NOTTINGHAM POLYTECHNIC
CLIFTON CAMPUS
CLIFTON LANE
NOTTINGHAM NG11 8NS

NOTTINGHAM POLYTECHNIC
CLIFTON CAMPUS
CLIFTON LANE
NOTTINGHAM NG11 8NS

PERMEATION THROUGH POLYMER LATEX FILMS

BRIAN JOHN ROULSTONE B.Sc. M.R.S.C. C.Chem

This thesis is submitted in partial fulfilment of the requirements for the degree of Doctor of Philosophy of the Council for National Academic Awards. The work reported in this thesis was carried out in the Department of Physical Sciences, Trent Polytechnic, Nottingham, in collaboration with the Physical Protection Division, Chemical Defence Establishment, Porton Down, Salisbury.

Parts of this work were presented at the NATO Advanced Study Institute Conference on Polymer Colloids, Centre Culturel Saint Thomas, Strasbourg, France July 1988.

September 1988

ACKNOWLEDGEMENTS

The author wishes to express his gratitude to the many people who have contributed to the work described in this thesis. First and foremost to Dr J.Hearn for his continued guidance and support, and to Dr M.C.Wilkinson for his considerable input and guidance to the project. The author also wishes to give thanks to Trent Polytechnic for the provision of facilities and financial support, and also the technical support of its staff.

PERMEATION THROUGH POLYMER LATEX FILMS

BY

BRIAN ROULSTONE

ABSTRACT

The permeabilities of polymer latex films prepared from surfactant free latices were studied. The work involved studies on surfactant free emulsion polymerisation, the morphology and permeation through model latex films, and latex films containing common latex additives. Also reported is the potential use of surfactant free latices as controlled release drug coatings.

The surfactant free emulsion polymerisation of butylmethacrylate was investigated, and the Smith and Ewart case III was used to describe the reaction kinetics. The emulsion polymerisation of 2-hydroxy-ethylmethacrylate was studied in the absence of surfactant; weakly stabilised latices were produced with significant gel contents.

The morphology of latex films was shown to be a result of the coalescence of the original latex particles, although the films were found to be essentially non porous.

The permeability of latex films to solutes was found to obey Ficks laws. The film permeability was shown to decrease with increased coalescence of the latex particles and a reduction in the permeability with film age was found. Permeation through latex films was postulated to be a combination of diffusion through the bulk polymer and the interparticle boundaries. The permeability of core-shell and copolymer latex films showed a reduction in permeability with film age, and the final value was consistent with the presence of a network of the more permeable polymer.

The inclusion of surfactants into clean latex resulted in an increase in the water vapour permeability. These films did not show any reduction in permeability with film age.

CONTENTS

CHAPTER 1

INTRODUCTION

I.1 EMULSION POLYMERISATION.

The earliest attempts at polymerising monomers in aqueous dispersion were performed just after the turn of the century[1-3]. These first polymerisations were very slow, being performed at ambient temperatures and in the absence of initiators, and could take up to six weeks to reach completion. With the use of soap and initiator, some twenty years later, the production of a synthetic latex became viable[4,5]. It was, however, the shortage of rubber during the second world war that prompted more intensive work in the field, notably work by Harkins[6] on the preparation of a styrene/butadiene latex. Harkins proposed the mechanism for particle formation in systems containing surfactant above its critical micelle concentration(CMC), and this mechanism is still widely accepted today. At about the same time Smith and Ewart[7] put forward a quantitative theory describing the kinetics of emulsion polymerisation of styrene. The agreement between experiment and their theory was good for styrene but less so for more water soluble monomers[8] such as vinyl acetate.

A typical recipe for an emulsion polymerisation consists of four components, water, monomer(s), surfactant, and initiator (usually water soluble). Other components may be found in some systems, such as chain transfer agents and buffers, to control the latex characteristics. The polymerisation is performed by stirring the mixture, and heating to a temperature above the decomposition point of the initiator. The product of such a reaction would typically be a polydisperse latex

with an average particle size of less than 500 nm . With sufficient surfactant in the system a latex of this type could be as concentrated as 60% solids and would be stable against coagulation over a wide range of conditions. Although these reactions often produce a polydisperse latex, by carefully controlling the surfactant type and concentration, and the particle number density by seeded growth, it is possible to produce a latex with a narrow particle size distribution[9]. Such latices were supplied by the Dow Chemical Company (Dow Chemical Company, Midland, Michigan, U.S.A.) and are used routinely as calibrants for Coulter counters, light scattering equipment and other particle sizing techniques.

Emulsion polymerisation in the absence of surfactant has been known for polystyrene since 1946[10], and it was shown by Matsumoto and Ochi[11] that the process could yield monodisperse poly(styrene) latices, both easily and reproducibly. The absence of surfactant in emulsion polymerisations is of limited interest industrially because the reactions often take longer to complete and the solids content must be low, i.e., <25% to avoid coagulation. However, the process has been widely used in academic studies to make model colloids.[12-15].

Fitch and his co-workers[16-19] developed the homogeneous nucleation theory for particle nucleation of the relatively water soluble monomers such as methyl methacrylate. Similar theories have been proposed for particle nucleation for less water soluble monomers such as styrene by Roe[28] and more recently by Napper.[35]

I.1.1 MECHANISM AND KINETICS OF EMULSION POLYMERISATION.

Emulsion polymerisation, as with other free radical mechanisms, can be split into three separate reactions, namely initiation, propagation and termination. Initiation takes place by the thermal decomposition of the initiator (I), to form free radicals (R):

$$I \xrightarrow{k_d} 2\ R^{\cdot} \qquad (I.1)$$

These radicals quickly react with monomer molecules to form monomer radicals which then can add further monomer units. The propagation step is given by:

$$R^{\cdot} + M \xrightarrow{k_i} RM^{\cdot} \ , \qquad (I.2)$$

and

$$RM^{\cdot} + nM \xrightarrow{k_p} R(M)_n M^{\cdot} \ , \qquad (I.3)$$

where nM is a polymer chain of n monomer units(M) and k_p, k_i and k_d are the propagation initiation and decomposition constants, respectively. The termination reaction can take place either by (i) combination, (ii) disproportionation or (iii) transfer reactions. Combination is the process whereby two growing polymeric radicals terminate by joining together, i.e.,

$$R(M)_m M^{\cdot} + R(M)_n M^{\cdot} \xrightarrow{k_t} R(M)_{m+n} + 2\ R \ , \qquad (I.4)$$

where k_t is the termination rate constant. The disproportionation reaction proceeds as follows;

$$R(M)_m M^{\cdot} + R(M)_n M^{\cdot} \xrightarrow{k_t} R(M)_n M' + R(M)_m M'' \qquad (I.5)$$

Termination by an initiator radical is also possible, i.e.,

$$R(M)_m M^{\cdot} + R^{\cdot} \longrightarrow R(M)_{m+1} R \qquad (I.6)$$

Other possible reactions include transfer to monomer, initiator and polymer. In each case the growing polymer radical usually terminates by hydrogen abstraction from the particular molecule and then the molecule itself becomes a free radical.

Since the early theories of Harkins[6] and Smith and Ewart[7], the mechanism and kinetics of emulsion polymerisation, mostly for styrene and methyl methacrylate has been studied by many workers, with some of the more notable work coming from Gardon[20], Napper[21] Ugelstad[23] and Fitch[16]. Only a brief summary of the main points is included here and more detailed discussions are given by Blackley[24] Vanderhoff[8] and Ugelstad[25].

I.1.2 MECHANISM OF POLYMERISATION IN THE PRESENCE OF SURFACTANT.

Monomer and surfactant are dispersed in water, with the surfactant at a concentration above it's critical

micelle concentration (CMC). The monomer and surfactant can be considered to be in three loci, (i) dissolved in the aqueous phase, (ii) monomer solubilised in surfactant micelles, and (iii) monomer emulsion droplets stabilised by absorbed surfactant. Upon initiation the free radicals formed by the initiator molecule react with the solute monomer molecules to form radicals. These radicals continue to grow in the aqueous phase until they either become surface-active or insoluble, at which stage particles begin to nucleate. There are several theories as to the mechanisms of particle nucleation and these fall into four classes, depending on the loci in which radicals initiate polymerisation:

(i) the aqueous phase,
(ii) micelles,
(iii) monomer droplets,
(iv) adsorbed surfactant layer,

The characteristics of the monomer is the principal factor which determines which mechanism prevails, but mechanism (iv), which is similar to initiation in micelles and (iii) which is only significant when the size of the monomer droplets is very small, are generally less favoured than mechanisms (i) and (ii).

(i) Initiation in the aqueous phase: This mechanism, put forward by Fitch,[16] is known as homogeneous nucleation. Here, the growing oligomers grow to the extent where they are no longer water soluble and precipitate to form primary particles. This mechanism is

favoured by the more water soluble monomers since they can polymerise more rapidly and the oligomers become insoluble before being captured by micelles. Once formed the primary particles can absorb surfactant and monomer. Polymerisation can then occur in the particle.

(ii) Initiation in micelles: The oligomeric ion radicals are captured by monomer swollen micelles, possibly by exchange with surfactant ions. Oligomers, rather than initiator radicals, are favoured for this capture process since the transfer of inorganic water soluble initiator radicals from the polar to the non polar enviroment is less likely. Since the micelle is swollen by monomer, polymerisation can take place rapidly until it is terminated by the entry of a second radical. Polymerisation can continue with the absorption of a third oligomer and termination by the fourth and so on. Only a small percentage of the initial micelles capture an oligomer and these continue to absorb monomer and surfactant from the aqueous phase. The remaining monomer droplets and surfactant micelles merely act as reservoirs to replace the monomer and surfactant lost from the aqueous phase. At the point when all the micelles have disbanded no new particles can be formed.

The role of surfactant micelles as the loci for particle nucleation has been disputed by Roe[28]. Roe suggested that the surfactant in the system was merely a source of stablisation for the polymer particles and he proposed a homogeneous nucleation mechanism essentially the same as that of Fitch[16]. Hansen and Ugelstad[29] presented a modified model for homogeneous nucleation

under submicellar or surfactant-free conditions. They also, however, presented a strong case for nucleation in micelles for surfactant concentrations above the CMC. Sutterlin[30] showed that the effect of monomer polarity was important in particle nucleation. He demonstrated that the more water soluble monomers produced a greater number of particles than predicted by the Smith and Ewart model. This was attributed to the greater number of monomer molecules dissolved in the aqueous phase being able to form polymer particles. An alternative mechanism for particle nucleation has been proposed by van der Hoff[31] and more recently by Hearn and Wilkinson et. al[32,33]. Essentially, this model suggests that the growing oligomers in the aqueous phase may become surface active and then associate with one another in the absence of surfactant, or with the surfactant molecules leading to the formation of mixed micelles. These associations could then become the loci for particle formation. Similar observations have also recently been reported by Chen and Piirma[34] who studied the polymerisation of acenaphthylene, a solid monomer with limited water solubility. It was concluded that the particle nucleation, both in the absence and presence of anionic surfactant, was initiated by mixed micelles or self micellisation. Lichti et. al[35] have also considered the mechanism of particle formation in a system containing surfactant above its CMC. They used electron microscopy to determine the particle size distribution directly after the cessation of particle nucleation. A mathematical model was also used to predict the rate of particle nucleation that would reproduce the observed particle volume distributions as a

function of time. Their calculations showed that the rate of particle nucleation was time dependent, and that there was a volume dependence on the efficiency of radical capture by latex particles, with the efficiency decreasing with particle size. They also applied their model to existing mechanisms for particle nucleation. Both the micellar and homogeneous nucleation mechanisms did not predict the increasing rate of particle nucleation that was needed to explain the observed particle volume distributions.

In order to explain the observed particle size distribution Lichti et. al. proposed a mechanism similar to homogeneous nucleation, with the additional consideration of primary particle coagulation. The model accounts for both the time-dependent nucleation rate and the size dependence of radical capture found from their calculations. The mechanism was presented in four steps:

i) Primary particles are formed in the aqueous phase by homogeneous nucleation. These primary particles grow at a relatively slow rate since there is no clear hydrophobic interior surrounded by a hydrophilic shell, as in mature latex particles and therefore, they are less able to absorb the equilibrium monomer concentration and do not polymerise rapidly. These particles have adsorbed surfactant on the incompletely formed outer surface.

ii) Primary particles may coagulate with each other and eventually there is enough polymer to absorb the equilibrium amount of monomer. Thereafter, the entity is considered as a latex particle and grows rapidly.

iii) Primary particles may coagulate with existing latex particles as well as with each other. The larger latex particles are unaffected by this except when the primary particle contains an active radical; this is then considered as radical entry into the large latex particle. Water soluble radicals also enter the latex particle by the accepted mechanism.

iv) When all the surfactant is exhausted the surface coverage on the latex particles decreases as its size increases. The same is not true for the much slower growing primary particles. This situation leads to coagulation between existing particles and primary particles predominating over primary particles coagulating with themselves. Thus, the rate of particle nucleation rapidly decreases.

Hansen[29] studied the number of new particles formed as a function of surfactant concentration in seeded and unseeded systems. He found that the number of new particles formed in a seeded polymerisation was much lower than in the unseeded system for low surfactant concentrations. However, above the CMC the numbers were the same. Lichti[35] explains this as follows. At low surfactant concentrations the rate of primary particles coagulating with existing particles is much higher than the primary particles coagulating with each other, and thus forming new particles. At very high surfactant concentrations the coagulation steps that lead to the formation of a latex particle from the primary particles are reduced to such an extent that the existing particles cannot compete kinetically in the coagulation process.

Thus, the seed particles have little or no influence on the number of new particles formed above the CMC.

In summary there seems to be no all-embracing model for particle nucleation in the presence of surfactant, and perhaps it would be a misleading to suggest there could be. Carra and Morbidelli[36] suggest that both the micellar and homogeneous nucleation mechanisms need to be applied, depending on the surfactant concentration. Some of the main evidence for the micellar mechanism comes from the large increase in particle number density at the CMC. In surfactant-free, or sub CMC systems, true micellar initiation can be ruled out, and the number of particles formed is due to the limited coagulation. This number increases as the surfactant concentration increases, because the particles undergo less coagulation. At concentrations above the CMC Carra suggests that the micellar mechanism becomes more important, and the two mechanisms coexist. At very high surfactant concentrations the micellar mechanism dominates. Lichti's[35] model would contradict this and suggest that micellar initiation was not as significant, although Lichti admits his evidence does not rule out the role of micelles in the mechanism for particle formation.

I.1.3 KINETICS OF SURFACTANT PRESENT POLYMERISATION.

Smith and Ewart[7] proposed a mathematical model of emulsion polymerisation based on the Harkins theory[6]. The model was presented in the form of a recursion equation for the steady state concentration of particles containing n free radicals, i.e. :

$$N_{n-1}(\rho/N) + N_{n+1} k_o a[(n+1)/V] + N_{n+2} k_t [(n+2)(n+1)/V]$$

$$= N_n \{(\rho/N) + k_o a(n/V) + k_t [n(n+1)/V]\} \qquad (I.7)$$

where N_n is the number of particles per unit volume containing n free radicals, ρ is the rate of entry of free radicals into all N particles, k_o is the rate constant for the transfer out of a particle of interfacial area a and volume V, k_t is the rate constant for termination inside the particles. They found solutions for this equation for three limiting cases. Firstly, when the average number of radicals per particle was much less 0.5. Secondly, when n was approximately equal to 0.5. Thirdly, when n was much greater than 1.

Case 1 applies when the rate of radical transfer out of the particle is much greater than radical entry. In such systems termination can take place in either the aqueous phase or the polymer particle. For termination in the aqueous phase the rate of polymerisation is given by:

$$R_p = k_p [M] V_p a(\rho/2k_{t,w})^{1/2}, \qquad (I.8)$$

where k_p is the propagation rate constant, [M] is the concentration of monomer in particles of volume V_p, a is the radical partition coefficient, i.e. the ratio of the average number of radicals in the polymer and aqueous phase, respectively. ρ is the rate of formation of free radicals in the water phase, and $k_{t,w}$ is the termination rate constant in the aqueous phase. For termination in the

polymer particles the rate of polymerisation is given by:

$$R_p = k_p [M] (V_p \rho / 2 k_o a)^{1/2} \qquad (I.9)$$

Case 1 kinetics would favour more water soluble monomers producing hydrophilic polymer.

Case 2 is widely acknowledged as describing the emulsion polymerisation of styrene. Case 2 is realised if termination in the particle takes place immediately a second radical is absorbed. It was considered that the polymer particles were so small that more than one radical could not exist in a single particle without rapid termination. Thus, in the absence of radical transfer out of the particle, a given particle would contain either 1 or 0 propagating polymer chains. Therefore, the average number of radicals per particle is 0.5. For case 2 kinetics the number of particles is given by:

$$N = k(\rho/\mu)^{0.4} (a_s S)^{0.6}, \qquad (I.10)$$

where μ is the rate of change of the volume of the particle and the term $a_s S$ is the surface area of the emulsifier in the recipe. The rate of polymerisation is given by:

$$R_p = 0.5\ k_p [M] N \qquad (I.11)$$

There is considerable evidence[8] to suggest that the emulsion polymerisation of styrene obeys case 2 kinetics provided that the particle size is small, i.e., < 150nm,

and that the rate of primary free radical generation is low. The agreement of this part of the theory with experiment is, however, less successful for more water soluble monomers such as vinyl acetate and the lower aliphatic acrylic and methacrylic esters.

Case 3 applies when more than one radical can exist in a given polymer particle. This situation is possible for systems producing large particles. Case 3 will occur if either k_t is small or V is large. The rate of polymerisation is given by:

$$R_p = k_p [M] (V_p \rho' / 2k_t)^{0.5} \qquad (I.12)$$

If $\rho = \rho'$, that is if the rate of radical production equals the rate of radical absorption, then the above equation is the same as that of bulk or solution polymerisation.

Several modifications to the Smith and Ewart model have been postulated. Stockmayer [37] obtained a general solution to the recursion equation and O'Toole[38] extended that work by considering that radical transfer out of the particles was significant. Ugelstad and Hansen[23] considered that the absorption of radicals by micelles and particles was not irreversible and developed expressions for the rate of radical absorption under varying circumstances. They concluded that the absence of a maximum in the rate of polymerisation during interval I, which was predicted by the Smith and Ewart treatment, was a consequence of small particles containing a radical

tending to absorb radicals from the aqueous phase at a higher rate than micelles and small particles containing no radicals. They also showed that during interval II the value of n = 0.5 held true since for particles > 100nm the rate of radical absorption is the same for particles containing either one or no radicals. Also, as the particle size increases the tendency for irreversible absorption of radicals increases.

It has been assumed that the monomer is uniformly distributed throughout the polymer particle during polymerisation. Williams[39] postulated that, even for compatible systems, the polymer particle consisted of a monomer-rich shell and a polymer-rich core, and polymerisation took place at or near the surface of the particle. Williams based his core-shell proposal on kinetic data, electron micrographs and thermodynamic arguments. Vanderhoff[40] has reviewed the literature on the subject of core-shell morphology in latex particles. He has proposed another hypothesis to explain the experimentally observed core-shell morphology without invoking the contentious monomer concentration gradient. Vanderhoff proposed that, initially, a polymer particle of ca. 15 nm in size contains only one polymer molecule and an equal amount of monomer. The polymer molecule has a random coil configuration with both the sulphate end groups at the particle surface. Initiation and termination results in the formation of new polymer chains with the same configuration. Thus, the newly formed polymer chains will tend to force the older chains towards the centre of the particle. These older chains will distort and strive to keep their end groups at the surface of the particle.

Eventually the strain forces some of the end groups to be buried by fresh polymer.

I.1.4 MECHANISMS OF SURFACTANT-FREE EMULSION POLYMERISATION.

The role of surfactant micelles in surfactant present emulsion polymerisation is one of great contention. However, in the surfactant-free systems there are no such entities to initiate particle formation. The homogeneous nucleation mechanism which was described by such early workers as Priest[26] and developed in more recent times by Fitch and his co-workers[16-19] has become widely accepted. Fitch[19] gives both a qualitative and quantitative model for particle nucleation and the number of particles formed. Initially, monomer dissolved in the aqueous phase reacts with the initiator radicals and goes on to form oligomeric ion radicals as described earlier. These oligomers can suffer one of three fates:

(i) the oligomers can grow to a critical chain length and precipitate, and at this point may nucleate a new particle (homogeneous nucleation),

(ii) they can flocculate with an existing polymer particle,

(iii) they may be terminated in the aqueous phase. At this point the newly formed particles may not be colloidally stable, and will coagulate with other particles in order to achieve this.

Thus, the rate of particle nucleation is given by:

$$dN/dt = R_i - R_c - R_f, \qquad (I.13)$$

where R_i is the rate of radical formation, R_c the rate of soluble oligomer capture and R_f is the rate of flocculation. Initially, the rate of particle formation will equal the rate of radical generation. As particles are formed the rate of oligomer adsorption becomes important and the rate of nucleation decreases. In considering the role of oligomer capture Fitch applied an adaptation of Gardon's collision theory[27] which predicts that the rate of capture is proportional to the square of the particle radius,i.e.,

$$R_c = R_i (N\pi r^2_p) L, \qquad (I.14)$$

where L is the average distance an oligomeric radical diffuses in the aqueous phase before it self nucleates, and r_p is the radius of the capturing particle. Fitch modified the above expression to take into account the motion of the polymer particle and the size of the oligomer. Using that equation, and assuming an initiator efficiency of 0.11, he predicted particle numbers for methyl methacrylate that were in good agreement with experiment. Fitch also considered a diffusion theory controlling the oligomer capture. This model describes the particle as a sink for the oligomers and gives a diffusion boundary layer around the particle. This boundary layer gives rise to a concentration gradient of oligomers around

the particle, ranging from zero concentration at the particle surface to the steady state concentration of oligomers in the solution beyond the boundary. In this situation the rate of oligomer capture is governed by Ficks law:

$$R_c = 4 D_{op} C_s N r_p r_h / (r_h - r_p), \qquad (I.15)$$

where D_{op} is the average diffusion coefficient determined by the relative motion of the oligomers and polymer particles, r_h is the radius of the boundary layer and r_p is the radius of the particle, and C_s is the number concentration of radicals beyond the boundary layer. In an experimental attempt to decide which of these two models was pertinent for methyl methacrylate, calculations showed that while the collision theory gave results of the right order of magnitude the diffusion theory was more correct. As mentioned earlier, Hearn et. al.[32,33] have described the formation of oligomeric micelles for particle initiation in the surfactant-free emulsion polymerisation of styrene. They based their conclusions in part on the low molecular weight material found by GPC studies in samples taken during the early stages of the polymerisation. Also analysed, by vapour phase osmometry, was the polymer in the aqueous phase, this suggested that water soluble polymer had achieved a degree of polymerisation between 2 and 4. It was thus suggested that these water soluble oligomers were surface active and could form an aggregate in a similar fashion to a micelle. Material of molecular weight 1000 was believed to be the result of termination of two water soluble oligomers.

It was also shown that the primary particles undergo extensive aggregation during the early stages of the reaction. Using light scattering and photon correlation spectroscopy data, they argued that the primary particles swelled with monomer and became unstable and thus formed aggregates. The observation that the number density of particles decreases rapidly in the initial stages of the reaction is a consequence of this aggregation. Recently, Yeliseyeva[41] has also demonstrated the presence of flocculation during particle formation. She has shown that the primary particles undergo limited flocculation and their presence was demonstrated by oxygen etching and electron microscopy.

I.1.5 KINETICS OF THE SURFACTANT-FREE REACTION

Of the various theories describing emulsion polymerisation kinetics, Hearn et al[42] cite four theories that may be capable of treating surfactant-free polymerisations. Firstly, the Smith and Ewart case III could be applied owing to the larger particle sizes obtained in surfactant-free reactions. These larger particles could contain more than one radical per particle at any given time, without the radicals terminating instantly. Secondly, the Smith Ewart case III was applied to the core-shell model of polymerisation mentioned earlier[29]. This theory predicts:

$$R_p = \frac{k_p [M]}{N_A} \left[\frac{\rho_A S L}{2 k_{ts}} \right]^{0.5} , \qquad (I.16)$$

where the subscript, s, refers to the shell of thickness L and S is the surface area per dm^3. The third model quoted was that of Wessling[43].He describes an absorbed monomer layer as being the locus of polymerisation. The kinetic treatment was quantitatively similar to the core-shell applied to case three. The last theory considered by Hearn was that of Gardon[44]. Gardon derived general equations to describe polymerisation from initiation to the end of interval II. Although the equations were derived for systems in the presence of surfactant above the CMC, they are readily adaptable for surfactant-free systems. This is done by replacing the term involving the surfactant with the observed value of N. Gardon's treatment predicts:

$$P_v = At^2 + Bt, \qquad (I.17)$$

were A and B are constants defined by

$$A = 0.102 \frac{k_p^{1.94} \Phi_m^{1.94} d_m \rho_A}{k_t^{0.94} (1-\Phi_m)^{0.94} d_p N_A}$$

and (I.18)

$$B = \frac{k_p \Phi_m N}{2 N_A} \qquad (I.19)$$

were d_m and d_p are the densities of the monomer and polymer, respectively, and Φ_m is the volume fraction of monomer in the particle.

I.2 FILM FORMATION BY POLYMER LATICES

Traditionally, polymer films have been made by casting from a suitable solvent or by industrial processes such as extrusion and compression moulding. Polymer films can also be prepared from latices in a manner similar to solvent casting, i.e., the solution or dispersion is spread over a suitable substrate and the water or solvent evaporated to leave the polymer behind as a film. The formation of latex films is, however, a little more complicated than the formation of polymer films from solution. For a latex to form a continuous film when dried down , the temperature must be above the minimum film forming temperature (MFFT) of the polymer. This temperature is usually similar to the glass transition temperature. Polymer latices dried below their MFFT form friable discontinuous films which crumble to a powder. Such differences in the properties of latex films have been attributed to the submicroscopic morphology of the film [45]. In continuous films the latex particles appear coalesced , but in discontinuous films they appear as a regular array of uncoalesced spheres.

Drying of latices to form films has been studied by several authors [46,47,48] using a range of different techniques. The results of these studies indicate that a plot of the volume fraction of polymer versus time yields a sigmiodal curve for film forming polymers above their MFFT. Vanderhoff el al.[47] interpreted this curve by dividing the drying process into three stages, as shown in Figure I:1. During the first stage of drying , water

evaporates from the surface of the latex. The rate of this evaporation is similar to the evaporation rate from dilute electrolyte or surfactant solutions. The rate of evaporation remains constant as long as the surface area of the latex is unchanged by disjoining or retraction of the latex on the casting substrate. The second stage begins when the particles come into irreversible contact and fuse to form a continuous film. Here, the particles are deformed from spheres into dodecahedra. The rate of water evaporation is considerably reduced during this period due to the reduction in the air/water interfacial area; however, the rate per unit area remains unchanged. The completion of coalescence marks the beginning of the final stage. The rate of evaporation is very slow as residual water escapes from the film through capillary channels or by diffusion through the polymer.

I.2.1 INITIAL STAGES OF FILM FORMATION

In order to understand fully the process of film formation it is necessary to explain particle coalescence. The first mechanisms for particle coalescence were proposed by Dillon, Matheson and Bradford[49], and later by Brown[50]. Dillon et. al. argued that the large reduction in surface area which accompanies particle coalescence would produce sufficient shearing stress to cause viscous flow. An expression for the rate of coalescence by viscous flow that was developed by Frenkel[51]:

$$\Theta^2 = 3\gamma t/2\pi r\eta \qquad (I.20)$$

where t is the time ,η is the polymer viscosity, γ the surface tension, r is the radius of the particle and Θ the half angle of coalescence (see Figure I:2).

Brown[50] suggested that, for a film to be formed the forces causing coalescence must exceed those opposing it. i.e.,

causing coalescence:

F_S, the force produced by the negative curvature of the particle surface i.e. surface tension causing a reduction in surface area.

F_C, the capillary pressure resulting from a water surface of negative curvature.

F_V, the van der Waals attractive forces between particles.

F_g, the gravitational force acting on the particles.

opposing coalescence:

F_E, the electrostatic repulsion between particles.

F_G, the resistance of spherical particles to deformation.

Thus, for coalescence to occur the following must apply:

$$F_S + F_C + F_V + F_g > F_E + F_G \qquad (I.21)$$

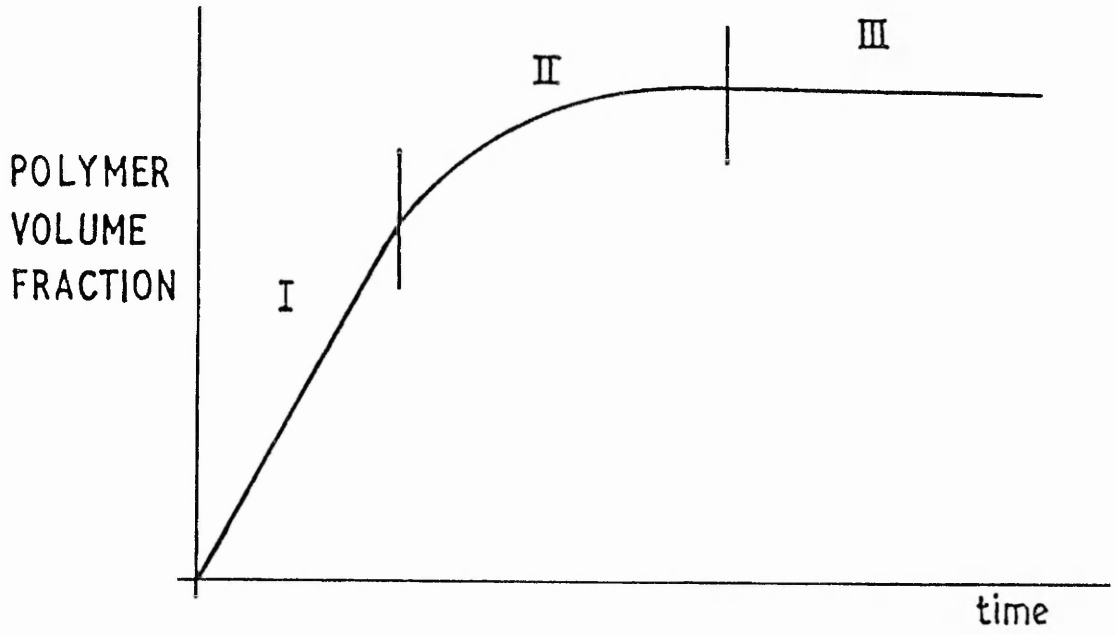

Figure I:1 Water loss during latex film formation

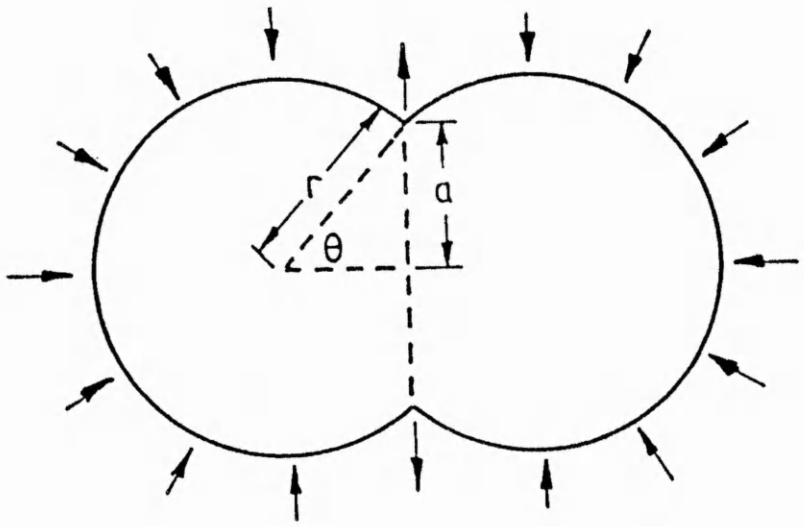

Figure I:2 Coalescence of latex particles according to Dillon

Brown was critical of the dry sintering mechanism for particle coalescence proposed by Dillon et al. and proposed an alternative wet sintering mechanism. The points raised by Brown to support this were as follows:

(i) film formation occurs concurrently with the evaporation of water , and therefore the surface tension of the polymer could not provide the driving force for coalescence. Alternatively, Brown suggested that the polymer surface tension should be replaced by a water/polymer interfacial tension and suggested 0 - 10 mN m^{-1} would be a realistic value for it.

(ii) The observation that the rate of water removal influences the coalescence of borderline film forming latices.

(iii) That porous, incompletely coalesced films were formed by latices dried down below their MFFT

(iv) That lightly crosslinked polymer latices formed films even though the crosslinking would prevent viscous flow of the polymer.

Brown went on to eliminate some of the originally suggested forces that could influence particle coalescence. The gravitational force, F_g , was considered to be insignificant and the repulsion force, F_E , was greater than the Van der Waals attraction, F_V , for stable dispersions. The influence of the surface tension force,

F_S was also considered to be small as it could only operate when a concave polymer surface existed. Having eliminated these forces the original inequality was reduced to:

$$F_C > F_G \qquad \text{(I.22)}$$

Brown went on further to give a more quantitative solution. Using the gap that exists in the plane passing through the centres of three adjacent particles as the capillary(see Figure I:3) he calculated that the capillary pressure, F_C, was given by;

$$F_C = 12.9\gamma A/r \qquad \text{(I.23)}$$

Taking the force required to deform the particles to be the product of the shear modulus of the polymer G_1 and another geometrical constant, i.e.,

$$F_G = 0.37\ G_1 A \qquad \text{(I.24)}$$

From these two results the condition for coalescence, and hence film formation, is given by:

$$G_1 < 35\gamma/r \qquad \text{(I.25)}$$

Both the mechanisms proposed by Dillon et al. and Brown predict that the pressure causing coalescence is inversely proportional to the particle radius. Thus, for large particles with radii greater than 1μm the calculated pressures would seem inadequate to bring about

coalescence. Vanderhoff et.al.[52] showed that a series of monodisperse particles of styrene-butadiene copolymer latices in the range 0.1 to 1 μm, all formed continuous films, regardless of particle size. Vanderhoff et al. argued that during the early stages of particle coalescence the initial polymer-polymer contact generates very small radii of curvature. This curvature has a strong influence on the surface forces exerted, causing coalescence.(see Fig. I:4) They maintained that any treatment involving the Young-Laplace equation must make use of these radii. According to their analysis the pressure difference across the particle/water interface is given by:

$$P_2 - P_1 = 2\gamma/r \quad , \qquad \text{(I.26)}$$

and in the region of coalescence is given by:

$$P_3 - P'_2 = (1/r_1 - 1/r_2) , \qquad \text{(I.27)}$$

where γ is the polymer/water interfacial tension and the pressures, P_1, P_2, P_3 and the radii, r_1 and r_2, are shown in Fig. I:4. Assuming that $P_3 = P_1$, the above equations can be combined to give:

$$P = P_2 - P'_2 = (1/r_1 - 1/r_2 + 2/r) \qquad \text{(I.28)}$$

Brodnyan and Konen[53] attempted to verify Brown's mechanism by correlating the MFFT of a latex with its particle size, surface tension and polymer shear modulus. They found that the ability of a latex to form a film was

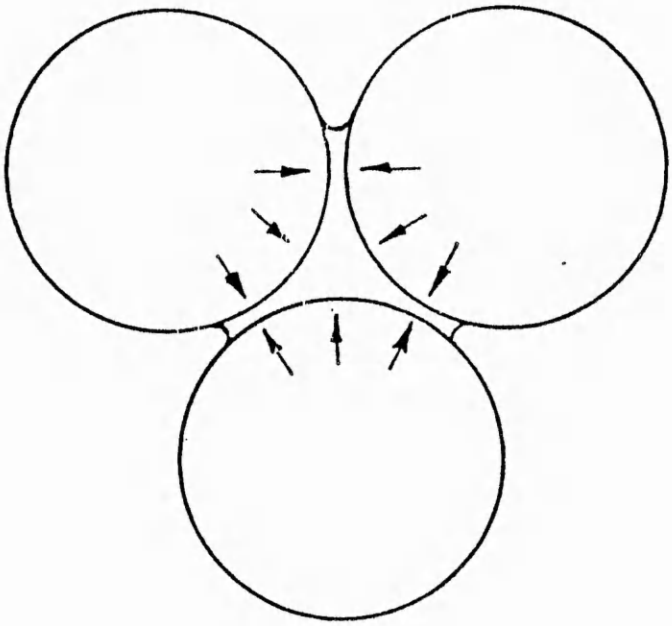

Figure I:3 Capillary pressure during particle coalescence

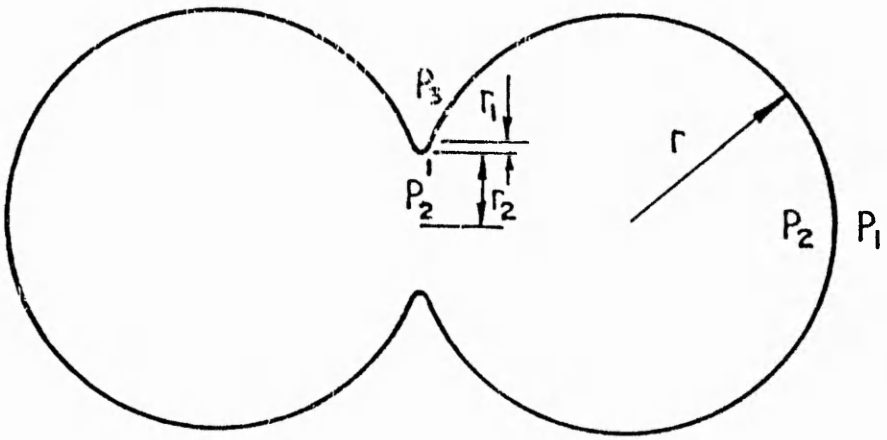

Figure I:4 Particle coalescence according to Vanderhoff

not strongly dependent on particle size or surface tension. They also found that the shear modulus of the polymer did fall rapidly with increasing temperature in the region of film formation as predicted by Brown. Although reasonable agreement was found for the Brown condition for film formation, $G_1\gamma/r$ was constant for different sized latices of the same polymer, but this same value varied greatly for latices of different polymers. Values ranging from 0.58 for a non-polar copolymer to 260 for a polar one were reported. They also noted the difference between the MFFT and the glass transition temperature, Tg. The MFFT was found to be 10°C higher than the Tg for a non-polar copolymer, whilst it was found to be 3°C lower for a polar one. It was suggested that the variation in polymer polarity and the value of $G_1\gamma/r$, was due in part to the plasticisation of the polymer by water. However, this factor alone would not be enough to account for the differences.

Myers and Shultz[54] investigated the influence of drying rates on film formation of acrylic latices. They showed that slow drying rates resulted in continuous films being formed below the MFFT. This was attributed to the removal of residual stress due to creep relaxations under longer periods of film formation. The notion of internal stress in film formation is a well known phenomena in the coatings industry and many studies have been reported; details of which can be found in a review by Paul[55].

A more recent model for film formation has been developed by Bierwagen[48]. The kinetics of film drying were examined, using the onset of coalescence as a transition point in the film forming process. The

qualitative description of the drying process is much the same as that described by Vanderhoff[52], where the process is divided into three stages. In stage one the rate of water loss is constant and proportional to the free surface area, and is governed by:

$$\text{Rate} = A\ K_E, \qquad \text{(I.29)}$$

where A is the surface area for evaporation and K_E is the rate constant for evaporation. Stage two of the drying process marks the transition point, where the particles are at their random most dense packing. Mixed drying kinetics are found in this stage; evaporation from the free surface area not closed by coalescence and diffusion controlled drying through the closed area of the film. The drying rate is now given by:

$$\text{Rate} = (1-\theta)R_e + R_D, \qquad \text{(I.30)}$$

where θ is the fraction of the surface closed by coalescence and R_D is the diffusion controlled evaporation rate. In stage three the surface of the film is completely closed and the rate of drying is solely diffusion controlled. At this point $\theta = 1$, and the drying rate is given by:

$$R_D = \{(C_o - C)D/h\}(AM/\rho_l), \qquad \text{(I.31)}$$

where C_o and C are the concentrations of water in the film and the volumetric concentration of water external to the film, respectively. D is the diffusion coefficient of

water in the film and h is the coalesced layer thickness. M is the molecular weight and ρ_l is the density of water. Using the above model a computer programme was generated to predict the influence of varying parameters in the drying process. The conclusions from this were as follows:

(i) under identical conditions, drying is sensitive to the thickness of the film. The thicker films contain more water than thinner ones at an equivalent time even though they have reached the diffusion controlled stage and have a closed surface.

(ii) films with low initial solids content will finish drying quicker than films of higher solids content even though the latter have less water to lose. The higher solids films reach the diffusion controlled stage faster and then lose water at a much slower rate.

(iii) films with different original thickness and volume fraction solids, but the same amount of solids and hence the same final film thickness show different initial drying characteristics. In the final stages the drying rates converge and become identical.

The final point made by Bierwagen was with reference to stress during the final stages of film formation, leading in some cases to the so called 'mud cracking '. The stress due to capillary pressure can cause the coalescence of particles in stage two and in stage three there exists an osmotic pressure. All the stresses

of film formation must be dissipated by the polymer for a complete film to be formed. When a film dries such that the surface area of the film remains the same but there is is a reduction in thickness due to the evaporation of water, stress is induced in the x-y plane. If the stresses cannot be released then cracks will occur in the film. For films formed above the glass transition temperature the polymer has a high elasticity, thus when surface closure takes place the coalesced layer can support the horizontal stresses generated at all times. Mudcracking may occur if the temperature is lower than the glass transition temperature, if there is some flocculation or surface defects. Thicker films are more likely to suffer 'mudcracking' and this is probably caused by slip between the coalesced layer and the fluid layer beneath which has no strength.

Another recent treatment of the film forming process has been proposed by Lamprecht[56]. He accepted the physical model proposed by Brown[50], but modified the calculation to take into account the influence in the rate of water removal. This was done by treating the physical properties of the polymer (such as creep compliance and shear modulus) to be time dependent. Lamprecht showed that the force resisting deformation of the particles was that generated when two viscoelastic bodies are pressed together, and gave the condition that this force must be less than the external pressure generated.Thus:

$$1.33\left(\frac{K}{t}\right)^{3/2}\int_0^{t^*} G(t^* - \tau)\sqrt{\tau}\, d\tau \leqslant P_{max} \qquad (I.32)$$

where k is the constant rate of evaporation per unit area, t is the relaxation time and t* is the time taken for complete coalescence to occur (and is equal to 0.2861/k). Lamprecht estimated the value of P_{max} to be 1.3 $x10^8 N\ m^{-2}$, which is similar of value given by Brown[50].

I.2.2 FINAL STAGES OF FILM FORMATION

According to all of the above models, a latex film is formed from coalesced latex particles held together by physical forces. Voyutskii[57] considered that these forces alone could not explain the mechanical properties of the films. To account for this he postulated the mutual interdiffusion of polymer chain ends, termed 'autohesion'. Essentially, autohesion is the process by which polymer chain ends from one particle interdiffuse with the polymer chains of a neighbouring particle. Thus, this process changes a latex film into a more homogeneous film by reducing the interparticle boundaries. This process accounts for the strength of latex films and other properties of polymers such as adhesion. The concept of autohesion has been studied experimentally and reviewed by Voyutskii[58,59]. From this work it was found that the rate and extent of autohesion were inversely related to molecular weight and degree of crosslinking.

In studies by Bradford and Vanderhoff[60,61] and Vanderhoff[62] it was demonstrated that latex films behaved in a manner consistent with the autohesion theory. Using a replication technique and transmission electron microscopy to examine styrene-butadiene copolymer latex film surfaces, they found that freshly formed films clearly

showed the contours of the coalesced particles, even though the film was continuous and transparent. Further replicas were produced at various times after film formation and showed that the contours became less distinct and after 14 days were no longer visible. Also, during this time blister like eruptions had appeared on the surface of the film, growing larger and eventually flowing over the surface of the film. It was later shown that the exudations were surfactant which had stabilised the particles in suspension, and was not compatible with the polymer. This aging process which was termed 'further gradual coalescence', was also found to take place in the film interior. The variation in the amount of aging with respect to polymer molecular weight and degree of crosslinking was studied. Divinyl benzene was added to the polymerisation reactions to study the effects of crosslinking, whilst tert-dodecyl mercaptan was added as a chain transfer agent to reduce the molecular weight. It was found that decreasing molecular weight increased the degree of coalescence and increasing degrees of crosslinking reduced it.

The postulate that latex films become completely homogeneous on aging was contradicted by Distler and Kanig[63]. It was suggested that some interdiffusion of polymer chain segments was inevitable, but this would be restricted by the incompatibility of hydrophilic surface groups, such as grafted surfactant and charged end groups arising from initiation, with the bulk polymer. The evidence they used to support this was that clear latex films became turbid on swelling in water. This effect was attributed to water penetrating the interior of the film

along the hydrophilic interparticle boundaries. In order to confirm that this effect was not due to the deposition of water soluble impurities, such as initiator fragments and surfactant, a latex containing 1 % acrylic acid was cast into a film. This film was treated with uranyl acetate, thus leaving the uranyl ions bound to the carboxyl groups of the acrylic acid as well as acid residues from initiator fragments and surfactant, which were considered to be concentrated at the surface. After washing the excess uranyl acetate away, the film was sectioned for inspection by transmission electron microscopy. The section showed a regular pattern of points connected by a fine web of dark lines. The web was interpreted as the particle boundary and the points as water soluble material in the interstices. The same authors used a staining technique involving hydrazine hydrate vapour and osmium tetroxide [64], again observing the particle contours in an acrylic latex film. Films treated by this method clearly showed a honeycomb structure, highlighting the deformed latex particle boundaries, with the honeycomb spacing agreeing very well with the original particle size of the latex. Distler and Kanig[65] also examined films cast from dilute solutions of freeze dried polymer dissolved in tetrahydrofuran. Solvent cast films of poly(ethyl acrylate) and poly(n-butyl acrylate) showed the same honeycomb structure whereas films cast from poly(n-butyl methacrylate) were featureless. This was attributed to the acrylate polymers being crosslinked and the particles not being in true solution. The source of the crosslinking was chain transfer with the labile tertiary hydrogen of the acrylate

polymers[66]. The methacrylate polymer did not have the labile hydrogen atom, and therefore did not crosslink, and this was given as the explanation for the lack of any structure in the solvent cast methacrylate film.

A recent paper by Kast[67] has considered the film forming mechanisms when applied to homogeneous and heterogeneous copolymer systems, where the homogeneity refers to a latex particle that contains only one polymer phase. A heterogeneous copolymer particle would be one that contained two or more separate polymer phases, such as core-shell copolymers. Kast suggests that homogeneous copolymer latices do not differ from homopolymers in their behaviour during film formation. There are exceptions, however, when comonomers are added which impart hydrophilic polymer to the system, such as vinyl acetate and methyl acrylate. Kast suggests that water may act as a plasticiser and cites experimental evidence to show an increase in the mechanical properties of a wet film as compared to a dry film. Heterogeneities due to water soluble or hydrophilic monomers, such as acrylic and methacrylic acid, often result in particles with core-shell morphologies. This is because the hydrophilic material is not homogeneously polymerised, but accumulates at the particle surface or in the aqueous phase. Kast cites the work of Distler[63] and uses the same staining technique to show the differences in film morphology of a acrylic acid containing copolymer with the same copolymer without acrylic acid. He showed that the acrylic acid collected at the particle surface in the form of a shell, which formed a continuous network throughout the film during film formation. Kast also showed that the storage

modulus of the polymer had increased above the major glass transition temperature, for the acrylic acid containing film and that a second higher transition was detected, indicating that the acrylic acid was present as a second phase. In the case of latex particles which have multidomain morphologies, that is where one polymer is dispersed in the second to form a complex structure, the polymer with the highest glass transition is dispersed in the polymer with the lowest. However, there are exceptions to this, i.e., when the volume fraction of the polymer with the lower Tg is insufficient to form the continuous phase. Normally, it will be the low Tg polymer that will govern the film formation process, and if the film formation takes place below the glass transition of the second polymer, a film with the harder polymer dispersed in the softer polymer results. This shown in Figure I:5. These films also exhibit a unique feature of a further stage of film formation which occurs in the dry film when it is heated at temperatures above the Tg of the second polymer. The dispersed domains start to coalesce and tend to form an inverse morphology with a matrix of the second polymer (also shown in Figure I:5). Kast demonstrates this experimentally with a styrene-ethyl acrylate copolymer; using the storage modulus of the polymer and electron microscopy to demonstrate changes in morphology. In the first case the poly(ethyl acrylate) phase dominates with only a small contribution from the dispersed poly-(styrene). After annealing and phase inversion the modulus versus temperature plots are typical of two-phase polymer systems. Kast attributes the driving force for this phase inversion to the polymer-polymer interfacial tension.

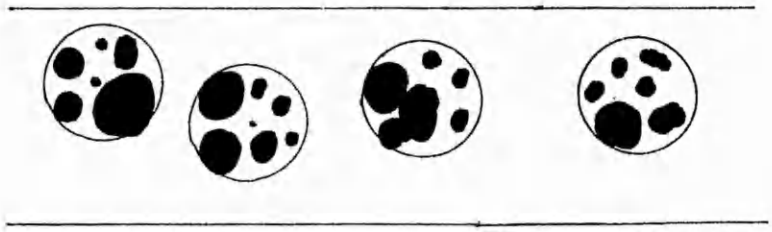

$T_{G1} < T < T_{G2}$

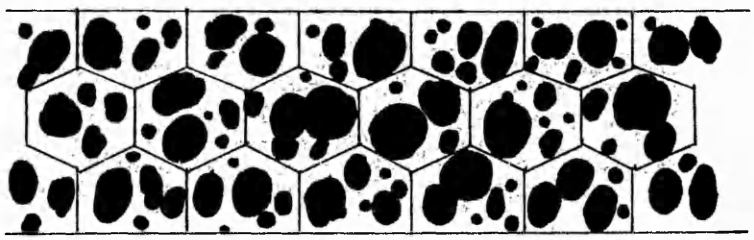

$T_{G1}, T_{G2} < T$

POLYMER 1 T_{G1}

POLYMER 2 T_{G2}

Figure I:5 Domain structure in copolymer latex films

CONCLUSIONS

The various theories of film formation provide a good description of the processes occuring when a latex dispersion is dried. For the first stage in film formation the model proposed by Brown[50] is most widely accepted. However, in a recent paper[56] only capillary forces opposed by the resistance of the particles to deformation are considered. The question of such factors as flocculation, softening of the polymer by water, surface tension in the last stages of coalescence and van der Waals forces have yet to be quantified[56].
Studies of the longer term properties of latex films show that changes in the morphology of these films continues some time after the film is completely dry. Voyutskii's autohesion theory explains these observations and work by Distler and Kanig show that latex films may never completely become homogeneous, since hydrophilic moieties on the particle surface would be incompatible with the hydrophobic particle interiors. All the work on the long term processes in latex films concentrates on the interparticle boundaries and work by Kast highlights this as well as demonstrating that drastic changes in film morphology can result in hetergeneous copolymer systems.

The morphology of latex films will undoubtedly influence their transmission properties. Measurement of transmission of gases through latex films has been used recently[68] to study the aging in latex films and highlights the importance of the interparticle boundaries in this process.

I.3 DIFFUSION AND PERMEATION.

The discovery that natural rubber membranes were permeable to gases was made in the early nineteenth century. The most notable of these early works was that of Graham[69]. He described rubber as being more liquid-like than solid, and postulated that permeation was a three stage process involving condensation and solution of the gas at one face of the membrane, diffusion as a liquid to the other face, and finally dissolution and evaporation. With the advent of the airship at the turn of the century many advances in the measurement of permeability were made, especially of hydrogen and helium through rubber coated fabrics. In 1920 Daynes[70] gave a solution to Fick's second law of diffusion which enabled diffusion coefficients to be determined from the so called 'lag-time'. However, it was not until 1939 that Barrer[73] developed the experimental techniques to exploit this.

I.3.1 DETERMINATION OF DIFFUSION AND PERMEABILITY COEFFICIENTS

When considering the transport of gases across a barrier the terms Diffusion and Permeability can be defined as follows: Diffusion is the process by which matter is transported from one part of a system to another by means of random molecular motions. Permeation of a gas through a polymer film under a partial pressure difference occurs by condensation and solution of the gas in one face of the film, followed by diffusion to the other face, and

finally dissolution and evaporation[69]. When the transport of species in solution is considered the processes of diffusion and permeation are essentially the same as for gases and can be described in the following manner. A transport system is created when there is passage of a solute across a barrier which separates the solution from the solvent. The passage of the solute occurs when there is a concentration gradient (or more correctly a chemical potential gradient) of the solute across the barrier, and is such that there is a tendency to equalise the concentration of the solute in all parts of the system. In a non porous barrier the solute must have a finite solubility in the barrier material for diffusion to take place. In porous barriers the solute molecules can pass through the spaces within the barrier.

In determining the diffusion and permeability coefficients the use of Fick's laws of diffusion are essential. Fick[72] reasoned that the flow of matter along a concentration gradient was analogous to the flow of heat along a temperature gradient. From this analogy Fick proposed that J, the rate of flow of particles per second across unit area in a plane x, perpendicular to the direction of the concentration gradient, is directly proportional to the concentration gradient $\delta c/\delta x$, thus,

$$J = -D(\delta c/\delta x), \qquad (I.33)$$

where c is the concentration and D is the diffusion coefficient. The negative sign in the above equation signifies that the diffusant is progressing towards regions of lower chemical potential. If the concentration

gradient at all points in the barrier were equal at any instant, then the flux, J, would be readily determined from a knowledge of the concentration gradient and film thickness. In practice the concentration gradient, and hence J, vary from point to point in the barrier, and their values will be time and position dependent. If the diffusion coefficient is concentration independent then Fick's second law takes the following form:

$$\frac{\delta c}{\delta t} = \frac{D \delta^2 c}{\delta x^2} \qquad \text{(I.34)}$$

This states that the concentration gradient, $\delta c/\delta t$, at any given point, x, is proportional to the rate of change in the concentration gradient, $\delta^2 c/\delta x^2$. Initially the barrier contains no permeating molecules. On exposure to the permeant the concentration gradient at any point in the barrier is not constant, and increases with time. After a certain period of time, the concentration gradient within the film becomes essentially zero at all points, and after this time the rate of transport of permeant across the barrier becomes constant. This is known as the steady state permeability. The time required for the steady state permeability to be established is termed the lag-time. Barrer[71] gave a solution to Fick's second law which exploited the time lag and gave a means of determining the diffusion coefficient. The practical form of the solution takes the following form:

$$Q = \frac{D(Co'-C1')}{L} \frac{(t - L^2)}{6D}, \qquad \text{(I.35)}$$

where Q is the cumulative mass permeated per unit area of the film, Co'-C1' is the concentration gradient within the film of thickness L. Figure I:6 shows a typical plot of Q versus time, often referred to as a Barrer plot. By extrapolation of the steady state permeability to zero mass of permeant the diffusion coefficient can be determined by the following relation:

$$t_{lag\text{-}time} = \frac{L^2}{6D} \qquad (I.36)$$

The linear portion of the plot in Figure I:6 can also be used to determine the diffusion coefficient. Differentiation of equation (I.35) yields the following equation:

$$\frac{dQ}{dt} = \frac{D(Co'-C1')}{L} \qquad (I.37)$$

The donor phase concentration, Co, is related to Co' by the solubility of the permeant in the film, i.e.,

$$Co' = K\ Co, \qquad (I.38)$$

where K is the partition coefficient. Thus, equation (I.37) can be written as:

$$\frac{dQ}{dt} = \frac{DK(Co-C1)}{L} \qquad (I.39)$$

The composite term DK is the permeability coefficient.

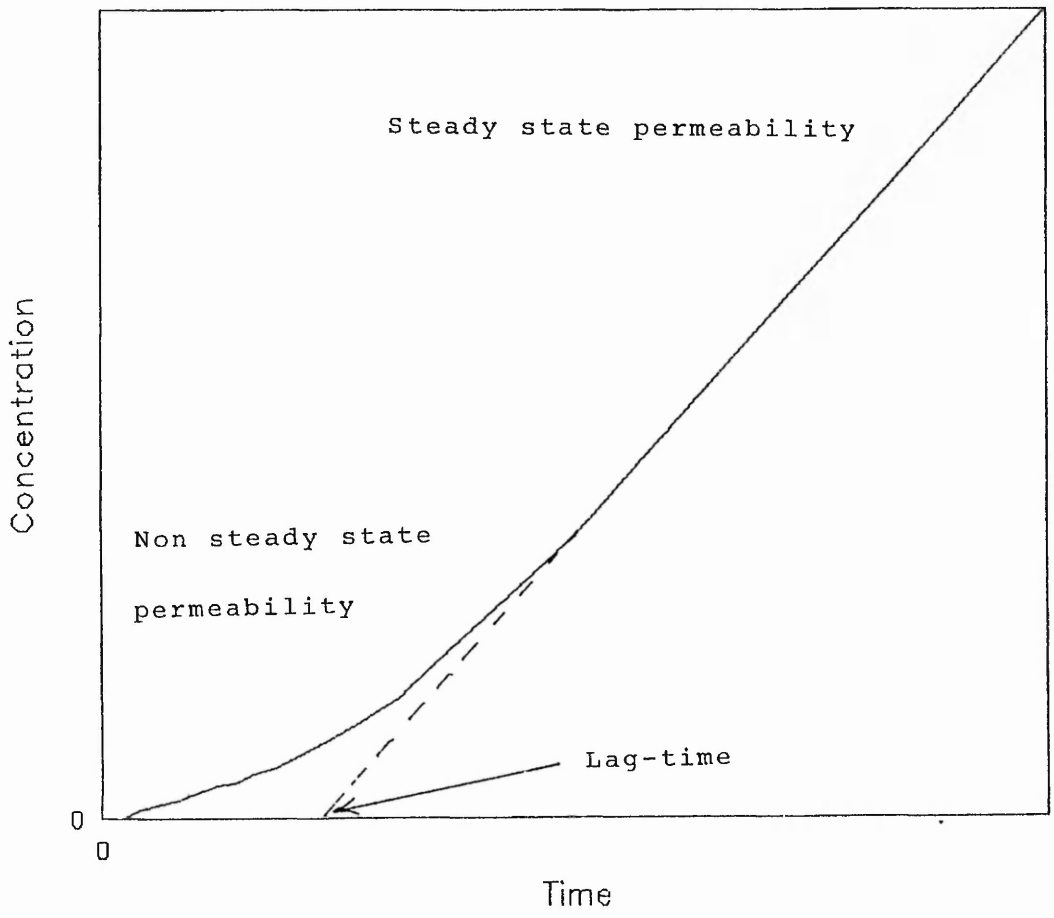

Figure I:6 'Barrer plot' cumulative concentration vs time

When permeation of gases is studied it is usually the pressure of the gas that is measured rather than its concentration. The pressure and concentration of a gas are easily related by Henry's law, which states that

$$C = SP \quad , \tag{I.40}$$

where C is the concentration, S is the solubility coefficient and P is the pressure. Thus equation (I.37) can be similarly rewritten as,

$$\frac{dQ}{dt} = \frac{DS(Po-P1)}{L} , \tag{I.41}$$

where the terms Po and P1 refer to pressures instead of concentrations. Since Henry's law only applies at low concentrations the above relationship only holds when that criteria is met. As described previously, the composite term DS can be replaced by the permeability coefficient. For practical purposes it is useful to remove the area term from the definition of Q as described in equation (I.35) such that Q represents the cumulative mass of permeant. Equation (I.39) may now be rearranged to give;

$$P = \frac{dQ}{dt} \frac{L}{A(Co-C1)} \quad , \tag{I.42}$$

where A is the exposed area of the film.

I.3.2 MECHANISM OF TRANSPORT THROUGH POLYMER FILMS

Transport of gases, vapours and solutes through polymeric films may take place by one or more mechanisms, according to the nature of the polymer film and the relationship between the film and the permeant molecules. In porous films where no partitioning of the solute occurs the diffusion rate is directly related to the pore size, and inversely to the diffusant molecular volume. This is known as the sieve mechanism. For non-porous films diffusion is often described by the free volume model.

I.3.2.1 THE FREE VOLUME MODEL FOR DIFFUSION

Diffusion in amorphous polymers can be visualised as the movement of permeant molecules through a tangled mass of polymer chains and holes. For polymers above their glass transition temperature the holes may be considered to be constantly disappearing and reforming, as a result of thermal fluctuations. The diffusion process can then be described by permeant molecules jumping from hole to hole as they are formed. A more detailed discussion of the free volume theory is given by Kumins and Kwei[73]. The diffusion process involves the permeant molecule making successive jumps between equilibrium positions of distance d in a random direction with frequency ν. The diffusion coefficient, D, is related to the jump length and frequency by:

$$D = \frac{\nu d^2}{6} \qquad (I.43)$$

The model for free volume theories stems from comparisons with simple liquids, and suggests that holes are discrete independent entities. When considering polymers the concept of co-operation of free volume is important in our understanding of segmental mobility, and hence the diffusion process. The idea that molecular diffusion in polymers occurs mainly through the co-operation of several degrees of freedom was advanced by Barrer[75] and was later incorporated into his activated zone theory[76]. This theory assumes that an activation energy is required by the chain segments involved in the diffusion step as well as the diffusant molecule. The activated zone thus comprises these polymer chain segments and the diffusant molecule. Each zone with f degrees of freedom must acquire an activation energy, E, before a diffusion step can take place. Thus, the diffusion coefficient can be given as:

$$D = \frac{\nu}{2} d^2 \sum_{f=1}^{f'_{MAX}} \left[\frac{p_f (E/RT)}{(f'-1)!} \right]^{f-1} \exp(-E/RT) \qquad (I.54)$$

where ν is the thermal vibration frequency of the diffusant molecule, f' is the number of degrees of freedom involved in a particular movement, f'_{MAX} is the value of f'for which the expression 1/(f'-1)! is a maximum, E is the activation energy of one mole of the activated zones, and P_f is the probability that the f' degrees of freedom will co-operate in a diffusion step. Barrer[75] found that values of f' in the neighbourhood of 12 to 14 were required to satisfy the above equation when experimental

values for D and E were used, and thus concluded that the motion of many polymer segments was required for the gaseous diffusion process.

A model for Fickian diffusion was proposed by Frisch[77]. He considered the diffusant size and the distribution of local free volumes within the polymer. Two classes of Fickian diffusion were proposed.

1. Type A, typified by small diffusant molecules such as hydrogen, has the following characteristics:

(i) low solubility of the gas and negligible departure from Henry's law,

(ii) concentration-independent diffusion coefficients,

(iii) an apparent temperature and concentration independent energy of activation.

2. Type B Fickian diffusion, generally observed for larger organic vapours, has the following characteristics:

(i) non-dilute diffusant polymer mixture,
(ii) concentration-dependent diffusion coefficients,
(iii) temperature-dependent activation energies.

The distribution function of local free volumes in a polymer may be denoted by f(v,t,c), which is the fraction of all local free volumes of sizes less than v at temperature t and diffusant concentration c. At temperatures above the Tg the average free volume may be

defined as:

$$\overline{V} = \int_0^1 V \, dF \qquad (I.45)$$

Type A Fickian diffusion occurs if the minimum void volume required to disperse the diffusant molecule is smaller than the average free volume, and Type B occurs when it is larger.

I.3.2.2 THE PORE FLOW MODEL FOR DIFFUSION

When considering the permeation of solutes, as in this study, the pore flow model can be described by water filled pores or channels constituting an internal aqueous pathway for diffusion. In such systems the polymeric barrier gives a greater resistance to diffusion than does the solvent filled pores. This is because of the lower activation energy required for molecular motions in liquids, as opposed to chain segment motion in polymers. When a solute molecule approaches a pore, factors such as the molecular size and shape of the solute, the pore size, and the chance that the molecule will strike the edge of the pore, influence the probability of the solute entering the pore. For cylindrical pores it is assumed[78] that the penetration of a pore of radius Rp by a molecule of radius Rm only occurs if the molecule chances to fall within the area of a circle described by the radius (Rp - Rm). If the actual and possible areas for penetration are Ap and Ao, respectively, then these areas can be expressed as follows:

$$Ap = n\ (Rp-Rm)^2 \quad \text{and} \quad Ao = n\ Rm^2 \qquad (I.46)$$

Based on the above assumption it was shown[78] that the ratio Ap/Ao, which is a measure of the steric hindrance, will be given by :

$$Ap/Ao = (1 - Rm/Rp)^2 \qquad (I.47)$$

As the size of the molecule increases and approaches the pore size the ratio of Ap/Ao tends to zero as does the probability of the molecule entering the pore. Once a molecule has entered a pore a viscous drag with the walls of the pores can impede the mobility of the molecule. An expression for this viscous drag M was given by Ladenburg[79] :

$$\frac{M}{Mo} = \frac{1 + 2.4\ Rm}{Rp}, \qquad (I.48)$$

where Mo is the viscous drag when the molecule radius is negligible compared with the radius of the pore. By assuming that the permeability will be proportional to the real area available for permeation, and inversely proportional to the viscous drag, the total restriction to permeability was expressed by[79] :

$$\frac{Dr}{Daq} = \frac{(1 - Rm/Rp)^2}{(1+2.4Rm/Rp)} \qquad (I.49)$$

where Dr is the restricted diffusion coefficient and Daq is the free aqueous diffusion coefficient.

I.3.3 FACTORS AFFECTING THE PERMEABILITY OF POLYMER FILMS

If diffusion can be described in terms of an energy activated process then obviously temperature will be a significant parameter. Also, the nature and size of the penetrant molecule and its interaction with the polymer will have an influence on the permeation process. Finally, the structure and morphology of the film will influence its permeability, and the presence of cracks, pores and voids will facilitate the diffusion process. The presence of extraneous material such as fillers or impurites may disrupt the film structure. In general diffusion is described by transport through amorphous polymer. The presence of crystallinity in the polymer film will represent regions of impermeability and again this will effect the overall transport process.

I.3.3.1 THE INFLUENCE OF TEMPERATURE

From the standpoint of the free volume theory, energy is required for the formation of holes and for the dissolution of the penetrant in the polymer. Therefore, as the temperature increases the rate of permeation is expected to increase. Over moderate temperature ranges the diffusion, solubility and permeation coefficients can be expressed by an Arrhenius type relationship[80]:

$$D = D_o \exp(-E_d / RT) \qquad (I.50)$$

$$S = S_o \exp(-{}^*H_s / RT) \qquad (I.51)$$

$$P = P_o \exp(-E_p/RT) \qquad (I.52)$$

where E_d and E_p are the activation energies of diffusion and permeability, and $^*H_s$ is the heat of solution. The terms D_o, S_o and P_o are the diffusion, solubility and permeability coefficients at infinite temperature. For gaseous permeability, an inflection in the Arrhenius plot sometimes occurs at the Tg, with higher activation energies occurring above the Tg. Yasuda[81] showed inflections in the Arrhenius plots for the permeation of several permanent gases through an acrylonitrile-methyl acrylate copolymer, helium, however, showed no inflection. Stannett and Williams[82] found no such inflections for the permeation of similar gases through poly(ethyl methacrylate) films, but did, however, for water vapour. These differences were attributed to the effect of the molecular size of the permeant with respect to the 'hole' size in the polymer. Stannett suggested that the water molecules plasticised the polymer to some degree. Similar Arrhenius relationships have been reported for solute permeation of relatively hydrophobic polymer films[83,84]. However, a linear dependence of permeation with temperature was found for urea permeation through relativley hydrophilic acrylate-methacrylate copolymers[85]. This deviation from the usual Arrhenius relationship was attributed to an asymmetric structure within the film and zones of differing permeabilities and the dependence of P on temperature differing from zone to zone.

I.3.3.2 EFFECT OF THE PERMEANT MOLECULE

As the penetrant molecule gets larger the size of the 'hole' required for diffusion also increases. Therefore, for a given polymer the permeation rate tends to decrease with increasing permeant size. This has been demonstrated for the permeation of gases through several different polymers[80,86-88]. When considering solute permeation the effect of permeant size was demonstrated by Huang[89]. He used a homologous series of poly(ethylene glycols) permeating a cellophane film, and found that the permeability decreased with increasing molecular weight of the permeant. Gonzales et. al.[83] showed that permeant size or molecular weight are not the only considerations. He reported higher diffusion and permeability coefficients for benzaldehyde than benzyl alcohol and benzoic acid. This was attributed to the acid and the alcohol forming dimers and trimers through hydrogen bonding and thus increasing the effective size of the permeating species.

For solute permeation, the permeant species must leave the aqueous environment to enter the polymer and therefore, the affinity of the permeant for either phase is an important consideration. Serota et. al.[90] showed that the permeability coefficient for several substituted anilines obeyed the same rank order as the partition of the permeant between water and hexane. For the pore flow model the permeant size only becomes significant when the molecular size is comparable with the pore size. For hydrated permeant molecules the hydrodynamic size will be the controlling factor. In microporous films the effect of permeant size is not always noticeable.

I.3.3.3 EFFECT OF FILM STRUCTURE

The influence of film structure on permeation may be interpreted in many ways. Firstly, the effect of pores, voids and cracks will tend to increase the permeability. Secondly, the presence of regions of differing properties, such as crystallinity and greater polymer density will serve to decrease the permeability. Lastly, the presence of heterogeneities, either in terms of a second polymer phase or in terms of additives such as fillers and plasticisers can reduce, or enhance, the permeability.

The influence of film asymmetry was shown by Abdel-Aziz[91] and Leob[92]. Films dried from an organic solvent tend to have a more compact layer at the upper surface (exposed to the atmosphere during drying). The permeability is lower when this compact layer is exposed to the permeant. The film preparation technique was shown to influence the film permeability by Pickard et al[93] where the water vapour permeability of methylcellulose films were higher for sprayed films rather than those cast on glass. This was explained in part by the surface roughness of the sprayed films. The effect of casting solvent and substrate was reported by Katz[94] and Yaseen[95]. Katz[94] showed that the substrate affected the water vapour permeability of polar polymers, but this was insignificant for non polar polymers. Polar substrates such as glass and metals were found to give films of higher water vapour permeability and a film asymmetry was found[95]. Heterogeneous regions in films, such as those with added fillers, may affect the permeability in several ways. If the filler is less permeable than the polymer the

diffusion coefficient would be decreased[96], but if the filler is highly adsorbent, large lag-times are often encountered[97] because the filler absorbs the permeant preferentially until it is saturated. When the heterogeneity in the film is caused by two polymer phases being present the overall permeability is governed by the relative permeability and volume fraction of each polymer. Theoretical treatments to describe such situations are derived from analogy with dielectric permittivity, where the film is considered as the dielectric between the plates of a large plane capacitor. Various expressions have been presented to account for the overall permeability of a heterogeneous film; some of the more notable ones are briefly described below. In the following expressions the permeability of the composite film is denoted by P_M, the volume fractions by V, and P_1 and P_0 refer to the dispersed and continuous phase permeability, respectively.

De Vris[98] reviewed the literature and found that when the continuous phase was more permeable than the dispersed phase, an expression given by Maxwell adequately described the available experimental data. Maxwell's treatment assumed that the dispersed particles were dilute enough so that interactions between them could be ignored. The resulting expression,

$$P_M = P_0\{1+3V_1/[(P_1+2P_0)/(P_1-P_0)-V_1]\}, \qquad (I.53)$$

is therefore expected to apply only for small volume fractions of dispersed material. Higuchi[99] derived an expression for a random dispersion of spheres in a

continuum, where particle-particle interactions were accounted for, i.e.,

$$P_M = \frac{2P_o^2(1-V_1)+P_oP_1(1+2V_1)-KP_o[(P_1-P_o)/(2P_o+P_1)]^2(2P_o+P_1)}{P_o(2+V_1)+P_1(1-V_1)-K[(P_1-P_o)/(2P_o+P_1)]^2(2P_o+P_1)(1-V_1)} \quad (I.54)$$

The symbol K is a constant and to a first approximation is a fraction of V_1. Higuchi claimed that the expression was in agreement with available permittivity data[99]. The expression was later used by Higuchi[100] to explain the barrier properties of ointments. Peterson[101] used the equation to predict the permeability of a polymer film containing a random dispersion of a second polymer and found good agreement between experiment and theory. In more recent times the Higuchi expression was found to give the best agreement for permeation of helium through polymer latex films[102]

I.3.4 PERMEATION THROUGH POLYMER LATEX FILMS

The main area of study in latex film permeation is connected with changes in film morphology with time. Many authors (see below) have shown that latex film properties, such as permeability and mechanical strength, change with time. Isaacs[103] showed that the permeability of several latex films to electrolyte solutions decreased when the films were aged for one week. Vanderhoff[104] found similar results for water and water vapour permeation of styrene-butadiene and acrylate-methacrylate copolymer

latex films. The reduction in permeability was attributed to the further gradual coalescence of the original latex particles to form a more homogeneous film. In a more recent study Padget and Moreland[105] have commented on the improved corrosion protection of polymer latex films that showed a high degree of particle coalescence. Work by Chainey et al[68,102,106] has shown the reduction in permeability of helium through several acrylate, methacrylate and styrene-ethyl acrylate copolymer latex films upon aging. The rate of reduction in permeability was related to the polymer type, with the softer polymers aging quicker. However, the final permeability was shown to be slightly higher than results obtained for the same polymers cast from solution. In all the above cases the reduction in permeability is described in terms of the degree of coalescence of the original latex particles, and that further gradual coalescence or autohesion is responsible for the increased coalescence and the reduction in permeability.

I.4. AIMS AND SCOPE OF THE PROJECT

BACKGROUND TO THIS STUDY

Surfactant-free emulsion polymerisation is known to produce monodisperse latices of controllable particle size[12] and easily characterisable surfaces[13]. Latices prepared by this method contain impurites and reaction by-products resulting from the initiator decomposition and side reactions. These impurities, which are in the main water soluble, can easily be removed by microfiltration, leaving a model polymer colloid system containing only polymer particles and water. These surfactant-free latices can then be used to prepare polymer films where the properties of the film are dependent only on the physical properties of the polymer and the film internal morphology. The need to use the surfactant-free technique rather than the conventional surfactant containing polymerisations arises from a need to totally remove surfactant from the latices in order to form these model films. The presence of surfactant in polymer films is highly undesirable since the fate of the surfactant after particle coalescence is uncertain. In certain cases[60] exudations of surfactant from latex films have been found, whilst in others no exudations were found, indicating that the surfactant remained within the film interior, either as an interpenetrating network or dissolved in the polymer. Either of these two situations would be detrimental to a study of the properties and morphology of model latex films. Grafting of surfactant to latex

particles during the polymerisation reaction is known[108], and this surfactant would remain with the particles, and ultimately be present in the films whether the surfactant is, or is not, compatible with the polymer.

Films prepared from surfactant-free latices have been studied using helium permeability, where the film internal morphology resulting from the incomplete particle coalesence was investigated[68,102,106]. The film permeability was found to be dependent on the polymer type, film age, and preparation temperature. The difference in permeability was attributed to the amount of further gradual coalescence between the original latex particles, even though the films were apparently homogeneous. It was postulated[68] that permeability through such films was probably by a combination of permeation through an interpenetrating network of interparticle boundaries, and through the bulk polymer.

In the present study, surfactant-free polymer latices were used to study the permeation of water vapour and aqueous organic solutes through polymer latex films. Permeation through latex films has not been widely reported in the literature, but has several potential applications, such as drug coatings for controlled release systems, and may find many uses in the future because of the present trend away from solvent based systems.

Three different types of latices were prepared for this study. Firstly poly(butyl methacrylate), PBMA. This polymer has a glass transition temperature at room temperature, and thus films made from it would be easy to handle. Secondly, poly(2-hydroxyethyl methacrylate),

PHEMA, which was chosen because of its biocompatibility and general use in biomedical applications[107]. A study of the kinetics of emulsion polymerisations of PBMA and PHEMA was also of interest, given the large difference in water solubility of these two monomers. The last type of latices used were core-shell and copolymers of PBMA and poly (methyl acrylate), PMA and these were used to study the influence of more hydrophilic polymers in the interparticle regions in the latex films.

OBJECTIVES

1. To study the kinetics and preparation of PHEMA and PBMA latices.

2. To prepare surfactant-free polymer latex films.

3. To compare the permeability of solvent-cast films with films cast from latices of the same polymer.

4. To study the effect of variations in film formation times and casting temperature, on the permeability of latex films.

5. To study the effect of film age on permeability.

6. To investigate the nature of permeation through latex films by studies of film morphology, and the use of different permeants and conditions.

7. To investigate the effect on permeability of the inclusion of common additives found in latex, such as surfactants.

8. To study heterogeneous latex films to test the effect of hydrophilic polymers at the interparticle boundaries in latex films.

9. To investigate the potential use of surfactant-free latices for use as controlled-release drug coatings.

I.5 REFERENCES

1. F.Hofmann, K.Delbruk; German patent, 250 690, (1909).

2. Idem. German patent, 254 672, (1912).

3. Idem. German patent, 255 129, (1912).

4. R.P.Dinsmore; U.S. patent, 1 732 795, (1927).

5. M.Luther, C.Henck; German patent, 558 890, (1927).

6. W.D.Harkins; J. Am. Chem. Soc. 69, 1428 (1947).

7. W.V.Smith, R.H.Ewart; J. Chem. Phys., 16, 597 (1948).

8. J.W.Vanderhoff in " Vinyl Polymerisation," Vol I, pt II, G.E. Ham (Ed) Marcel Dekker (1969).

9. J.W.Vanderhoff in "Characterisation of Metal and Polymer Surfaces", Leing-Huang Lee(Ed), Academic Press (1977).

10. W.P.Hohenstein, H.Mark; J.Polym.Sci., 1, 127 (1946).

11. T.Matsumoto, A.Ochi; Kobunshi Kagaku, 22, 481 (1965).

12. J.W.Goodwin, J.Hearn, C.C.Ho, R.H.Ottewill; Brit. Polym. J., 5, 347 (1973).

13. Idem, Colloid Polym. Sci., 252, 464 (1974).

14. J.Hearn, Ph.D Thesis, University of Bristol, 1971.

15. A.R.Goodall, Ph.D Thesis, Trent Polytechnic, 1976.

16. R.M.Fitch, C.H.Tsai; "Polymer Colloids"
R.M.Fitch (Ed), Plenum, New York (1971).

17. R.M.Fitch, L.B.Shih; Prog. Colloid Polym. Sci.,
56, 1 (1975).

18. R.M.Fitch, R.C.Watson; J. Colloid & Interface Sci.,
68, 14 (1979).

19. R.M.Fitch; Br. Polym. J., 56, 467 (1973).

20. J.L.Gardon; J. Polym. Sci., Part A1 6,
623,643,665,687 2853,2859 (1968).

21. A.E.Alexander, D.H Napper; in "Progess in Polymer
Science," A.D. Jenkins (Ed) Pergamon press (1971).

23. J.Ugelstad, F.K.Hansen; Rubber Chem. Technol.,
49, 536 (1976).

24. D.C Blakely; in "Emulsion Polymerisation"
Applied Science Publishers, London (1975).

25. J.Ugelstad, F.K.Hansen; in "Emulsion Polymerisation"
I.Piirma (Ed), Academic Press, New York (1982).

26. W.J.Priest; J. Phys. Chem., 56, 1077 (1952).

27. J.L.Gardon; J. Polym. Sci. A1. 6, 623 (1968).

28. C.P.Roe; Ind. Eng. Chem., 60, 20 (1968).

29. F.K.Hansen, J.Ugelstad; J. Polym. Sci., Polym. Chem. Ed., 17, 3047 (1979).

30. N.Sutterlin in "Polymer Colloids II" R.M.Fitch (Ed) Plenum Press, New York (1980).

31. B.M.E.van der Hoff; J. Polym. Sci., 44, 241 (1977).

32. A.R. Goodall, M.C. Wilkinson, J. Hearn; J. Polym. Sci. Polym. Chem. Ed., 15, 2193 (1977).

33. D.Monro, A.R.Goodall, M.C.Wilkinson, J. Hearn K. Randle; J. Colloid & Interface Sci., 68, 1 (1979).

34. Chi-Yu Chen, I.Piirma; J. Polym. Sci., 18, 1979 (1980).

35. G.Lichti, R.G.Gilbert, D.H.Napper; J. Polym. Sci., Polym. Chem. Ed., 21, 269 (1983).

36. S.Carra, M.Morbidelli, G.Storti; Proc. Int. Sch. Phys., 90, 483 (1985).

37. W.H.Stockmayer; J. Polym. Sci., 24, 314 (1957).

38. J.T.O'Toole; J. Appl. Polym. Sci., 9, 1291 (1965).

39. D.J.Williams; J. Polym. Sci., Polym. Chem. Ed., 12, 2123 (1974).

40. J.W.Vanderhoff in "Symposium on Water Borne Polymers and High Solids Coatings", New Orleans, (1979).

41. V.I.Yeliseyeva in "Emulsion Polymerisation" Chapt. 7, I.Piirma (Ed), Academic Press (1982).

42. J. Hearn, M.C.Wilkinson, A.R.Goodall, M.Chainey; J. Polym. Sci., Polym. Chem. Ed., 23, 1869 (1985).

43. R.A.Wessling, I.R.Harrison; J. Polym. Sci., A-1 9, 3471 (1971).

44. J.L. Gardon; Brit. Polym. J., 1, 1 (1979).

45. E.B.Bradford; J. Appl. Phys 23, 609 (1952)

46. R.Myers, R.K.Shultz; J. Appl. Polym. Sci., 8, 755 (1964).

47. J.W. Vanderhoff; J.Polym. Sci., Symp.(41) 155 (1973).

48. G.P. Bierwagen; J. Coatings Technol., 51(658), 117, (1979).

49. R.E. Dillon, L.A.Matheson, E.B.Bradford; J. Colloid. Sci., 6, 108 (1957).

50. G.L Brown; J. Polym. Sci., 22, 423 (1956).

51. J.Frenkel; J. Phys. USSR, 9, 385 (1945).

52. J.W. Vanderhoff, E.B.Bradford, H.Tarkowski
M.C. Jenkins; J. Macromol. Chem., 1(2), 361 (1966).

53 J.G. Brodnyan, T. Konen; J. Appl. Polym. Sci.,
8, 687 (1964).

54. R.R Myers, R.K.Shultz; J. Appl. Polym. Sci.,
8, 755 (1964).

55. S.Paul; in "Surface Coatings Technology,"
Wiley-Interscience, New York, 1978.

56. J.Lamprecht; Colloid Polym. Sci., 258, 960 (1980).

57. S.S. Voyutskii; J. Polym. Sci., 32, 528 (1958).

58. S.S. Voyutskii; in "Autohesion & Adhesion of High
Polymers", Polymer Reviews. Vol4,
Wiley-Interscience (1963).

59. S.S. Voyutskii, N.L. Vakula, Rubber Chem. Technol.,
37, 1153 (1963)

60. E.B Bradford, J.W. Vanderhoff; J. Macromol. Chem.,
1, 335 (1966).

61. E.B.Bradford, J.W. Vanderhoff; J. Macromol. Sci.

Phys., B6, 671 (1972).

62. J.W. Vanderhoff; Br. Polym. J., 2, 161 (1970).

63. D.Distler, G.Kanig; Colloid Polym. Sci., 256, 1052 (1978).

64. G.Kanig, H.Neff; ibid, 253, 29 (1975).

65. D. Distler, G.Kanig; Org. Coatings Plastics Chem., 43, 606 (1980).

66. F.W. Billmeyer; "Textbook of Polymer Science," Second Edition, Wiley-Interscience (1971).

67. H.Kast; Makromol. Chem. Suppl. 10/11, 447 (1985).

68. M.Chainey; Ph.D Thesis, Trent Polytechnic, 1984.

69. T.Graham; Phil. Mag., 32, 401 (1866).

70. H.A.Daynes; Proc. Roy. Soc. Ser.A, 97,286 (1920).

71. R.M.Barrer; Trans. Faraday Soc., 35, 625 (1939).

72. J.Crank; "The Mathematics of Diffusion" Second Edition, Oxford University Press, 1975.

73. C.A.Kumins, T.K.Kwei; in "Diffusion in Polymers," Chapt 4, J.Crank, G.S.Park (Ed), Academic Press, 1968

75. R.M.Barrer; in "Diffusion in and Through Solids," Cambridge University Press, 1941.

76. Idem. Trans. Faraday Soc., 38, 322 (1943).

77. H.L.Frisch; J. Polym. Sci. B., 3, 13 (1965).

78. J.R.Poppenheimer; Physiol. Rev., 33, 387 (1953).

79. R.Ladenburg; Ann. Der. Physik., 22, 287 (1907).

80. V.Stannett in "Diffusion in Polymers." Chapt 2 , J.Crank G.S.Park (Ed), Academic Press, 1968.

81. H.Yasuda, T.Hirotsu; J. Appl. Polym. Sci., 21, 105 (1977).

82. V.Stannett, J.L.Williams; J. Polym. Sci. Pt C, 10, 45 (1965).

83. M.A.Gonzales, J.Nemotollahi; J. Pharm. Sci., 56, 1288 (1967).

84. E.R.Garrett, P.B.Chemburker; J. Pharm. Sci., 57,949 (1968).

85. S.A.M. Abdel-Aziz, Ph.D Thesis, University of Strathclyde, 1976.

86. A.S.Michaels, H.J.Bixler; J. Polym. Sci., 50, 413 (1961).

87. F.H.Muller; Kolloid Zt., 100, 335 (1944).

88. F.J.Norton; J. Appl. Polym. Sci., 7, 1649 (1963).

89. R.Y.M.Huang, N.R.Jarvis; J. Polym. Sci., Symp.(41) (1972).

90. D.G.Serota, M.C.Meyer, J.Autian; J. Pharm. Sci., 61(3), 417 (1972).

91. S.A.M. Abdel-Aziz, W.Anderson, P.A.M.Armstrong; J. Appl. Polym. Sci., 19, 1181 (1975).

92. S.Leob, S.Sourirajan, Adv. Chem.Ser., 38, 117 (1962).

93. Pickard, J.E.Rees, P.H.Elworthy; J. Pharm. Pharmac., 24, suppl., 139 (1972).

94. R.Katz, B.F.Munk; J. Oil Col. Chem. Assoc., 52, 418 (1969).

95. M.Yaseen; Prog. Org. Coat., 10, 125 (1982).

96. G.L.Flynn, T.J.Roseman; J. Pharm. Sci., 60, 1788 (1971).

97. G.L.Flynn, S.H.Yalkowsky, T.J.Roseman; J. Pharm. Sci., 63, 479 (1974).

98. D.A.De Vris; in "The Thermal Conductivity of Granular Materials", Bull Inst. Intern. Du Froid, Paris 1952.

99. W.I.Higuchi; J. Phys. Chem., 62, 649 (1958).

100. W.I.Higuchi, T.Higuchi; J. Am. Pharm. Assoc. Scientific Edition., 49, 598 (1960).

101. C.M.Paterson, J. Appl. Polym. Sci., 12, 2649 (1968).

102. M.Chainey, M.C.Wilkinson, J.Hearn; Makromol. Chem., suppl. 10/11, 435 (1985).

103. F.K.Isaacs; J. Macromol. Chem., 1(1), 163 (1966).

104. J.W.Vanderhoff, E.B.Bradford, W.K.Carrington; J. Polym. Sci., Polymer Symp.(41), 155 (1973).

105. J.C.Padget, P.J.Moreland; J.Coatings Technol., 55, 39 (1983).

106. M.Chainey, M.C.Wilkinson, J.Hearn; J.Polym. Sci., Polym. Chem. Ed., 23, 2947 (1985).

107. D.G.Pedly, P.J.Skelly B.J.Tighe; Brit. Polym. J., 12, 99 (1980).

108. R.M.Fitch, W.T.McCarvill; J. Colloid & Interface Sci., 66, 20 (1978).

Chapter II

Experimental

II.1 MATERIALS

II.1.1 MONOMERS

The monomers used in this study were obtained from BDH Chemicals Limited, Broom Road, Poole, and were laboratory reagent grade. They were stabilised with small amounts of hydroquinone. The monomers were purified by distillation under reduced pressure in an inert nitrogen atmosphere, with the first and last 10% of each distillate being discarded. The distilled monomer was then flushed with nitrogen and stored in Pyrex containers at 253K.

II.1.2 WATER

All the water used was double distilled from an all-Pyrex glass still, and stored in sealed Pyrex containers. The conductivity of each batch was tested routinely and found to be less than 1.5 $\mu S\ cm^{-1}$.

II.1.3 OTHER CHEMICALS USED IN POLYMERISATIONS.

Fisons analytical grade potassium persulphate (Fisons Scientific Apparatus Ltd., Bishop Meadow Road, Loughborough, Leicester), recrystallised from double distilled water was used to initiate all polymerisations. The recrystallised material was dried under vacuum and stored in a desiccator in a dark cupboard. Sodium chloride was supplied as the Analar grade by Fisons and used as received. Sodium dodecyl sulphate was supplied by Fluka (Fluorochem Ltd., Dinting Vale Trading Estate, Peakdale

Road, Glossop, Derbyshire) as the Puriss grade and used as received. Nitrogen gas was the oxygen free white spot grade as supplied by BOC (BOC Limited, Millbank Road, Southampton) and was also used as received.

II.1.4 AQUEOUS SOLUTES

All chemicals were Analar grade and obtained from Fisons. 4-Nitrophenol was recrystallised from toluene, and the liquid aniline derivatives were used without further purification.

II.1.5 FILM ADDITIVES

Sodium dodecyl sulphate was used as previously described (II.1.3), Dodecyl ethyldimethyl ammonium bromide was supplied by Fluka and was Puriss grade. Dodecyl tetraoxyethylene glycol monoether was supplied by A.B.M. Chemicals Ltd. Woodley, Stockport, Cheshire.

II.2 METHODS

II.2.1 EMULSION POLYMERISATIONS

a. HOMOPOLYMER POLYMERISATIONS

Polymerisations were carried out in 1 litre, three necked round bottom flasks equipped with a reflux condenser, PTFE paddle stirrer and nitrogen bleed. See Figure II:1. The flask, bleed and stirrer were assembled and washed with double distilled water until the washings

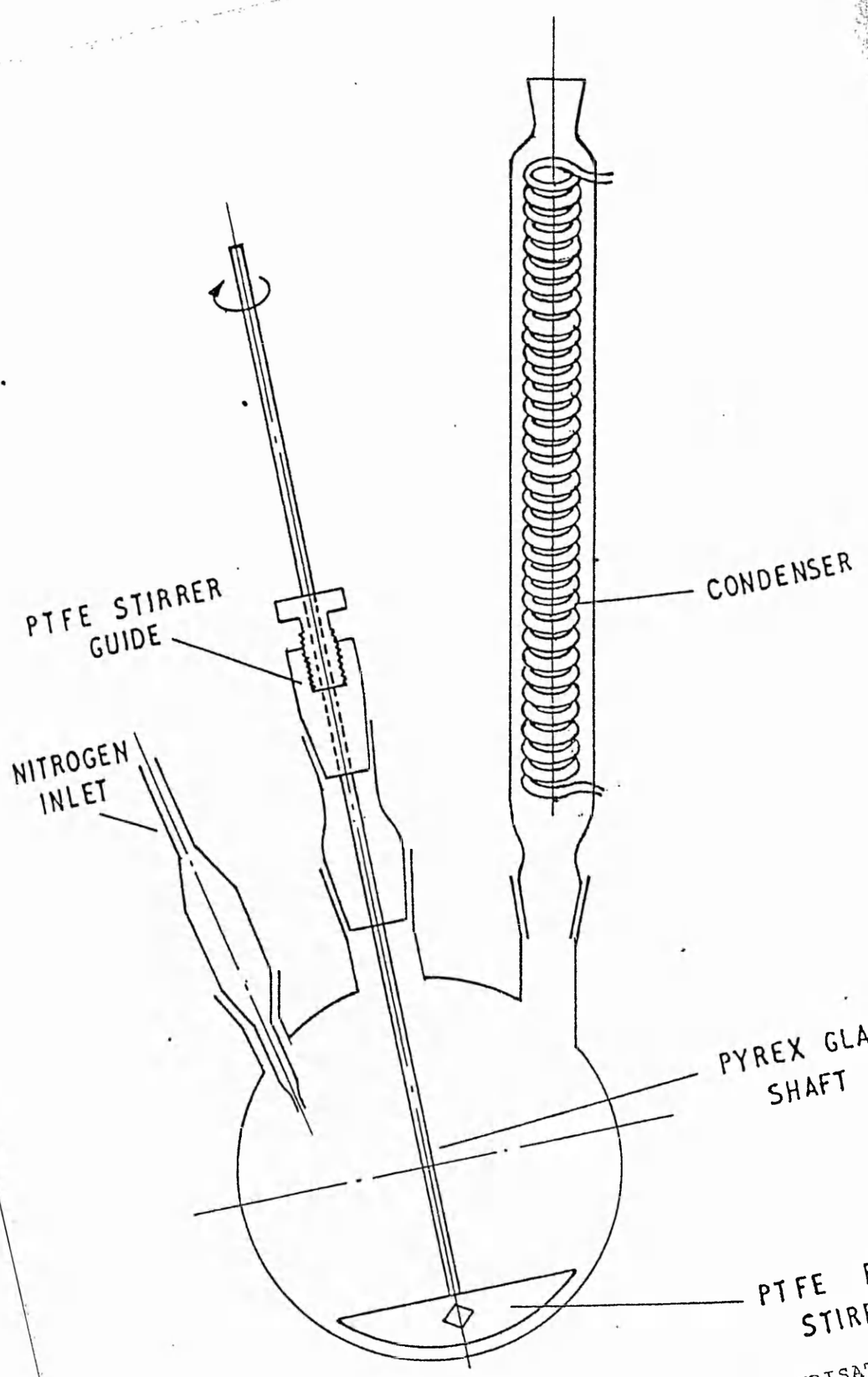

FIGURE II:1 APPARATUS FOR EMULSION POLYMERISATION REACTIONS

were of the same conductivity as that of the clean water. The flask was then charged with most of the water to be used in the reaction and mounted in a water bath at the reaction temperature. The water was flushed with nitrogen for at least thirty minutes while the water reached the reaction temperature; the stirrer was in operation during this time, and was set at 250 rpm unless otherwise stated. The monomer charge was added and allowed ten minutes to reach the reaction temperature. The reaction was initiated by the addition of potassium persulphate dissolved in 50 cm^3 of water, and the nitrogen bleed was substituted for a shorter one to prevent blockage during the reaction. At this stage the nitrogen flow rate was reduced so as to just maintain an inert atmosphere but not to aid evaporation of the monomer. The reaction was allowed to proceed for six hours at 75° C, which was more than adequate for the systems under study to reach full conversion. Samples of each polymerisation were taken and the fractional conversion was determined by a gravimetric method, see II.2.2a. The particle size was determined by photon correlation spectroscopy. For the multisampled reactions the stirrer was stopped for 30 seconds before sampling and a pipette was used to extract a sample (ca. 3 cm^3) from beneath the separated monomer layer. A typical recipe was:

monomer	50 g
double distilled water	450 g
potassium persulphate	0.5 g
temperature	75° C
stirrer	250 rpm

b. CORE-SHELL POLYMERISATIONS

The core shell polymers were prepared by the 'shot growth' method[1]. For the poly(butyl methacrylate-co-methyl acrylate) latices produced in this study, the method was as follows. The butyl methacrylate monomer was polymerised as usual, and after 180 minutes the reaction was sampled for solids content and particle size. At this point the butyl methacrylate was at about 80 % conversion. The second monomer was then added and the reaction allowed to continue for another four hours.

c. COPOLYMERS

Copolymers of butyl methacrylate and methyl acrylate were prepared and supplied by Dr. M.Chainey. The method of preparation was similar to that described above for homopolymer latices with the following exception. The polymerisation was allowed to proceed under monomer starved conditions, i.e., the monomer mixture was added, via a metering pump, to the reaction vessel at a rate slower than the polymerisation rate of the slowest polymerising monomer. This precaution was necessary to produce a copolymer latex particle of uniform composition. The author would like to express his gratitude to Dr. M. Chainey* for this part of the work.

* Dr M.Chainey c/o International Paint Ltd.,
Stoney Gate Lane, Felling, Gateshead, Tyne & Wear

II.2.2 LATEX CHARACTERISATION

a. SOLIDS CONTENT

The solids content was used as a measure of the percentage conversion and was determined as follows. An aluminium planchet was cleaned with butanone and rinsed with acetone, dried and weighed. A sample of the latex (ca. 3-4 cm^3) was added and the planchet reweighed. The sample was then dried under partial vacuum (400 mm Hg) at 323K, until apparently dry, and then stored under vacuum until constant weight was attained.

b. PARTICLE SIZE

Owing to the soft nature of poly(butyl methacrylate), particle sizes could not easily be determined by electron microscopy, since particle coalescence and damage by the electron beam distorted the particles. Routinely, particle sizes were determined by photo correlation spectroscopy using the Malvern Autosizer, Malvern Instruments Ltd Spring Lane South, Malvern, Worcestershire.

c. FREEZE DRYING

Latices were freeze dried for the determination of molecular weights and for the preparation of solvent cast films. A round bottomed flask was cooled in a slush bath containing solid carbon dioxide and methylated spirits. The latex was slowly added to the cooled flask and rotated

so as to form a frozen film around the walls of the flask. The flask was then pumped under vacuum until the polymer was fully dry.

d. POLYMER MOLECULAR WEIGHTS

Polymer molecular weights were determined as part of a SERC funded service by the 'Rubber and Plastics Research Association', RAPRA Technology Ltd., Shawbury, Shrewsbury, Shropshire. The molecular weights of the freeze dried latices were determined by gel permeation chromatography using tetrahydrofuran as the solvent. For the routine measurements four columns of 30 cm length and packing size 10 μm were used with nominal pore sizes 10^6, 10^5, 10^4, 10^3 Å respectively. For the low molecular weight analysis two columns were used of 30 cm length, packing size 5 μm and nominal pore sizes of 100 and 500 Å, respectively. The molecular weights were quoted as poly(styrene) equivalents as poly(styrene) molecular weight standards were used for the calibration.

e. CONDUCTOMETRIC TITRATIONS

Surface charge densities were determined by conductometric titrations. The latex sample was cleaned by microfiltration (see II.2.3) and acid washed with 0.05 mol dm^{-3} hydrochloric acid, using the microfiltration cell to replace the latex serum. Finally the latex was cleaned again with double distilled water. A known weight of latex, of previously determined solids content, was placed in a Pyrex glass beaker and covered with a Perspex lid.

The lid was equipped with a hole to permit the addition of the titrant and the conductivity electrode. The latex was stirred with a PTFE coated stirrer bar and a stream of nitrogen was passed through the latex to remove any carbon dioxide. Prior to titration, the nitrogen bleed was removed and a nitrogen atmosphere was maintained above the latex during the titration. Freshly prepared sodium hydroxide was standardised and delivered to the latex via an autoburette and fine bore syringe needle. Small aliquots of sodium hydroxide were added, and the conductivity of the latex was measured using a dip type conductivity cell and a Wayne Kerr Universal Autobalance bridge (model B642. Wayne Kerr Co. Ltd Durban Road, Bognor Regis, Sussex), and measurments were made within thirty seconds of each addition.

II.2.3 CLEANING OF POLYMER LATICES

All latices were cleaned by microfiltration[2,3] prior to use. This method was chosen as the quickest and most efficient cleaning process for the removal of both inorganic material resulting from the initiation reaction, and residual monomer. The microfiltration cell shown in Figure II:2 was made from PTFE. Prior to use the cell was dismantled and cleaned with butanone, then rinsed with acetone followed by distilled water. The cell was then reassembled and rinsed with double distilled water. Membrane filters of pore size approximately 60 % of the latex particle size were used and were obtained from Millipore UK Ltd. Millpore House, Abbey Road, London NW10 7SP. The filters were placed in the cell and distilled

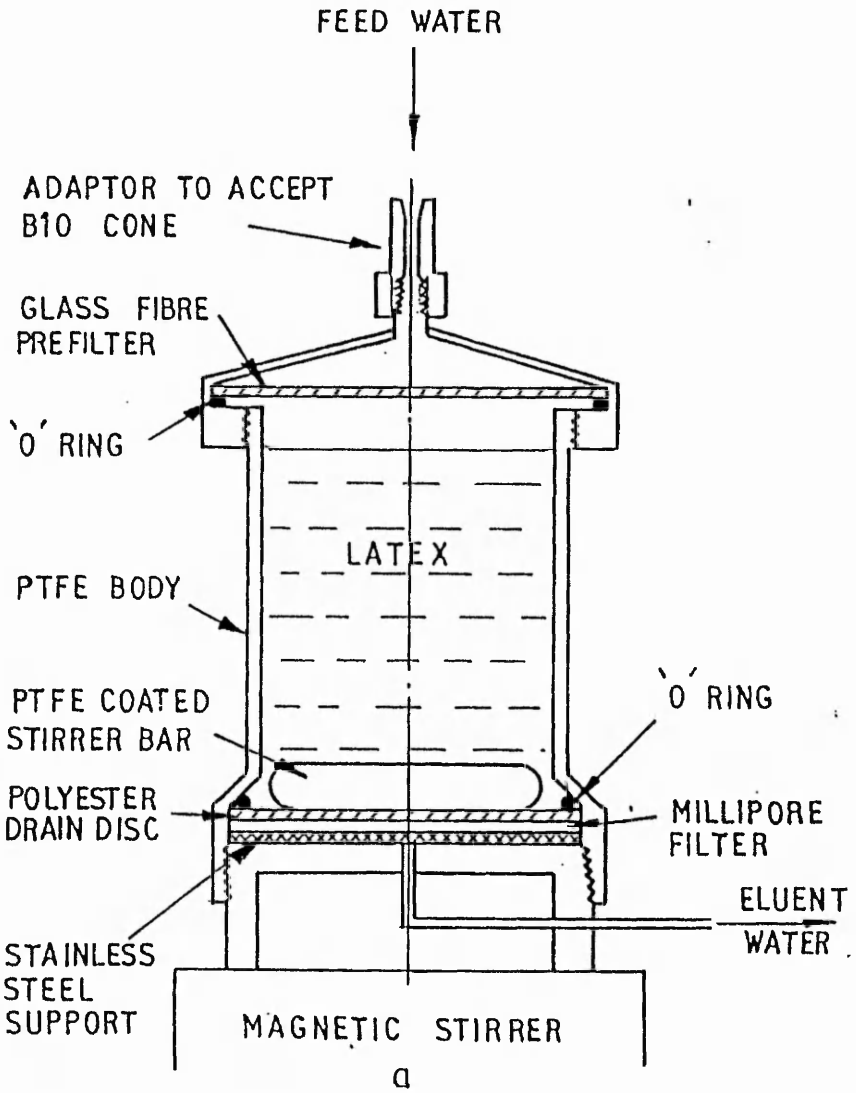

FIGURE II:2 MICROFILTRATION CELL

water was run through the system until the conductivity was the same as that of the clean water. The latex was then introduced and double distilled water was constantly fed through the system. A PTFE coated stirrer bar was used at the minimum stirrer speed, typically less than 100 rpm, to (i) reduce filter blockage, and (ii) prevent coagulation caused by high shear rates. The system was typically left running for 24 hours, after which time the conductivity of the effluent was checked. A conductivity of approximately 1.5 $\mu S\ cm^{-1}$ indicated the latex was clean. A clean latex was usually obtained when approximately 10 to 15 times the latex volume of water had eluted. Sometimes the elution rate slowed after a few hours; replacement of the filter with a new clean one restored the elution rate; it was assumed that residual monomer attacked the filter in these instances, as the problem did not recur after the filter was replaced.

II.2.4 FILM PREPARATION

The choice of substrates for casting surfactant-free latices was limited, since the requirements of the substrate and final film were stringent. The substrate must be clean and not contaminate the film, have a smooth surface, and release the film when formed. In general, the low surface energy substrates such as PTFE cannot be used since the latex tends to disjoin prior to film formation, especially with surfactant-free latices. The higher energy substrates do not suffer from this problem but metals, such as mercury, contaminate the film surface, and glass tends to have too good adhesion with the films. It was

found that poly(butyl methacrylate) latex films could be released from glass by a short period of soaking in warm water. It is presumed that the hydrated glass surface allows water to penetrate the interface between the polymer film and the glass on contact with the water, and thus assists release of the film.

For films with added water-soluble material, such as surfactants, the soaking process was unacceptable since the water soluble material may be leached from the film, and hence affect its properties. In these instances it was found that a compression moulded Nylon substrate was suitable since it allowed the films to be peeled off the substrate without the water soaking stage. Since the initial work was performed on films cast on glass plates, this method was used throughout the work for consistency, unless otherwise stated

a. LATEX FILMS CAST ON GLASS PLATES.

Pyrex glass plates were cleaned using chromic acid, usually by soaking for 24 hours. The plates were rinsed with distilled water before use. If after this period water retracted up the the glass the plate was cleaned again in fresh acid. The plates were placed on a levelled platform in an oven at the prescribed drying temperature. Brass or PTFE frames were placed on the glass and the required volume of latex was poured inside the frame. The frame merely acted to confine the latex to a fixed area during the film formation process. The films were left in the oven for a set time depending on the temperature, and removed from the glass plate soon after

this time. The relative humidity inside the oven was essentially zero as a large vat of silica gel was kept in the oven at all times.

b. LATEX FILMS CAST ON NYLON PLATES

The nylon plates were initially cleaned with butanone and then rinsed with acetone followed by distilled water, and then allowed to dry. They were then used in the same manner as described for glass plates, except that the film was removed while still warm and above the glass transition temperature of the polymer.

c. SOLVENT CAST FILMS

Solvent cast films were prepared on PTFE substrates since this gave the best film release performance. The PTFE was cleaned in the same way as the nylon plate. Solvent cast films were not dried in an oven since the solvent was sufficiently volatile to dry at ambient temperatures. The solvent mostly used was butanone, although some films were prepared using toluene. The required weight of freeze dried latex was dissolved in the solvent to give a solution of apparently similar viscosity to the solvent, then filtered through ashless filter paper. The filtered solution was poured onto the level PTFE plate and covered, although not sealed so that evaporating solvent could escape, but dust dropping into the film would be eliminated. The film was allowed to dry overnight and was peeled off the substrate after slight warming to raise the film above its glass transition temperature.

d. EVALUATION OF FILM THICKNESS

Film thickness was measured using a dial gauge with a plane foot. Between 10 and 20 measurements were taken across the film surface, depending on the size of the sample, and the average reading taken. Typically, the film thicknesses were in the range 20 to 80 μm, with the standard deviation in the thickness measurment being on average about 5% of the mean value.

II.2.5 MEASUREMENT OF PERMEABILITY

a. HELIUM PERMEABILITY

The helium permeability was determined using the British Standard BS 2782[4]. Figure II:3 shows a diagram of the apparatus. Essentially, the method is a volume change method at constant pressure. The cell consists of a large volume upper cavity and a small volume lower cavity. Connected to the lower chamber was a mercury manometer which was used to follow the volume of gas permeated. The film under test separated the two chambers. The top chamber was flushed with the permeant gas of interest, and was open to the atmosphere, and thus the pressure of the permeating gas was that of the atmosphere. The lower half of the cell was evacuated, and at a known time the mercury was introduced into the manometer. The mercury level was followed as a function of time, and from this the permeability was calculated.

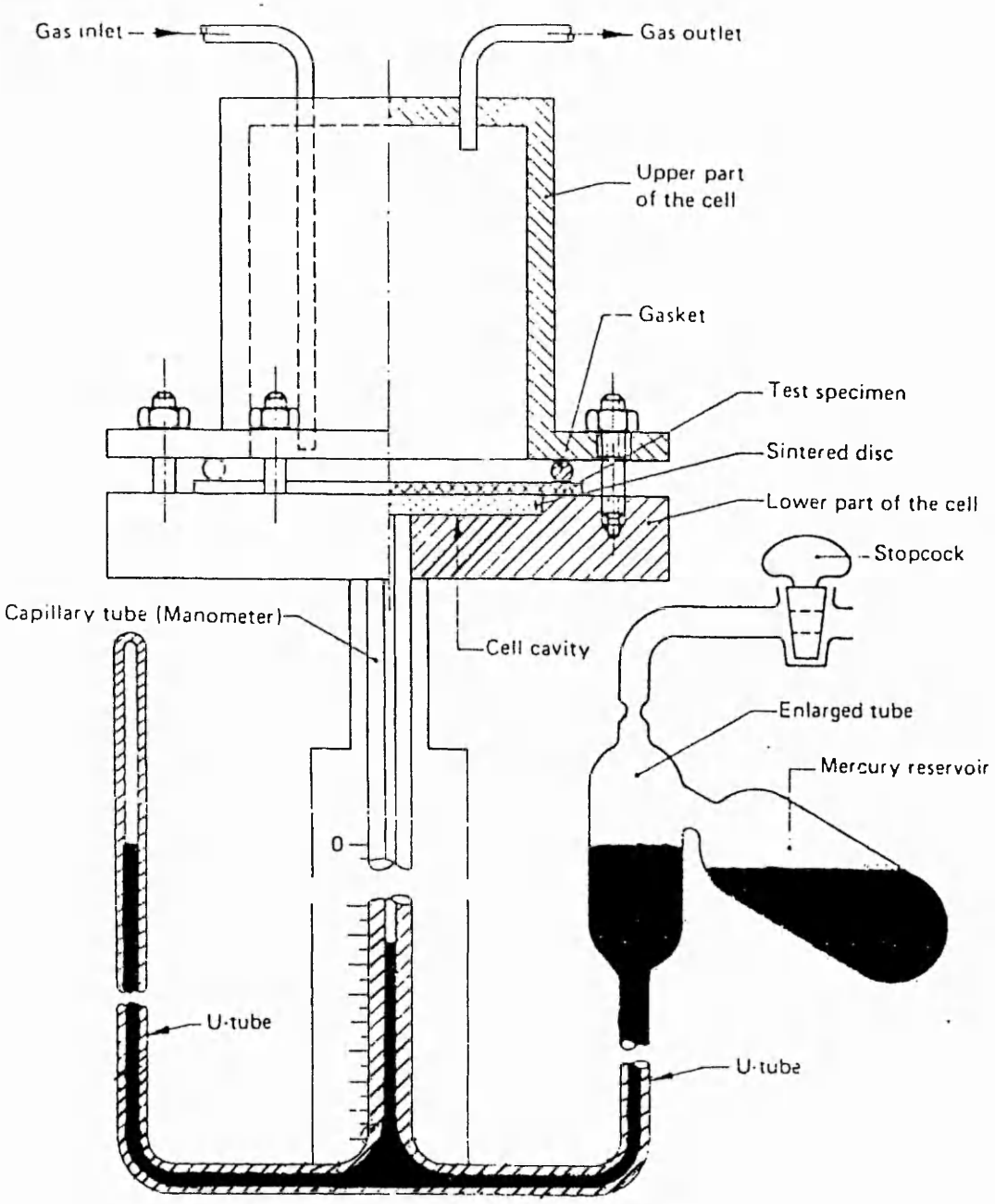

FIGURE II:3 DAVENTEST GAS PERMEATION APPARATUS

B. WATER VAPOUR PERMEABILITY

Water vapour permeabilities were determined by a method similar to that used by Banker[5] and Patel[6]. A 10 cm^3 glass sample bottle was used for the reservoir of water vapour. 5 cm^3 of a saturated solution of ammonium sulphate were placed in the bottle. This solution would give a constant relative humidity of 81%, which corresponds to a water vapour pressure of 19.2 mm Hg at 25° C. A sample of the film under test was fixed to the top of the bottle using a concentrated solution of the polymer in butanone as an adhesive. The bottle was left 3 to 4 hours for the solvent to evaporate and was then weighed. For each film under test 5 identical bottles were prepared in the same fashion. The test bottles were stored in a desiccator containing silica gel, and therefore the relative humidity was effectively zero. The bottles were removed and weighed over an eight day period, and the weight loss / time plot was used to determine the permeability coefficient.

To test the limits of the method for measuring the water vapour permeability, weight losses were determined for a bottle with no film in place, and for a bottle sealed with aluminium foil. The weight losses were 6.7 $x10^{-3}$ g/hour and 0.074 $x10^{-3}$ g/hour for the open bottle and the totally closed bottle, respectively. The weight loss of the open bottle was due entirely to evaporation of the water, whereas the aluminium sealed bottle tested the quality of the seal, with the assumption that the aluminium was impermeable. The experimental values for the films tested in this study ranged from 0.67 to

3.2×10^{-3} g/hour. This indicates that the rate of weight loss was not controlled by the evaporation of the water, and that permeation through the adhesive, joining the film to the bottle, was negligible compared with the film permeability.

Although this method has many drawbacks in the determination of true permeability coefficients the method was applied here as only comparisons were being made. Among some of the objections to this kind of method are: the lack of any attempt to reduce the effect of boundary layers on either side of the film, and the long exposure time of the sample to the water vapour. This long period could give rise to some swelling of the polymer by the water vapour.

c. SOLUTE PERMEABILITY

The solute permeability was determined using the type of cell shown in Figure II:4, which has been widely used[7,8,9]. The cell consists of two chambers separated by the film sample under test. In one chamber, referred to as the donor chamber, a concentrated solution of the solute was added. To the second chamber, referred to as the receiver chamber, distilled water was added. Both halves of the cell were stirred at a constant and equal rate, driven by a common motor. The cell was constructed of glass, with ground glass flanges forming the mating faces between both halves. The stirrers were glass rods with PTFE paddle blades, and driven from above. The film under test was clamped between the two cell halves, on the ground glass flanges. A smear of high melting vacuum

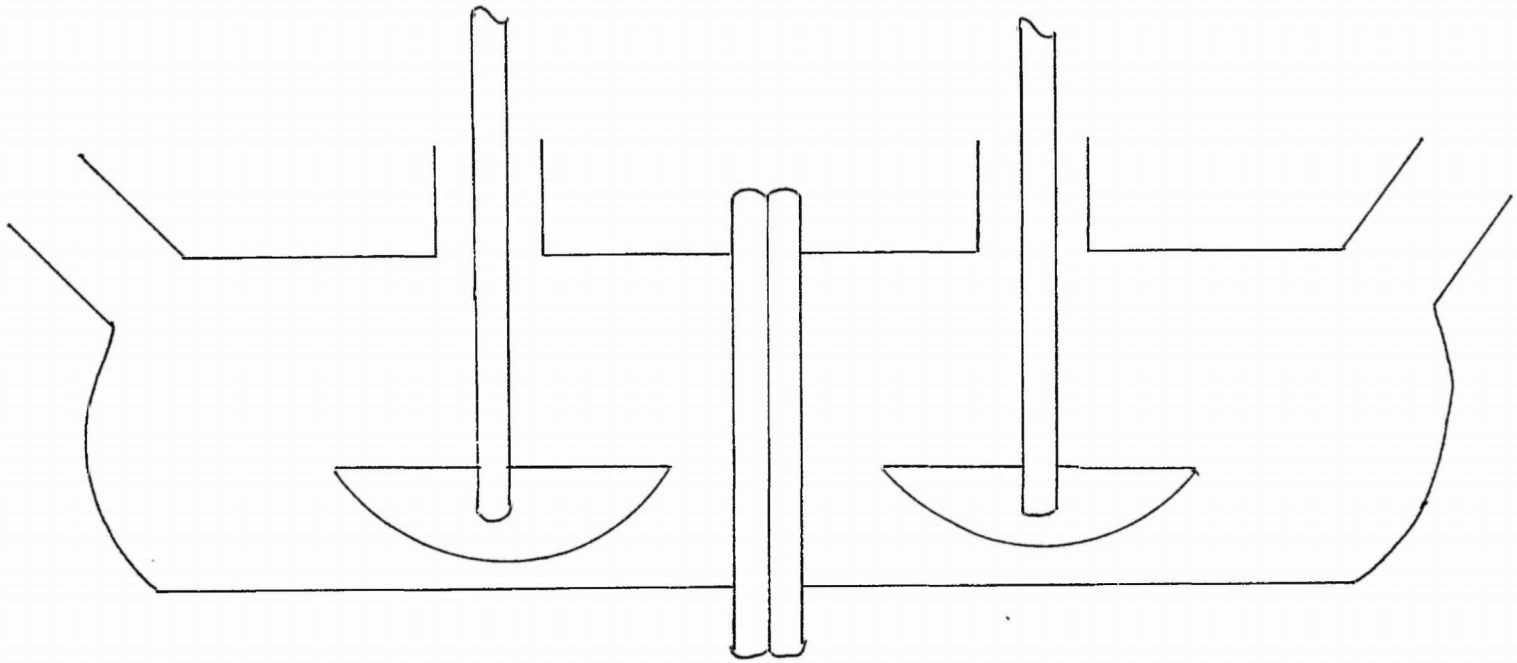

FIGURE II:4 SOLUTE PERMEATION CELL

grease was used to ensure a water tight seal. The assembled cell was then placed in a water bath at 30°C and allowed to equilibrate. Both the donor solution and the distilled water were also equilibrated to the same temperature before the experiment commenced. The donor solution concentration was chosen such that the concentration in the receiver side, at the end of the experiment, would never exceed 1% of this value. This was done to maintain an essentially constant concentration gradient across the film. Both the donor and receiver solutions were poured into the cell simultaneously, to prevent any distortion of the film. The stirrers were started, and this marked time zero. The concentration of the solute in the receiver side was monitored spectrophotometrically. In initial experiments the receiver solution was circulated through a flow cell in the spectrophotometer and back to the cell, and the absorbance was recorded on a chart recorder. This method was adopted because of the long times required to achieve a steady state flux of solute, and in order to measure the flux with sufficient accuracy. A typical experiment would last approximately 16 to 20 hours. This system only allowed one sample to be examined and was inefficient since film failures, such as pin holes made some determinations worthless. A film failure was readily recognisable by the rapid transmission rate compared with a good film. To improve this situation the system was modified to use up to six cells simultaneously, see Figure II.5 . An eight port rheodyne valve was used to circulate the receiver solution of each cell in turn to the spectrophotometer. The spectrophotomer was fitted with

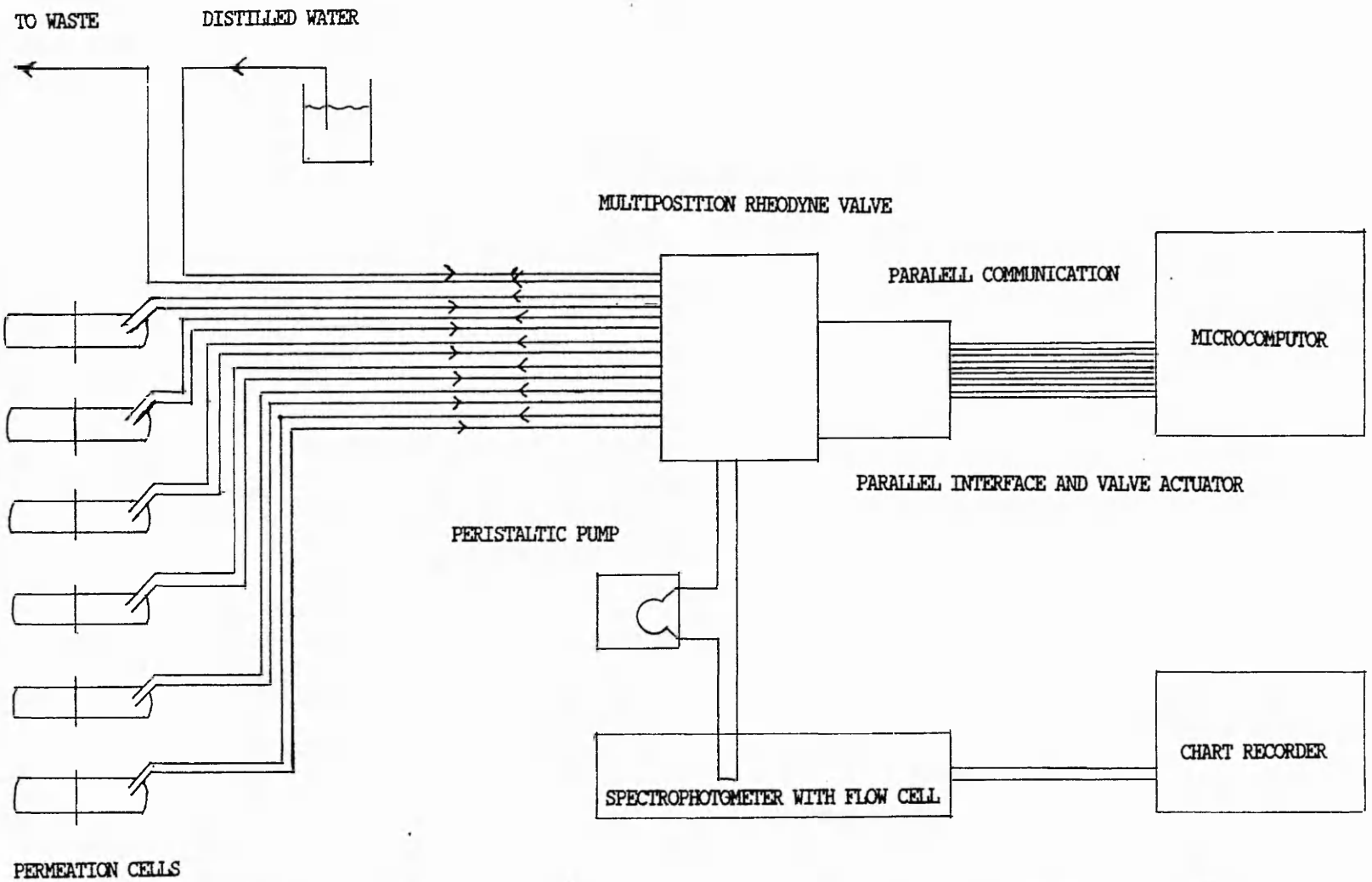

FIGURE II:5 COMPUTER CONTROLLED MULTI-CELL PERMEATION APPARATUS

a flow cell of volume 0.2 cm^3, and the dead volume of the associated plumbing was less than 1 cm^3, which was small compared to the 200 cm^3 used in the receiver cell. An IBM computer was used to control the position of the rheodyne valve such that each cell was sampled for a prescribed period, with the solution being returned to the original cell. After a known time the valve was changed to flush the flow cell by pumping with distilled water before the next cell was sampled. This flushing did introduce a small dilution in the receiver cell (because of the flow cell and associated plumbing) but this volume was less than 1 cm^3 per sample. It was found not to be significant for the 10 to 20 samples taken from each cell.

II.2.6 TABLET COATING AND DISSOLUTION STUDIES

The following materials were used to prepare beads containing either ascorbic acid or 2-(4-isobutylphenyl) propionic acid (Ibuprofen). The materials and the beads were prepared and supplied by Dr P.York of the University of Bradford.(The author would like to express his gratitude to Dr. York and his staff for their co-operation and assistance in this part of the work.)

The beads had the following composition:

Ascorbic acid beads :- 50% Lactose
25% Ascorbic acid
25% Cellulose
30% final weight of water

Ibuprofen beads :- 30% Cellulose
30% Lactose
40% Ibuprofen
50% final weight of water

The beads were prepared by the usual method employed in the laboratory, i.e., the components were intimately mixed and an extruder was used to form small tubular shaped particles from this mixture (2-3 mm length and 1 mm thickness). These still soft and deformable particles were then spheronised by spinning at high speed on a notched plate. The resulting spherical particles were allowed to dry overnight and were sieved with the fraction between British sieve size 8 to 12 being collected.

Initially the bead coating was attempted using the ascorbic acid beads and was performed using a rotating copper pan as the coating method. The beads were placed in the slowly rotating pan so as to get full mixing, and latex was added dropwise to the tumbling mass of beads; the temperature and drying control was via a hot air blower.

For more accurate control of the coating temperature a laboratory scale fluidised bed was used to coat the beads. The coating procedure in the fluidised bed was as follows; 400g of the beads were placed in the bed which was run until the temperature of the air leaving the bed was constant. The latex was sprayed vertically down into the bed of beads. The beads were in the bed for a total time of twenty minutes from the start of spraying, whereupon they were removed and allowed to dry at room temperature.

A sample of each set of beads was dried at 45° C for 5 hours. In both types of coating a sufficient amount of latex was added so as to give a final loading of polymer of 10% based on the weight of beads used.

The release profiles were determined using the following method. Approximately 0.5g of the coated beads were accurately weighed into gelatine capsules. The capsules were placed in wire baskets and immersed into the dissolution medium. The sample baskets were rotated at 100 rpm throughout the dissolution process. The dissolution medium consisted of 600 cm^3 of a pH 6.3 phosphate buffer which was allowed to equilibrate to 37° C., that being the temperature at which the dissolution experiment was performed. Each experiment was performed simultaneously on six samples of the beads. The rate of dissolution was determined by measuring the absorbance of the dissolution medium at 220 nm with a spectrophotometer.

II.3 REFERENCES

1. M.Chainey, M.C.Wilkinson, J.Hearn;
   Ind.Engng.Chem., Prod.Res.Dev., 21, 171 (1982)

2. M.C.Wilkinson, J.Hearn, P.Cope, M.C.Chainey;
   Brit. Polym. J., 13, 82 (1981)

3. S.M.Ahmed, M.S.El-Aasser, G.W.Poehlein, C.H.Pauli
   J.W.Vanderhoff; J.Colloid & Interface Sci.,
   73, 388 (1980)

4. Daventest. British Standard 2782 Pt8 Method 821 A

5. G.S.Banker, A.Y.Gore, J.Swarbrick;,
   J. Pharm. Pharmac., 18, 457 (1966)

6. M.Patel, J.M.Patel, A.P.Lemberger; J. Pharm. Sci.,
   53(3), 286 (1964)

7. S.Wicks; Ph.D Thesis, Univeristy of Bath, 1978.

8. D.G.Serota, M.C.Meyer, J.Autian;
   J. Pharm. Sci., 61(3), 417 (1972)

9. M.B.Rodell, W.L.Guess, J.Autian; ibid., 56, 1288 (1967)

CHAPTER III

EMULSION POLYMERISATION

The nature of emulsion polymerisation is a complex one. The production of synthetic polymer latices is the result of both the interplay of various polymerisation reactions, and colloidal phenomena governing reactions occurring at interfaces. Since there is a great variety in the types of monomers now employed, the absence of any single unifying mechanism is understandable. Blackley[1] gives the following definition for emulsion polymerisation; 'a polymerisation reaction which produces polymer in the form of a stable lyophobic colloid'. This definition encompasses many situations including non-aqueous polymerisations, reactions which are initially homogeneous and microsuspension polymerisations. Despite the wide spectrum of possible reactions, in the main there appear to be two approaches to describing particle formation. In the presence of surfactant above its CMC micellar initiation is often cited as the mechanism for particle formation. In the absence of micelles homogeneous nucleation has been put forward as the explanation. Of the many factors which can affect the mechanism of particle formation the monomer solubility in the polymerisation medium, namely water, is one of the most important. It is generally accepted that the homogeneous nucleation mechanism describes the reactions of the more water soluble acrylate and methacrylate monomers, but there is less evidence for its applicability to particle nucleation in reactions of less water soluble monomers in the absence of micelles, when the self-micellisation theory has been suggested[2,3].

In this study the emulsion polymerisation of butyl methacrylate and 2-hydroxyethyl methacrylate was

studied; the latter being very water soluble and the former having a water solubility similar in magnitude to styrene.

III.1 THE KINETICS OF THE EMULSION POLYMERISATION OF BUTYL METHACRYLATE

III.1.1 THE DEPENDENCE OF CONVERSION AND PARTICLE RADIUS WITH TIME

A plot of the conversion, and particle radius, versus time, for the surfactant free emulsion polymerisation of PBMA is shown in Figures III:1a, and III:1b, respectively. The conversion versus time, after a short induction period, appears to be linear up to 70% conversion. The radius versus time plot shows the same trends, and this was generally true for all the reactions studied. The shape of the conversion curve agrees well with those reported by Brodnyan[4] and Gardon[5], and shows no clear evidence for an auto-acceleration step, such as that described by Trommsdorff[6], and evident in methylmethacrylate[7] and styrene[8] emulsion polymerisations.

The equilibrium solubility of the BMA monomer in the polymer was determined by measuring the swollen and unswollen particle sizes using PCS. The unswollen particle size was 415 nm and this increased to 560 nm on swelling with the monomer. The volume fraction of the monomer in the swollen particles was found to be 0.66, which agrees well with the values of 0.6, found by Gardon[5], and 0.65 found by Bartoh[9]. This value implies that the

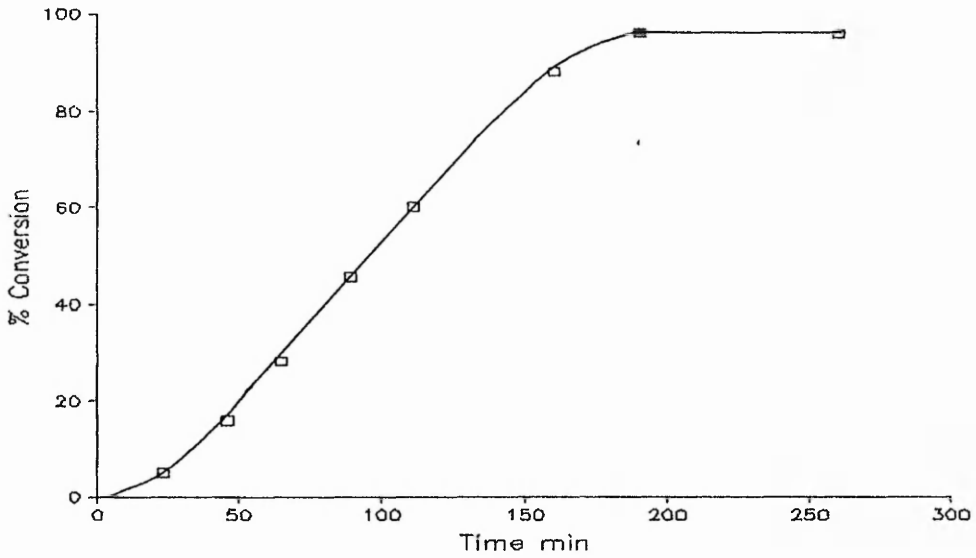

FIGURE III.1A % CONVERSION VERSUS TIME FOR BMA EMULSION POLYMERISATION

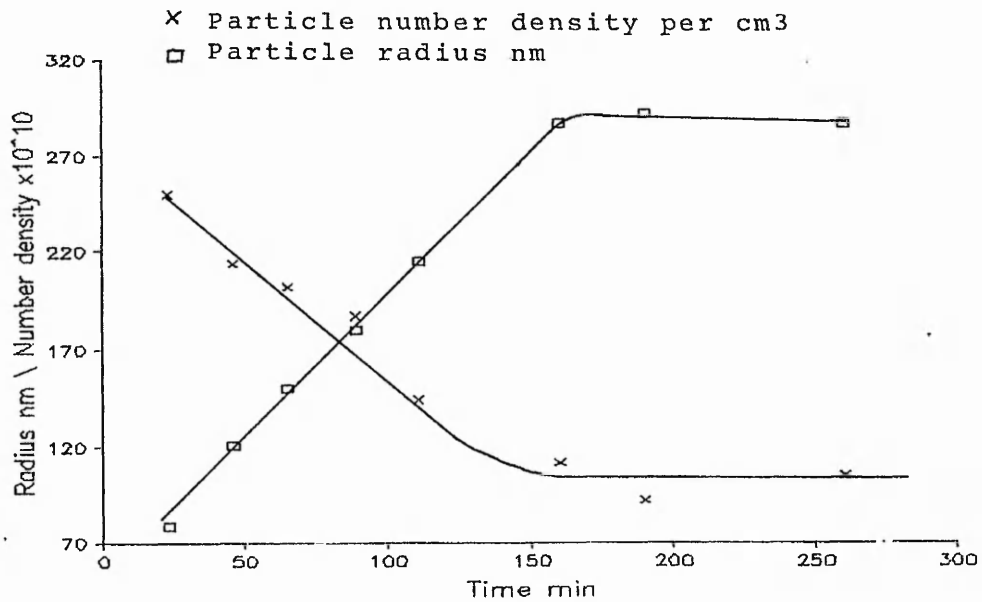

FIGURE III.1B PARTICLE SIZE AND NUMBER DENSITY VERSUS TIME FOR THE REACTION SHOWN IN FIGURE III.1A

disappearance of monomer droplets occurs at 34% conversion, and this would mark the end of interval II in a true emulsion polymerisation system, and thus, the conversion rate would be expected to decrease in interval III. The continuation of the constant rate period after the disappearance of monomer droplets has also been observed for the persulphate initiation of ethyl acrylate[10]. However, the same behaviour was not found when an oil soluble initiator was used,[10] and this difference was attributed to different particle nucleation mechanisms which resulted in a very low average number of radicals per particle in the persulphate initiated case[11].

Figure III:1b shows the change in particle number density with time for PBMA. It clearly shows that the number of particles during the constant rate period is decreasing, and this is contrary to the behaviour during interval II for conventional emulsion polymerisations, where the particle number density remains constant after an initial decrease.

The particle size as a function of conversion was estimated by transmission electron microscopy, in order to compare the sizes with those obtained from PCS measurments. Because of the low beam currents needed to measure soft polymers such as PBMA, the definition of the individual particles in the micrographs was poor. However, the size of at least thirty particles for each sample was estimated and the results are shown in Table III:1 in conjunction with the PCS sizes.

Conversion %	T.E.M size nm	% Standard deviation	PCS size nm	% standard deviation
12	147	5	157	1
41	214	5	221	1
54	371	2	297	6
62	405	2	370	1
69	384	3	406	1
76	416	4	428	1
Final	440	2	428	1

TABLE III:1 COMPARISON OF TEM AND PCS PARTICLE SIZES

The agreement between the two methods is reasonably good, and therefore, the decrease in particle number density throughout the reaction is probably not a function of the method of particle size measurement. An apparent decrease in particle number density would be found if either the conversion was over estimated or the particle size was underestimated, at early times in the reaction.

For a constant rate during a period of decreasing particle number density the polymerisation rate per particle must be increasing, and this in turn implies that the average number of radicals per particle is increasing with increasing conversion.

For butyl methacrylate, Gardon[5] showed that the peak in the number of radicals per particle was reached at approximately 45% conversion, and had a value typically of 3, although in the same paper he gave values as high as 9. The ability of particles to sustain, on average, more than one radical is increased as the particle size increases,

and in general is described by the Smith and Ewart[12] case III, where the average number of radicals per particle is much greater than 0.5.

III.1.2 THE EFFECT OF VARYING IONIC STRENGTH AT CONSTANT INITIATOR CONCENTRATION

It has been established[13] for latices prepared in the absence of surfactant, using ionic initiators such as potassium persulphate, that the particle stability is provided by the charged end groups of the polymer chains resulting from the initiator decomposition. The concept of limited flocculation[14] during the early stages of particle formation is a consequence of the colloidal stability of the primary particles and it has been shown that the particle number density, and therefore the size can be controlled by varying the ionic strength of the aqueous medium.[15]

A similar study was undertaken here, where the ionic strength in several reactions was varied, but the initiator and monomer concentration were kept constant at 3.7×10^{-3} and 0.7 mol dm^{-3}, respectively. The results for the particle size and number are shown in Table III:2 The effect of ionic strength on the particle size and number density was similar to those shown by Goodwin et al,[14] for styrene. The particle size increased with increasing ionic strength, and the particle number density decreased accordingly. A log-log plot of the ionic strength versus the particle number density gives a straight line of gradient -7.3, and is shown in Figure III:2.

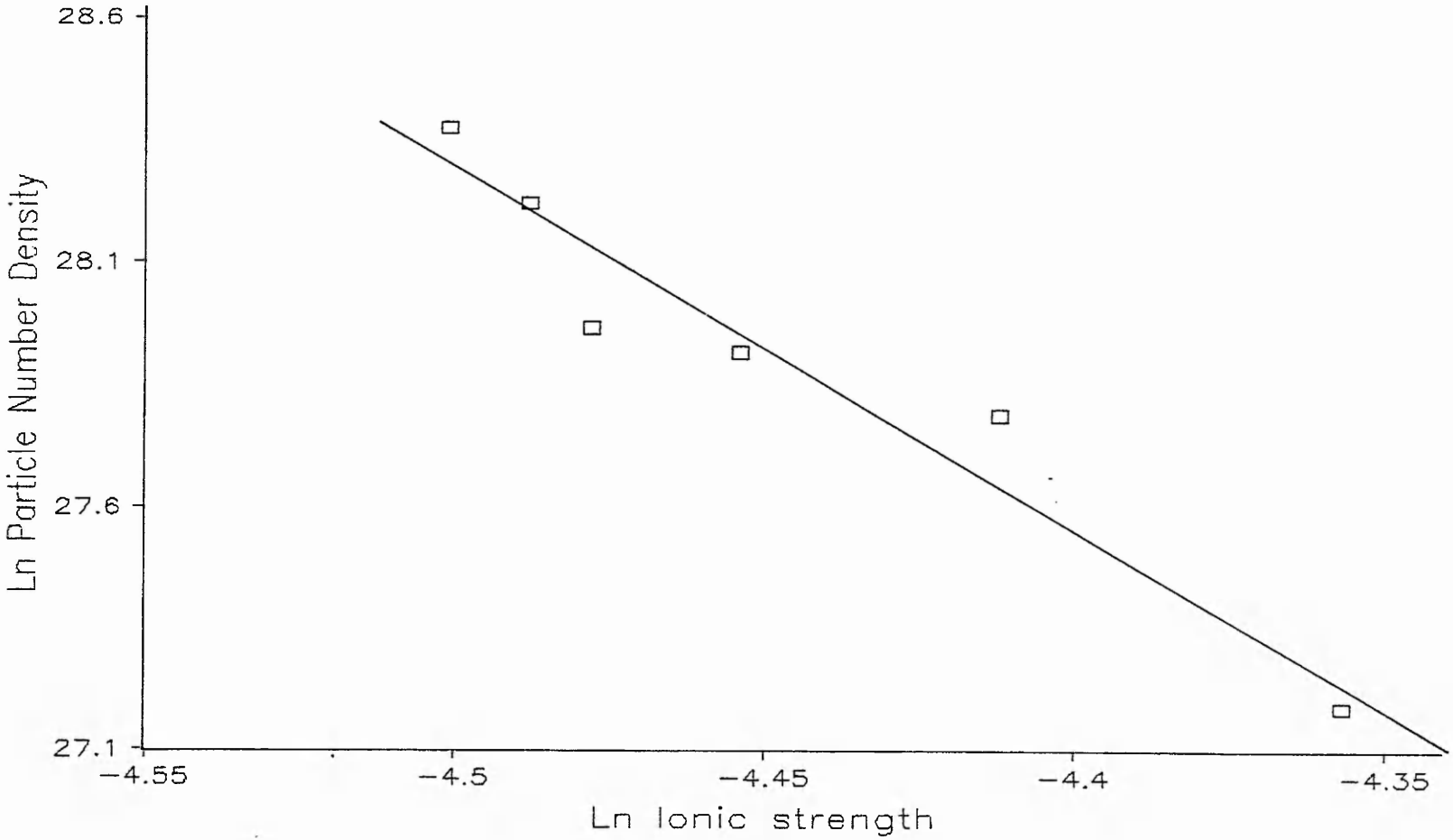

FIGURE III.2 THE EFFECT OF IONIC STRENGTH ON THE PARTICLE NUMBER DENSITY

code	Ionic strength $x10^{2}$ mol dm^{-3}	particle size nm	number density per cm^{3} $x10^{-12}$	molecular weight Mn $x10^{-5}$	Rate % min^{-1}
63	1.11	410	21	2.3	0.65
61	1.12	430	18	2.4	0.65
60	1.13	483	14	2.7	1.02
53	1.16	496	13	1.4	0.79
52	1.21	517	12	1.3	0.60
50	1.28	634	6	1.3	0.70

TABLE III:2 THE EFFECT OF VARYING IONIC STRENGTH AT CONSTANT INITIATOR CONCENTRATION

This implies that the particle number density is inversely proportional to the ionic strength as follows:

$$N \propto [I]^{-7.3}$$

Similar experiments on the surfactant-free polymerisation of styrene gave the number density to be inversely proportional to the power 0.78 of the ionic strength[16]. From the above it appears that the particle number density is more sensitive to the ionic strength compared with polystyrene[15]. Four of the above latices were acid washed and conductometric titrations were performed in order to determine the number of end groups per chain and surface charge density. A typical titration curve is shown in Figure III:3, and clearly demonstrates the presence of both strong and weak acid end groups. Table III:3 shows the titration data along with the

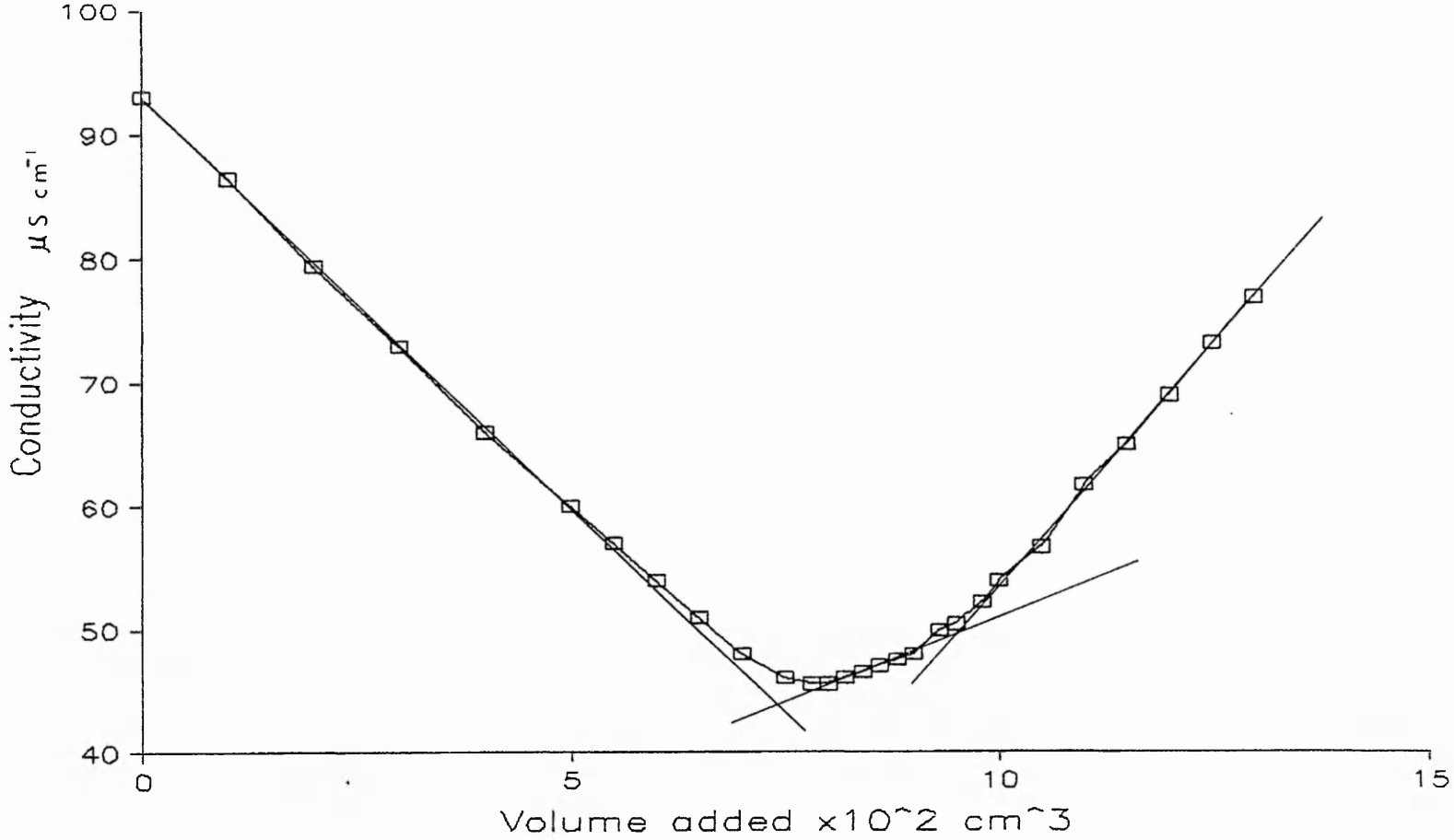

FIGURE III.3 TYPICAL TITRATION CURVE FOR A PBMA SURFACTANT FREE LATEX

calculated surface charge densities and the number of end groups per chain. All the samples were polymerised using the same initiator concentration, but the ionic strength was used to change the particle size. There was no real trend in either the strong or weak acid end group concentrations, and the total titratable acid concentration was also reasonably constant.

Code	particle size nm	Strong acid $x10^6$ moles/g	Weak acid	Molecular weight Mn $x10^5$	Surface charge $\mu C\ cm^{-2}$	Number of end groups per chain
50	624	3.2	1.9	1.27	5.1	0.6
52	517	4.3	1.8	1.35	5.0	0.8
53	496	1.3	4.1	1.39	4.3	0.7
63	410	5.4	0.7	2.3	4.0	1.4

TABLE III.3 SURFACE CHARGE AND END GROUP ANALYSIS

The surface charge density showed a small trend with ionic strength. However, the number of end groups per chain was smallest for the larger particles. This may be due to coagulation causing some of the end groups to be buried within the particle, and thus, not detected by titrations.

The polymerisation rates in Table III:2 were determined from the slope of the linear portion of the conversion time plots, and here again no real trend was found. However, if the rate is plotted against the square root of the total volume of polymer formed, at a fixed

conversion, a linear relationship is found for a series of reactions of constant initiator concentration and variable ionic strength. The data is shown in Figure III:4, and the gradient of the line was 5.56 $x10^{-4}$. From the Smith Ewart relationship for case III:

$$R_p = k_p [M] (\rho V / 2k_t)^{0.5}, \qquad \text{(III.1)}$$

the gradient of the line is given by:

$$\text{gradient} = k_p [M] (\rho / 2k_t)^{0.5}, \qquad \text{(III.2)}$$

where k_p and k_t are the propagation and termination rate constants, [M] is the equilibrium monomer concentration in the particles, and ρ is the rate of absorption of radicals and can be approximated to the rate of radical production in the aqueous phase.

$$\rho = 2k_d \, EXP(-k_d \, t + LnP) N_a \quad , \qquad \text{(III.3)}$$

where k_d is the rate constant for the decompostion of potassium persulphate and was equal to 2.68 $x10^{-5}$ mol dm^{-3}[16], P is the initial initiator concentration. k_p = 931 $mol^{-1} dm^3 sec^{-1}$ (calculated from k_p =369 at 30°C[27] and an activation energy of 20.4 kJ mol^{-1}[28]), k_t = 1.02 $x10^7$ $mol^{-1} dm^3 sec^{-1}$[27] and [M]= 3.8 mol dm^{-3}[26]

Using equation III.2 with the above constants the predicted gradient to the line in Figure III.4 is 3.2 $x10^{-4}$. Although this figure is somewhat smaller than that found experimentally, the agreement is reasonably good,

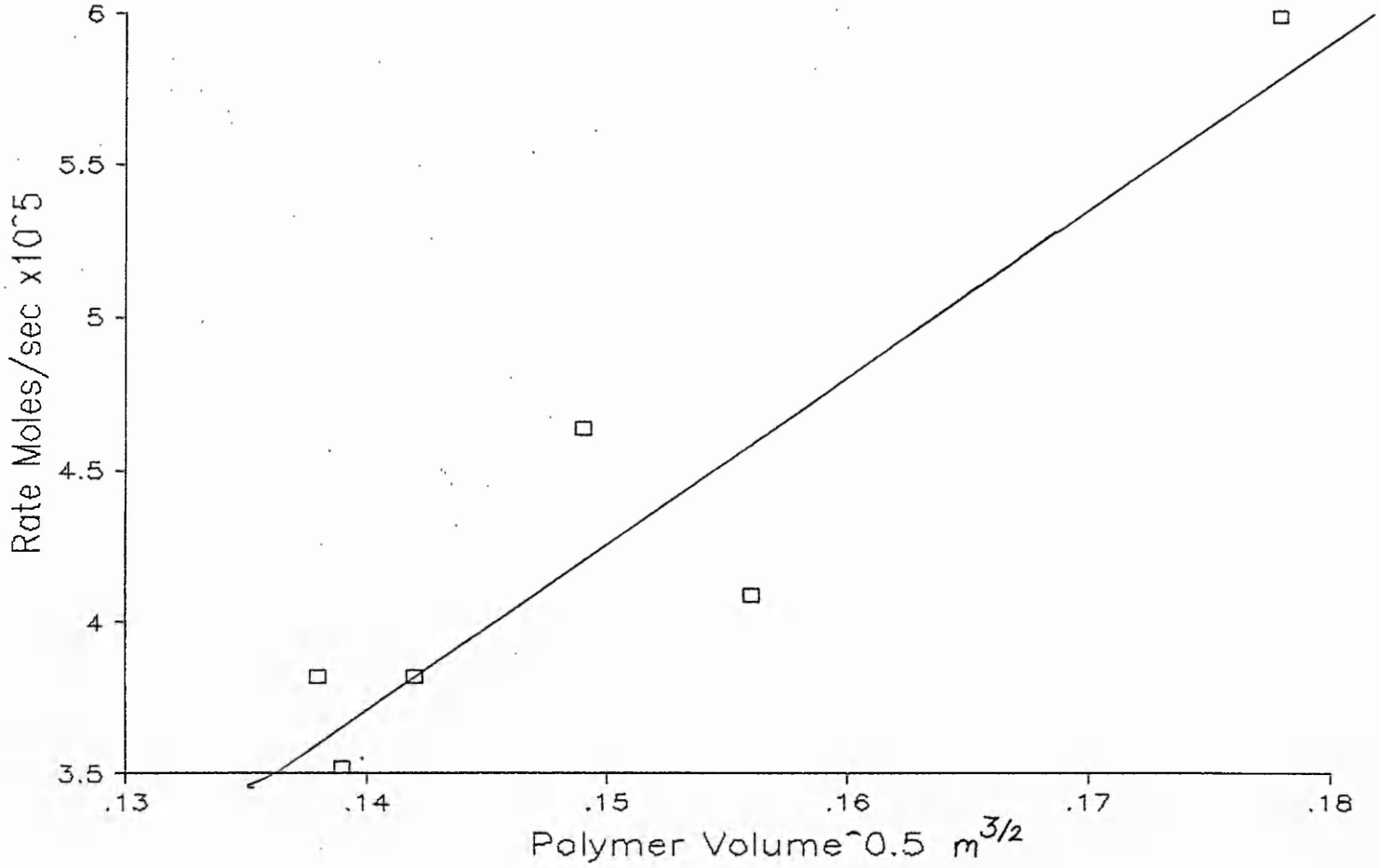

FIGURE III.4 RATE OF CONVERSION VERSUS THE SQUARE ROOT OF THE TOTAL VOLUME OF POLYMER

given the variability of literature values for the rate constants

III.1.3 THE EFFECT OF VARYING INITIATOR CONCENTRATION AT CONSTANT IONIC STRENGTH

The effect of initiator concentration was studied at constant ionic strength by the addition of sodium chloride. In all the reactions the monomer concentration was 0.7 mol dm^{-3}, the reaction temperature was 75° C, and the ionic strength was 1.11 $x10^{-2}$ mol dm^{-3}. The results are shown in Table III:4

code	initiator concentration $x10^{3}$ mol dm^{-3}	particle size nm	number density $x10^{-12}$	molecular weight M_n $x10^{-5}$	reaction rate % min^{-1}
63	3.7	400	21	2.3	0.65
58	3.5	493	12.5	2.5	0.74
55	2.9	530	10.2	1.5	0.82
57	2.4	551	8.6	1.4	0.75
105	2.2	592	8.7		1.18
54	1.8	561	8.8	1.5	0.68
92	1.1	608	6.9		0.86

TABLE III:4 THE EFFECT OF INITIATOR CONCENTRATION AT CONSTANT IONIC STRENGTH

For low initiator concentrations, the particle size was relatively large and the number density was small. Increasing the initiator concentration caused a

decrease in the particle size and the particle number density increased accordingly. The decrease in particle size with increasing initiator concentrations was probably due to more free radicals being initially available, and thus the chances of nucleating new particles was greater.

A log-log plot of the particle number density versus the initiator concentration is shown in Figure III:5. The gradient of the straight line, found by linear regression, was 0.46. This value is in reasonable accord with the Smith and Ewart prediction of 0.4. Medvedev[25] considered adsorption on the particle surface as being a dominant feature, and with this consideration the dependence of the number on the initiator concentration was 0.5. Since the value in this study was determined from a log-log plot, the accuracy of the measurement is insufficient to prove the applicability of either model.

III.1.4 THE EFFECT OF INITIATOR CONCENTRATION AT VARIOUS IONIC STRENGTHS

The effect of initiator concentration was determined for a similar range of reactions as described previously. No attempt was made to compensate for changes in ionic strength, and thus, the ionic strength of the medium increased as the initiator concentration increased. The results are shown in Table III:5. The trends in particle size and number density differ greatly from those obtained earlier for constant ionic strength. At the highest initiator concentration, the particle size was large and the number density accordingly small. For the intermediate initiator concentrations, the particle size

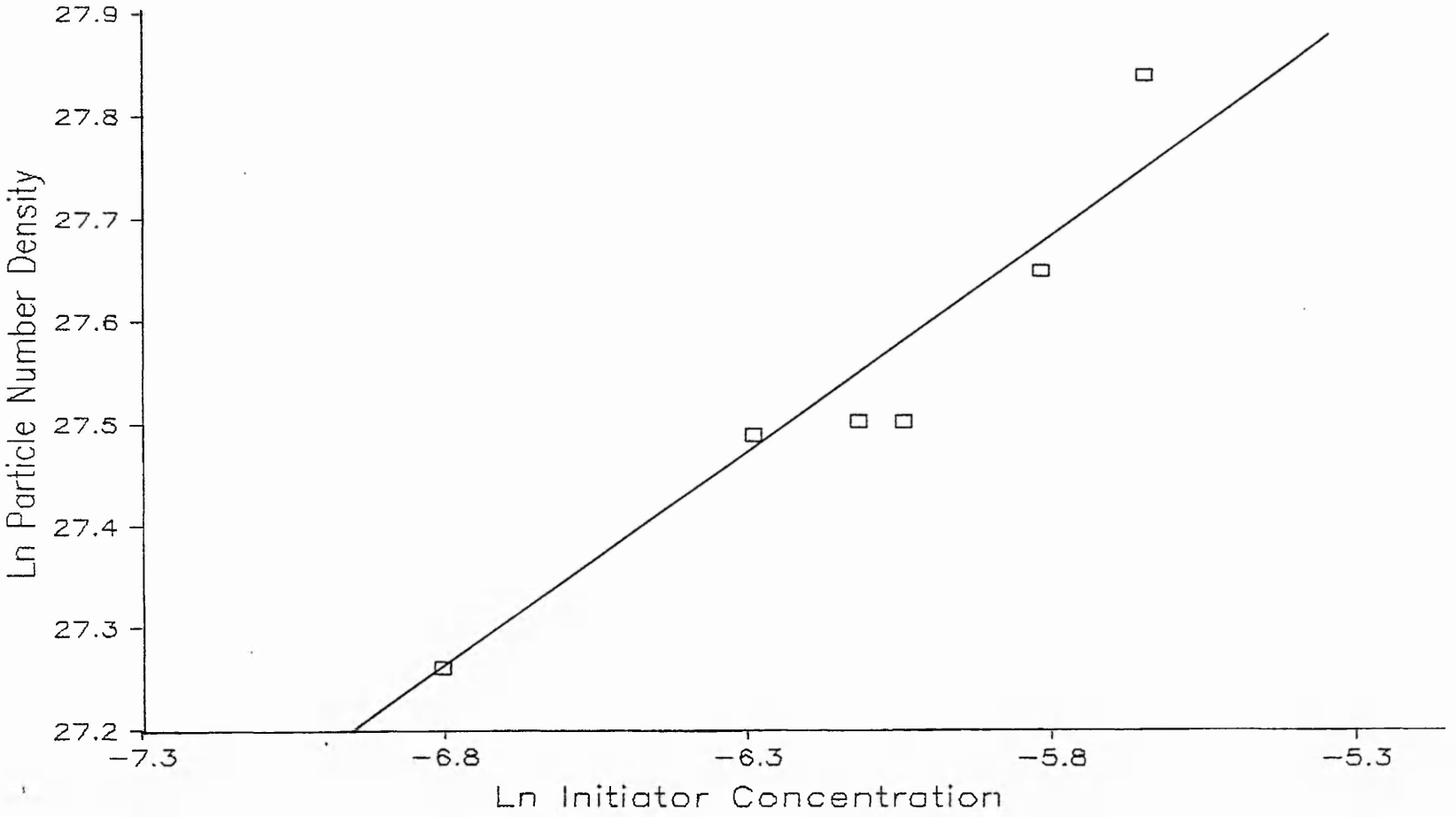

FIGURE III.5 THE EFFECT OF INITIATOR CONCENTRATION ON THE PARTICLE NUMBER DENSITY

was smaller than the corresponding reactions carried out at constant and higher ionic strength. Also in this intermediate region the particle size remains fairly constant. At the low initiator strengths employed the particle size increased, with a corresponding drop in the particle number density. These observations are in keeping with the particle size and thus, the number density being controlled by coagulation type mechanisms. It was shown earlier that the particle number was strongly dependent on the ionic strength of the reaction medium. In these reactions, the ionic strength was lower than the corresponding reactions in Table III:4.

code	initiator concentration $x10^{3}$ mol dm^{-3}	particle size nm	number density per cm^{-3} $x10^{-12}$	rate % min^{-1}
90	5.5	613	7.4	1.36
63	3.7	410	21	0.65
72	3.6	408	36	0.90
73	3.5	421	22	0.64
74	2.9	425	26	0.55
76	2.4	423	25	0.89
77	1.8	426	20	0.75
82	1.5	618	7.5	0.71
81	1.1	635	6.8	0.83

TABLE III:5 THE EFFECT OF INITIATOR CONCENTRATION

It is only at the extremes of initiator concentration that the ionic strength contribution from the initiator outweighs the stability given to the particles via the number of charged end groups. As was previously observed, there was no real trend in the rate of polymerisation with respect to initiator concentration.

III.1.5 THE RATE OF POLYMERISATION

The rates of polymerisation shown above were all derived from the slope of the linear portion of the conversion time plot. This region of constant rate of polymerisation is usually described as interval II, and typically the particle number density is constant in this region. In the present study the particle number density was found to decrease during this constant rate period. Thus, for a constant rate to be maintained, the polymerisation must either be :

(i) independent of particle number density, and thus, polymerisation in the aqueous phase rather than the monomer swollen polymer particle would be the principal locus of polymerisation. This would seem unreasonable given the low solubility of the monomer in the aqueous phase, and its high solubility in the polymer or

(ii) the average number of radicals per particle must increase as the number of particles decrease.

The second hypothesis would seem more likely, since, during the constant rate period the particle size would typically grow from 200 to 400 nm. The large size of these particles would allow the existence of more than one radical per particle without immediate termination taking place. An expression for the average number of radicals was given by Napper[26], and takes the form:

$$\frac{dx}{dt} = \frac{k_p N_c C_m M \, n(t)}{N \, g_m} \quad , \qquad \text{(III:4)}$$

where dx/dt is the fractional conversion with respect to time, k_p is the propagation rate constant, N_c is the number of latex particles per dm^{-3}, M is the molecular weight and g_m is the initial mass of monomer, C_m is the monomer concentration in the particles, N is Avogadro's number and n(t) is the average number of radicals per particle at time t.

Ugelstad[29] gave an approximation of $\bar{n}$ which was

$$\bar{n} = (0.25 + \alpha/2)^{0.5} \quad , \qquad \text{(III:5)}$$

where $$\alpha = \frac{\rho_a \, V_p}{N \, K_t} \qquad \text{(III:6)}$$

A comparison between the experimentally determined number of radicals per particle from Equation III:4, and those predicted by Ugelstad, equation III:5, is shown in Table III:6

Conversion %	Particle Diameter nm	Particle No density $x10^{-14}$	$\bar{n}$	
			Experimental	Ugelstad
16	230	22.4	2.8	3.1
20	255	21.4	3.0	3.8
30	300	19.4	3.3	4.9
40	345	18.0	3.6	6.4
50	390	16.2	3.9	8.2
60	430	14.6	4.4	9.9

TABLE III:6 THE AVERAGE NUMBER OF RADICALS PER PARTICLE

The values predicted by the Ugelstad expression increase with increasing conversion as do the experimental values. However, the Ugelstad values are much larger than experimental ones at higher conversions. Also, the above values are much larger than the 0.7 quoted by Napper[26], for butyl methacrylate. However, the system used by Napper contained surfactant and the seed particles used in his study were approximately 40nm, and thus, nearly an order of magnitude smaller than particle sizes encountered in the present study. The much greater particle size here may account for the relatively large number of radicals per particle. Values for $\bar{n}$ of 10 and greater have been quoted for the surfactant-free polymerisation of styrene[16], where the particle size was also large, i.e., 500nm.

The lack of any trend in the polymerisation rate with increasing initiator concentration is at first a surprising result. However, considering the fact that, both the particle size, and particle number density change

considerably with initiator concentration (at constant ionic strength), then the situation becomes much more complicated. Table III:7 shows the calculated number of radicals per particle as a function of initiator concentration. The number of radicals per particle and the total number of radicals in the system was estimated from at 40% conversion. In general, the number of radicals per particle increases with decreasing initiator concentration. This is, however, easily rationalised, since the particle size increases with decreasing initiator concentration, and thus, the number of radicals that could exist in each particle without immediately terminating, increases.

Code	Initiator Conc. $x10^{3}\,dm^{-3}$	Particle Number $x10^{12}$	Radicals per particle	Total number of radicals $x10^{12}$
63	3.70	24.5	2.6	63.7
73	3.52	20.3	3.5	71.0
74	2.96	18.6	4.4	81.8
57	2.37	10.6	6.5	68.9
91	2.2	16.0	7.1	113.6
54	1.85	11.8	5.3	62.5
92	1.11	4.6	16.5	75.9

TABEL III:7 THE AVERAGE NUMBER OF RADICALS PER PARTICLE

When the total number of radicals is considered, there is no trend with respect to the initiator concentration. The number of radicals in the system is reasonably constant at a fixed conversion. It would therfore appear that the total polymer volume governs the total number of radicals rather than the particle size or number. Therefore, the lack of any trend in the rate of polymerisation rate with respect to initiator concentration is caused by the principal locus of polymerisation. The polymerisation rate did not increase with the initiator concentration for the following reasons: Increase in the particle size permits more radicals to freely polymerise within the particles; however, the increase in size is accompanied by a decrease in the total number of particles, and thus, there is a balance between the number of particles, and the rate of polymerisation per particle.

III. MOLECULAR WEIGHT DEVELOPMENT

As described in chapter II, the GPC molecular weights were determined as polystyrene equivalents. To test the validity of the results obtained in this way the weight average molecular weight of a poly(butyl-methacrylate) sample was determined in three ways. Firstly, by using poly(styrene) standards to calibrate the instrument, and the Mark-Houwink parameters for poly(styrene) in THF, and secondly, using chloroform, a solvent for which the Mark-Houwink parameters for PBMA are known[17]. Thirdly, low angle light scattering was also used to directly determine the molecular weight of the same sample. The various molecular weights are shown in

Table III:8. The best agreement between the light scattering and the GPC results comes from the poly(styrene) equivalent results determined in THF. The GPC results from chloroform solutions were much higher than the light scattering values. The Mark-Houwink parameters for PBMA in chloroform were used to calculate a universal molecular weight from the poly(styrene calibration curve[38], however, there is some doubt as to their validity[18]. Therefore it would seem that the poly(styrene) equivalent values quoted are in reasonable agreement with the absolute values at this molecular weight, although the values are slight underestimates. Light scattering could not be used universally, since it would not be suitable for the lower molecular weights which were encountered during this study.

	M_w x10^5	mean M_w x10^5
GPC in THF	2.95	
	3.06	3.0
GPC in $CHCl_3$	6.22	
	6.07	6.1
Light scattering	3.77	
	3.88	3.8

TABLE III:8 MOLECULAR WEIGHT DETERMINATIONS

The molecular weight was determined as a function of conversion for two multi-sampled reactions. The weight average molecular weight became constant at an early stage

in the reaction and was between 4 and $5x10^5$. The corresponding number average molecular weights were in the range 1.3 to 1.5 $x10^5$. The molecular weight distributions showed the constant presence of peaks at poly(styrene) equivalent molecular weights of 300 and 1500. The peak at 300 could be due to an oligomer of 2-3 monomer units, or less likely, residual initiator. The peak at approximately 1500, could be attributed to a molecular species containing 10-11 monomer units. Similar studies were performed by Goodall[21] on the surfactant-free emulsion polymerisation of styrene. Goodall reported the occurrence of a low molecular weight peak of 1000, and this was a result of precipitation or micellization of 500 mol wt water soluble oligomers, which then nucleated new polymer particles. Thus, the critical chain length of polymer upon precipitation from the aqueous phase was approximately 8 for styrene (assuming 2 sulphate end groups per chain). Fitch[22] reported that the critical chain length of the relatively water soluble methyl methacrylate was approximately 65, and that these chains collapsed onto themselves to form new polymer particles, i.e., homogeneous nucleation occurred. If the low molecular weight material found in this study can be attributed to the critical chain length for solubility, then the degree of polymerisation required to cause precipitation is 10, assuming only one sulphate end group per chain, and this value is similar to the value for styrene. This value would seem reasonable, since the solubility of butyl methacrylate and styrene in water are 4.23 and 1.92 mmol dm^{-3} respectively[23], and thus the solubility of their

oligomers would likely be in similar proportions. Also, this proposed value is much lower than that found for methyl methacrylate, which has a water solubility of 159 mmol dm^{-3}[24]

The role of the low molecular weight material in particle nucleation is by no means certain, particularly when the material is present in the reaction at conversions where the particle number density is falling. The results reported for styrene[21] showed that the low molecular weight material could only be detected at low conversions, and was not detected at the higher conversion found in this study. This was taken to imply that further nucleation of particles, followed by heterocoagulation was not a significant mechanism for particle growth.

The molecular weight distribution shown in Figure III:6 is for a sample at 5% conversion. The major molecular weight peak is at 1.22 $x10^5$, but the presence of a small peak at approximately 1500 is clearly visible. The ratio in size of the two peaks was similar for all the samples studied. In order to aid interpretation of this data a reaction was performed using a monomer concentration fifty times less than normally employed and the reaction was terminated immediately after turbidity had set in. The termination was accomplished by quenching the reaction in ice. The sample was also analysed by GPC. The molecular weight distribution is shown in Figure III:7. Here, the low molecular weight peak is much more prominent, although the higher molecular weight peak is still a major feature, presumably being associated with particle growth. Also, the 1500 molecular weight chains would be formed in the aqueous phase constantly, provided

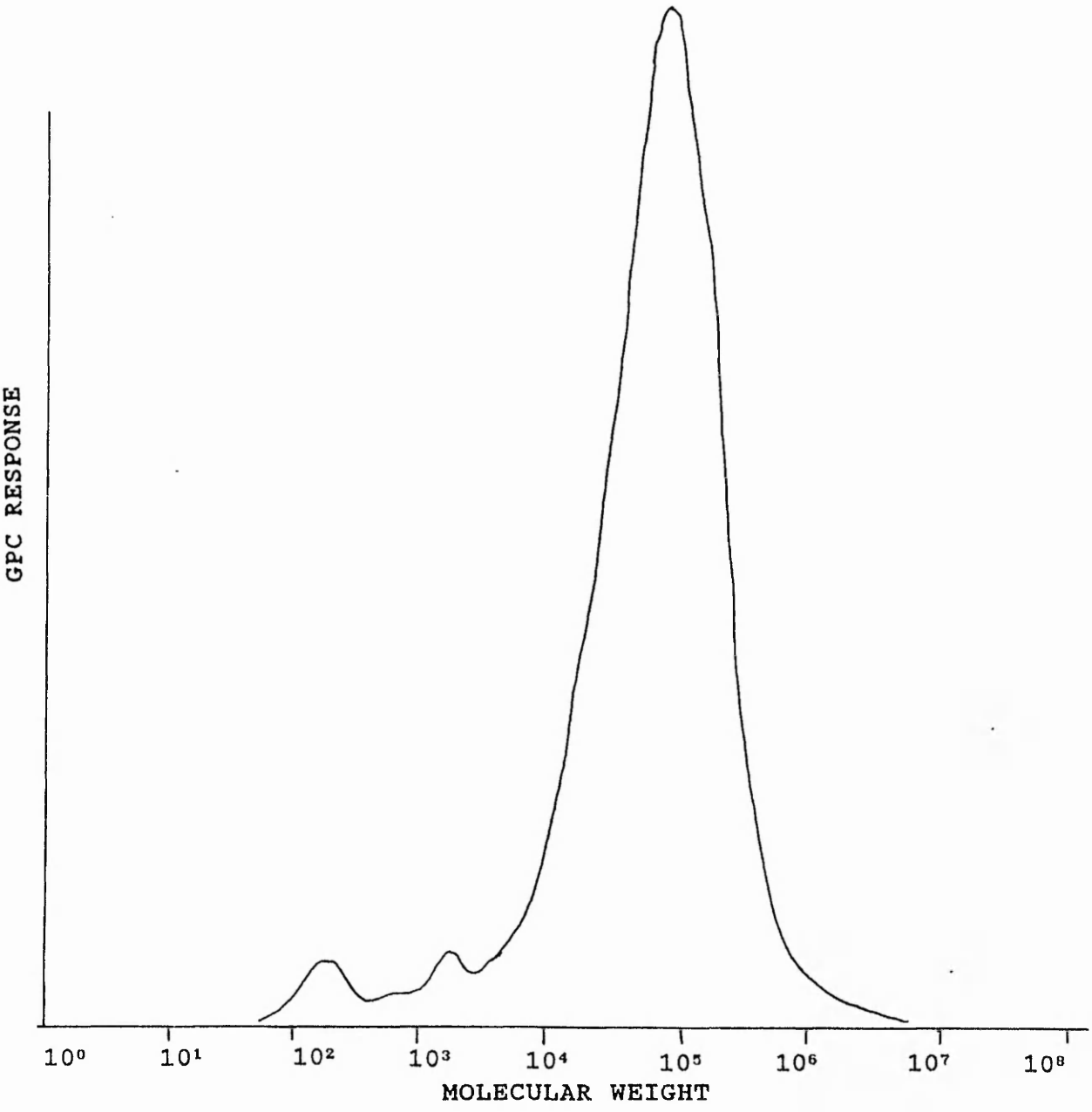

FIGURE III.6 MOLECULAR WEIGHT DISTRIBUTION FOR A SAMPLE OF PBMA AT 5% CONVERSION

code 93

FIGURE III.7 MOLECULAR WEIGHT DISTRIBUTION FOR A SAMPLE OF PBMA IMMEDIATELY AFTER PARTICLE NUCLEATION

code 85

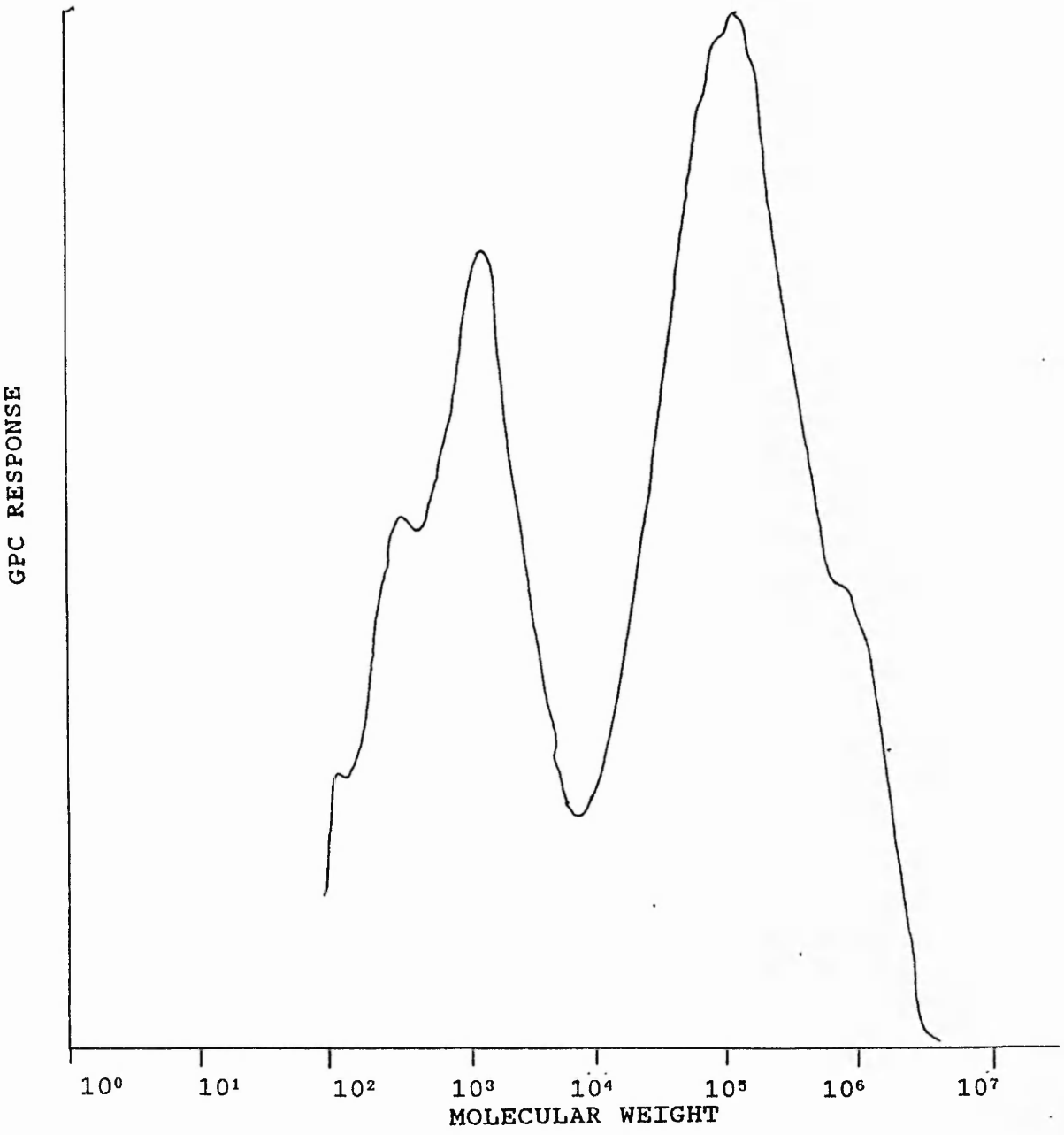

that there was dissolved monomer. The fact that there was no observable increase in the particle number density (in fact a decrease in number density was found as a function of conversion) would suggest that either the 1500 mol wt chains did not homonucleate new polymer particles initially, or that these chains tended to heterocoagulate once the number of particles formed gave sufficient surface area to preferentially adsorb or coagulate with the low molecular weight chains. Since the low molecular weight peak is not the major feature in the molecular weight distributions of samples taken at significant conversions, then the heterocoagulation mechanism is not likely to be the major route for particle development. The presence of this material, even at high conversions, indicates that heterocoagulation may occur continually, but since the major molecular weight peak is at much higher molecular weights, it is suggested that polymerisation principally occurs within the monomer swollen polymer particle.

III.2 THE EMULSION POLYMERISATION OF 2-HYDROXYETHYLMETHACRYLATE (HEMA) IN THE PRESENCE AND ABSENCE OF SURFACTANT

In this study the monomer used (HEMA) was miscible with water in all proportions. When the reaction was attempted using a similar recipe to that described by Kamei et al[30] a latex was produced with a particle size of 900 nm, but the solids content was less than 1% and there was a large amount of aggregated material. Several further reactions were attempted in which the initiator

and monomer concentrations were increased and the stirrer speed reduced. It was found that the latex was sensitive to shearing and that at high stirrer speeds the latex aggregated extensively. The polymerisation with no stirring produced a slightly larger latex than normal, with a particle size of 1μm, and there was no coagulum. The tendency of the latex to aggregate at higher stirrer speed was probably due to the particles having a low surface charge density, arising from the low initiator concentrations used. The initiator concentration was increased to 8.23×10^{-4} mol dm^{-3}; this produced a latex of particle size of about 850 nm and a solids content of 3%. Attempts to increase both the solids concentration, and surface charge, by increasing the monomer and initiator concentration, failed to produce a latex of either greater solids content, or smaller particle size. In all the reactions prepared in the absence of surfactant, the latex particles sedimented in a few days and coagulated and could not be redispersed. The polymer, with a density of 1.278 g cm^{-3} [31], in conjunction with the large particle size, would sediment quickly. The sedimentation rate, calculated using Stokes law, was approximately 1 cm per day. This, accompanied by the low surface charge, gave a latex that was very unstable. The surface charge was not measured directly by titration since the latex coagulated in cleaning and acid washing, but the critical coagulation concentration using sodium chloride was determined and found to be 5×10^{-2} mol dm^{-3}.

III.2.1. THE DEPENDENCE OF CONVERSION AND PARTICLE SIZE WITH RESPECT TO TIME

The particle size, number density and conversion for a typical surfactant-free reaction are shown in Table III:9 and displayed graphically in Figure III:8. There is a rapid increase in particle size during the early part of the reaction accompanied by a reduction in the particle number density. This drop in number density has been well documented in the literature, and was demonstrated by Fitch[14] for a methyl methacylate reaction, and by Munro et. al.[32] for styrene. As can be seen from Figure III:8 the conversion-time plot shows no linear portion as was found for butyl methacrylate, and the conversion was found to be first order for conversions less than 80%.

Time min	% conversion	particle size nm	particle number density per cm^3 $x10^{-10}$
5	10	312	37.7
10	23	523	9.1
15	40	640	8.8
24	61	740	8.8
32	70	820	8.5
48	85	960	6.0
60	83	936	6.4
108	84	941	6.6
360	84	890	7.6

TABLE III:9 CONVERSION TIME DATA FOR THE SURFACTANT-FREE EMULSION POLYMERISATION OF HEMA

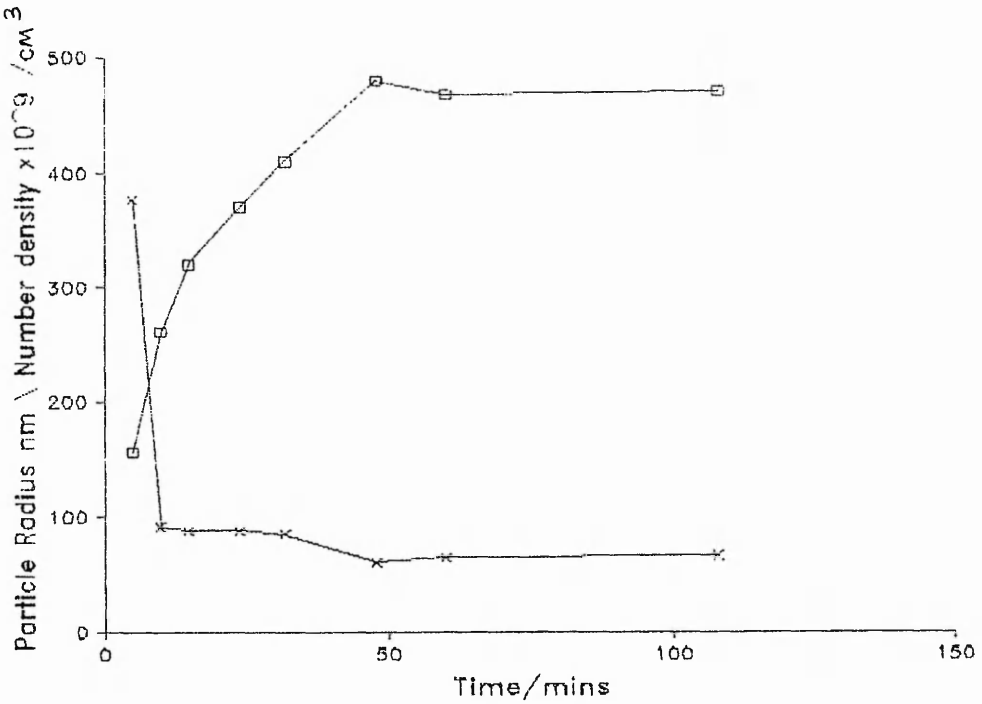

FIGURE III.8B PARTICLE SIZE AND NUMBER DENSITY VERSUS TIME FOR THE REACTION SHOWN IN FIGURE III.81A

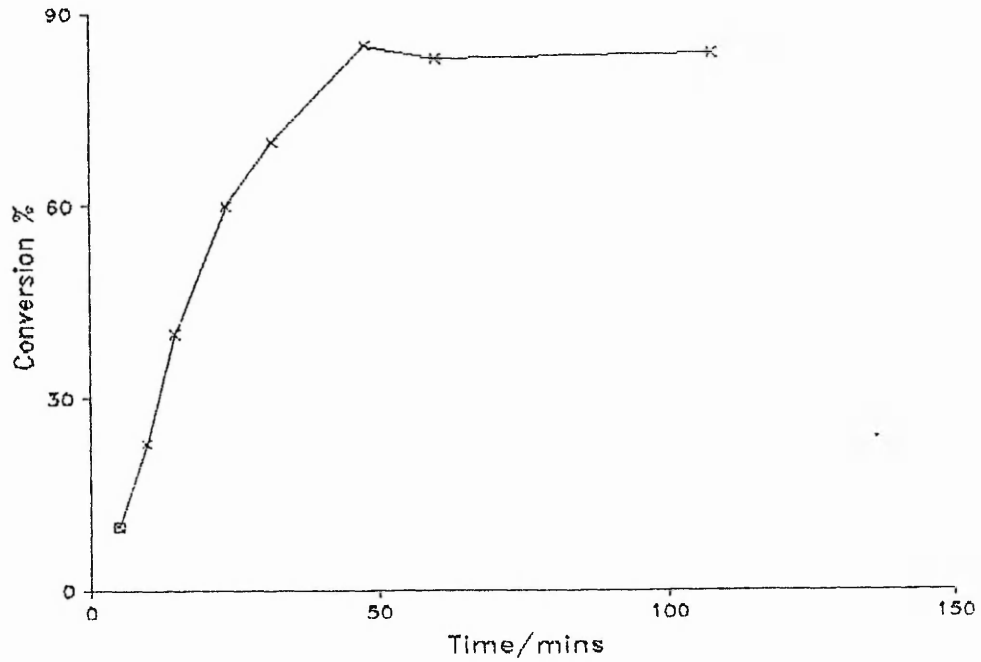

FIGURE III.8A % CONVERSION VERSUS TIME FOR PHEMA EMULSION POLYMERISATION

code 46

III.2.2. THE EFFECT OF VARYING INITIATOR CONCENTRATION AT CONSTANT IONIC STRENGTH

The effect of the initiator concentration at constant ionic strength was studied and sodium chloride was added to maintain the ionic strength. In all the following reactions the monomer concentration was 0.052 mol dm^{-3}, the stirrer speed was 90 rpm and the reaction temperature was 75° C. The results are tabulated in Table III.10. The reaction rate was determined from a first order type plot. The results show that the reaction rate and particle number density decrease, and the particle size increases with decreasing initiator concentration. The results are similar to those for butylmethacrylate and the same reason can be used to explain the changes in particle size and number density, i.e., particle stability, especially during the early stages of the reaction. However, the overall reaction rate increased with increased initiator concentration and this was not found for PBMA. For PHEMA, not only does the overall reaction rate increase, but also the rate per particle increases. It was argued previously for PBMA that the larger particles could sustain greater numbers of radicals without instantaneous termination, and hence the rate per particle was greater for the larger particles.

Since the monomer has a high solubility in water, solution polymerisation cannot be ruled out. Established theory suggests that the rate of polymerisation is proportional to the square root of the initiator concentration for solution polymerisation, and to the power of 0.4 for Smith and Ewart case II.

I=2.496 x10^{-3} mol dm^{-3}				
Code	Initiator conc mol dm^{-3} x10^{4}	particle size nm (final)	No density per cm^{3} (final) x10^{-10}	1st order rate constant min^{-1} x10^{2}
32	8.23	856	10	4.16
46	6.58	890	7.6	2.91
45	4.11	920	6	1.47

TABLE III:10 THE EFFECT OF INITIATOR CONCENTRATION AT CONSTANT IONIC STRENGTH

A plot of the limited data, shown in Figure III:9 implies that the dependence of the rate on the initiator concentration is to the power 1.49. Clearly this figure is far from either of the predicted values, indicating that a process more complicated than either solution or emulsion polymerisation is taking place. A possible explanation is given later in this chapter.

III.2.3 THE EFFECT OF VARYING IONIC STRENGTH AT CONSTANT INITIATOR CONCENTRATION

It was found that PHEMA latices were not produced at high initiator concentrations, probably because of the high ionic strength arising from the initiator itself. In the following reactions the initiator concentration was kept constant and the ionic strength adjusted by the addition of sodium chloride. The results are shown in Table III:11.

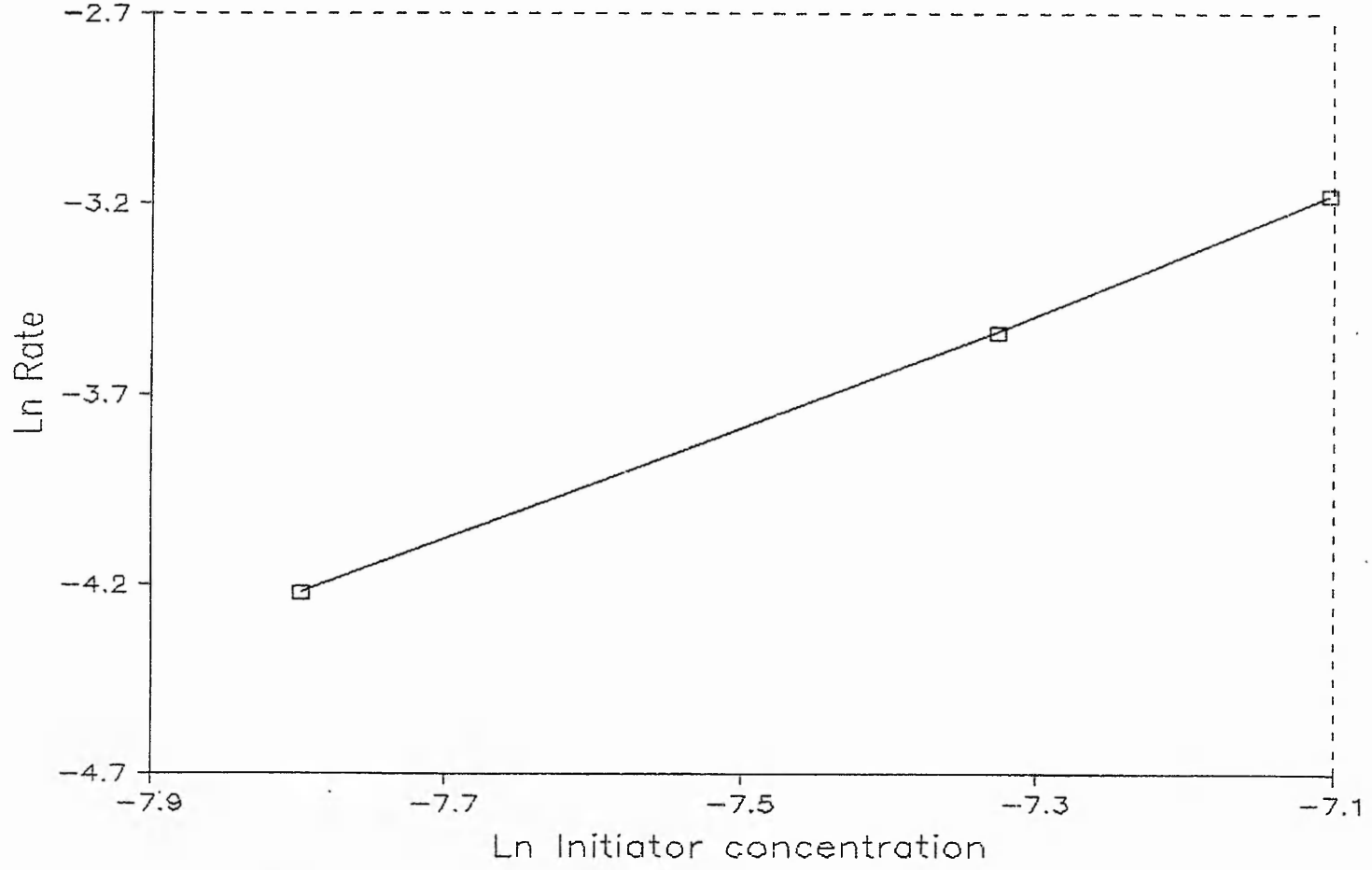

FIGURE III.9 THE FIRST ORDER RATE CONSTANT VERSUS THE INITIATOR CONCENTRATION

Initiator conc.= 8.23×10^{-4} mol dm^{-3}				
Code	Ionic strength mol dm^{-3} $\times 10^{3}$	particle size nm (final)	No density per cm^{3} $\times 10^{10}$	1st order rate constant $min^{-1} \times 10^{2}$
47	0.197	750	13	6.9
46	2.49	856	10	4.16
48	2.81	963	5	2.18

TABLE III:11 THE EFFECT OF VARYING IONIC STRENGTH AT CONSTANT INITIATOR CONCENTRATION

The influence of ionic strength on the particle size and number density was as expected and again similar to that found for PBMA. However, the overall reaction rate increased with decreasing ionic strength although the initiator concentration was constant. When the rate per particle is considered there is no increase in reaction rate. This may imply that the principle locus of polymerisation was the polymer particles. It is also possible that the increased ionic strength could have caused the water soluble polymer to precipitate out of solution at lower degrees of polymerisation and terminate upon coagulation with other precipitating chains, and thus remove reacting species from the water phase. This may be of importance if solution polymerisation is dominant, although it would seem unlikely that such large changes in the reaction rate would result from such small changes in ionic strength. Therefore pure solution polymerisation does not seem likely, but it cannot be ruled out totally.

III.2.4 THE EFFECT OF TEMPERATURE

All the reactions were carried out at an initiator concentration of 8.23 $x10^{-4}$ mol dm^{-3}. The effect of reaction temperature is shown in Table III:12. The particle size decreases and the polymerisation rate and particle number density increase with increasing temperature. An Arrhenius plot shown in Figure III:9 gives an activation energy of 14.6 kJ mol^{-1}. This value is very low in comparison with values for surfactant-free styrene polymerisations where figures of 69 and 71 KJ mol^{-1} have been quoted[16].

Code	Temperature °C	particle size nm (final)	No density per cm^3 (final) $x10^{10}$	1st order rate constant min^{-1} $x10^2$
44	60	1004	8	0.221
32	75	856	10	4.16
49	90	725	14.9	17.47

TABLE III:12 THE EFFECT OF REACTION TEMPERATURE

III.2.5 THE EFFECT OF ADDED SURFACTANT

Since PHEMA latices produced in the absence of surfactant were quite unstable and changes in the reaction conditions did not improve the latex properties, surfactant was added to the reaction recipe, to both reduce the particle size and hence the sedimentation rate,

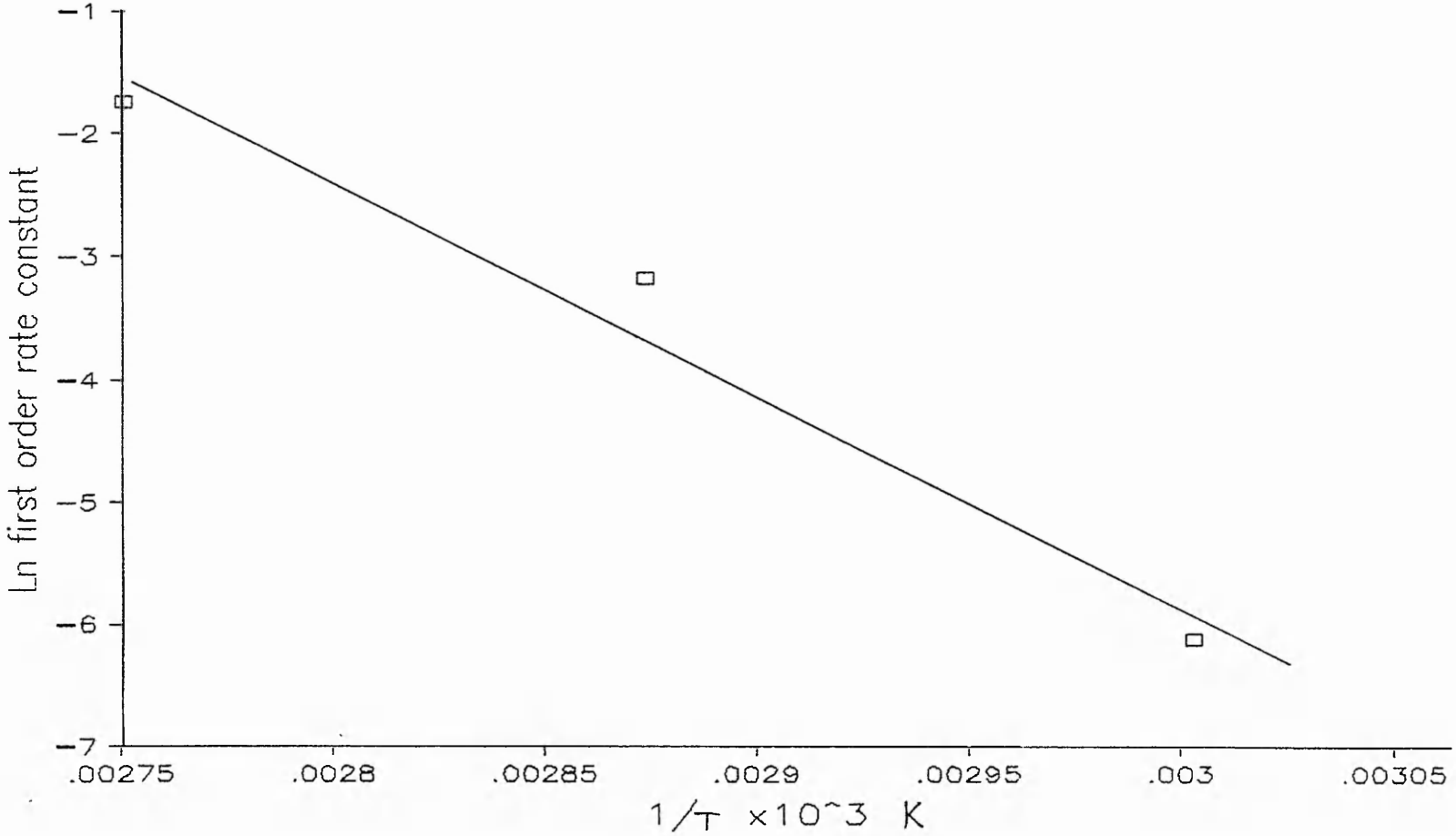

FIGURE III.10 ARRHENIUS PLOT OF THE Ln(RATE CONSTANT) VERSUS 1/T

and to increase the stability by increasing the surface charge. Sodium dodecyl sulphate(SDS) was chosen as the surfactant. Initially a typical emulsion recipe[37] was attemped. The conditions and concentrations were 1.69 mol dm^{-3} monomer, 9.57 $x10^{-3}$ mol dm^{-3} initiator (potassium persulphate) and 6.9 $x10^{-2}$ mol dm^{-3} surfactant (SDS), temperature 60°C and 350 rpm stirrer speed. The final product was a 420nm latex at 8.9% solids. However, a large amount of the polymer was lost as coagulum. A more systematic study of the effect of surfactant was undertaken and the results are shown in Table III:13. In all the reactions the monomer and initiator concentrations were 0.052 $x10^{-3}$ and 8.23 $x10^{-4}$ mol dm^{-3}, respectively and the reaction temperature was 60°C. A plot of the ln particle number density versus ln surfactant concentration is shown in Figure III:10. The gradient of the line was found to be 3.14. This value is much greater than the figure of 0.6 predicted by Smith and Ewart. Values higher than 0.6 have been found for other methacrylates when using SDS as the surfactant. Brodnyan[4] quotes a figure of 3 for n-butyl methacrylate and Fitch[22] quotes values of 1.08 and 3.87, depending on the initiator, for methyl methacrylate. Although the Smith Ewart model applies to styrene which has a low water solubility, the methacrylates in general are more water soluble and thus, deviation from the Smith and Ewart model is not unexpected. Vinyl acetate, however, has a higher water solubility than methyl methacrylate and shows a reasonable agreement with the predicted value of 0.6, with quoted figures being in the range 0.2 to 0.78[14]. French[33] gave theoretical reasons why the number of particles would

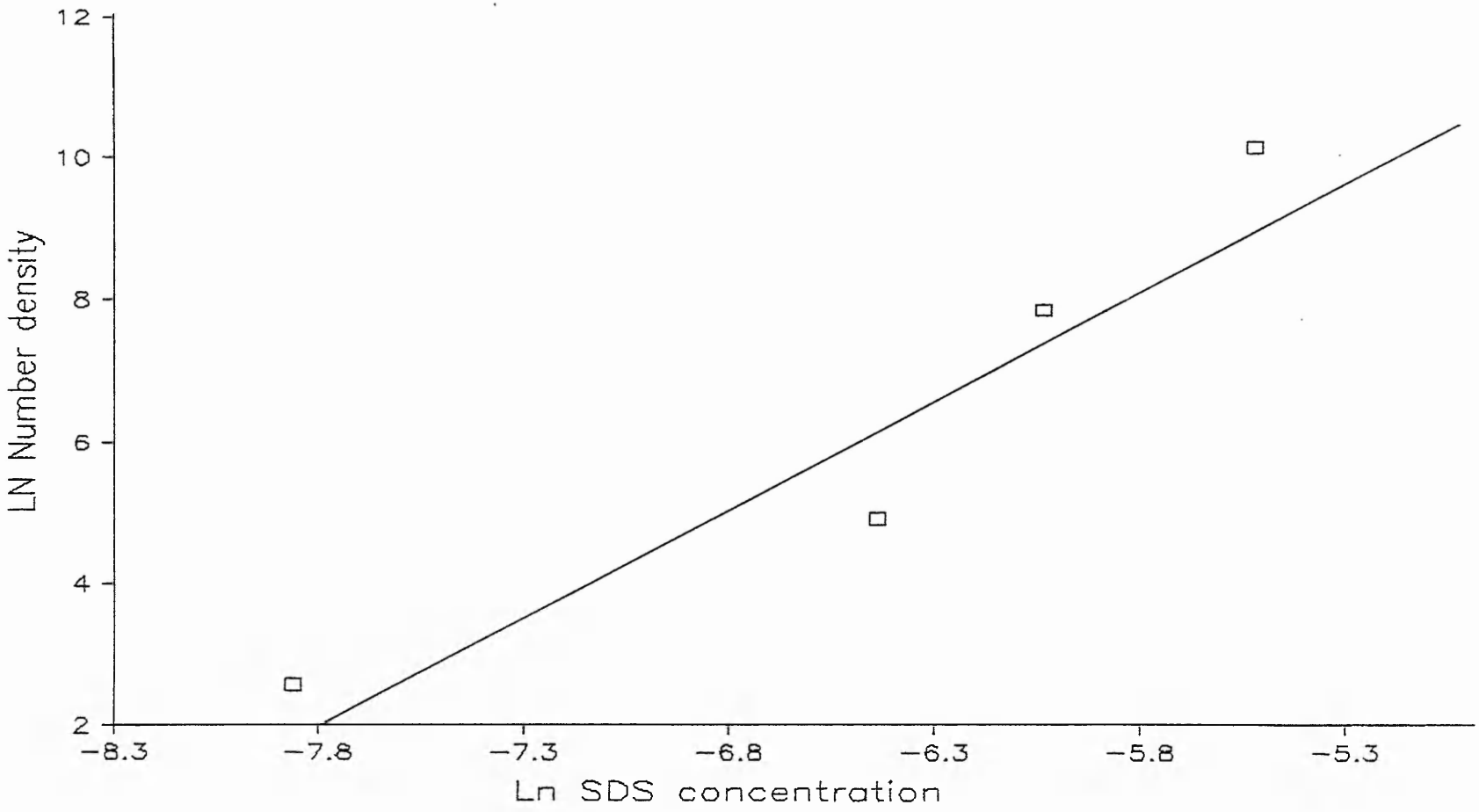

FIGURE III.11 THE EFFECT OF SDS CONCENTRATION ON THE PARTICLE NUMBER DENSITY

be dependent on the cube of the surfactant concentration. French argued that the surfactant stabilised a fixed surface area, and thus only so many particles could be stabilised for each given surfactant concentration. The large increase in both the reaction rate and particle number indicate that the polymer particles play a dominant role in the reaction mechanism, and further helps to rule out solution polymerisation.

Code	Conc [SDS] mol dm^{-3} $x10^{3}$	particle size nm(final)	No density per cm^{3} $x10^{-10}$	1^{st} order rate constant $min^{-1} x10^{3}$
32	0.0	1004	8	2.21
35	0.386	701	13	9.09
36	1.6	350	140	11.14
38	2.4	126	2600	18.89
34	4.0	60	26000	*

* No rate could be determined as this reaction was not sampled until turbidity had set in, at which time the reaction had gone to high conversion.

TABLE III:13 THE EFFECT OF SDS CONCENTRATION

III.2.6. MOLECULAR WEIGHT DETERMINATION

A selection of the latices described above were freeze dried and the molecular weight distributions of the polymers determined by GPC using dimethylformamide as the solvent. All the molecular weights are quoted as

poly(ethylene glycol)/poly(ethylene oxide) equivalents.

The first feature to note was the large amount of gel found in all of the samples, sometimes accounting for 90% of the weight of the polymer. This would imply that some degree of crosslinking or branching reactions had occurred. A typical example of the molecular weight distribution is shown in Figure III:12. The broadness of the peak, with the tailing towards lower molecular weights was a feature found in all the samples analysed. There appears to be a second and third peak that could be masked by the main peak as shown in Figures III:13 and III:14. This may be indicative of polymeristion in several loci, or more than one polymerisation mechanism taking place. Transfer reactions may also account for the broadness of the distribution.

The number average molecular weights varied from 5 $x10^4$ to 13.1 $x10^4$ and the weight averages were mostly in the range 20 $x10^4$ to 35 $x10^4$, although two of the samples gave values of 65 $x10^4$ and 96 $x10^4$ respectively.

III.2.7. IMPLICATIONS FOR THE REACTION MECHANISM

For a monomer with a high water solubility, solution polymerisation would be favourable. However, uncrosslinked PHEMA would in fact be expected to be water soluble. The evidence of high gel contents in the polymer from the GPC analysis indicates that a high degree of branching or crosslinking occurred, and this would account for the water insoluble polymer being formed. The formation of large amounts of gel are not usually attributed to the common methacrylic monomers, and thus

the presence of the hydroxy group is expected to be the cause of the gel formation. There is evidence to suggest that the decomposition of persulphate to give radicals is increased in the presence of alcohols[34] by hydrogen abstraction, and the following mechanism has been proposed[35]:

$$S_2O_8^{2-} \longrightarrow 2\ SO_4^{\cdot-}$$

$$SO_4^{\cdot-} + ALCOHOL \longrightarrow HSO_4^- + ALCOHOL^{\cdot}$$

$$ALCOHOL^{\cdot} + S_2O_8^{2-} \longrightarrow ALDEHYDE + HSO_4^- + SO_4^{\cdot-}$$

In the presence of monomers, both the persulphate and the alcohol radicals can initiate polymerisation[36]. In the present case the alcohol is the hydroxy monomer, and hydrogen abstration by the initiator would be the site for branching or crosslinking to occur. This fact alone could explain the discrepency between the rate dependence on the initiator concentration and accepted theories for emulsion or solution polymerisation. Also of note is evidence that the rate of decomposition of persulphate is dependent on its concentration to the power 1.5 in the presence of alcohol[35]. This may explain the rate dependence on the initiator concentration of 1.5 found in this study.

When considering a mechanism for particle formation, again the branching of the polymer would be significant. Water soluble polymer could undergo branching reactions and termination with other growing polymer chains to form very high molecular weight species which would precipitate from solution. Since this reaction scheme would form particles with polymer chains terminating in

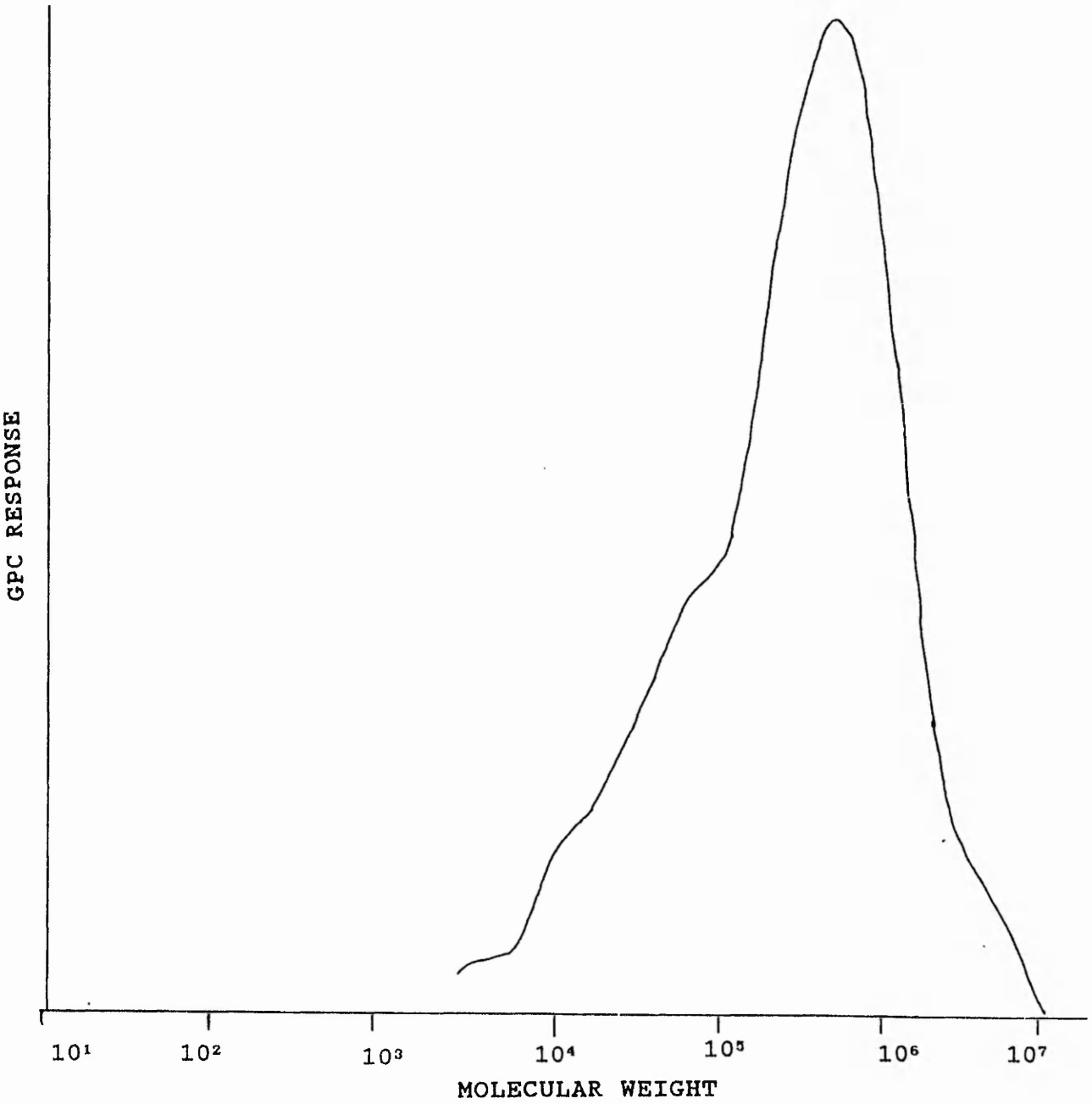

FIGURE III.12 MOLECULAR WEIGHT DISTRIBUTION FOR PHEMA LATEX

code 46

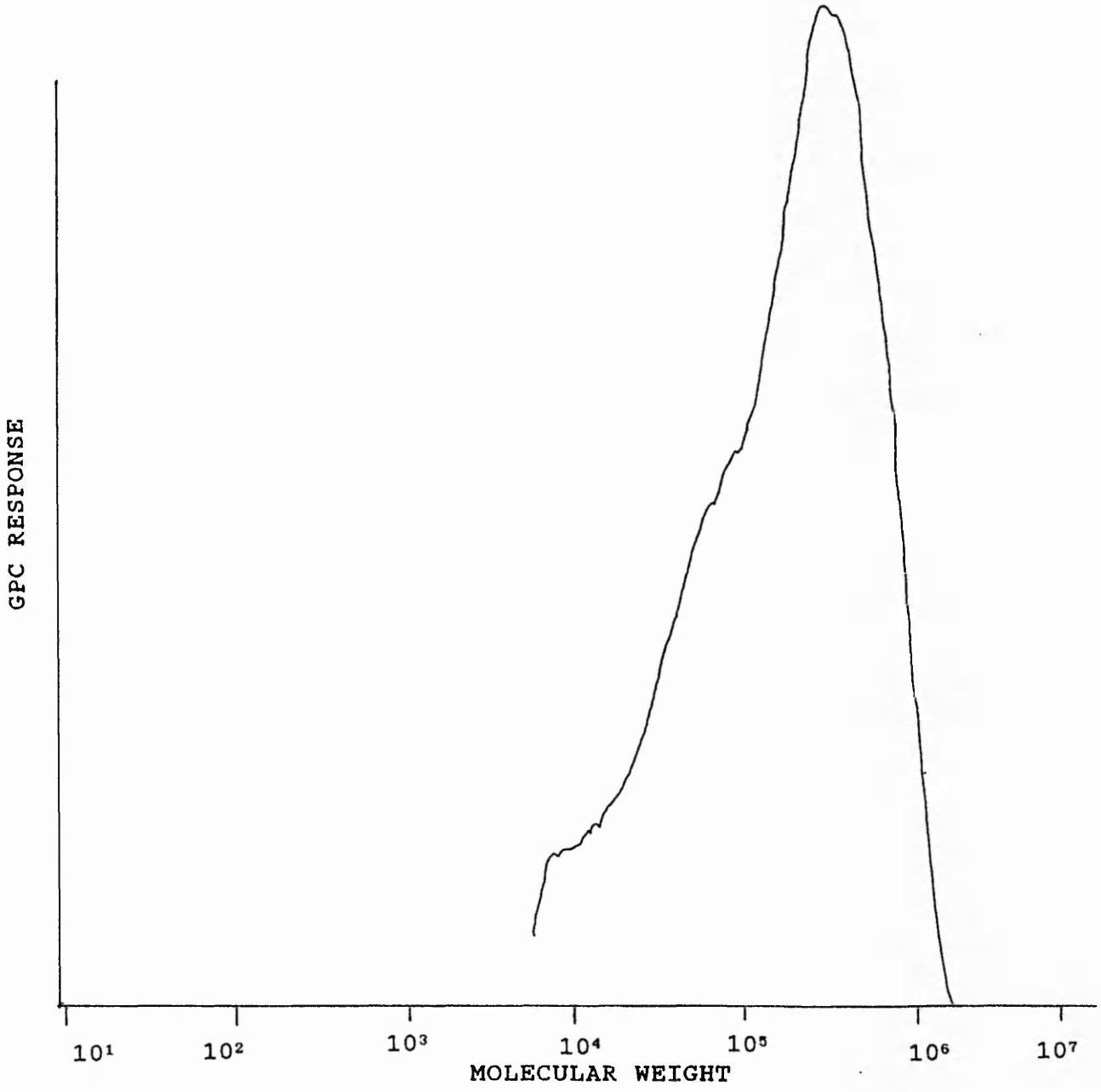

FIGURE III.13 MOLECULAR WEIGHT DISTRIBUTION FOR PHEMA LATEX code 36

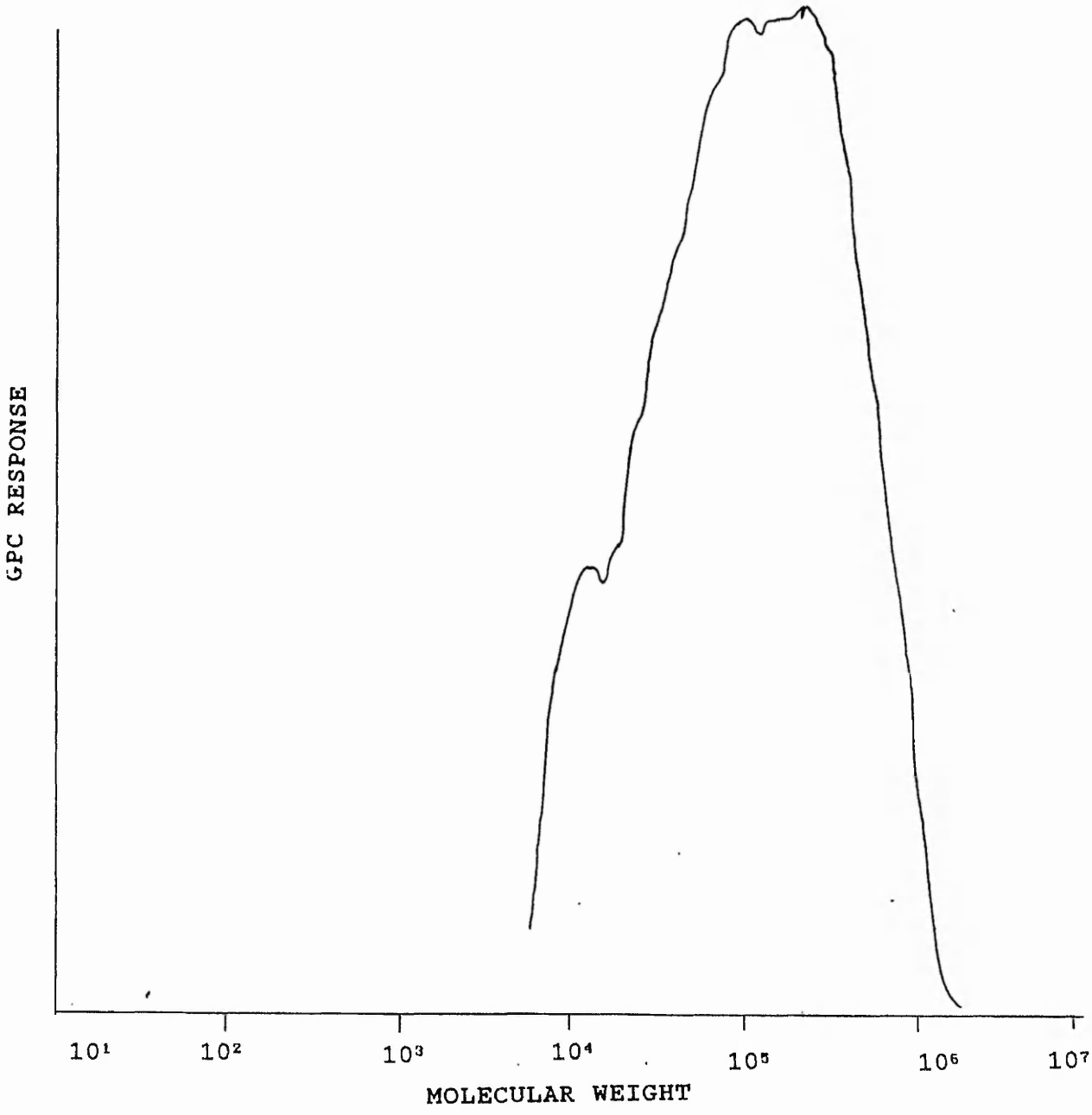

FIGURE III.14 MOLECULAR WEIGHT DISTRIBUTION FOR PHEMA LATEX code 32

both a sulphate ion and a species derived from the monomer, the surface charge would be low. This would explain the large particle size and the low stability of the latices. It is also possible that some of the water soluble polymer could be adsorbed on the polymer particles and behave like a surfactant. Measurement of the surface tension of a surfactant-free PHEMA latex by the Du Nouy ring method gave a value of 60.5±0.72 mN m^{-1}, indicating the presence of some surface active material. Electron micrographs of the surfactant-free polymer does in fact show some material on the particle surface which could be surfactant-like polymer. Whilst this mechanism would account for the production of water insoluble polymer in the form of a latex with poor stability it does not indicate how particle size develops, or the principal loci of polymerisation when polymer particles are present. Obviously polymerisation in the aqueous phase followed by heterocoagulation with existing particles is a strong possibility in this case. However, polymerisation in or on the particle surface could still be significant. When considering the effect of ionic strength on the polymerisation rate, the increase in the overall rate with increased particle number density in conjunction with a constant rate per particle indicates that polymerisation takes place in the particle to a significant degree. Also the large increases in polymerisation rate in the presence of surfactant indicates the particles as being a major loci for polymerisation.

In conclusion it is suggested that hydrogen abstraction from the monomer as well as the usual free radical opening of double bonds are responsible for the

initiation of polymerisation in HEMA and also that this abstraction leads to branching and crosslinking of the polymer to render it water insoluble. The polymer that becomes insoluble homogeneously nucleates new particles that are stabilised by sulphate end groups and adsorbed water soluble polymer. Although a rigorous study of the kinetics was not performed, existing models would seem not to predict the behaviour found here.

III.3 REFERENCES

1. D.C.Blackley; Makromol Chem., 1, 61 (1980).

2. A.R.Goodall, M.C.Wilkinson, J.Hearn;
   J.Polym. Sci. Chem. Ed., 15, 2193 (1977).

3. Chi-Yu Chen, I.Piirma; J.Polym. Sci., 18, 1979 (1980)

4. J.G.Brodnyan, J.A.Cala, T.Konen, E.L.Kelly;
   J. Colloid & Interface Sci., 18, 73 (1963).

5. J.L.Gardon; J.Polym. Sci., PtA-1, 6, 687 (1968).

6. E.Trommsdorff, H.Kohle, P.Lagally;
   Makromol. Chem. 1, 169 (1948).

7. W.S.Zimmt; J.Appl.Polym.Sci., 1(3), 323 (1959).

8. S.M.Hasan; J.Polym.Sci.Poly.Chem.Ed., 20, 3031 (1982).

9. I.Capek, J.Bartoh, A.Karpatyova; Makromol. Chem.,
   188, 703 (1987).

10. V.I.Yeliseyeva; in "Emulsion Polymerisation"
    I.Piirma (ed) Academic Press London 1982.

11. A Mamadaliev; Candidates dissertation, Institute of
    Physical Chemistry, Akad, Nauk, SSSR Moscow.

12. W.V.Smith, R.H.Ewart; J.Chem.Phys., 16,597 (1948).

13. R.H.Ottewill, J.N.Shaw; Kolloid Z.u.Z. Polymere, 218, 34 (1967).

14. R.M.Fitch; Br. Polym.J., 5, 467 (1973).

15. J.W.Goodwin, R.H.Ottewill, R.Pelton, G.Vianello, P.E.Yates; Brit. Polym.J., 10, 173 (1978).

16. M.Chainey; Ph.D Thesis, Trent Polytechnic, 1984.

17. J.Brandrup, E.H.Immergut (Eds); "Polymer Handbook" Second Edition, Wiley Interscience (1975).

18. Private communication, S.Holding, RAPRA, Shawbury, Shrewsbury, Shropshire.

19. J.L.Gardon; J.Poly.Sci., PtA-1 6, 687 (1968).

20. Idem, Ibid, 6, 665 (1968).

21. A.R.Goodall, M.C.Wilkinson, J.Hearn; in "Polymer Colloids II", Plenum Press, New York (1980).

22. R.M.Fitch, C.H.Tsai; in "Polymer Colloids" R.M.Fitch (ed) Plenum Publishers (1970).

23. N Sutterlin; in "Polymer Colloids II" Plenum Press, New York (1980).

24. S.Carra, M.Morbidelli, G.Storti; Proc. Int. Sch. Phys., 90, 483 (1985).

25. S.S.Medvedev; Int. Symp. Macromolecular Chemistry Pergamon press (1959).

26. L.F.Hahnan, D.H.Napper, R.G.Gilbert; J.Chem. soc Faraday Trans., 80, 2851 (1984).

27. G.M.Burnett, P.Evans, H.W.Melville; Ibid 49, 1096 (1953).

28. S.Lora, G.Palmo, L.Busulini, B.Castilletti; Eur. Polym.J., 10, 1223 (1974).

29. J.Ugelstad, P.C.Mork; Brit. Polym.J., 2, 31 (1970).

30. S.Kamei, M.Okubo, T.,Matsumoto; J.Polym.Sci., (1985).

31. Private communication B.J.Tighe, Aston University.

32. D.Monro, A.R.Goodall, M.C.Wilkinson, J.Hearn; J. Polym. Sci. Chem. Ed., 15, 2193 (1979).

33. D.M.French; J. Polym.Sci., 32, 395 (1958).

34. Marie, Bunel; Bull. Soc. Chim. Paris Ser.3, 29, 930 (1903).

35. P.D.Barlett J.D.Cotman; J.Am.Chem.Soc., 71, 1419 (1949).

36. Sankalia, Chandhuri, Hermans; Canad. J. Chem., 40, 2249 (1962).

37 J.Hearn; Private communication, Trent Polytechnic (1987).

38 H.Itagaki,J.E.Guillet, K.Sienicki, M.A.Winnik; J. Polym. Sci. Pt(c) 27, 21 (1989)

CHAPTER IV

THE MORPHOLOGY OF LATEX FILMS

Polymer films derived from synthetic latices have been shown, in several cases, to have some internal structure resulting from the film formation process.[1,5,6] This structure is said to be the result of the original latex particles only partially coalescing during film formation. In this study several techniques have been used to investigate the internal structure of latex films with a view to interpreting the permeability of the films, which is discussed in Chapter V.

IV.1 MERCURY POROSIMETRY

To test the applicability of mercury porosimetry to studying latex films a poly(stryene)/poly- (ethyl acrylate) 72:28 core shell latex was prepared by the shot growth technique[3]. This composition was such that there was insufficient shell polymer to form a complete non-porous film below the glass transition temperature of the core polymer[4]. The latex was cleaned by microfiltration and dried for six hours at 60°C. The resulting film was opaque and discontinuous, and as a result of the low drying temperature the film would be expected to be porous. Samples of this film were analysed in the mercury porosimeter, and Figures IV:1 and IV:2 show the cumulative and the differential pore volume respectively. The total cumulative pore volume was 385 $mm^3 g^{-1}$ with the bulk of the pores being in the region 188 to 15 nm radius, and the peak at 37.5 nm. There was also a small amount of porosity at pore radii of 5 nm. The total pore volume agrees well with the value of 383 $mm^3 g^{-1}$ predicted from close packing. A low magnification micrograph (Plate IV:1) shows a cross section of the film, and it is clear that the film is porous. Samples of the same film were heated for a further 2 hours at 95°C and Figures IV:3 and IV:4 show the cumulative and differential plots on samples of this film. The total cumulative pore volume had decreased slightly to 332 $mm^3 g^{-1}$, and the previously large peak at 37 nm was significantly reduced. The size of the pores had decreased with the further heating and now appeared to exhibit radii of 300nm and 9.4 nm. The micrograph of this sample (Plate IV:2) is similar

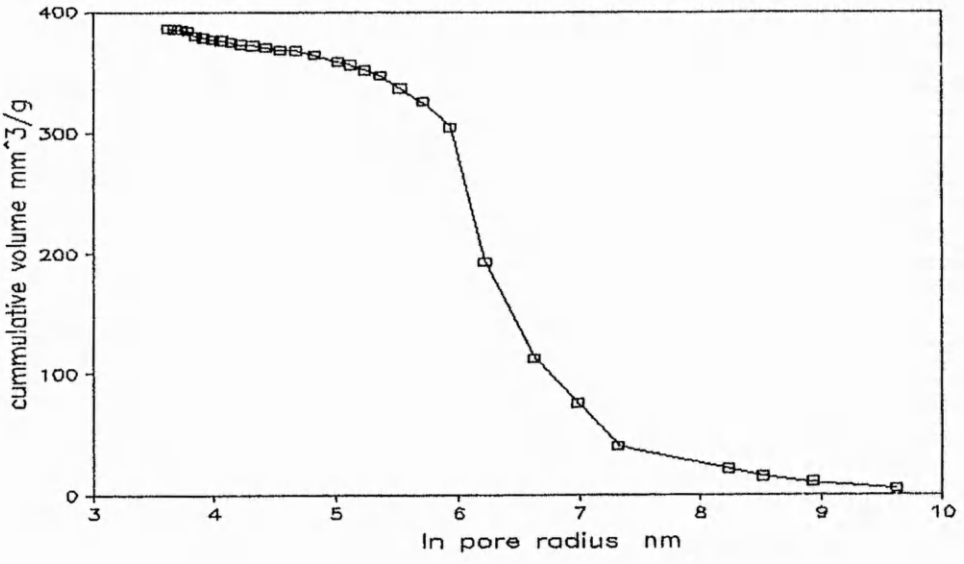

FIGURE IV:1 CUMULATIVE PLOT FOR 72:28 PS/EA LATEX FILM DRIED FOR 6 HOURS AT 60° C

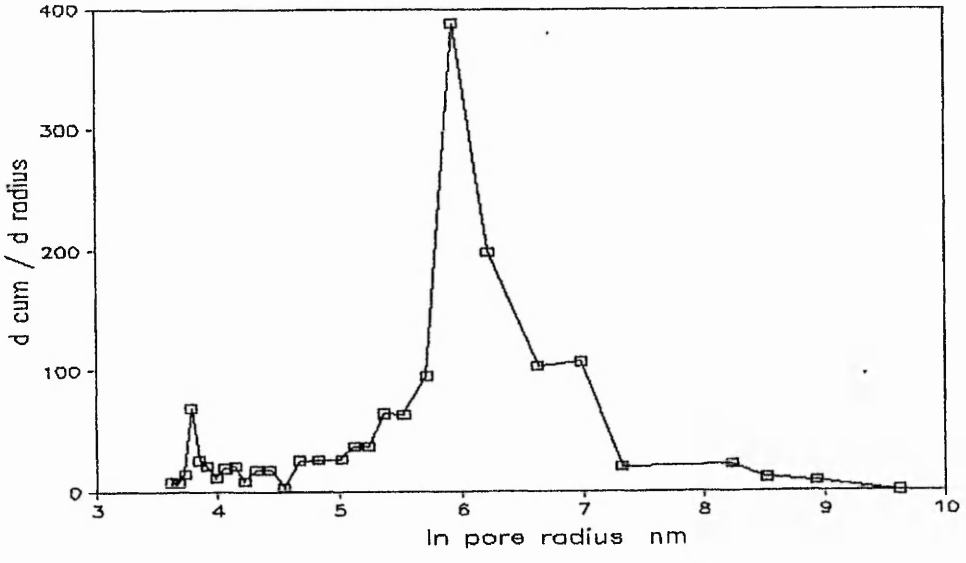

FIGURE IV:2 DIFFERENTIAL PLOT OF FIGURE IV:1

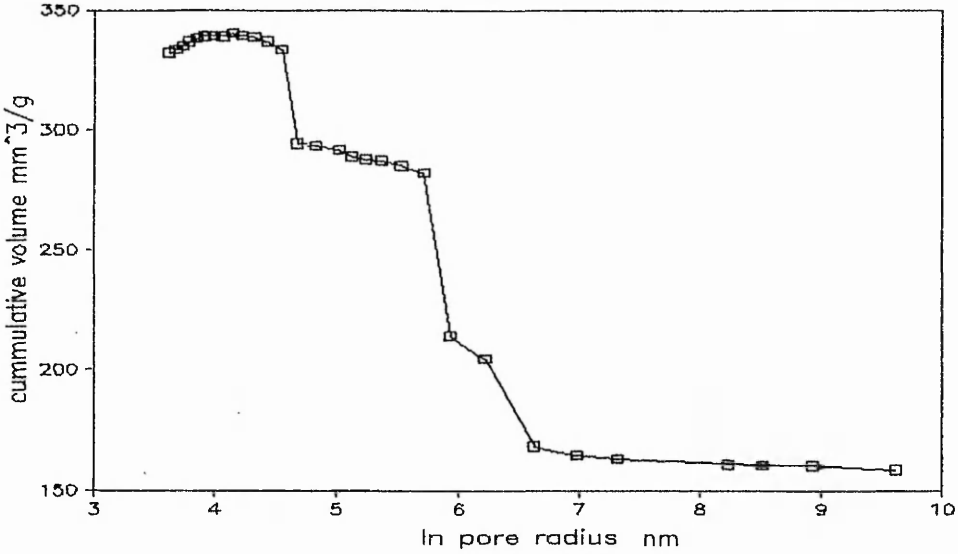

FIGURE IV:3 CUMULATIVE PLOT FOR 72:28 PS/EA LATEX FILM CURED FOR A FURTHER 2 HOURS AT 95°C

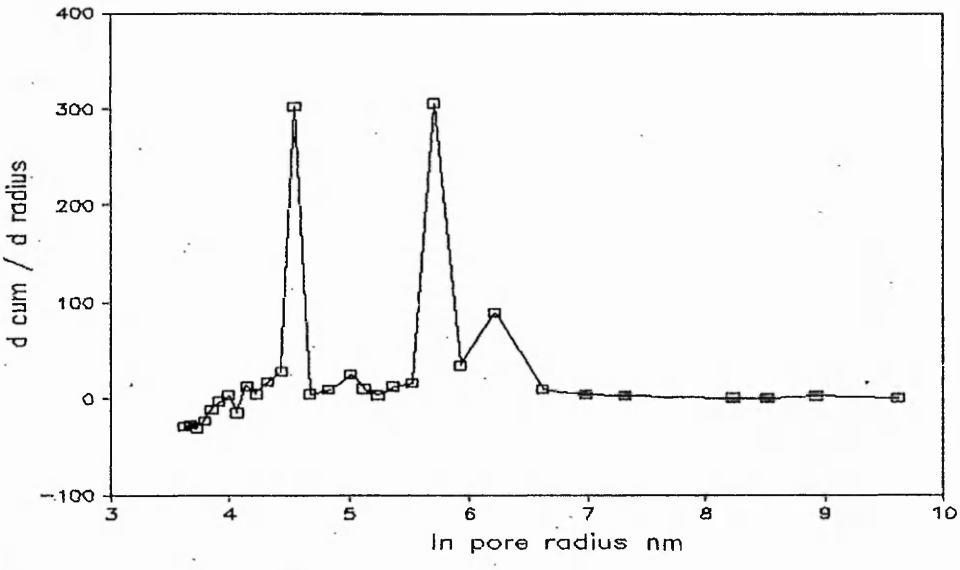

FIGURE IV:4 DIFFERENTIAL PLOT OF FIGURE IV:3

in appearence to the previous one. A further sample of the same film was heated for 2 hours at 130 °C. (this was higher than the glass transition temperature of the poly(styrene) core.[8]) The micrograph of this sample (Plate IV:3) shows the film to have no visible structure at this low magnification. The mercury porosimetry results for this sample are shown in Figures IV:5 and IV:6. In this case the cumulative pore volume has been drastically reduced to 40 $mm^3 g^{-1}$, and there is only slight evidence of pores with radii of <10 nm.

The film was deliberately prepared to be porous and the results clearly demonstrate that this was the case. Heating the film at tempertures below the glass transition temperature of the core polymer still gave a porous film. When the film was exposed to a temperature above the glass transition temperature of the core polymer the film underwent further sintering to produce a homogeneous film. This was indicated by the large reduction in the cumulative pore volume from 385 to 40 $mm^3 g^{-1}$ and also by the reduction and subsequent disappearance of the largest pores. Although the above results indicate that porosity in polymer films can be measured, the validity of the pore radii found by this method is questionable because of the extremely high pressures employed during the measurements.

A similar set of experiments was undertaken using poly(butylmethacrylate) latex. A sample of the cleaned latex was allowed to dry at room temperature (approximately 25° C) for 48 hours. This produced an opaque discontinuous film, as the film was formed at a temperature in the region of the glass transition temperature of the polymer. (There are conflicting

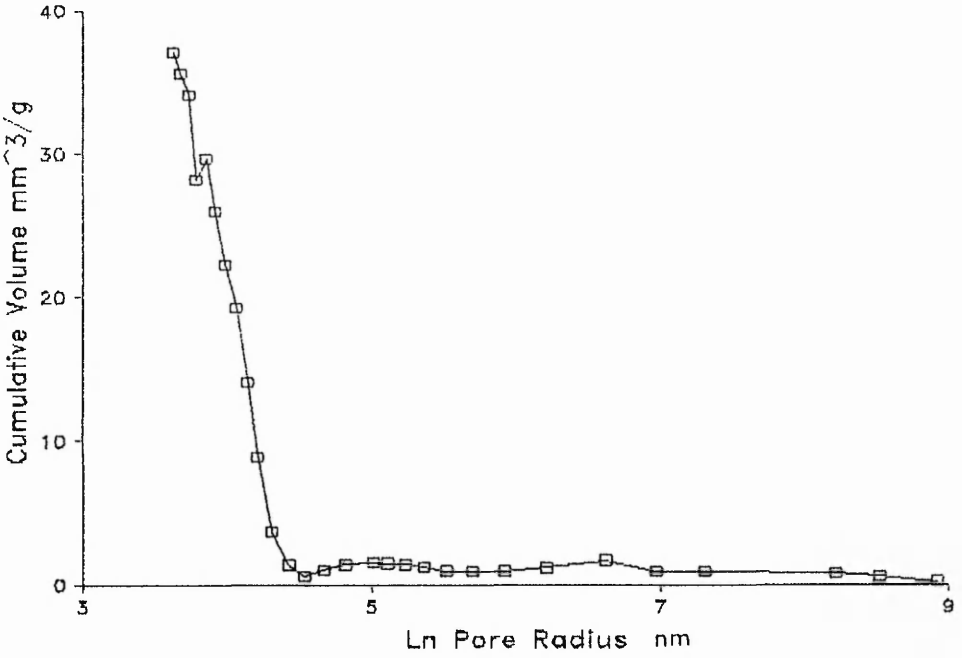

FIGURE IV:5 CUMULATIVE PLOT FOR 72:28 PS/EA LATEX FILM CURED FOR A FURTHER 2 HOURS AT 130°C

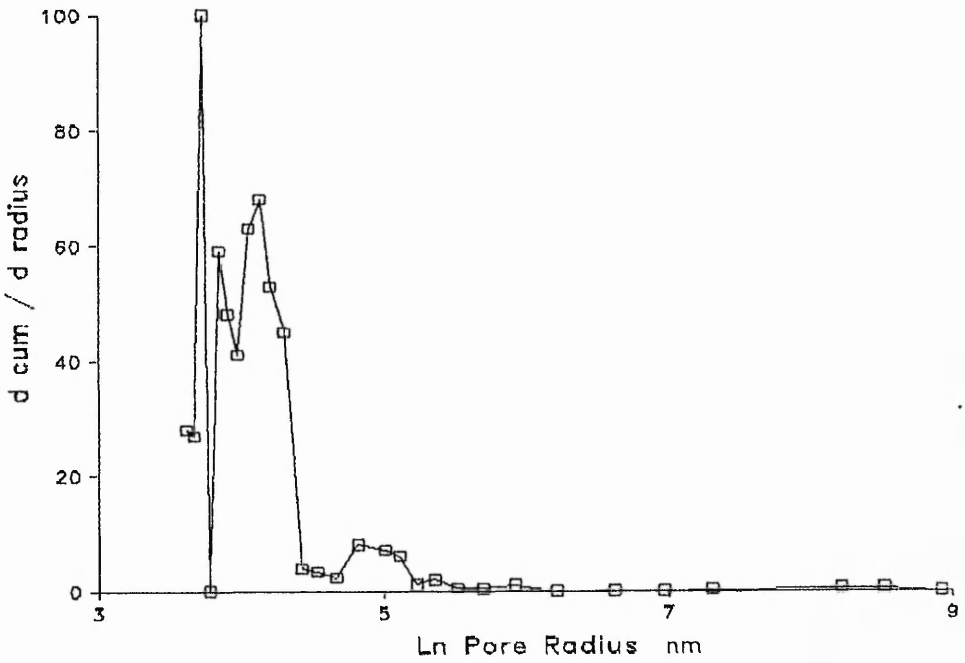

FIGURE IV:6 DIFFERENTIAL PLOT OF FIGURE IV:5

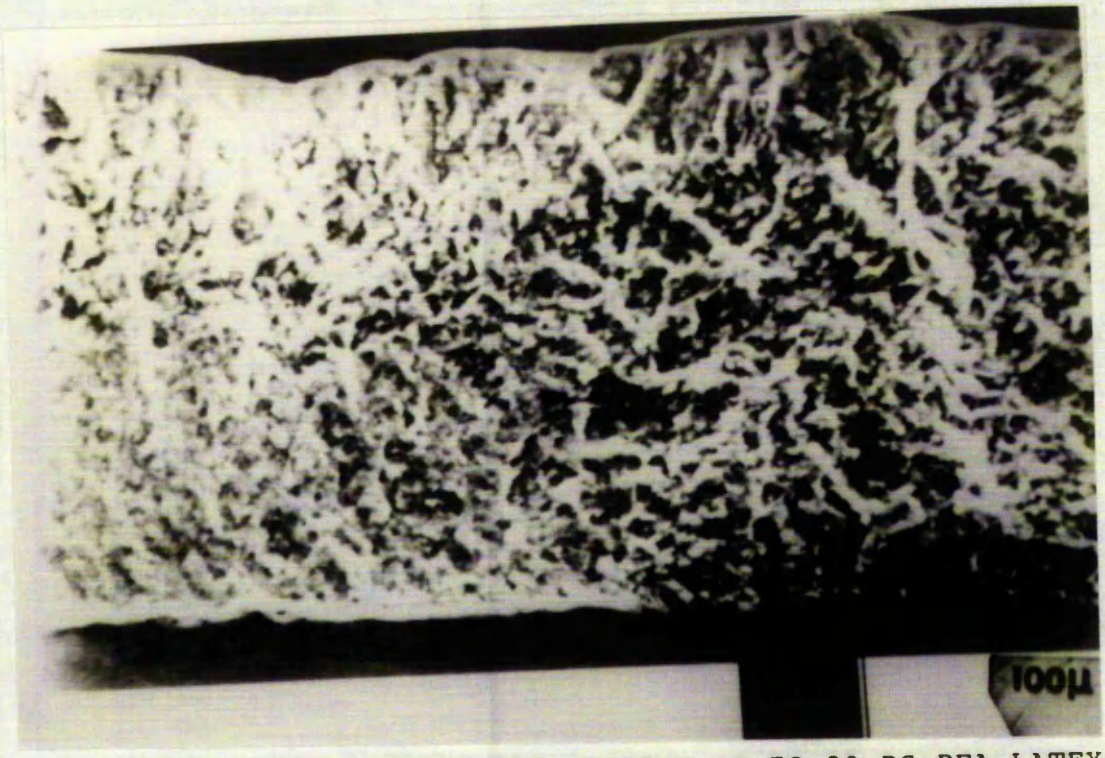

PLATE IV.1 SEM FRACTURE X-SECTION OF 72:28 PS:PEA LATEX FILM DRIED AT 60°C FOR 6 HOURS

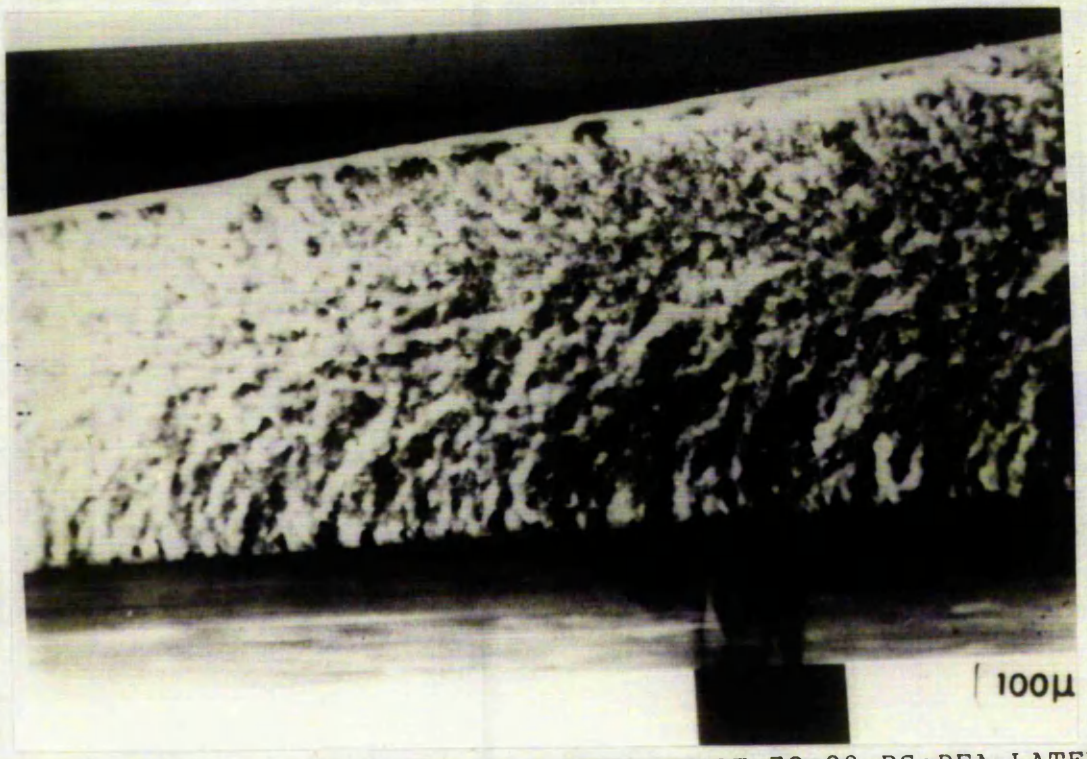

PLATE IV.2 SEM FRACTURE X-SECTION OF 72:28 PS:PEA LATEX FILM CURED AT 95°C FOR 2 HOURS

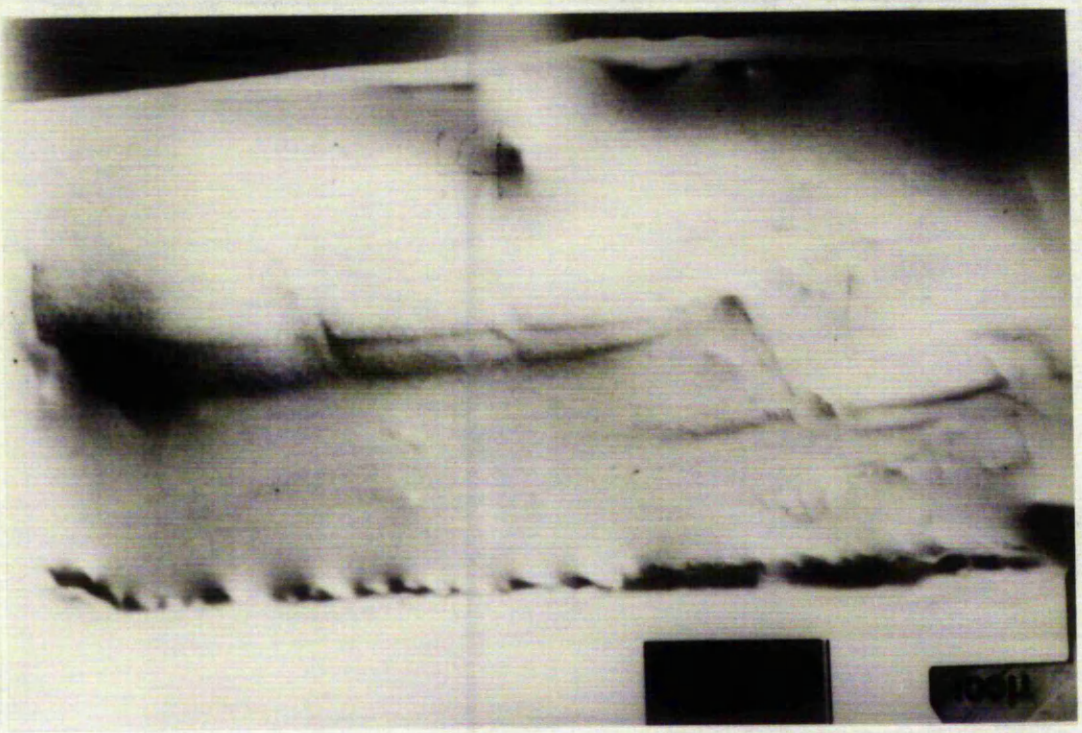

PLATE IV.3 SEM FRACTURE X-SECTION OF 72:28 PS:PEA LATEX FILM CURED AT 130°C FOR 2 HOURS

references to the actual value and several are quoted in the range 9 to 30°C in the Polymer Handbook[8]) Samples of this film were analysed using mercury porosimetry and the cumulative and differential plots are shown in Figures IV:7 and IV:8. The total cumulative pore volume was 58 $mm^3 g^{-1}$. The cumulative plot does not show the large steps as seen in Figures IV:1 and IV:3 indicating a low amount of porosity. The differential plot shows evidence for pores of radii < 20 nm. A fresh film was prepared from the same latex using the standard conditions employed for films used in the permeability experiments. This sample was dried for three hours at 80°C on a glass plate and formed a clear continuous film. The cumulative and differential plots are shown in Figures IV:9 and IV:10. The total cumulative pore volume was 37 $mm^3 g^{-1}$ and was lower than than that for the film dried at room temperature. i.e., 58 $mm^3 g^{-1}$. The differential plot shows there are pores of radii of approximately 19nm and in the region 4 to 10 nm. Melting range studies and differential scanning calorimetry (DSC) showed that poly-(butyl methacrylate) began to flow at about 120°C. The DSC result is shown in Figure IV:11. A sample of the film dried for three hours at 80°C was cured at 150°C for a further three hours which was sufficient to bring about partial melting of the polymer, and maybe remove the internal structure resulting from the particle coalescence. The cumulative and differential plots of a sample of this film are shown in Figures IV:12 and IV:13. The total cumulative pore volume was 45 $mm^3 g^{-1}$, and the differential plot shows that the porosity is almost non existent. The value for the cumulative pore volume is slightly higher than that found

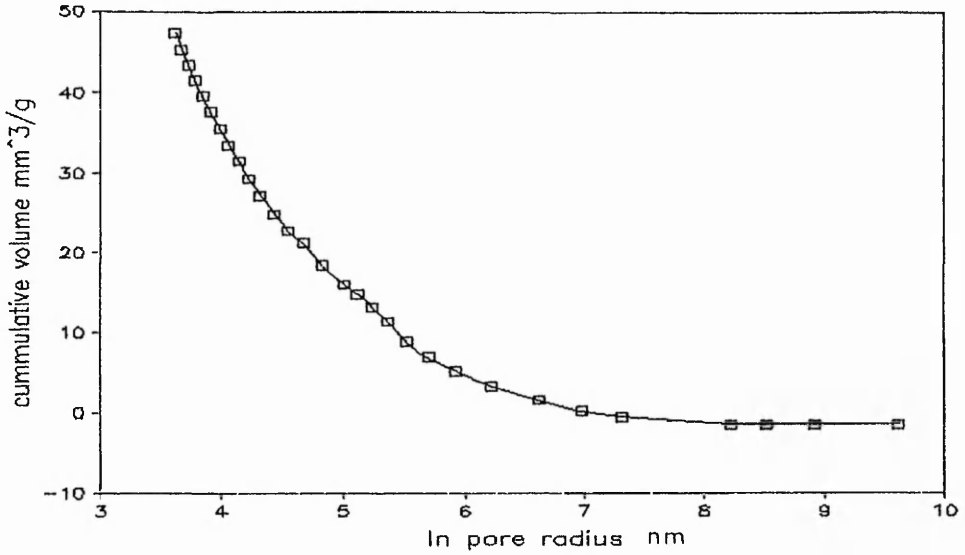

FIGURE IV:7 CUMULATIVE PLOT FOR PBMA FILM DRIED AT ROOM TEMPERATURE

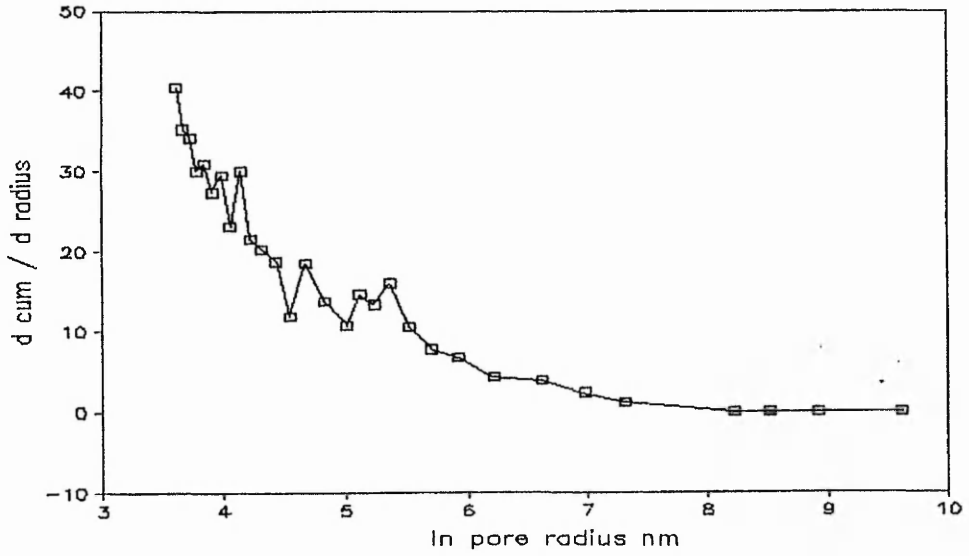

FIGURE IV:8 DIFFERENTIAL PLOT OF FIGURE IV:7

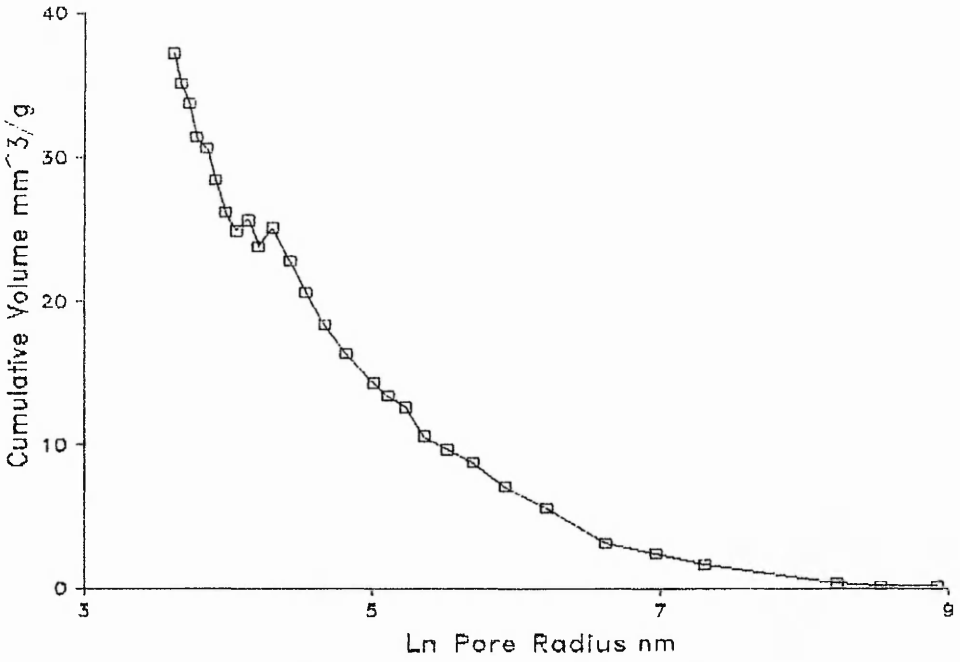

FIGURE IV:9 CUMULATIVE PLOT FOR PBMA FILM DRIED FOR 3 HOURS AT 80°C

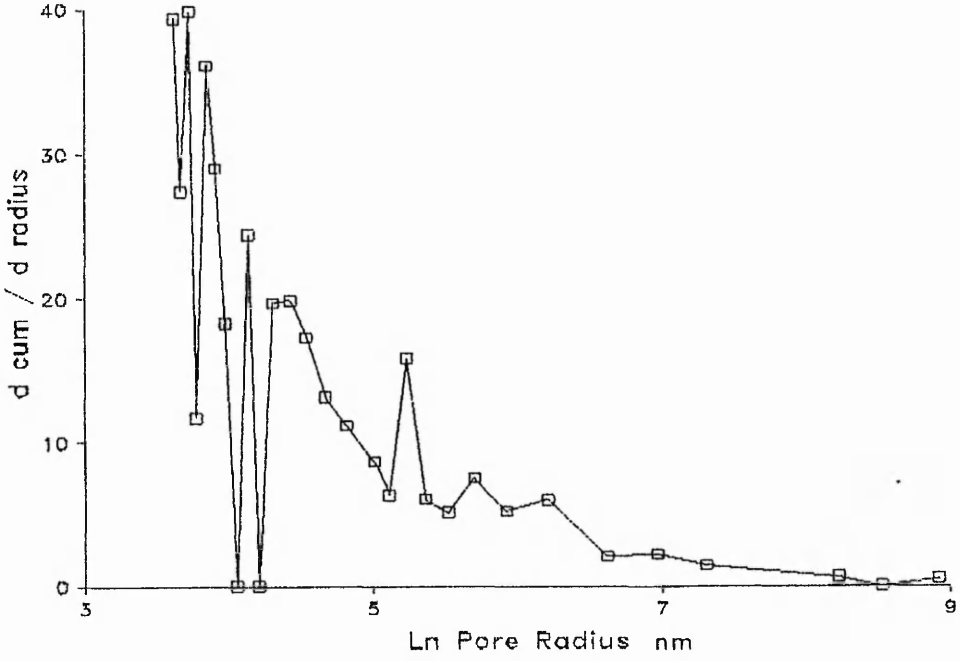

FIGURE IV:10 DIFFERENTIAL PLOT OF FIGURE IV:9

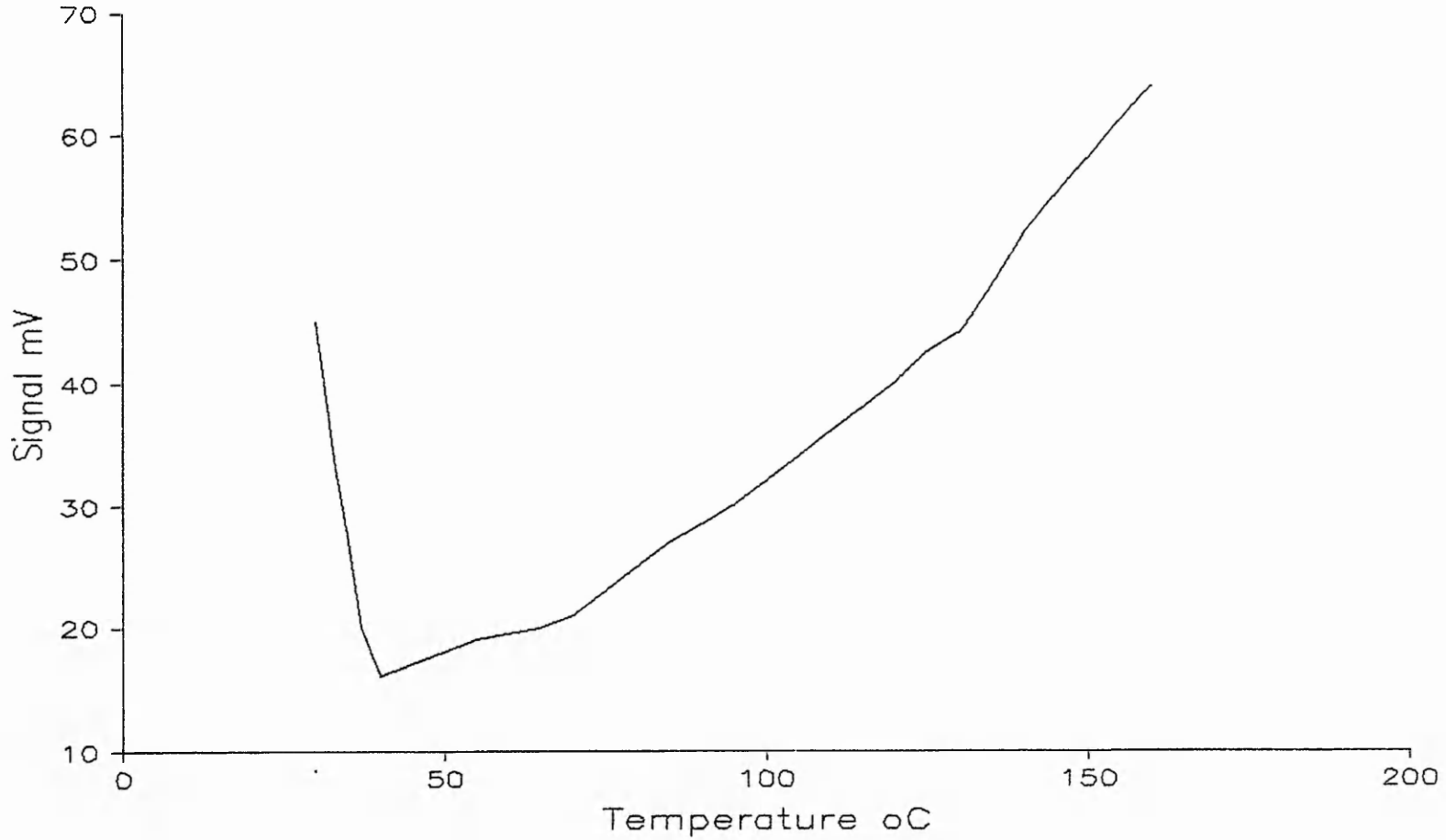

FIGURE IV:11 DSC PLOT FOR PBMA LATEX FILM

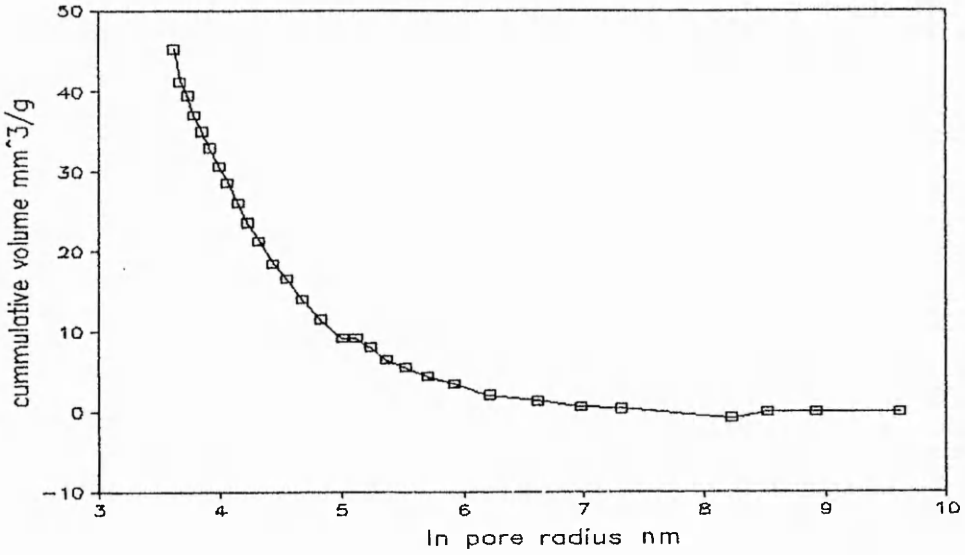

FIGURE IV:12 CUMULATIVE PLOT FOR PBMA FILM CURED AT 150° C FOR TWO HOURS

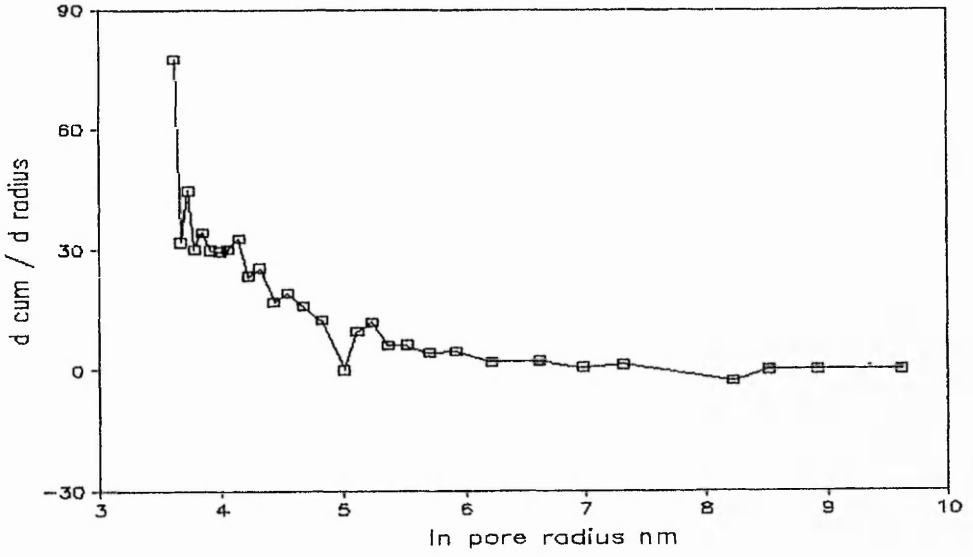

FIGURE IV:13 DIFFERENTIAL PLOT OF FIGURE IV:12

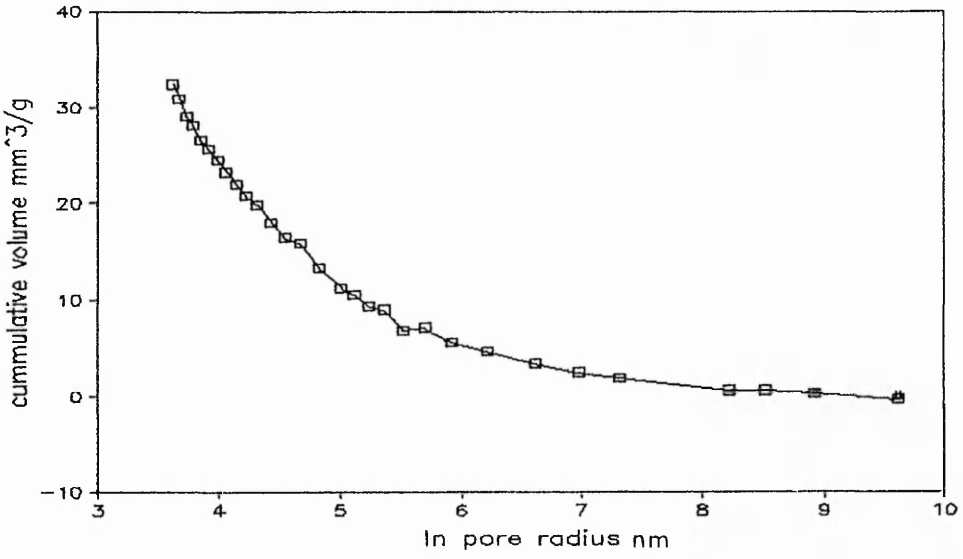

FIGURE IV:14 CUMULATIVE PLOT OF PBMA SOLVENT CAST FILM

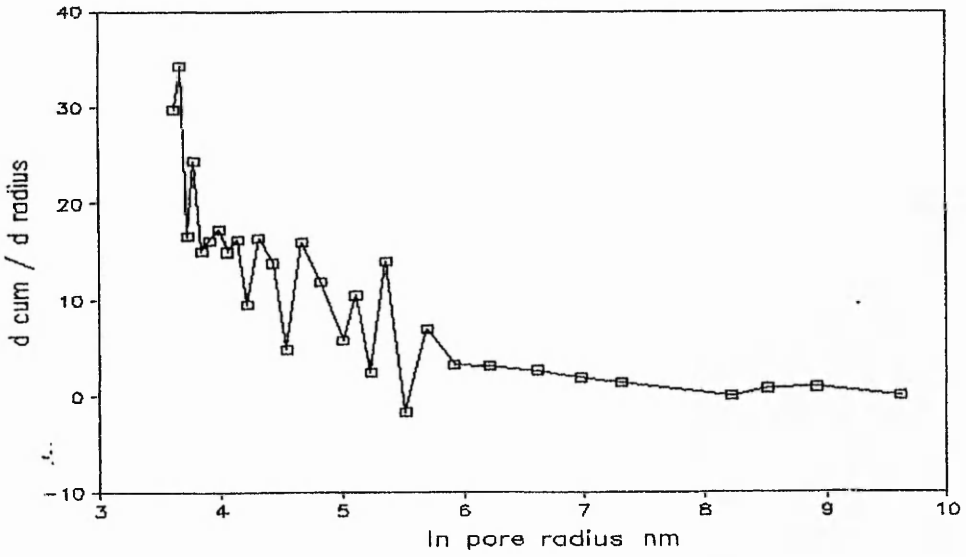

FIGURE IV:15 DIFFERENTIAL PLOT OF FIGURE IV:14

for the film prepared at 80°C, i.e., 37 $mm^3 g^{-1}$. This difference is probably due to the experimental errors in this technique, which is usually of the order of 10 $mm^3 g^{-1}$

The porosity of a solvent cast film was also determined by the same method; the cumulative and differential plots are shown in Figures IV:14 and IV:15. The total cumulative pore volume was 32.5 $mm^3 g^{-1}$. This value is similar to the lowest values obtained for latex films, and thus, may only be a reflection of the polymer compressibility. The differential plot shows slight evidence of porosity in the region 5 to 20 nm. This may be due to errors in the experiment rather than any significant porosity.

From the above results it seems clear that little or no porosity is present in the latex films when formed at temperatures significantly greater than the glass transition temperature of the polymer. The total cumulative pore volumes are all similar, and may simply be a measure of the polymer compressibility. The lack of any significant features in the differential plots also indicates the general absence of porosity.

IV.2 FREEZE FRACTURE ELECTRON MICROSCOPY

Samples of the same films as described above were examined using transmission electron microscopy*. The samples were freeze fractured and platinum/carbon replicas

* The author would like to express his gratitude to Dr A.Wilson, Centre for Cell and Tissue Research, University of York, for his part in this work.

were made whilst the sample was still at liquid nitrogen temperatures. This technique allowed the internal structure of the film to be examined at very high magnifications. Conventional scanning electron microscopy methods proved to be inadequate since at the magnifications required, the polymer distorted under the electron beam. Also, the fact that the samples were both fractured and replicated at liquid nitrogen temperatures allowed the 'true' internal structure to be examined. A sample of the PBMA latex film dried at room temperature is shown in Plates IV:4 to IV:6. In Plate IV:4 the regular array of the latex particles can be seen and the structure appears highly ordered although there is some evidence of disruption in the overall particle packing. Also shown in this micrograph are cracks in the film. These may either be a result of the fracturing process or stress induced during the film drying. Plate IV:5 shows the same film at higher magnification. Again the ordered structure is evident. Also, hexagonal(marked A) and diamond shapes (marked B) are clearly visible. The hexagonal shapes correspond roughly in size to the cross section of the original latex particles (400 nm in diameter). At the magnification concerned a latex particle would be 9 mm in diameter. The smooth diamond shapes represent the surface of a particle in the layer below the plane of the fracture. The hexagonal shape corresponds well with the findings of Distler[7] who used a staining technique to reveal a honeycomb structure in latex films, where the honeycomb spacing agreed with the latex particle size. Plate IV:6 shows the same film at a higher magnification, and as before the particles are clearly visible. A film

PLATE IV.4 TEM REPLICA OF FREEZE FRACTURE X-SECTION PBMA LATEX FILM DRIED AT ROOM TEMP.

2μm

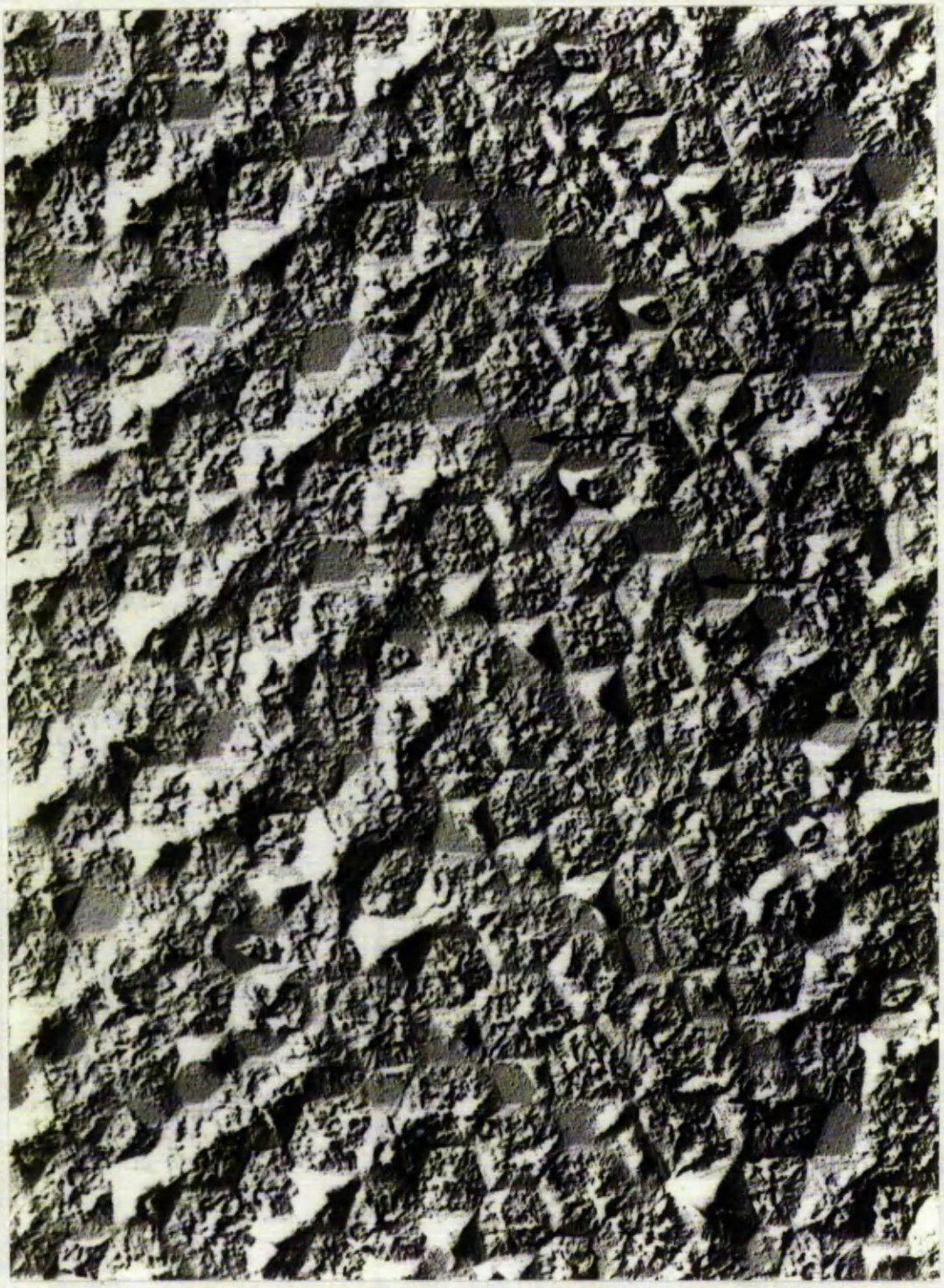

PLATE IV.5 TEM REPLICA OF FREEZE FRACTURE X-SECTION PBMA LATEX FILM DRIED AT ROOM TEMP.

PLATE IV.6 TEM REPLICA OF FREEZE FRACTURE X-SECTION PBMA LATEX FILM DRIED AT ROOM TEMP.

400nm

made from the same latex was dried for three hours at 80° C and micrographs were prepared in the same way. Plate IV:7 shows that the particles are regularly packed; however, there are several grain boundaries in the packing order. . As before, the individual particles are visible as hexagonal shapes. Plate IV:8 shows that the particle packing is not an idealised close packed structure, with the particles in clearly defined layers. The pattern is interrupted with particles from other layers breaking up the packing uniformity.

The evidence in the above plates suggests that the latex particles are, to a first approximation, close packed. This would imply a coordination number of twelve, i.e., each particle has twelve near neighbours, six in the same plane, and three in the plane above and below. Therefore, the hexagonal features could be due to fractures through the particles, and the sides of the hexagon represent the interface between the centre particle and its six near neighbours. If each particle around the centre particle caused it to deform in a uniform manner, then it would be reasonable to assume that the particle formed one of the space filling dodecahedra shapes. The faces of the dodecahedron would correspond to the interface between the centre particle and its twelve near neighbours. Of the space filling dodecahedra known, the rhombohedral dodecahedron has all the surface features that are seen in the micrographs (see Figure IV.16). This shape is made up of twelve rhombuses, each forming a face of the dodecahedron. The overall shape is not perfectly symmetrical, the main difference being the two types of vertices. The first type of vertex is similar to that

found on a trigonal based pyramid, and there are four of this type. The second type of vertex forms a square based pyramid, and there are three of this type.

Plates IV:6 and 8 show good examples of all the features which would correspond to the deformed latex particle taking the shape of a rhombic dodecahedron. In both of the plates the smooth areas correspond to the rhombohedral faces, and the rougher hexagons correspond to fractures through a particle. Also clear in Plate IV:8 are the raised trigonal and square based pyramid features which would represent one of the two types of vertex from a particle in the layer below the plane of the fracture. Plate IV:9 shows similar indented features where a particle was removed from the fracture plane. Although the choice of the rhombic dodecahedron implies that the particle packing is cubic closed packed, there is little evidence to prove that either cubic or hexagonal close packing is the dominant feature in latex film formation. One argument in favour of cubic close packing is that the symmetry of the rhombic dodecahedron leads to three axes for fractures which would produce a regular hexagonal cross section, but in a hexagonal close packed structure only one such fracture plane is possible.

The degree of coalescence of latex particles is known to increase with time[1,5,6], although it is not clear whether the interparticle boundaries ever completely disappear. In order to study coalescence two films were prepared, one at 80°C for three hours and one at 95°C for six hours. Both films were allowed to age at room temperature for one month. Plate IV:9 shows the sample cast at 80°C. The individual particles are just visible,

but the interparticle boundaries are indistinct, as is the case in Plates IV:6 to 8 which was of the same film 24 hours after preparation. Plate IV:10 shows the film prepared at 95°C; here there is some structure indicative of the original particles but the interparticle boundaries are not obvious. The loss of the identifiable boundaries agrees well with the notion of autohesion, and correlates with permeability data given in Chapter V, and else where[2].

A sample of the film prepared at 80°C was aged at 120°C for two days; the Plates IV:11 and IV:12 show that no particles or interparticle boundaries are evident. In Plate IV:11 the features are caused by differences in the fracture plane giving rise to cliffs and shadows. In Plate IV:12 the latex particles would measure 2.4 cm. The Plate shows no structure other than the morphology of the fractured polymer.

A sample of solvent cast PBMA film was also analysed and the micrograph is shown in Plate IV:13 . This Plate shows that the solvent cast film has no structure that corresponds to latex particles. The morphology shown is the same as in Plate IV:12

All the micrographs decribed above have been of freeze fractured samples, and thus, only the internal morphology has been discussed. Plates IV:14 and 15 show the upper and lower surface respectively, of a PBMA latex film cast at 80°C for three hours and aged one month at room temperature. The surfaces of the film are of interest for two reasons. Firstly, the upper surface of the film has a less glossy appearance than the lower surface. Here the upper surface is the film surface which formed the

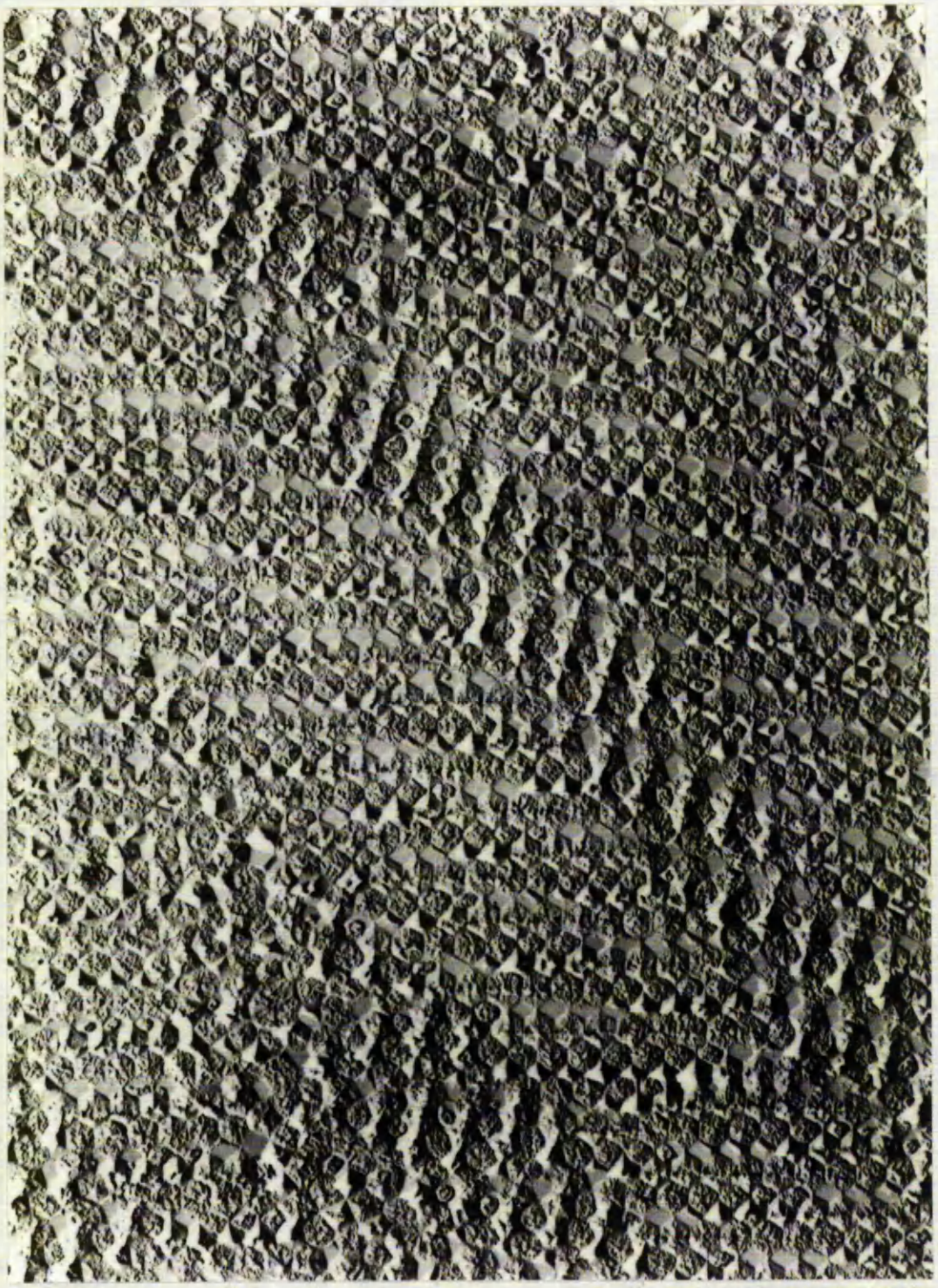

PLATE IV.7 TEM REPLICA OF FREEZE FRACTURE X-SECTION PBMA LATEX FILM DRIED AT 80°C FOR 3 HOURS.

400nm

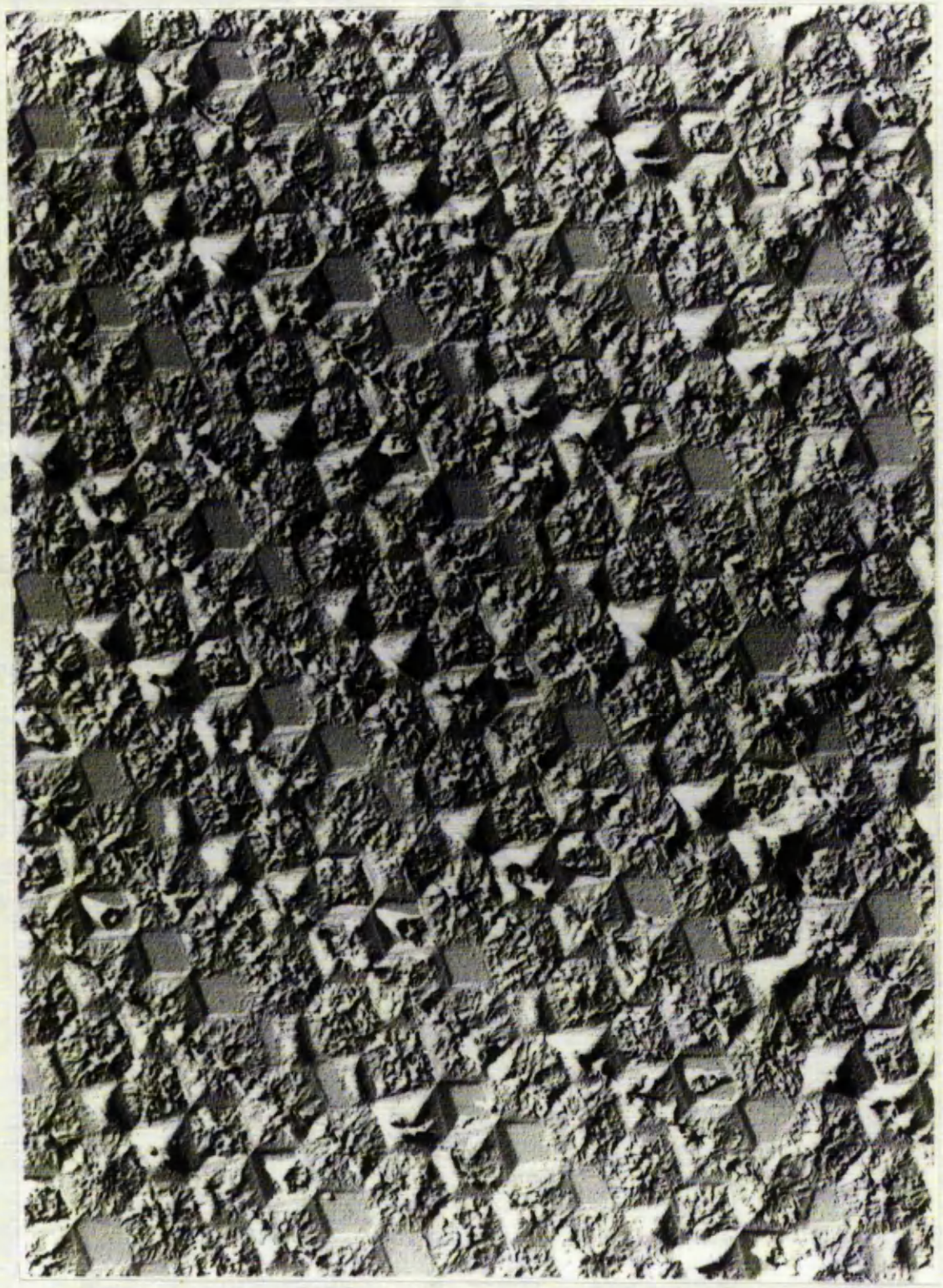

PLATE IV.8 TEM REPLICA OF FREEZE FRACTURE X-SECTION PBMA LATEX FILM DRIED AT 80°C FOR 3 HOURS.

400nm

PLATE IV.9 TEM REPLICA OF FREEZE FRACTURE X-SECTION PBMA LATEX FILM DRIED AT 80°C FOR 3 HOURS.

PLATE IV.10 TEM REPLICA OF FREEZE FRACTURE X-SECTION PBMA LATEX FILM DRIED AT 95°C FOR 6 HOURS.

PLATE IV.11 TEM REPLICA OF FREEZE FRACTURE X-SECTION PBMA LATEX FILM DRIED AT 120°C FOR 60 HOURS.

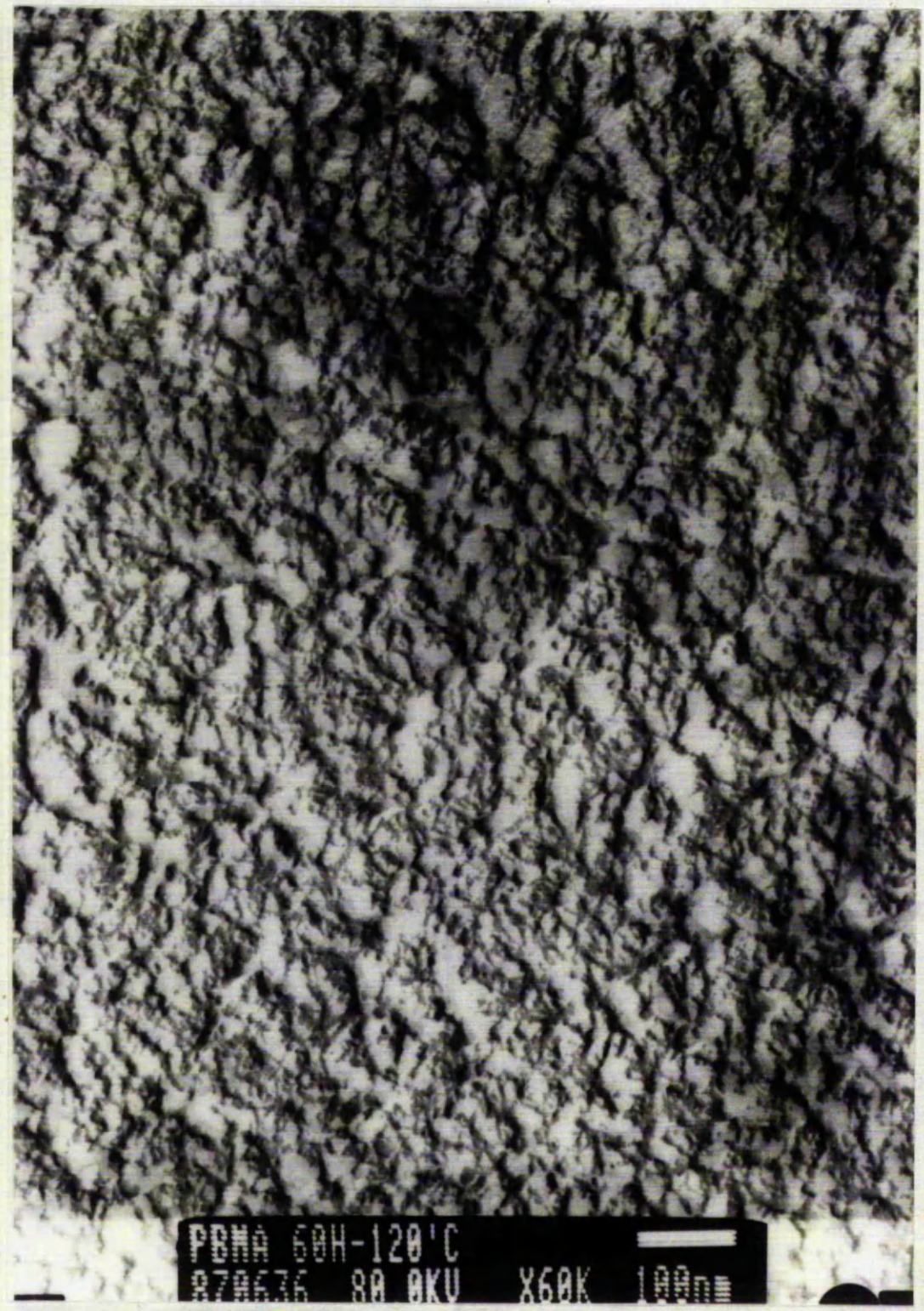

PLATE IV.12 TEM REPLICA OF FREEZE FRACTURE X-SECTION PBMA LATEX FILM DRIED AT 120°C FOR 60 HOURS.

PLATE IV.13 TEM REPLICA OF FREEZE FRACTURE X-SECTION PBMA SOLVENT CAST FILM.

PLATE IV.14 TEM REPLICA OF UPPER SURFACE OF PBMA LATEX FILM DRIED AT 30°C FOR 3 HOURS.

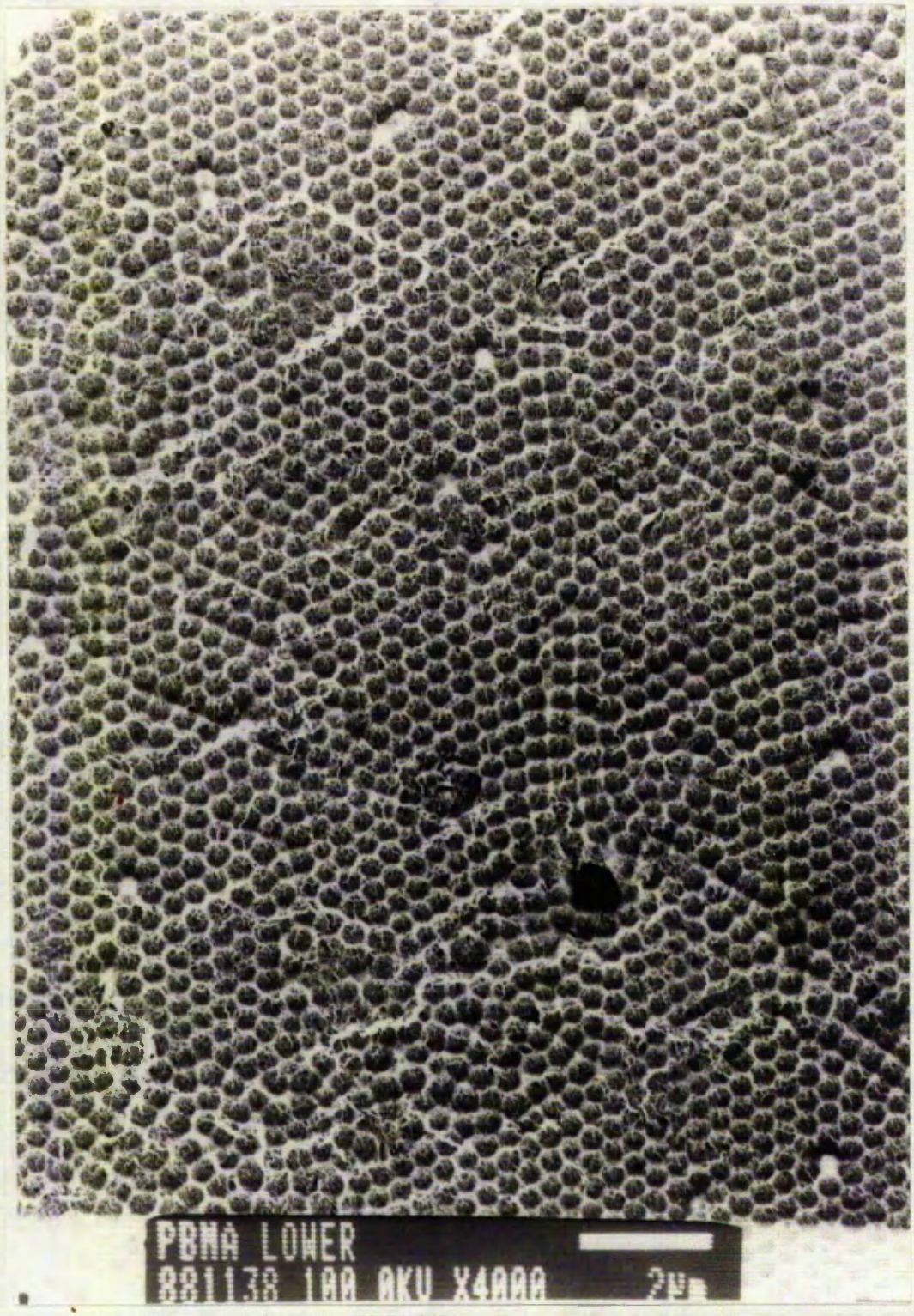

PLATE IV.15 TEM REPLICA OF LOWER SURFACE OF PBMA LATEX FILM DRIED AT 80°C FOR 3 HOURS.

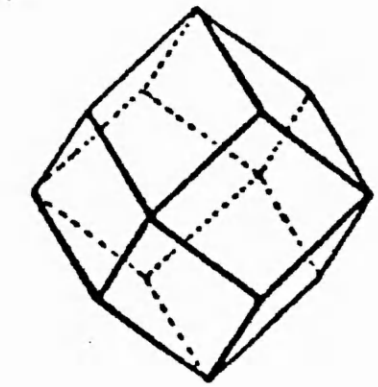

FIGURE IV.16 THE RHOMBIC DODECAHEDRON

air/latex interface during drying, and the lower surface is the one in contact with the substrate during film formation. Secondly, the permeabilities (discussed in Chapters V an VI) show a marked trend with respect to film orientation to the permeant. In Plate IV:14 the original latex particles are still clearly visible, and appear close packed. Two other quite striking features can also be found in the micrograph. Firstly, the dislocated nature of the surface disrupts the particle packing order, and the film surface is not made up of one continuous layer of particles, but is stepped. The second feature is the slight undulating appearance over the whole surface. These features are distincly different from those found in a replica of the lower surface (Plate IV:15). Here the particles still appear close packed. although there are regions of disorder. Also, this micrograph shows none of the undulations or stepped layers apparent in the upper surface. The flatness would account for the more glossy appearence in comparison with the upper surface.

IV.3 NITROGEN AND KRYPTON ADSORPTION*

A sample of the film prepared for three hours at 80°C was analysed using nitrogen adsorption. The BET surface area was determined in the range p/p_o 0.1 to 0.3 and was found to be 5.89 $m^2 gm^{-1}$. The value for the surface area was much greater than that of the flat sheet of

*The author is indebted to Dr.D Hall, Malvern Instruments, Spring Lane South, Malvern, Worcester, for his work on both the nitrogen, and krypton adsorption reported here.

polymer film used, (which would have been <0.01 $m^2 g^{-1}$). The surface area of a sample of a film dried for three hours at 80°C and then aged for one month at 25°C was determined using krypton adsorption. This gave a value of 0.37 $m^2 g^{-1}$. This value is much smaller than the surface area determined by nitrogen adsorption described above for sample prepared similarly. The large difference between the two results could be caused by capillary condensation of the nitrogen or more probably that the nitrogen was soluble in the polymer.

A further sample of latex film was prepared for krypton surface area analysis. The film was prepared by drying at 120°C for 60 hours. This heating should have completely removed all traces of the interparticle boundaries (see above) The surface area determined for this sample was 0.24 $m^2 g^{-1}$. The reduction in surface area is to be expected since most of the surface irregularities would have been removed by the partial melting of the polymer, and any penetration into the film via interparticle boundaries would be non existrnt. The surface area of a sample of a solvent cast film was also measured and was found to be 0.304 $m^2 g^{-1}$. This value is similar to the values found for latex films and indicates that the films have similar surface areas.

The measured surface areas by krypton adsorption are all greater than the geometric sizes of the samples, and this may either indicate porosity, or a certain degree of surface irregularity. The porosimetry and electron microscopy evidence does not support the idea of any appreciable porosity, and therefore it is suggested that the greater surface areas are derived from surface

irregularities.

IV.4 IMPLICATIONS FOR THE MECHANISM OF FILM FORMATION

The evidence presented above shows that whilst polymer films derived from latices have no significant porosity, at pore sizes greater than 3.75 nm, the latex particles retain some of their original identity after film formation. The main evidence comes from electron micrographs, which clearly show that the internal morphology of the film is due to the incomplete coalescence of the particles. The most striking feature found in all the micrographs showing particle structure is the high degree of packing order. This is taken to imply that the particles attained a high degree of order before irreversible contact was made. Because the electrostatically stabilised particles were dispersed in a medium of low ionic strength (all the latices were cleaned by microfiltration with double distilled water) the electrical double layers would have been extended. As the water evaporated the influence of these extended electrical double layers could have brought about particle ordering at reasonably low volume fractions of polymer, i.e., much lower than the 0.74 volume fraction for close packed spheres. Thus, when the double layers collapsed, through the loss of water from the film or the particles coagulated because of the lack of stability, then the polymer-polymer contacts would be made by particles already in a close packed arrangement. A similar notion was presented by Isaacs[9] who suggested a gelation stage during film formation.

The presence of particle identity in the majority of the film samples is in agreement with Distler and Kanig[1,7], who argued that latex particles would never undergo complete coalescence because the surface groups where incompatible with the particle interior. From the above work it seems that to achieve what appears to be total particle coalescence, the polymer film must be raised above the melting point of the polymer.

The higher degree of particle packing on the upper surface of the film is in keeping with findings of Durbin[10]. He showed micrographs indicating that the packing order was greatest at the upper surface, as this surface forms first, whilst the lower surface suffers some premature coagulation due to the ionic strength of the remaining water increasing due to concentration effects. A model for latex film formation given by Bierwagen[11] also included the upper surface of the film forming initially, and the film drying from the top to the bottom.

From the above arguments the process of latex film formation is believed to take place as follows:

(i) The volume fraction of the polymer increases as the water evaporates in a manner described by a number of workers[5,11].

(ii) At some point the particles form an ordered structure, due to the interaction of their electrical double layers, leading to a structure with an apparent volume fraction of 0.74

(iii) The particles begin to coalesce, forming an orderd array at the upper film surface, and this layer gets progessively thicker as the film forms towards the lower surface. The fractures shown in the upper surface are due to stresses arising form shrinkage during film formation. These stresses cannot be dissipated by the newly formed film, which cracks.

(iv) The film formation continues and the ionic strength of the water increases. The increase in ionic strength causes some coagulation of the particles at the lower surface.

(v) The particles retain their identity within the film forming a close packed array of hydrophilic boundaries which continue to become less distinct with time and can be fully removed by partial melting of the polymer.

IV:5 REFERENCES

1. D.Distler, G.Kanig; Colloid Polym. Sci. 256, 1052 (1978).

2. M.Chainey, Ph.D Thesis, Trent Polytechnic, 1984.

3. M.Chainey, M.C.Wilkinson, J,Hearn; Ind. Engng. Chem, Prod.Res.Dev., 21, 171 (1982).

4. L.J.Hughes, G.L.Brown; J.Appl. Polym. Sci., 5, 580 (1961).

5. E.B.Bradford, J.W.Vanderhoff; J. Macromol. Chem., 1, 335 (1966).

6. Idem; J.Macromol Sci-Phys, B6, 671 (1972).

7. D.Distler, H.Neff; Colloid Polym.Sci., 253, 29 (1975).

8. J.Brandrup, E.H.Immergut(eds.) "Polymer Handbook", second edition Wiley-Interscience (1975).

9. F.K.Isaacs; J.Macromol Chem., 1(1), 163 (1966).

10. D.P.Durbin, Ph.D Thesis, Lehigh University, 1980.

11. G.P. Bierwagen; J.Coating Technol., 51(658), 117 (1979).

CHAPTER V

PERMEATION THROUGH POLY(BUTYLMETHACRYLATE) LATEX FILMS.

The majority of the published work on film transmission properties has been carried out using film specimens prepared by such methods as solvent casting, compression moulding and extrusion. Even though latex films have been shown to have a distinct internal structure[1] there have been relatively few studies on the effect of film morphology on latex film permeability. However, recent studies[2,3] have shown that the permeability of latex films is influenced by the degree of particle coalescence. The influence of the film morphology is expected to affect the coating performance in any of the varied applications of polymer latices, e.g., adsorbent binders and barrier coatings. With this in mind a study of the effect of film morphology on the permeability of aqueous solutes through films cast from polymer latices was attempted. In the first part of this chapter the permeability of poly(butyl methacrylate) latex films is discussed, whilst the second half deals with the permeability of some heterogeneous films derived from copolymers and core-shell polymer latices.

V.1 A COMPARISON OF LATEX AND SOLVENT CAST FILMS.

The permeability of several permeants through both latex and solvent cast films was studied. The solvent cast films were studied with a view to determining the permeability coefficients of bulk polymer films so that the influence of the interparticle boundaries found in latex films could be determined.

V.1.1 HELIUM PERMEABILITY

The helium permeabilities were measured using the Daventest permeability apparatus, employing the British Standard method[4]. The average permeability coefficients were 2.69 ± 0.05 and 2.81 ± 0.16 $\times 10^{-16}$ sm^3kg^{-1} for butanone and toluene cast films respectively. These values are nearly three times larger than values reported by Chainey[3]. However, the values obtained by Chainey were determined using a dynamic flow system, with no net pressure difference across the film. The values obtained in this study were determined when the net pressure difference across the film was nearly one atmosphere. Since the method of film preparation, thermal history and particularly the method of measurement were significantly different, the discrepancy is understandable[5].

It has been suggested that residual solvent in polymer films can plasticise the polymer and may lead to an increased permeability coefficient[6]. To test whether residual solvent was responsible for causing higher permeability coefficients a sample of a PBMA film cast from butanone was heated to 70°C for two hours, and a helium permeability coefficient of 2.77 $\times 10^{-16}$ s m^3kg^{-1} was determined. A second sample of the same film was stored under vacuum for three days at 60°C and this yielded a permeability coefficient of 2.71 $\times 10^{-16}$ s m^3kg^{-1}. Both of these values are within one standard deviation of the results quoted above. Thus, it appears that the permeability coefficient was unaffected by the residual solvent since the values would be expected to be

lower if plasticising solvent had been removed.

Various latex films, prepared at temperatures between 55 and 95°C, all gave permeabilities greater than the apparatus could measure. Therefore, the permeability coefficients would be greater than 1 $x10^{-14}$ s $m^3 kg^{-1}$. As described in Chapter IV, PBMA has a melting range beginning at 120°C, and with this in mind a sample of PBMA latex film was conditioned at 125°C for 2 hours. This sample gave a helium permeability coefficient of 2.45 $x10^{-16}$ s $m^3 kg^{-1}$. Since the film was exposed to a temperature that would bring about a great deal of softening, if not partial melting, then a considerable amount of coalescence between the latex particles would have occurred. This was demonstrated in Chapter IV, where the interparticle boundaries were indistinguishable in the film sample heated above the softening point (120°C). Thus, it is suggested that the films prepared in the usual range of temperatures, i.e., less than 100°C, had particles that were coalesced, but not sufficiently so as to prevent permeation occurring through the interparticle regions, whereas the sample that had been heated to 125°C had little or no remaining interparticle boundaries where the permeation would be facilitated. This may also explain why Chainey[3] was able to measure helium permeabilities of latex films, since the film preparation was performed at temperatures in excess of 120°C.

V.1.2 WATER PERMEABILITY.

Water permeabilty coefficients were determined as described in Chapter II. The weight loss with respect to time was found to be linear after a short equilibration time (one hour) for both latex and solvent cast films. The permeability coefficients are shown in Table V:1. The latex films had been cast for three hours at 80°C and aged at ambient temperature for one month. The permeability coefficient for latex films was higher than for solvent cast films, and both films showed significant differences in permeability coefficients with respect to film orientation. The upper side was the film surface in contact with air during film formation and the lower side was the surface in contact with the substrate during formation. The effect of film orientation on water vapour permeability was also found for various latex films (see below).

V.1.3 WATER VAPOUR PERMEABILITY.

The water vapour permeabilities of solvent cast and latex films were determined as described earlier. The values for the latex films 24 hours old and one month old were 2.1 ± 0.3 and 1.4 ± 0.1 $\times 10^{-17}$ s $m^3 kg^{-1}$, respectively. The corresponding values for the solvent cast films were 1.7 ± 0.06 and 1.7 ± 0.10 $\times 10^{-17}$ s $m^3 kg^{-1}$ for the initial and aged values, respectively. From the above it is evident that

For latex films cast for 3 hours at 80°C after 24 hours			
Permeability coefficient $h\ m^{-2}$ $x10^7$	orientation to water	permeability coefficient $h\ m^{-2}$ $x10^7$	orientation to water
4.2	lower side	11.2	upper side
2.5	" "	11.8	" "
3.1	" "	16.5	" "
3.5	" "	15.0	" "
3.1	" "	14.9	" "
Mean result 3.3 ± 0.64		13.9 ± 2.28	
For solvent cast films from butanone at ambient			
permeability coefficient $h\ m^{-2}$ $x10^7$	orientation to water	permeability coefficient $h\ m^{-2}$ $x10^7$	orientation to water
1.8	lower side	2.3	upper side
1.6	" "	2.5	" "
1.9	" "	2.7	" "
Mean result 1.8 ± 0.13		2.5 ± 0.2	

Table V:1 THE EFFECT OF FILM ORIENTATION ON WATER PERMEABILITY

For latex films cast for 3 hours at 80° c after 24 hours			
Permeability coefficient s $m^3 kg^{-1}$ $x10^{17}$	orientation to water vapour	Permeability coefficient s $m^3 kg^{-1}$ $x10^{17}$	orientation to water vapour
1.7	lower side	3.0	upper side
2.3	" "	2.8	" "
1.9	" "	3.2	" "
2.0	" "	3.4	" "
2.4	" "	2.7	" "
Mean result 2.1±0.3		3.0±0.3	
For solvent cast films from butanone at ambient			
permeability coefficient s $m^3 kg^{-1}$ $x10^{17}$	orientation to water vapour	Permeability coefficient s $m^3 kg^{-1}$ $x10^{17}$	orientation to water vapour
1.7	lower side	1.7	upper side
1.7	" "	1.8	" "
1.6	" "	1.9	" "
Mean result 1.7±0.06		1.8±0.1	

Table V:2 THE EFFECT OF FILM ORIENTATION ON WATER VAPOUR PERMEABILITY

the permeability of latex films decreased over the period of one month, but the solvent cast films showed no aging at all during the same period. As was found for water permeability the latex films showed some effect of orientation with respect to the permeant, with the upper surface having the higher permeability (see Table V:2). A more detailed discussion of this is given in Chapter VI.

V.1.4 PERMEABILITY OF PBMA FILMS TO SOLUTIONS OF NITROPHENOL.

A detailed discussion of the permeability of latex films is given later in this chapter; results are quoted here only for comparison with solvent cast films. The permeability of solvent cast and latex films were determined for nitrophenol at a donor solution concentration of 0.16 gl^{-1}. As found previously, latex film permeability was dependent on the film age and orientation, whereas for solvent cast films only the orientation was significant. Table V:3 shows the permeability data for latex films cast at 80°C for three hours. The initial permeability refers to film permeability 24 hours after casting, and the final values for films aged one month at room temperature. The film orientation is described with respect to the permeant solution (i.e. the donor solution). The results in Table V:3 show the typical permeability coefficients found for latex films. However, to obtain these results 6 to 8 films were prepared and the average of the lowest coincidental values was chosen. Often the rejected values were factors of 10 greater than the quoted results, and because film

imperfections were the most likely cause of the higher results, the lower values were taken to be representative of the film permeability.

Initial permeability $h\ m^{-2}\ x10^{10}$		Final permeability $h\ m^{-2} x10^{10}$	
Orientation to donor		Orientation to donor	
Upper	Lower	Upper	Lower
5.6	11.1	4.5	2.8
4.5	9.6	3.1	2.5
5.4	11.2	2.8	3.8
	10.3		3.1
Mean result			
5.2±0.6	10.4±0.7	3.5±0.9	3.1±0.5
Solvent cast film (lower surface to donor) 6.3±0.06			

TABLE V:3 THE EFFECT OF FILM AGE AND ORIENTATION ON NITROPHENOL PERMEABILITY

To test whether the permeability of solvent cast films was dependent on film orientation a sample of solvent cast film was divided into two portions. The permeability coefficient was determined with the films in different orientations. When the lower side of the film was in contact with the donor solution the permeability coefficient was 6.3 $x10^{-10}\ h^{-1}m^{2}$. When the upper surface of the film was in contact with the donor solution the permeability coefficient was 9.83 $x10^{-10}\ h^{-1}m^{2}$. Therefore, the upper surface had the higher permeability, which the same trend as found for water permeation.

Activation energies for permeation were also determined for both types of film by measuring the permeability at several temperatures. For both latex films and solvent cast films the effect of increasing temperature was described by an Arrhenius type plot shown in Figures V:1,V:2. The permeability coefficient at 30°C for solvent cast films was 6.3 0.06 $x10^{-10}$ h^{-1} m^2, with a corresponding activation energy of 80 kJ mol^{-1}. For latex films the permeability coefficient and the activation energy were dependent on film age and casting temperature. The permeability coefficients were in the range 12 to 0.12 $x10^{-10}$ h^{-1} m^2 and the corresponding activation energies were between 65 and 143 kJ mol^{-1}. As found for water vapour permeability, the latex film had a lower permeability than the solvent cast film. In order to study this difference, the uptake of nitrophenol from solution was determined. Known weights of the film under test was immersed in a solution of nitrophenol of known concentration. The samples were agitated for 24 hours in a water bath at 30°C. The concentration of the solution was then tested. A blank determination was also performed. The uptake was calculated from the decrease in the nitrophenol solution concentration. The results are plotted in Figure V:3. It is clear that the uptake for solvent cast films is generally greater than the latex films. The latex film in this case was cast at 80°C for three hours, and then aged at ambient temperature for one month. At the donor concentration used in the permeability experiments (0.16 gl^{-1}) the solvent cast film had a considerably higher uptake. This may in part explain why the permeabilities of the solvent cast films were higher than the latex films,

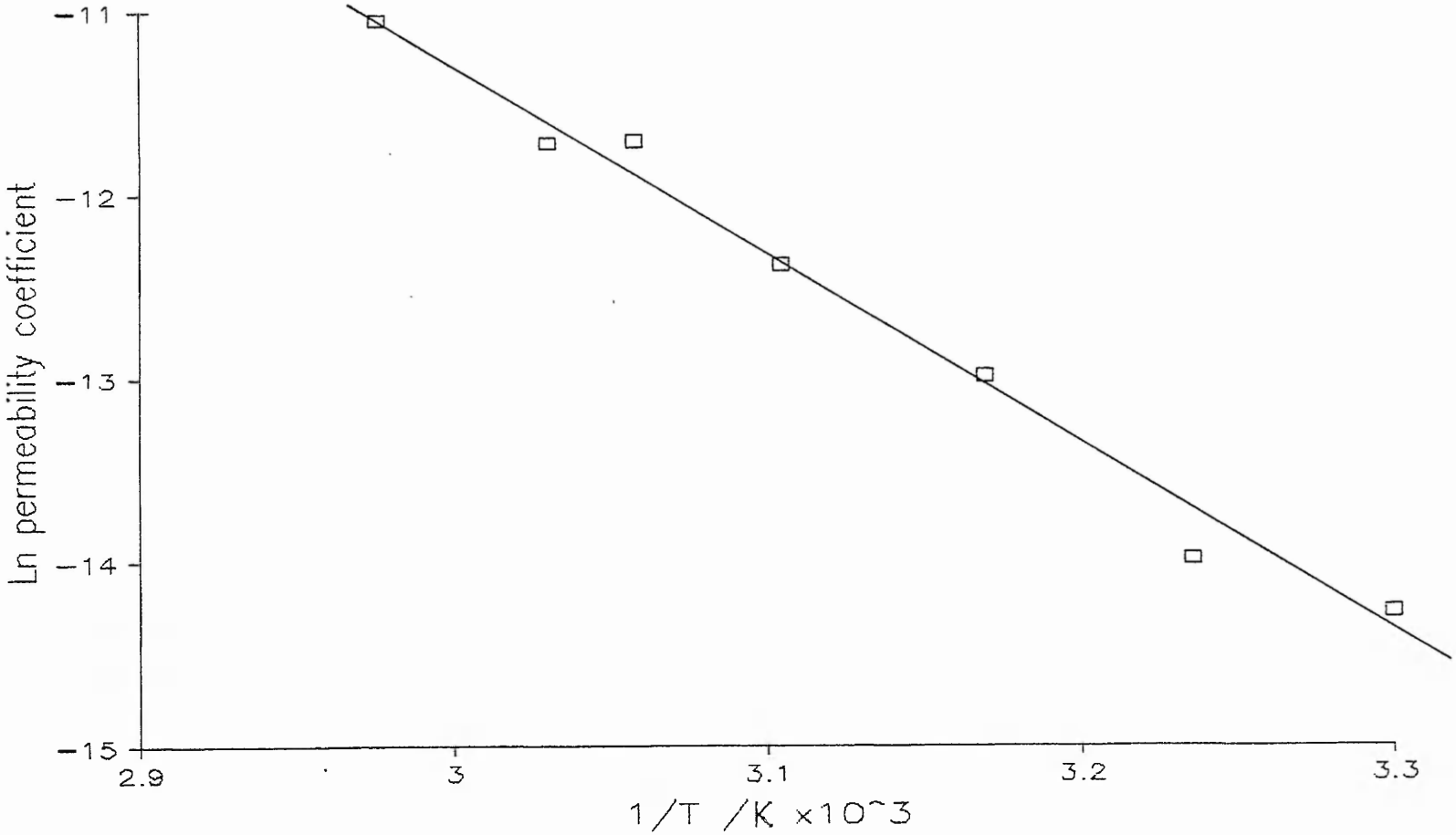

Figure V:1 Typical Arrhenius plot for PBMA solvent cast film

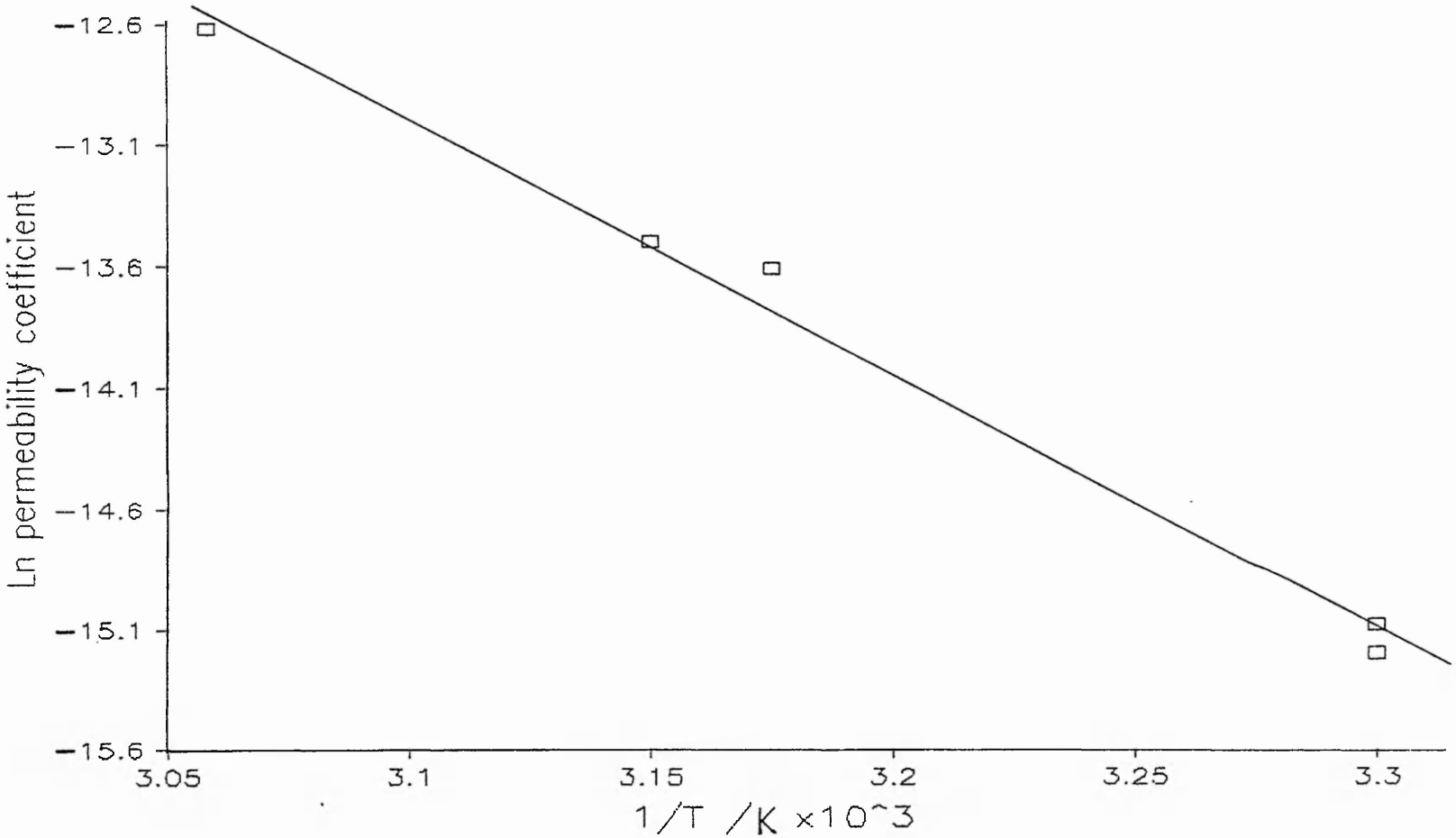

Figure V:2 Typical Arrhenius plot for PBMA latex film

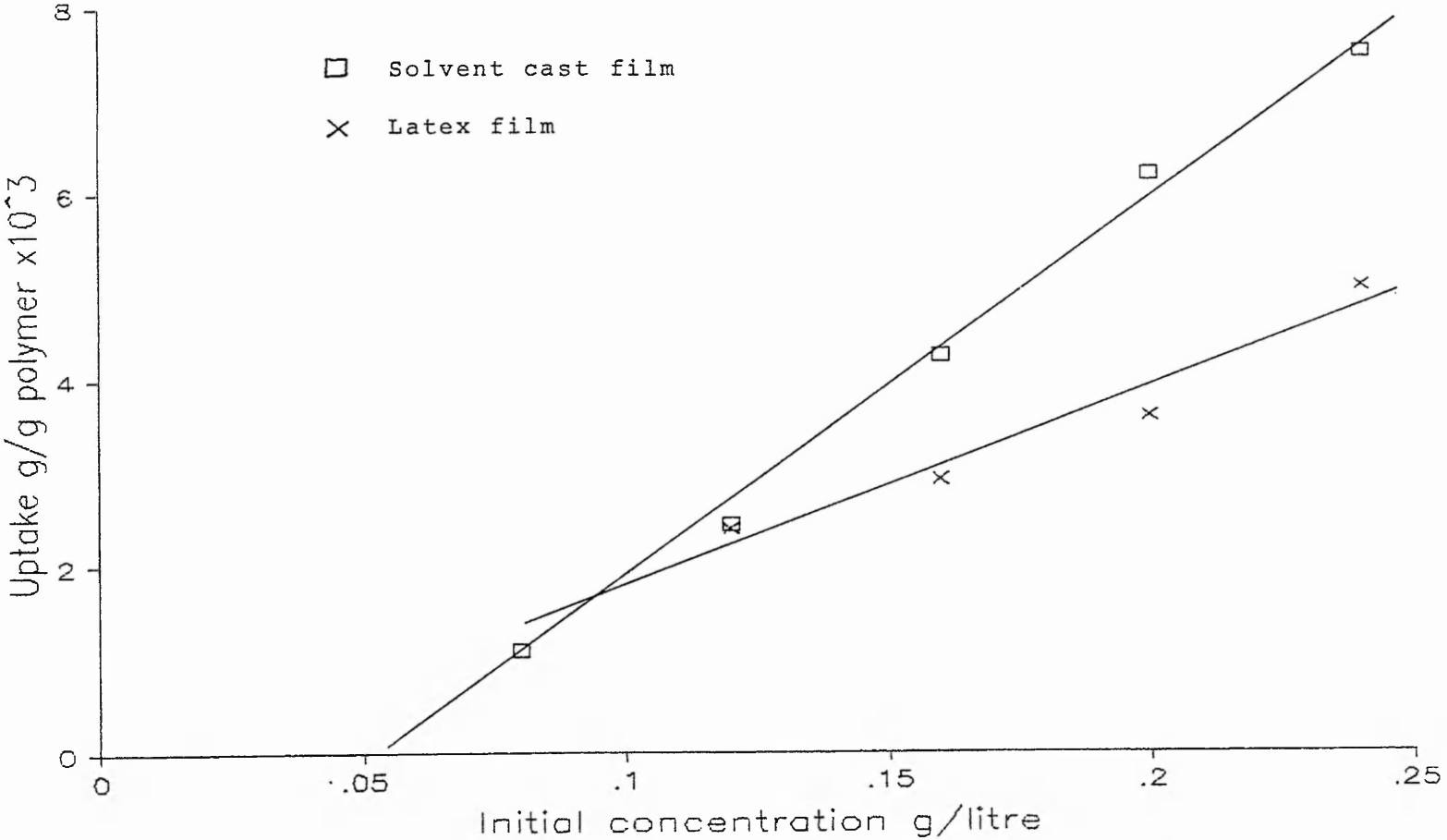

Figure V:3 Uptake of Nitrophenol from solution at 30°C

prepared as described earlier. Assuming the uptake from solution is equivalent to the solubility of the solute in the film, then the diffusion coefficient can be calculated, when the permeability coefficient is known. The calulated diffusion coefficients were found to be 0.15 and 0.13 h m^{-2} for solvent cast and latex films, respectively. Thus, both the solubility and diffusion coefficient were found to be greater for solvent cast films, in comparison with latex films, and this is the reason for the greater permeability of solvent cast films.

The reason and possible explanation for the greater values for the solvent cast polymer must lie in the polymer chain conformations. The diffusion coefficient is a measure of the free volume within the film, and the ability for holes of sufficient size to form and allow transport. Thus, a more open network would allow these processes to occur with greater ease than a more dense network. Thus, it would seem reasonable to suggest that the polymer chains in the solvent cast film are less tightly coiled, and more able to accommodate permeating molecules than the polymer in the form of the latex film. A similar observation was reported by Kassis and List[9], who found that latex films formed from a copolymer of acrylic and methacrylic acids and their methyl and ethyl esters, had lower permeabilities to water vapour than the same polymer cast from solvent. They argued that the difference was caused by different film morphologies. pre Density measurements showed that the more permeable solvent cast film was less dense than the latex film.

The densities of a solvent cast film and a latex film 24 hours and one month after casting were measured by

displacing a known weight of water from a specific gravity bottle. The film density was calculated from a knowledge of the film weight and the weight of water displaced. The densities of the films were 0.96, 1.05, and 1.09 g cm^{-3} for solvent cast, aged latex and unaged latex films, respectively. The different densities do not correlate directly with the observed film permeabilities, since the least permeable,(aged latex film) does not have the highest density. However, as with the findings of Kassis and List[9], the solvent cast film has the lowest density.

V.1.5 CONCLUSIONS

The above results indicate that solvent cast films, prepared in this way, cannot be used to give a base line value for the permeability coefficient in unstructured bulk polymer, as the lowest values were obtained from latex films which are known to contain the distinctive internal morphology. The solvent cast films were studied in order to compare the effects of the interparticle boundaries in latex films on the permeability, and these boundaries were expected to increase the permeability. It was found that solvent cast films had higher permeability coefficients than aged latex films but lower than new latex films. The most reasonable explanation for this is that the polymer chain conformation was markedly different in latex and solvent cast films. For the latex films, the influence of the interparticle boundaries would explain the higher permeability coefficients found, but on aging and heat treatment these boundaries would have diminished or

disappeared and the permeability was more prominent through the polymer itself. In the solvent cast films the polymer chains would have been more fully extended in solution and could have been 'frozen' in a more open conformation, leading to a greater free volume within the film, and thus a greater diffusion coefficient. It is therefore concluded that comparisons between latex and solvent cast films would not yield any direct information about the role of the interparticle region in latex films in the permeation process.

V.2 THE SOLUTE PERMEABILITY OF PBMA LATEX FILMS.

V.2.1 THE PERMEABILITY TO SOLUTIONS OF NITROPHENOL

The permeability of latex films has been shown to be dependent on the degree of coalescence in the film[2,3] and this was interpreted in terms of autohesion[7] or further gradual coalescence[8] leading to a reduction in permeation through the interparticle boundaries. To test whether these effects were found for solute permeability, latex films were prepared over a range of conditions and the effect of aging on the permeability of aqueous solutions of nitrophenol studied.

V.2.1.1 THE EFFECT OF CASTING TIME AND TEMPERATURE.

Since the degree of coalescence of latex particles can be envisaged to be dependent on both the temperature of film formation and the time the film is exposed to the

film forming temperature, a study of these parameters was undertaken. The films were prepared as described previously, but the times, and the temperatures at which the films were dried, were varied. Films were dried for 3,6, and 20 hours at oven temperatures of 52, 66, 80 and 95°C. The permeability coefficients for the permeation of aqueous solutions of nitrophenol are shown in Table V:4.

Permeability coefficient $x10^{10}$ h m^{-2} 24 hours after casting			
Drying temperature /°C	Drying Time /Hours 3	6	20
52	-	-	12.2
66	-	-	5.4
80	9.9	6.2	2.3
95	4.5	2.5	*

TABLE V:4 THE EFFECT OF CASTING TIME AND TEMPERATURE ON FILM PERMEABILITY

The blank values could not be determined because the latex would have not completely dried. The * value could not be determined as the films were extremely difficult to remove from the substrate after the prolonged exposure to the higher temperature.

From the above results it is clear that the higher

the drying temperature, and the longer the drying time, the greater the tendency towards a reduced permeability of the film. This reduction in permeability could be interpreted in terms of increasing particle coalescence, and hence a reduction in permeability through the interparticle regions and the permeability coefficients tended towards the value for the fully coalesced film.

The results in Table V:4 were analysed using multivariant regression analysis and the calculation was performed using a statistical computer package, called Minitab. The resulting analysis revealed that the permeability was inversely proportional to the drying time and temperature as shown in Equation V:1

$$\text{Permeability} = \frac{K}{\text{Time}^{a}\,\text{Temperature}^{b}} \qquad \text{V:1}$$

Where K, a and b are constants equal to 21.5, 0.702, and 4.23, respectively. No theoretical significance is attached to the above equation; it is simply included to demonstrate the experimental relationship between the film permeability and the film forming conditions. Table V:5 shows the experimental values compared with values derived from Equation V:1. Using the same equation the, permeability at several temperatures and dryng times were calculated. The curves are shown in Figure V:4. The figure shows that the permeability drops rapidly initially and then begins to level out. The values never actually approach the same base value, and this is probably a function of the mathematical approximation rather than a physical effect in film permeability. The general shape of

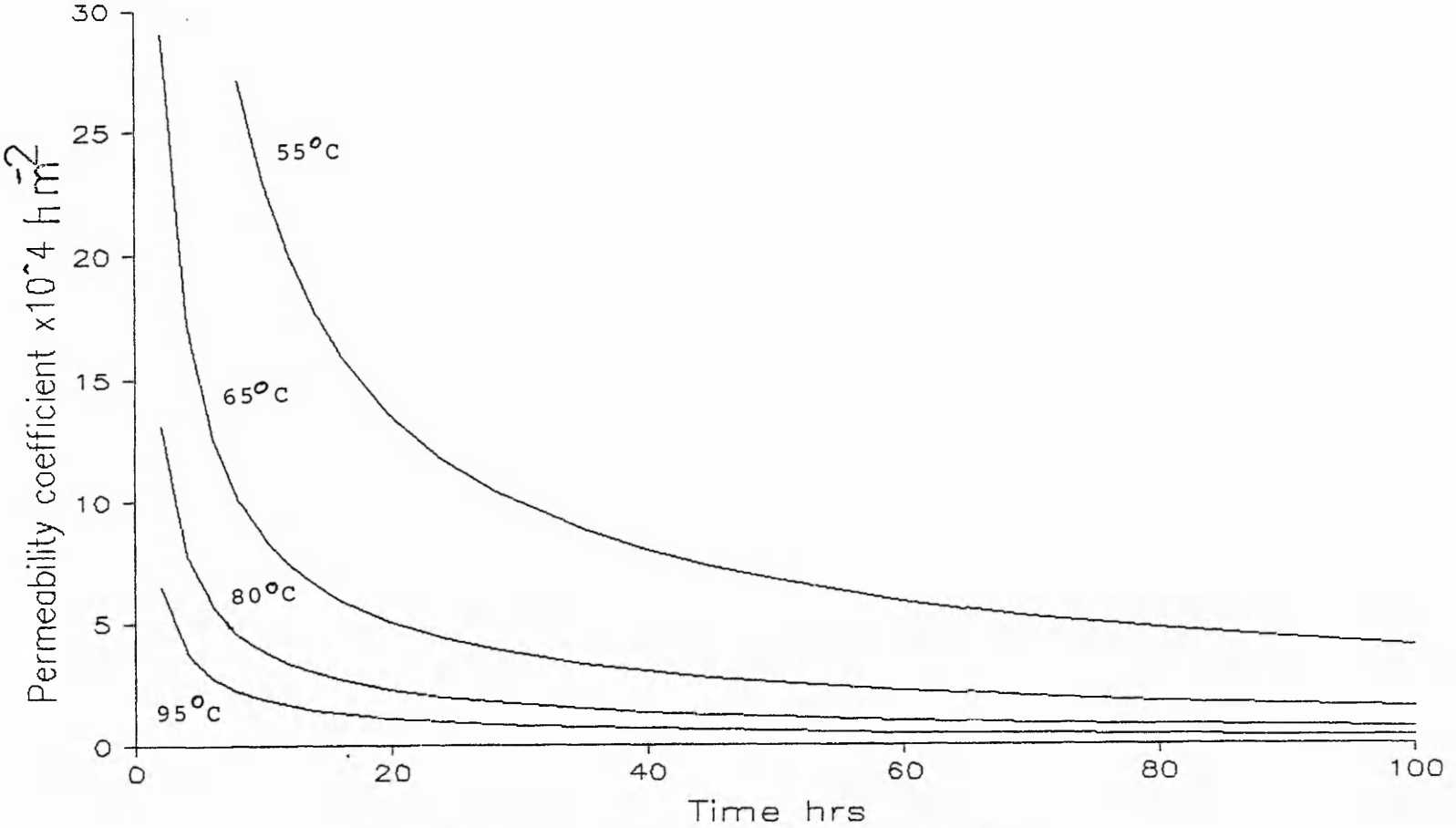

Figure V:4 Predicted permeability of film

Time Hours	Temperature °C	Permeability coefficient $x10^{10}$ h m^{-2}	
		Experimental	Calculated
20	80	2.3	2.28
6	95	2.5	2.80
3	95	4.5	4.74
20	66	5.4	5.05
6	80	6.2	5.70
3	80	9.9	9.65
20	52	12.2	13.52

TABLE V:5 COMPARISON BETWEEN EXPERIMENTAL AND CALCULATED PERMEABILITY

the curves in Figure V:4 compares well with the aging curves shown by Chainey[8] and Kassis[9], and indicates that the aging process causing lower permeability is dependent on both the temperature and time. These observations are consistent with the idea that permeation through latex films is, initially, dominated by permeation through the interparticle regions. The reduction in permeability is caused by an autohesion process[7] increasing the intimacy of contact between the latex particles and hence reducing permeability through the interparticle regions.

V.2.1.2 THE EFFECT OF FILM AGE ON PERMEABILITY.

Latex films were prepared under the same conditions as shown in Table V:4 and then allowed to age at room temperature for one month. The nitrophenol

permeability coefficients were then determined. The results are shown in Table V:6.

Permeability coefficient x10 ^{10}h m^2 after one month			
Drying temperature /°C	Drying Time /Hours 3	6	20
52	-	-	4.6
66	-	-	4.8
80	2.8	4.9	2.9
95	1.2	0.12	-

TABLE V:6 THE PERMEABILITY COEFFICIENTS OF AGED LATEX FILMS

Values in Table V:6 of less than 2 x10^{-10} h^{-1}m^2 were determined from the activation energy (see figure V:12) since the instrumentation was not capable of measuring permeabilities less than 2 x10^{-10} h^{-1} m^2.

In all cases the permeability decreased on storage, and this was consistent with earlier observations. Isaacs[11] showed that the electrolyte permeability of acrylic latex films was reduced over a period of one week. Bondy and Coleman[12] demonstrated a reduction in water vapour permeation upon aging for a variety of copolymer latex films, and Chainey[3,13] reported a reduction in helium permeability for a variety of acrylic, and methacrylic polymer and copolymer latex

films. In all these cases the reduction in permeability was attributed to changes in film morphology, which was caused by further gradual coalescence of the latex particles. The reason for the gradual disappearance of the interparticle regions on aging was discussed in Chapter IV. The film cast at 80°C for three hours initially showed quite distinct particle boundaries, but a sample of the same film aged for one month at room temperature showed that the particle identity was considerably reduced. For the film which gave the lowest permeability, i.e., prepared at 95°C for six hours, and aged for one month at ambient temperature, the particles were hardly identifiable. Similar observations of the loss of particle boundaries on aging have been reported[8,10] but were not correlated to a reduction in permeability.

The reduction in permeability could also be attributed to a relaxation process as suggested by Kassis and List[9]. They found that the permeability to water vapour was reduced on storage and was the result of a relaxation process, where the free volume of the system was lowered. They argued that films could be compared to glasses with a degree of free volume frozen within the system, but as glasses are thermodynamically unstable, they tend to form an energetically favourable more ordered state, which requires less space for movement and vibration of the molecules within the system. However, the same process should then apply to films cast from solution, and hence, a reduction in permeability would be noted, but this was not found in the present study. The explanation given by Kassis seems not to be appropriate here, where further coalescence is so obviously present in

latex films.

In order to determine how the film permeability decreased with film age upon storage at ambient temperatures, the permeability of several separate films was determined at different times after casting. The nitrophenol permeabilities coefficients are shown in Table V:7.

Film age Hours	Permeability coefficient $x10^{10}$ h m^{-2}
24	9.9
48	4.2
72	4.4
96	3.1
144	3.3
336	3.9
504	3.6
672	2.8

TABLE V:7 THE REDUCTION IN PERMEABILITY WITH TIME FOR FILMS STORED AT AMBIENT TEMPERATURE

Figure V:5 shows that the above data forms a curve similar to those shown by Chainey[8] and Kassis[9], and illustrates that films age rapidly over the first 3 days, and appear to have reached their lowest values at about 4 to 6 days. To test the effect of storage temperature on the reduction in film permeability, a sample of latex was dried for three hours at 80° C, then for a further three hours at 90° C. Samples of the same film

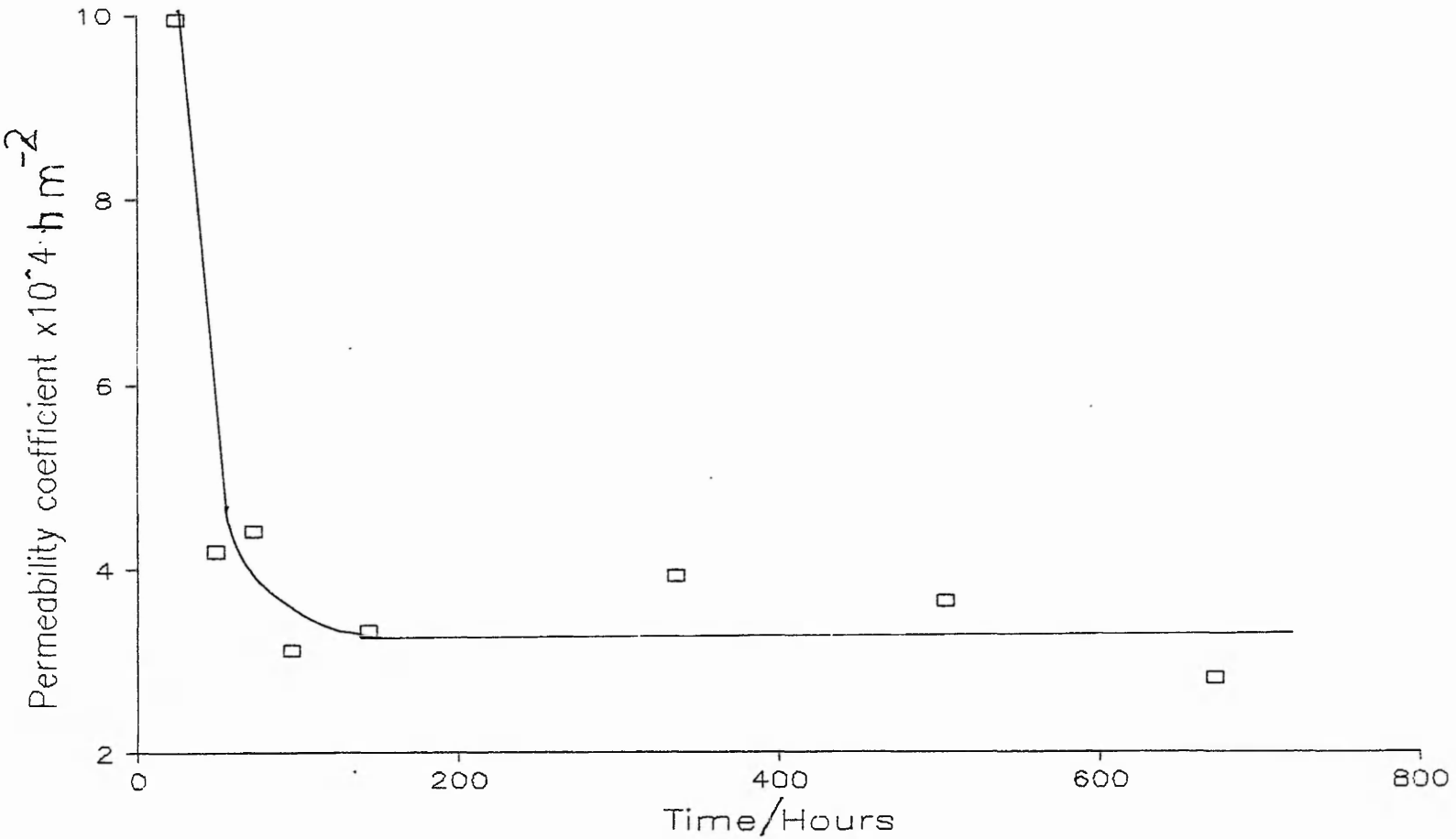

Figure V:5 The effect of film age on permeability

dried at 80° C for three hours were stored for one month in a freezer at -5° C. The nitrophenol permeabilities are shown in Table V:8

	Permeability coefficient $x10^{10}$h m^{-2}
After 3 hours at 80° C	10.4
After 3 hours at 90° C	5.1
After one month at -5° C	7.8
After one month at ambient	3.1

TABLE V:8 THE EFFECT OF STORAGE TEMPERATURE ON LATEX FILM PERMEABILITY

All the films show some reduction in permeability during the aging periods. Exposure of the film to 90° C for just three hours reduced the permeability coefficient by 50%. The sample stored at -5° C showed a less marked reduction in permeability over the period of one month. At this temperature the polymer would be in its glassy state and the autohesion process could no longer operate. The film stored at -5° C gave a permeability coefficient more than twice the value obtained from a similar film stored at room temperature. Thus the reduction in film permeability is both time-and temperature-dependent.

V.2.2. FACTORS AFFECTING FILM PERMEABILITY TO SOLUTES

V.2.2.1 THE EFFECT OF SOLUTE CONCENTRATION

The effect of nitrophenol concentration in the range 0.12 to 0.24 gl^{-1} on the permeability of latex films was determined. The permeability coefficient was found to be independent of the solution concentration. The results are listed in Table V:9

Nitrophenol concentration gl^{-1}	Permeability coefficient $x10^{10}$ h m^{-2}
0.12	10.5
0.16	10.4
0.20	12.3
0.24	9.2

TABLE V:9 THE EFFECT OF NITROPHENOL CONCENTRATION ON PERMEABILITY OF PBMA LATEX FILMS.

According to Fick's law, when applied to permeation[14], the permeability coefficient is independent of permeant concentration. However, the flux of permeant is directly proportional to the concentration. Several workers have shown the independence of the permeability coefficient on permeant concentration for solutes[15,16,17] and this was used to demonstrate the applicability of Fick's law. The absence of any trend in

permeability coefficient with nitrophenol concentration would imply that there were no interactions between the polymer and permeant, in the concentration range studied, which would otherwise give rise to non Fickian permeability.

V.2.2.2 THE EFFECT OF FILM THICKNESS

The effect of film thickness was determined for both latex and solvent cast films, and the plot of reciprocal thickness versus permeability is shown in Figure V:6. The straight lines drawn through the points are those predicted from Fick's law. In both cases the data points are in good agreement with the theory, which again implies that there was no specific interaction between the permeant and the polymer[18], and that Fick's law is applicable. Similar observations have been reported for solute permeability in Silastic[16] and polysiloxane membranes[15]. However, deviations from the theoretical line have been reported by Hwang[19,20] and these were attributed to boundary layer effects, which become more prominent as the film thickness decreased.

V.2.2.3 THE EFFECT OF TEMPERATURE

The effect of temperature on permeability was found to follow an Arrhenius type relationship and the plots for several film preparations are shown in Figures V:7 to V:12. The Arrhenius dependence of permeability upon temperature is well known[21], and has been shown to apply solute permeability in several different cases[16,22,23].

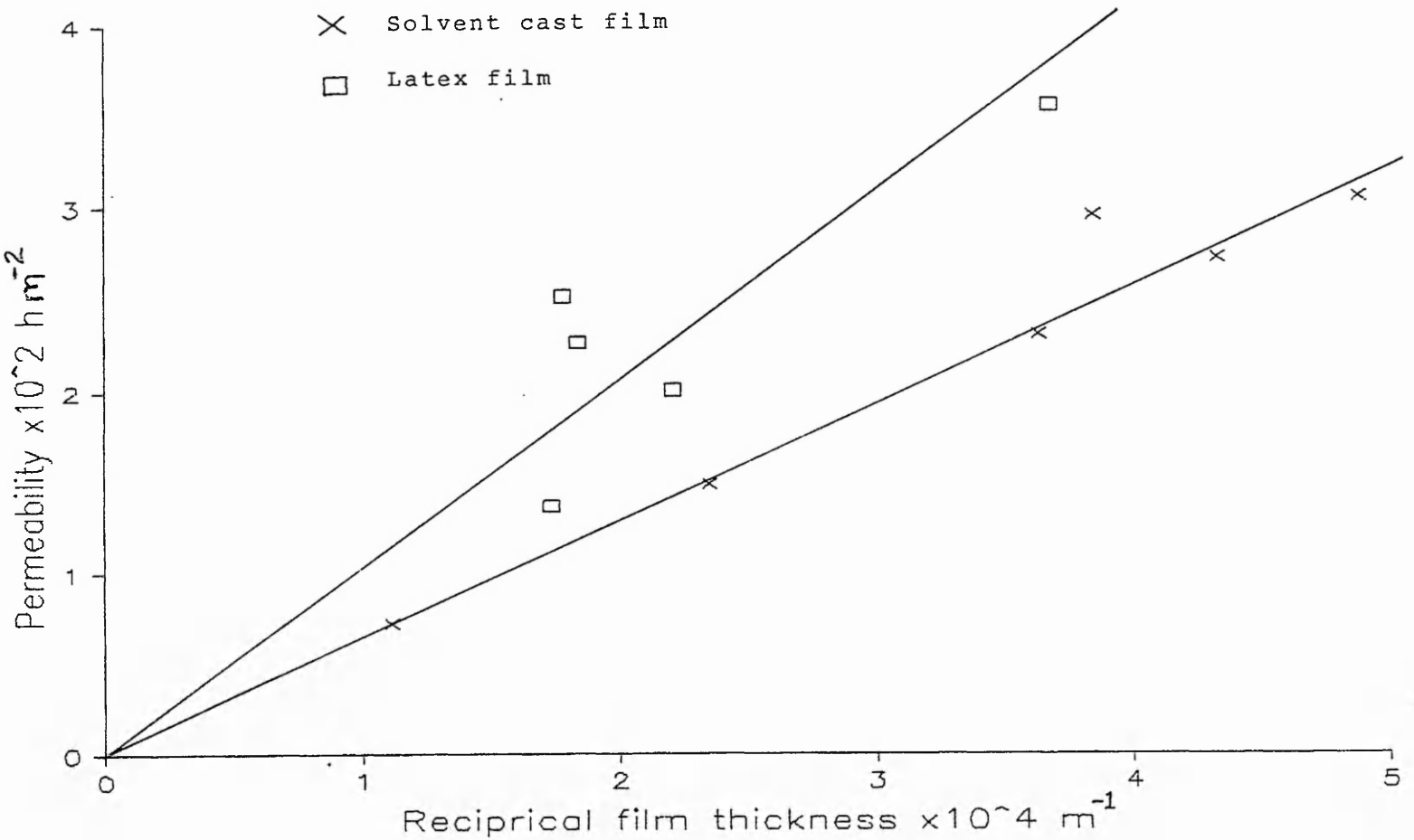

Figure V:6 Reciprocal film thickness vs Nitrophenol permeability

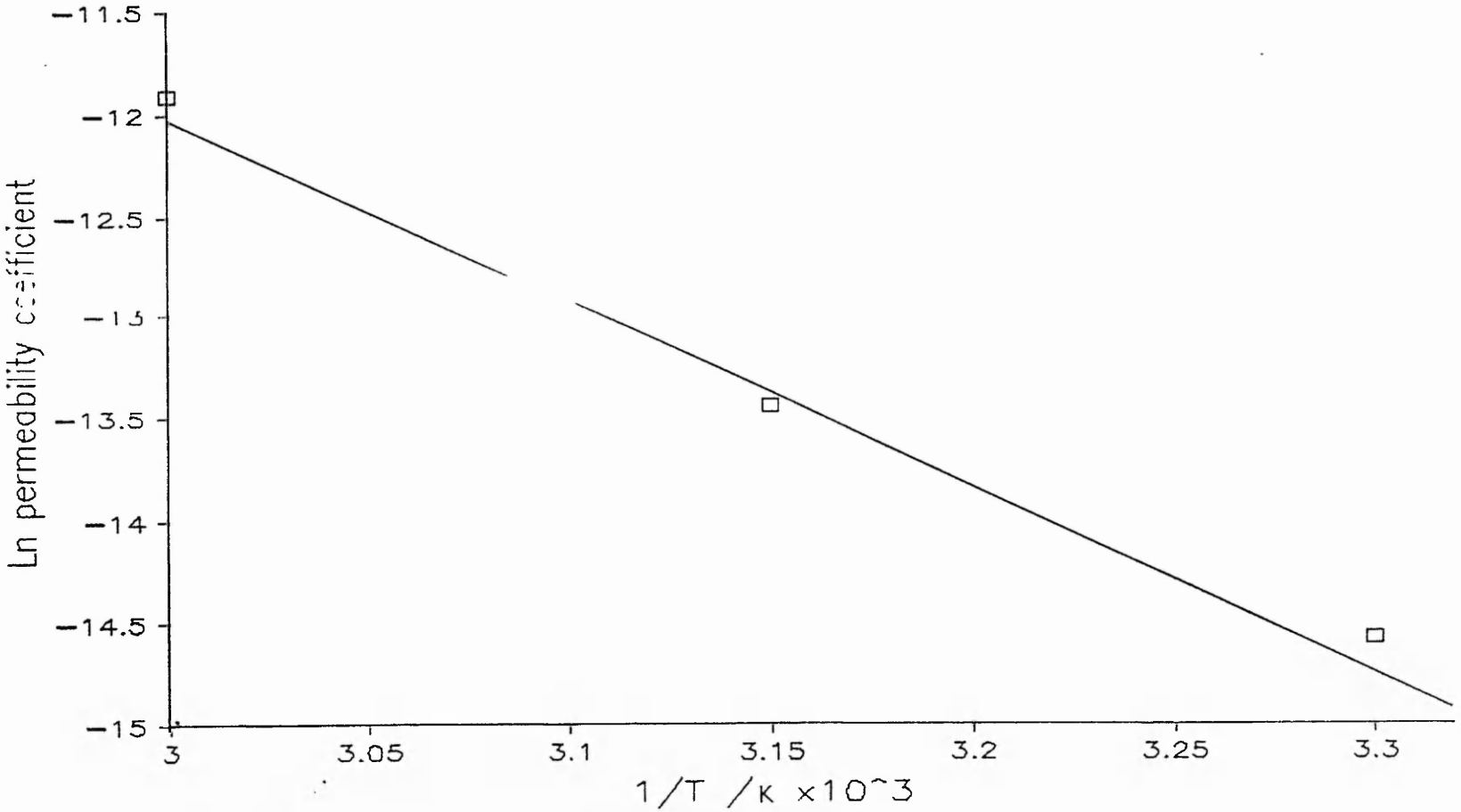

Figure V:7 Arrhenius plot for film cast at 55°C for 20 Hours

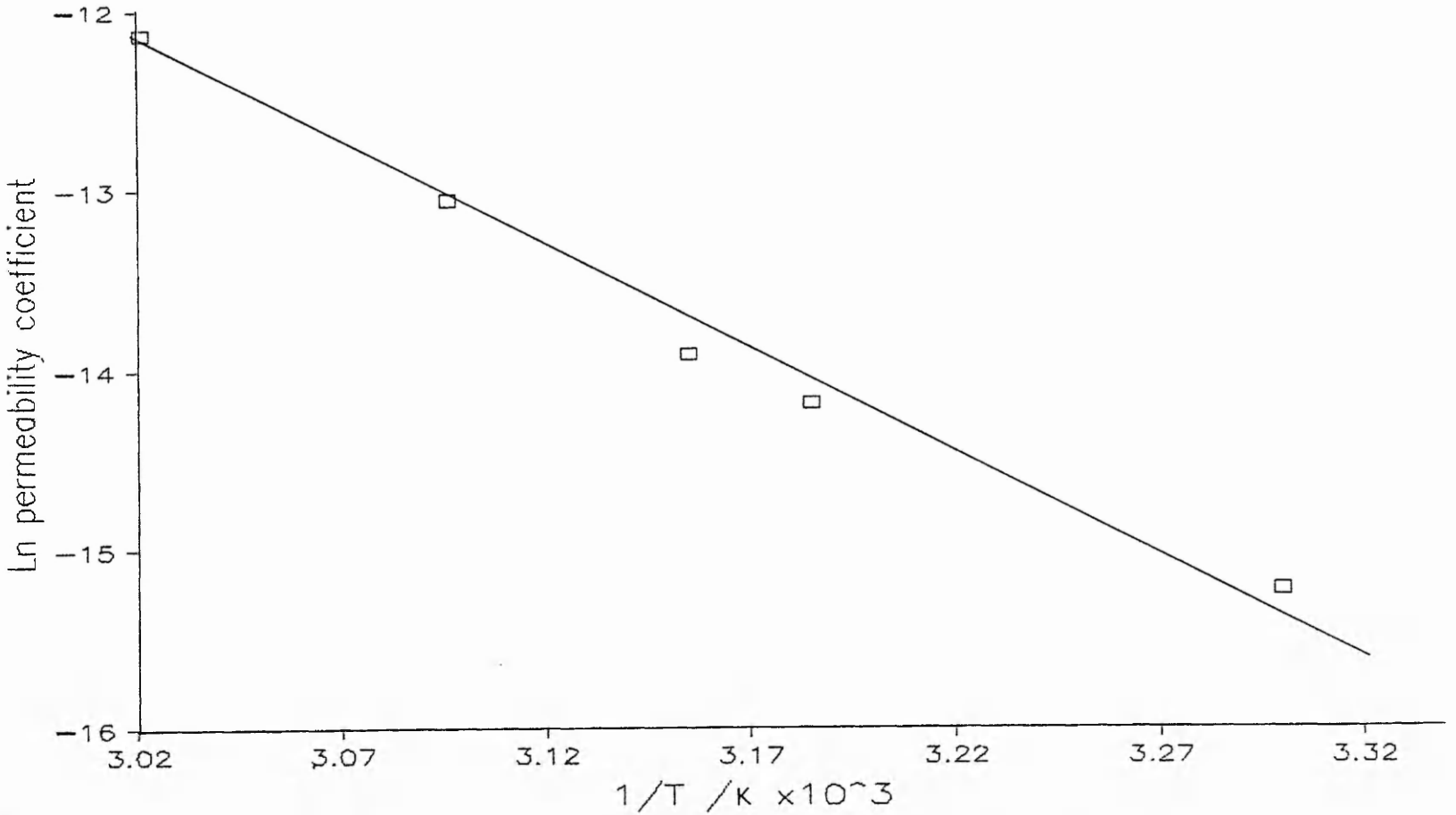

Figure V:8 Arrhenius plot for film cast at 65°C for 6 Hours

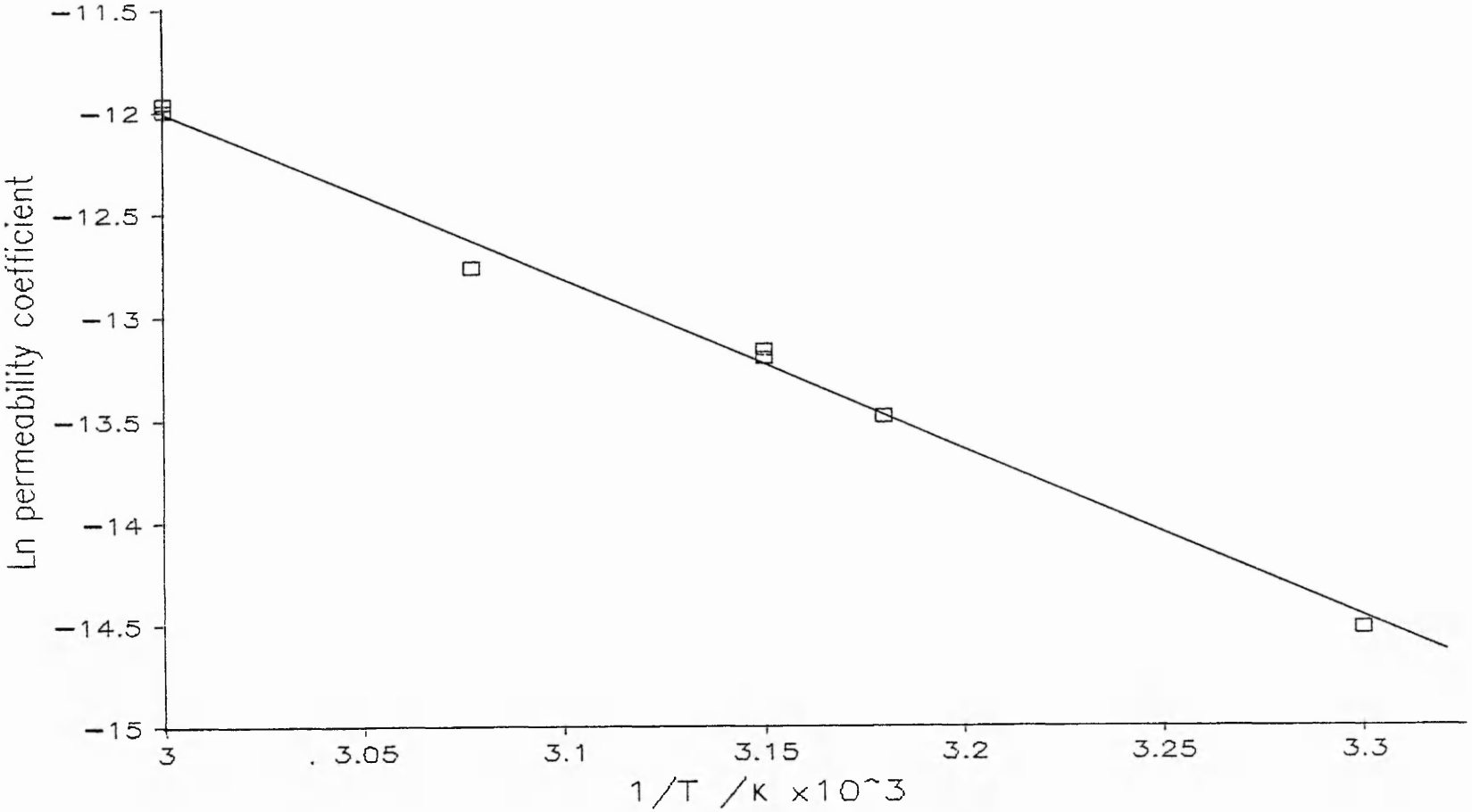

Figure V:9 Arrhenius plot for film cast at 65°C for 20 Hours

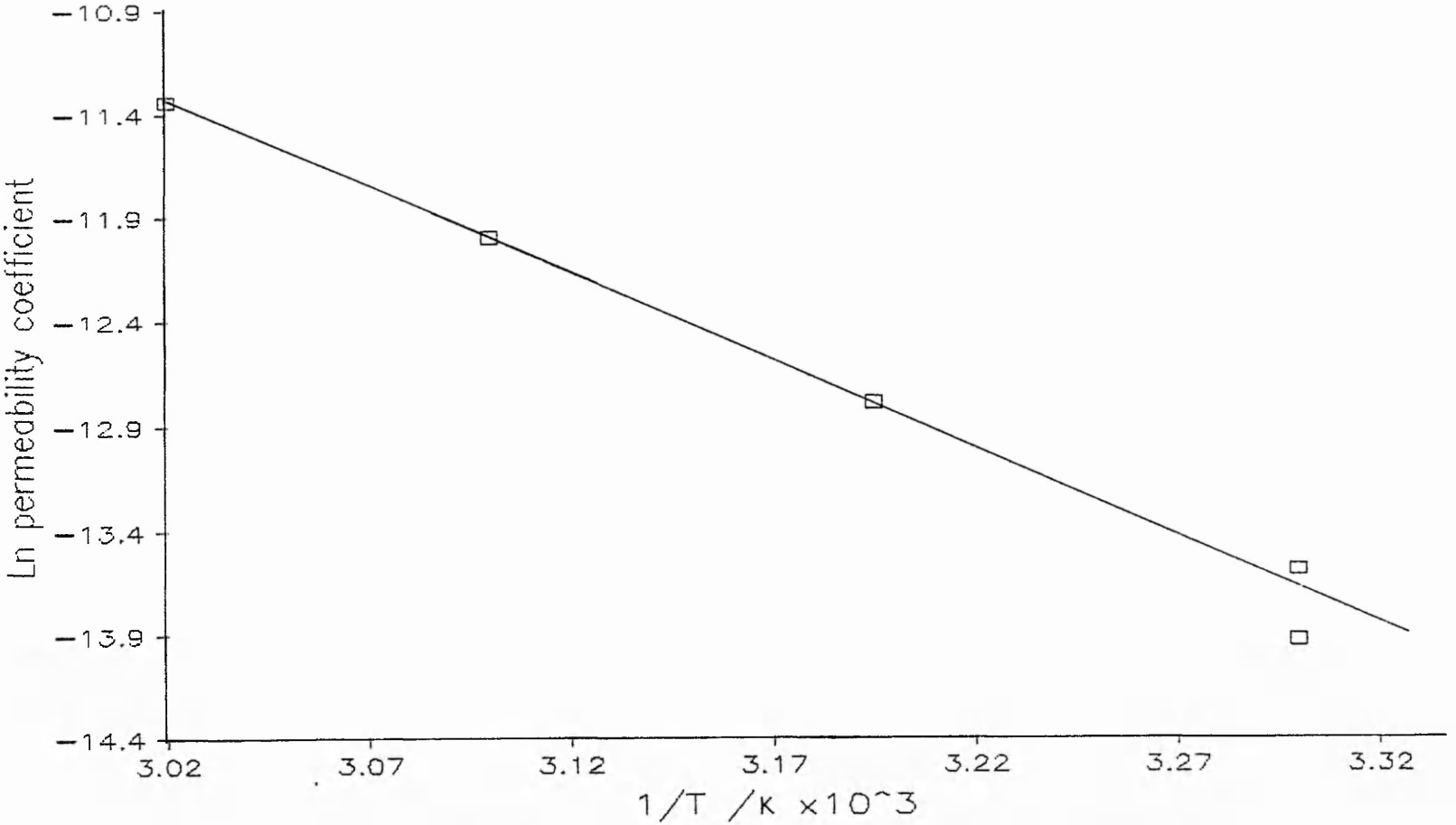

Figure V:10 Arrhenius plot for film cast at 80°C for 3 Hours

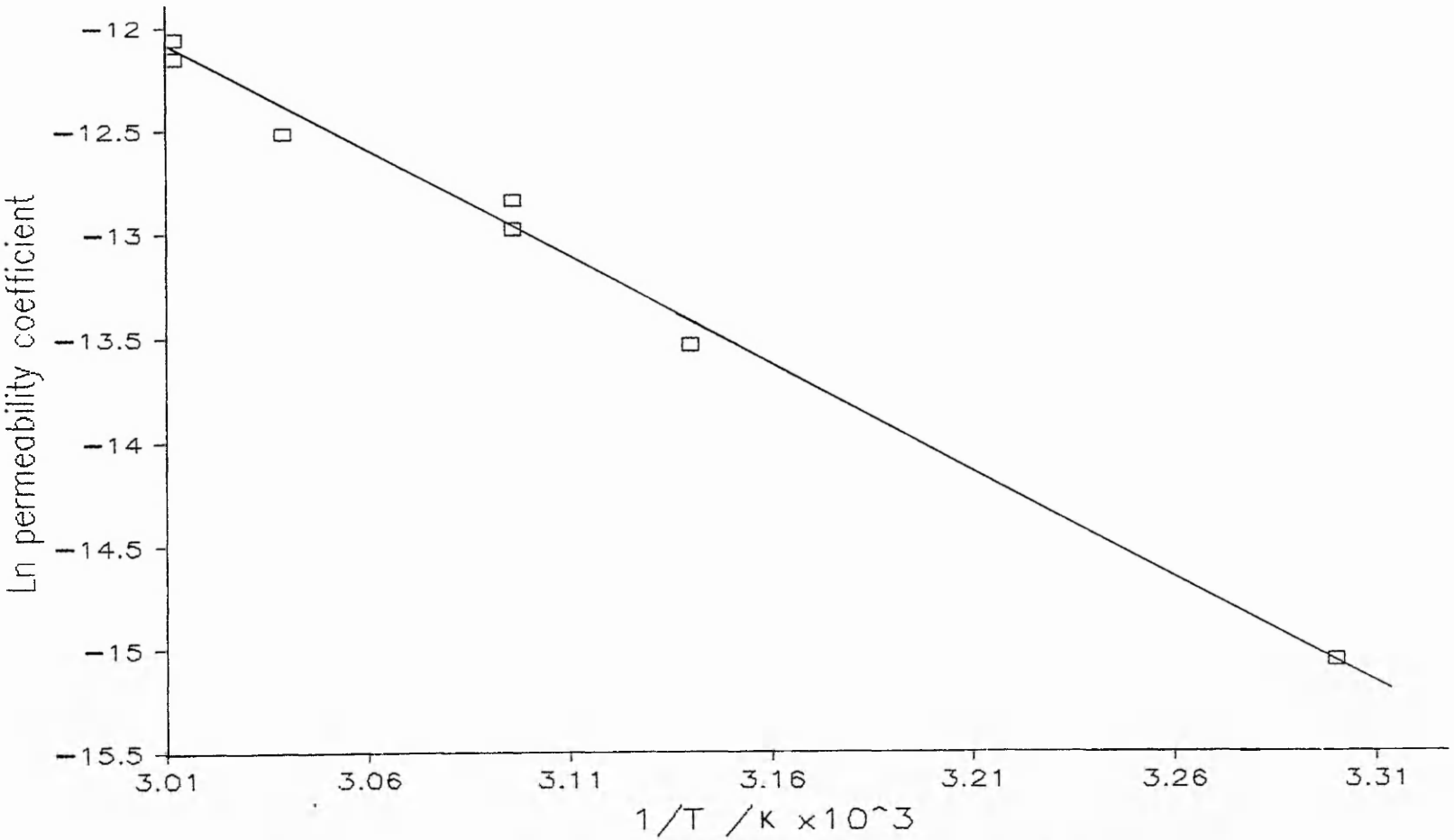

Figure V:11 Arrhenius plot for film cast at 80°C for 20 Hours

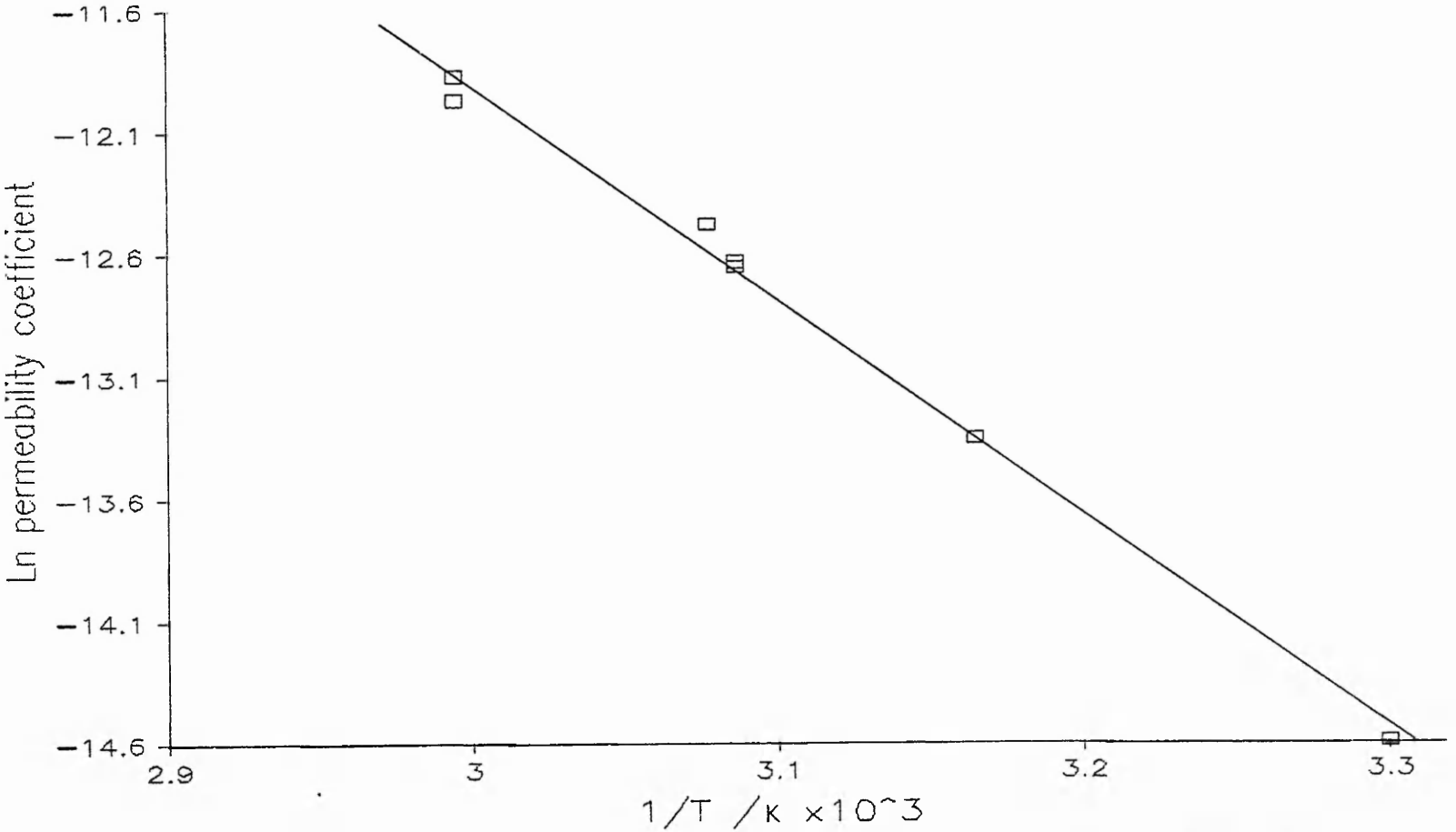

Figure V:12 Arrhenius plot for film cast at 95°C for 3 Hours

although Abdel-Aziz[24] reported a linear dependence of permeability with temperature.

Several films were prepared using the casting times and temperatures shown in Table V:6. The activation energies of films up to one month old were measured. The permeability coefficients at 30°C and the activation energies for permeation are given in Table V:10

The last value in Table V:10 is much higher than the other values, and was obtained from an aged film prepared at 95°C. Since this sample would have had little or no internal structure, the permeability may be close to the value for permeability through the bulk polymer, without the influence of the interparticle boundaries.

It would seem likely that morphological changes within the film are responsible for the decrease in permeability[25]. The decrease could be attributed to a reduction in chain segment mobility, and hence a reduction in the relative ease of hole formation. If the interparticle boundaries contribute to the permeation process[3], then the autohesion process[7] would be responsible for the reduction in chain mobility and thus a reduction in permeation through the interparticle regions. It was demonstrated earlier, that increased time and temperature for film formation reduced the permeability of the resulting films. Also, the decrease in the particle identity, and hence the interparticle boundaries were shown to be affected in the same manner. Therefore, it is suggested that permeation through the interparticle regions contributes significantly to the transport process, and that initially, when the amount of interdiffusion of polymer chains across the interparticle

Permeabiltity coefficient $x10^{10}$ h m^{-2} @ 30°C	Activation energy kJ mol^{-1}
4.8	69.9
4.6	73.9
4.5	67.3
4.2	68.7
3.6	84.6
2.9	84.4
2.8	88.1
2.5	89.9
2.1	103.3
1.2	96.2
0.12	142.0

TABLE V:10 A COMPARISON OF THE INITIAL FILM PERMEABILITY WITH THE ACTIVATION ENERGY FOR PERMEATION

boundary is small, that hole formation via chain segment mobility is relatively easy. This accounts for the initial high permeability and the low activation energy for permeability. When the autohesion process begins to operate and the polymer chains in the interparticle regions interdiffuse and tangle, the activation energy for hole formation in these regions increases. This is because a greater amount of co-operative chain segment movement is required for hole formation. Thus, as the activation energy increases the permeability decreases.

V.2.2.4 THE INFLUENCE OF FILM ORIENTATION TO THE PERMEANT SOLUTION

Previous results have indicated that the permeability of latex films is affected by the film orientation. When the upper surface of a film (dried for three hours at 80° C and used within 24 hours) was in contact with the nitrophenol solution the permeability coefficient was $4.3\pm1.3 \times10^{-10}$ $h^{-1}m^{2}$, i.e., lower than the value of $10.4\pm0.7 \times10^{-10}$ $h^{-1}m^{2}$ for similar films with the lower surface in contact with the donor solution. The water and water vapour permeability, however, gave results indicating that the upper surface was the more permeable. (a more detailed discussion of this is given in Chapter VI) There are several examples of polymer films showing this asymmetric property, where the side difference is attributed to film morphology or surface effects arising from the substrate. Abdel-Aziz[24,27] showed that solvent cast acrylic films had higher permeability when the lower surface was in contact with the permeant solution, and

this was attributed to a dense, less porous upper surface being less permeable than the lower, more porous surface. Katz and Munk[28] and Yaseen[29] demonstrated that polar casting substrates, such as glass, and metal foil gave films which were more permeable to water, particularly the lower surface and suggested that this was caused by the substrate orientating polar groups within the polymer. In these cases the casting substrates was glass, and thus the polarity explanation could be applicable, with the more polar surface allowing the solvated nitrophenol molecules to adsorb more easily. Another possible explanation stems from the physical appearance of the films. The lower surface, which was in contact with the glass substrate was glossy compared with the matt upper film surface.(electron micrographs of the film surfaces are shown in Chapter IV, Plates IV:13 and IV:14) If one of the interfacial processes (adsorption-desorption) is controlling the rate of permeation, then from a surface area point of view, desorption from the film would explain the observed side difference. The higher permeability was found when the rougher upper surface was in contact with the receiver solution. The rate of desorption from the film would be controlled by the relative affinity of the solute for the polymer and aqueous phase as well as the interfacial surface area. From studies of the equilibrium uptake of nitrophenol from solution by PBMA films (shown in Figure V:3) a PBMA latex film had an equilibrium uptake of 2.9 $x10^{-3}$ g of nitrophenol per gram of polymer, for an initial solution of 0.16 gl^{-1}. Therefore, on a weight for weight basis, the partition of nitrophenol between the polymer and aqueous phase is in the ratio

1.8:1. Thus, desorption from the film is likely to be slower than absorption into the film. In the case of solvent cast films, where the effect of film orientation is the opposite of that found for latex films, a similar argument can be applied. The asymmetric nature of solvent cast films has been attributed to a dense skin on the upper surface, and a more open structure in the rest of the film[24-27]. Thus, the presence of the dense layer would impede desorption from the film, whilst the presence of a more open lower surface would facilitate desorption, and hence the permeabilitiy of a solvent cast film would be greatest when the lower surface is in contact with the receiver solution.

V.2.2.5 THE ANOMALOUS BEHAVIOUR IN THE NON STEADY STATE REGION

When a transport system is set up, the rate of permeation is not initially constant. If a Barrer[26] plot is performed for permeability in the non steady state region then a curve concave to the time axis is obtained. This implies that the rate of permeation is increasing with time, and the rate continues to increase until the steady state region is reached, when it becomes constant, corresponding to the straight line portion of a Barrer plot. This kind of approach to the steady state permeation rate is well known and understood, and forms the basis of the so called 'lag-time' determination which allows the diffusion coefficient to be determined from Barrer plots. The approach to the steady state permeation rate for both solvent cast and latex films for the permeation of

nitrophenol was found not to follow this behavior. The Barrer plots are shown in Figure V:13 and V:14, and clearly show a convex curve with respect to the time axis, followed by the steady state region. This type of non steady state behaviour would lead to a negative lag-time, and thus, the diffusion coefficient cannot be determined; it also implies that the permeation rate is initially high and decreases towards the steady state rate. Several instances of negative lag times have been reported in the literature.[30-33] Serota et.al[17], showed that for a group of substituted anilines, the more hydrophilic derivatives showed a negative lag-time, but the hydrophobic anilines showed the normal time-lag behaviour. The authors tentatively suggested that the hydrophilic anilines caused some rearrangments of the polymer chains. Fujita[34] suggested three possible explanation to account for negative time-lags:

(i) the presence of convective or multiple diffusive flows having different diffusion coefficients,

(ii) the time dependence of the diffusion coefficients,

(iii) the relaxation of stress causing changes in the polymer structure.

Donbrow and Friedman[35] found similar lag-time behaviour for the permeation of salicylic acid and caffeine, and suggested that two types of diffusive flow through the copolymer membrane were the cause. Senf et.

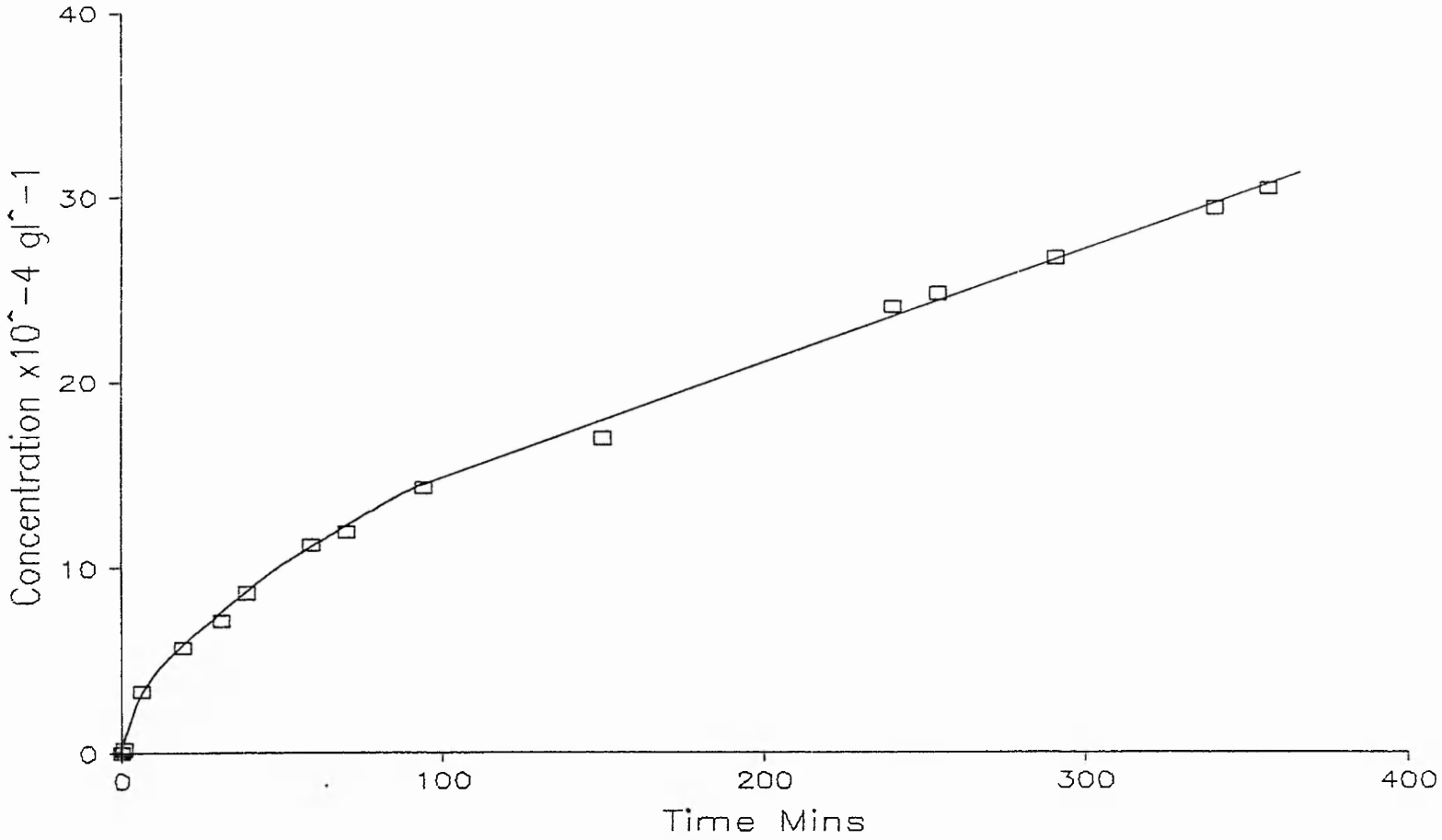

Figure V:13 Barrer plot for solvent cast PBMA film

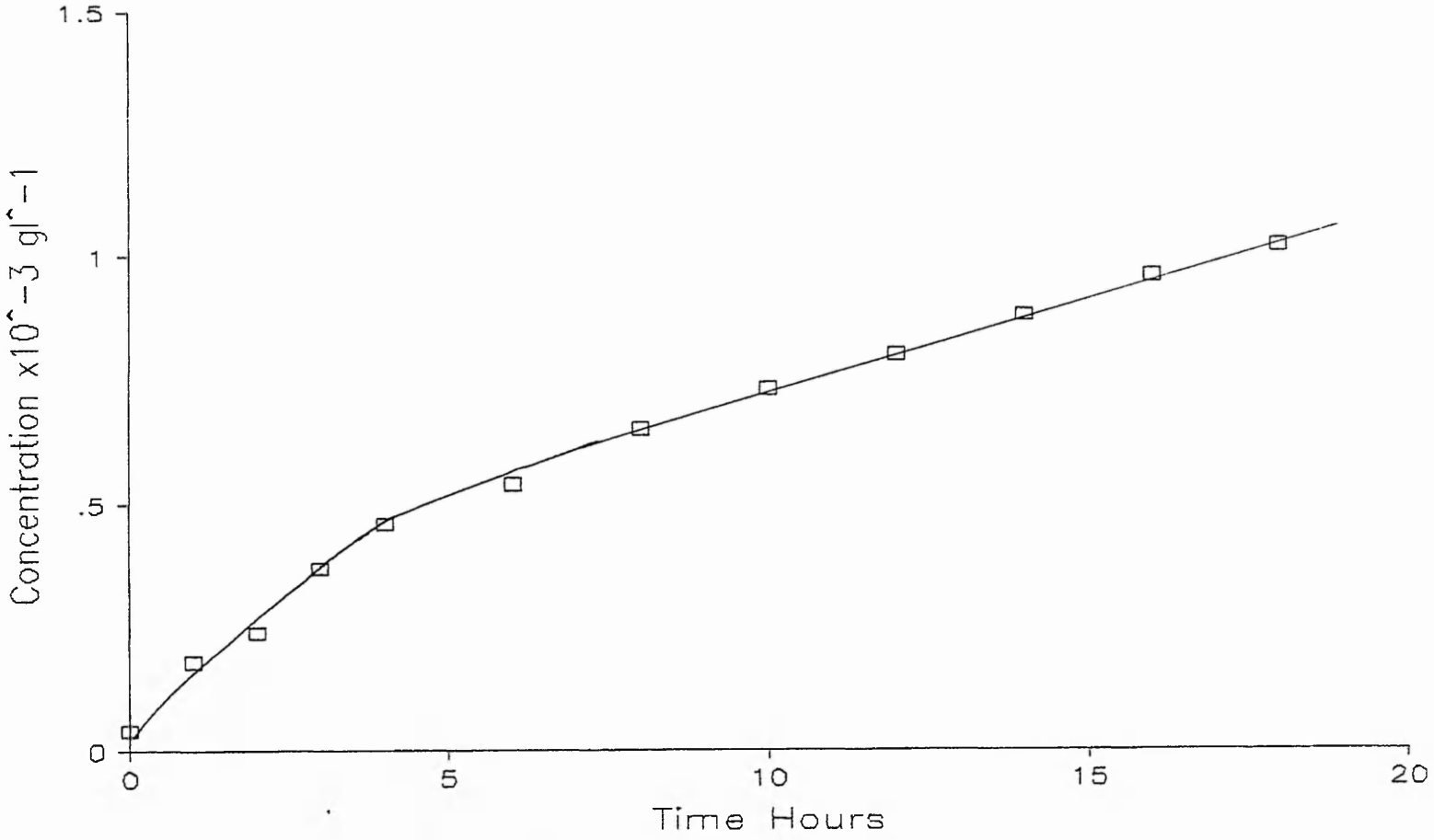

Figure V:14 Barrer plot for PBMA latex film

al.[36] demonstrated that the negative lag-times reported by Serota could be caused by impurities in the film leaching out and causing errors in the spectrophotometric analysis of the permeant. To test whether film leachates were causing the anomalous behaviour in this study, a sample of the receiver solution at the end of an experiment was analysed using HPLC, and no substances were found in the sample other than the permeant, and therefore the negative lag-time was not caused by impurities in the system. A possible explanation here is hydrogen bonding of the solute molecule with itself, with this interaction increasing as more permeant enters the film. This causes the permeation rate to decrease until the film is saturated with the permeant, when the steady state permeation results.

V.3 PERMEABILITY OF SEVERAL STRUCTURALLY RELATED ORGANIC SOLUTES

The permeability coefficient and the partition between the film and water were determined for several structurally related aniline derivatives. In all cases the latex film was dried for three hours at 80°C and used 24 hours after drying. Each of the partitioning experiments was performed using solutions of the same molarity as used in the permeability experiments. The partitioning, permeability coefficient and activation energies for the different solutes are shown in Table V:11

The occurrence of negative time-lags was not observed for any of the above permeants. This is contrary to the observations of Serota[17], who found aniline and

nitroaniline to have negative time-lags, whilst the others all behaved normally, when the films being studied were made from polyethylene. In the work presented here, the anomalous time-lag behavior was only found with the nitrophenol, and perhaps the effect of the phenolic hydroxyl group was significant, allowing hydrogen bonding with the polymer or itself. The permeability of Ibuprofen, which was used as a model drug permeant for controlled release studies discussed in Chapter VII also showed the more usual positive time-lag behaviour. Ibuprofen, whose chemical name is 2-(4-isobutylphenyl) propionic acid, contains a carboxy hydroxyl group, and might be expected to associate by hydrogen bonding, favouring a negative lag-time, and thus, the problem remains unresolved.

The data in Table V:11 is, however, otherwise in agreement with the findings of Serota. Namely, the rank order of permeability is the same, and the partition coefficient increased for increasing permeability coefficient. The permeability coefficient was found not to have the expected dependence on molecular weight, i.e., increasing the molecular weight, and hence, increasing molecular volume, would be expected to lead to a reduction in the permeability coefficient. The results indicate that the permeability coefficient was dependent on the partition of the solute from the water into the polymer. Several instances in the literature are in agreement with this hypothesis[17,37-39] for a number of permeants and polymers. Huang and Jarvis[40] demonstrated that the permeability coefficient was inversely proportional to the molecular weight for the permeation of poly(ethylene glycols) through cellophane membranes, and this

relationship was consistent with a porous flow model for permeation. The lack of any such trend here, and the strong dependence of the permeability coefficient on the partition coefficient indicates that the films were not porous, or that the pores were too small to allow permeation. Therefore permeability through the film is controlled by the partition of the permeant into the film.

Solute molecule	Molecular Weight	Partition coefficient $x10^3$ g/g	Permeability coefficient $x10^9$ h m^{-2}	Activation energy kJ mol^{-1}
Aniline	93	2.44	6.67	115.7
Methyl aniline	107	5.98	11.89	112.4
Ethyl aniline	121	10.69	43.05	40.7
Dimethyl aniline	121	14.76	70.45	13.9
mNitro aniline	138	5.42	5.24	37.0

TABLE V:11 THE PERMEABILITY OF SEVERAL ANILINE DERIVATIVES

V:4 PERMEABILITY OF HETEROGENEOUS LATEX FILMS

V.4.1 SOLUTE PERMEABILITY STUDIES ON CORE-SHELL AND COPOLYMER LATEX FILMS

Permeation through the interparticle boundaries that remain after film formation was postulated earlier. In this study the interparticle boundaries were made more permeable by coating PBMA latex with poly(methyl acrylate), PMA, to form a core-shell latex particle. Also, copolymers of the same proportions were prepared to check the effect of polymer composition as well as the effect of the interparticle boundaries. The latices were cleaned by microfiltration and dried on glass plates at 80°C for three hours. The film permeabilities were tested 24 hours and one month after the films were prepared.

The nitrophenol permeability coefficients were determined as described earlier. Since it has been shown that film orientation effects the permeability coefficient, the films were orientated with the glass cast side facing the nitrophenol solution for consistency.

The initial permeability of both the core-shell and the copolymer films increased as the volume fraction of the PMA increased. This is to be expected given the much greater permeability coefficient of PMA in comparison with PBMA. The 40/60 PBMA/PMA core-shell film had a much higher initial permeability than the corresponding copolymer film, whilst at lower volume fractions of PMA the agreement between the two was good. Considering the

core-shell			copolymer		
composition PBMA/PMA %	permeability coefficient h m^{-2} x10^{9}		composition PBMA/PMA %	permeability coefficient h m^{-2} x10^{9}	
	24 hours	1 month		24 hours	1 month
100/0	1.0	0.3	100/0	1.0	0.3
80/20	1.1	1.4	80/20	0.9	0.7
60/40	2.1	2.4	60/40	2.5	2.2
40/60	7.3	2.6	40/60	4.7	2.8
*			20/80	8.2	2.3
0/100	10.8	2.9	0/100	10.8	2.9

TABLE V:12 NITROPHENOL PERMEABILITY OF CORE-SHELL AND COPOLYMER LATEX FILMS

* the 20/80 core-shell latex could not be prepared by the process used here as the second monomer formed a secondary growth of particles.

films as two phase systems then it would seem likely that the low Tg material (PMA) would form a continuous phase in which the higher Tg material (PBMA) was dispersed, and this would be true for the core-shell films. However, Brown[41] pointed out for geometric reasons that volume fractions of less than 30-40% softer polymer, depending on the domain size distributions, was insufficient to form

the continuous phase. From the above table it can be seen that the permeability coefficient increased markedly above the 60/40 PBMA/PMA composition, perhaps indicating the strong influence of the PMA, due to a continuous phase of the softer material controlling the overall film permeability. Upon aging, the copolymer films all showed a reduction in permeability over the period of one month, and this observation is in keeping with findings by Chainey[13] for the permeability of copolymer latex films. The core-shell films, however, showed no signs of aging at the lower volume fractions of the shell polymer. The lack of appreciable aging was also noted by Chainey[13] when the volume fraction of the shell polymer was small. He suggested that this was caused by the movement of the shell polymer chains being impeded through grafting with the core particles[43]. The permeabilities of the aged films were all similar to that of PMA for both the copolymer and core-shell films, with the exception of the 80/20 composition. At the lowest volume fraction of PMA there would not have been sufficient polymer to form a continuous network, and hence the permeability is lower than the other films, where the permeability is dominated by a network of PMA.

The formation of a distinct PMA phase could not occur if the particles consisted of true random copolymer chains. If, however, the particles were made up of a heterogenous copolymer in which there were domains of one polymer dispersed in the other, or a core-shell morphology existed, then a continuous phase of PMA in the film would be possible. There are several circumstances which could lead to the formation of heterogeneous copolymer

particles, and in this instance the different solubilities of the monomers in the water and polymer could give rise to such heterogeneous particles. An example of copolymer latices forming distinct phases within latex films was demonstrated by Kast[42]. He showed that films formed at temperatures above the MFT for one polymer but below the MFT for the other polymer formed films that contained the second polymer dispersed in a continuous phase of the lower MFT polymer. However, when the films were heated to temperatures above the MFT for the dispersed polymer a phase inversion took place, with the softer polymer dispersed in a continuous phase of the harder polymer; the driving force for this process was the polymer-polymer interfacial tensions, which corresponded with the thermodynamically unfavourable situation of one phase dispersed in another[42].

For permeability to take place solely through the interparticle boundaries, then for the core-shell films the permeability would be independent of the coating thickness, since the interparticle regions would consist of the same material. This is clearly not the case for both the aged and unaged core-shell films. As suggested above the permeability was controlled by the partition of the permeant into the film, and also the similarity of the results found for copolymer and latex films on aging suggests that the permeability was principally through a network of PMA within the film.

A comparison of experimental results with the theories of Higuchi[44], Maxwell[45], and Rayleigh[46], for permeation through heterogeneous systems is given in Table V:13. The experimental permeation results are those

obtained for films after 24 hours. Of the three theories the Higuchi and Maxwell predictions are closest to the experimental results. The Maxwell theory shows better agreement for the lower volume fractions of PMA, and this is expected since the theory only applies to dilute dispersions of particles where no particle interactions are accounted for. The Higuchi theory however, was developed to account for particle interactions in dispersions.

%Composition PBMA/PMA	Permeability coefficient x10 ^{9} h m^{-2}				
	Experimental		Higuchi	Maxwell	Rayleigh
	core-shell	copolymer			
100/0	1.0	1.0	1.0	1.0	1.0
80/20	1.1	0.9	2.0	1.5	0.8
60/40	2.1	2.5	3.1	2.5	1.2
40/60	7.3	4.7	4.9	4.0	1.7
20/80		8.2	7.2	6.8	2.1
0/100	10.8	10.8	10.8	10.8	10.8

TABLE V:13 A COMPARISON OF VARIOUS THEORETICAL PREDICTIONS AND EXPERIMENTAL RESULTS

The data in Table V:14 compares the initial and final permeabilities obtained experimentally with those predicted by the Higuchi treatment.

Composition PBMA/PMA %	Permeability coefficient x10 ^{9} h m^{-2}					
	Experimental				Higuchi	
	core-shell		copolymer			
	initial	final	initial	final	initial	final
100/0	1.0	0.3	1.0	0.3	1.0	0.3
80/20	1.1	1.4	0.9	0.7	2.0	0.6
60/40	2.1	2.3	2.5	2.2	3.2	0.9
40/60	7.3	2.6	4.7	2.8	4.9	1.4
20/80			8.2	2.3	7.2	2.0.
0/100	10.8	2.9	10.8	2.9	10.8	2.9

TABLE V:14 A COMPARISON OF EXPERIMENTAL PERMEABILITIES WITH THE HIGUCHI PREDICTIONS

The theoretical predictions of the aged films are all lower than the experimental values indicating that the theory was incapable of predicting the permeabilities in these copolymer films. The same conclusions were reached by Chainey[13], where the calculated values were in better agreement with the experimental values at the higher volume fractions of the shell polymer. This may in part be due to the morphological changes within the film, described earlier giving rise to a film with a distinct polymer phase controlling the overall film permeability, and also permeability through the interparticle regions. If the interparticle regions had been richer in the more permeable polymer then higher permeability would be expected.

V.4.2 WATER VAPOUR PERMEABILITY THROUGH HETEROGENEOUS FILMS

As a test of whether the same trends were apparent for different permeants, the experiments were repeated using water vapour as the permeant. The permeability coefficients were determined as described previously. The permeability coefficients for the lower film surface in contact with the vapour are shown in Table V:15

There appears to be no significant effect of the PMA volume fraction, which was not the case for the solute permeability. The permeabilities are similar for each set of polymers, with the exception the 20/80 PBMA/PMA copolymer, and the core-shell films have a slightly higher permeability coefficient. This observation could imply that the permeability of water vapour is more dependent on transport through the interparticle regions than through the polymer itself. For the core-shell polymer the interparticle regions would all have a similar hydrophilic nature and thus be equally attractive to the water vapour. In the copolymer films the presence of a phase of the softer PMA dispersing the harder PBMA would also result in the interparticle regions consisting mainly of PMA, although the inclusion of the less permeable PBMA served to lower the overall film permeability. The much smaller difference in the homopolymer permeabilities to water vapour compared with nitrophenol results in films showing intermediate values irrespective of the volume fraction of polymer. Only the 20/80 PBMA/PMA shows any significant departure from the trend and it behaves more

like the PMA homopolymer, with the relatively small amount of PBMA having little effect on the overall film permeability. A comparison of the experimental values with those derived from the Higuchi equation is shown in Table V:16

As with the solute permeability there is poor agreement between theory and the observed permeability coefficients. Although Chainey[13] reported reasonable agreement between the experimental values and those predicted from the Higuchi equation for helium permeability, the application of these types of equations gives poorer agreement when applied to water vapour and solute permeability. The homopolymer permeability values reported by Chainey were similar such that the theoretical values would necessarily be similar to the observed permeabilities, given the accuracy of the measurments performed. In this study there was a large difference in the homopolymer permeability coefficients. The main reason that the theories do not predict the observed permeability is probably due to permeation through the interparticle boundaries in the film. For the core-shell polymers, these regions would be rich in the more permeable polymer, and for the copolymers, the possibility of a heterogeneous copolymer could also lead to these regions being rich in the more permeable polymer. This argument would seem reasonable, given the greater overall agreement between experiment and theory at the higher volume fractions of the more permeable polymer.

composition PBMA/PMA %	core-shell		copolymer		
	permeability coefficient s $m^3 kg^{-1}$ $x10^{17}$		composition PBMA/PMA %	permeability coefficient s $m^3 kg^{-1}$ $x10^{17}$	
	Initial	1 month		Initial	1 month
100/0	2.1	1.4	100/0	2.1	1.4
80/20	2.6	2.3	80/20	2.8	2.5
60/40	3.0	2.8	60/40	2.7	2.2
40/60	3.0	2.9	40/60	2.5	2.4
*			20/80	3.6	3.7
0/100	5.3	3.7	0/100	5.3	3.7

TABLE V:15 THE WATER VAPOUR PERMEABILITY OF CORE-SHELL AND COPOLYMER LATEX FILMS

Composition PBMA/PMA %	Permeability coefficient $x10^{17}$ s $m^3 kg^{-1}$					
	Experimental				Higuchi	
	core-shell		copolymer			
	initial	final	initial	final	initial	final
100/0	2.1	1.4	2.1	1.4	2.1	1.4
80/20	2.6	2.3	2.8	2.5	2.6	1.7
60/40	2.9	2.8	2.7	2.2	3.1	2.1
40/60	3.0	2.9	2.5	2.4	3.7	2.5
20/80			3.6	3.7	4.5	3.1
0/100	5.3	3.7	5.3	3.7	5.3	3.7

TABLE V:16 COMPARISON OF EXPERIMENTAL WATER VAPOUR PERMEABILITIES WITH HIGUCHI PREDICTIONS

V.5 References.

1. D.Distler, G.Kanig; Colloid Polym. Sci., 256, 1052 (1978).

2. J.C.Padget, P.J.Moreland; J. Coat. Technol., 55, 39 (1985).

3. M.Chainey, M.C.Wilkinson, J.Hearn; J. Polym. Sci., Polym. Chem. Ed., 23, 2947 (1985).

4. British Standard 2782 Pt8 Method 821A (1979).

5. B.J.Hennessy, T.C.Stenning, J.A.Mead in "The Permeability of Plastic Films". The Plastics Inst. London (1966).

6. P.H.List, G.Laun; Pharm. Ind., 42, 399 (1980).

7. S.S.Voyutskii; J. Polym. Sci., 32, 528 (1958).

8. E.B.Bradford, J.W.Vanderhoff; J. Macromol. Chem., 1, 335 (1966).

9. P.H.List, G.Kassis; Acta Pharmaceutica Technologica 28(1) (1982).

10. E.B.Bradford, J.W.Vanderhoff; J. Macromol.Sci. Phys B(6), 671 (1972).

11. F.K.Isaacs; J. Macromol. Chem., 1(1), 163 (1966).

12. C.Bondy, M.M.Coleman; J. Oil Col. Chem. Assoc., 53, 555 (1970).

13. M.Chainey, M.C.Wilkinson, J.Hearn; Macromol. Chem., Suppl. 10/11, 435 (1985).

14 J.Crank, G.S.Park; (Eds), in "Diffusion in Polymers" Academic Press, New York (1968).

15. G.L.Flynn, T.J.Roseman; J. Pharm. Sci., 60, 1788, (1971).

16. E.R.Garrett, P.B.Chemburker; ibid., 57, 949, (1968).

17. D.Serota, M.Meyer; ibid., 61, 419 (1972).

18. G.S.Banker, A.Y.Gore, J.Swarbrick; J. Pharm. Pharmac., 18, 457 (1966).

19. S.T.Hwang; Polym. Sci. Technol., 6, 197 (1974).

20. S.T.Hwang, G.Strong; J. Polym. Sci., Symp(41), 17, (1973).

21. V.Stannett in "Diffusion in Polymers"; J.Crank, G.S.Park (Eds). Academic Press, New York (1968).

22. M.B.Rodell, W.L.Guess, J.Autian; J. Pharm. Sci.,

55, 1429 (1966).

23. M.A.Gonzales, O.Nemotollahi, W.L.Guess, J.Autian; ibid., 56, 1288 (1967).

24. S.A.M. Abdel-Aziz; Ph.D Thesis, Univerisity of Strathclyde 1976.

25. C.E.Rogers, S.Stenberg; J. Macromol. Sci., Phys B5(1), 189 (1971).

26. R.M.Barrer; Trans. Faraday Soc., 35, 625 (1939).

27. S.A.M.Abdel-Aziz. P.A.M.Armstrong. W.Anderson; J. Pharm. Pharmac., 25 Suppl.137 (1973).

28. R.Katz, B.F.Munk; J. Oil Col. Chem. Assoc., 52, 418 (1969).

29. M.Yaseen, K.V.S.N.Raju; Prog. Org. Coat., 10, 125 (1982).

30. D.R.Paul, A.T.DiBenedetto; J. Polym. Sci., PtC 1017 (1965).

31. V.Stannett in "Permeability of Plastic Films and Coated Papers to Gases and Vapours", TAPPI Monograph Series No23, New York (1962).

32. R.M.Barrer; Trans Faraday Soc., 35, 644 (1939).

33. G.S.Park; ibid., 48, 11 (1952).

34. H.Fujita; Fortschr. Hochpolym-Forsch-Bd, 3, 51, (1961).

35. M.Donbrow, M.Friedman; J. Pharm Pharmac., 27, 633 (1975).

36. H.Senf, H.Wollman, U.Cyranka; J. Pharm. Sci., 62, 2059 (1973).

37. E.R.Garrett, P.B.Chemburker; ibid., 57, 1041 (1968).

38. O.P.Ho, J.M.Padfield, B.J.Meakin; J. Pharm. Pharmac., 29, 46 (1977).

39. A.Polack, M.Roberts, F.Schuman; Amer. J. Hosp. Pharm., 27, 638 (1970).

40. R.Y.Hwang, N.R.Jarvis; J. Polym. Sci. Symp(41) (1972).

41. L.J.Hughes, G.L.Brown; J. Appl. Polym. Sci., 5, 580 (1961).

42. H.Kast; Macromol Chem., Suppl.10/11, 447, (1985).

43. T.I.Min, A.Klein, M.S.El-Aasser, J.W.Vanderhoff; J. Polym. Sci. Chem. Ed., 21, 2845 (1983).

44. W.I.Higuchi; J. Phys. Chem., 62, 649 (1958).

45. D.A. de Vris; The Thermal Conductivity of Granular Materials, Bull Inst. Intern. du Froid, Paris (1952).

46. R.M.Barrer in "Diffusion in Polymers", J.Crank G.S.Park (Eds) Academic Press, Chpt. 6 pp 165 (1968).

47. M.Chainey, M.C.Wilkinson, J.Hearn; Ind. Eng. Chem. Prod. Res. Dev., 21, 171 (1982).

CHAPTER VI

THE EFFECT OF COMMON LATEX ADDITIVES ON THE WATER VAPOUR PERMEABILITY OF LATEX FILMS

In all industrial latex systems there are many components such as surfactant, inorganic material from initiator fragments, and a variety of other chemicals, such as biocides, which are added to the latex to improve its stability and shelf life. In this study, the effect of some of these materials on the resulting latex film permeabilities were studied. All the latices used were prepared by the surfactant-free method described earlier, and were cleaned by microfiltration prior to use. Latices were prepared in this manner for the same reasons as given in Chapter V, i.e., to produce a model system of monodisperse polymer particles, and to form it into a model polymer film, where any properties of the film are entirely due to the polymer and the film morphology.

Since the additives are all water soluble the films were not tested for their solute permeability as the effect of the additives leaching out of the film would both affect the film morphology and interfere with the analysis of the solute.

VI.1. THE WATER VAPOUR PERMEABILITY OF PBMA

In all the water vapour studies the latex films were prepared by drying in an oven at 80°C for three hours on nylon plates. The water vapour permeability was determined by a weight loss method similar to that used by Patel[1], and Banker[2] and was described in Chapter II. Figure VI:1 shows the weight loss versus time for PBMA latex and solvent cast films, where the lower surface of the film was facing the water vapour. The gradient of the

linear portion was used to calculate the water vapour flux through the films. The average water vapour permeabilities were 2.1 and 1.7 $x10^{-17}$ $Sm^3 kg^{-1}$ for the latex and solvent cast films, respectively. The permeability of latex films is known to decrease with film age[3,4]; thus the water vapour permeability of solvent cast and latex films were determined one month after preparation This was also demonstrated in Chapter V. of this study, for the permeability of solutes. The profiles are shown in Figure VI:2. The average values were 1.4 and 1.7 $x10^{-17}$ $Sm^3 kg^{-1}$ for the latex film and solvent cast film, respectively. The latex film showed a reduction in permeability on storage whilst the solvent cast film remained the same. This is in keeping with the findings of Chainey[3], and also the solute permeabilities shown earlier in this work. The only reference in the literature for water vapour permeability was given by Banker et. al.[2], who quotes the water vapour permeability coefficient for PBMA ranging from 3.54 to 4.16 $x10^{-17}$ s $m^3 kg^{-1}$. Since the casting solvent,[5] substrate[6], and thermal history[7] are all factors known to influence the film permeability, the difference between Banker's values, and those found in the present study is understandable.

List and Kassis[8] found that films prepared from an aqueous dispersion and an organic solution of Eudragit L 30 D showed a reduction in permeability with time. (Eudragits are copolymers of acrylic and methacrylic acid and their methyl and ethyl esters.) The films prepared from the aqueous dispersion were found to attain their lowest permeability after a few days, and this value was

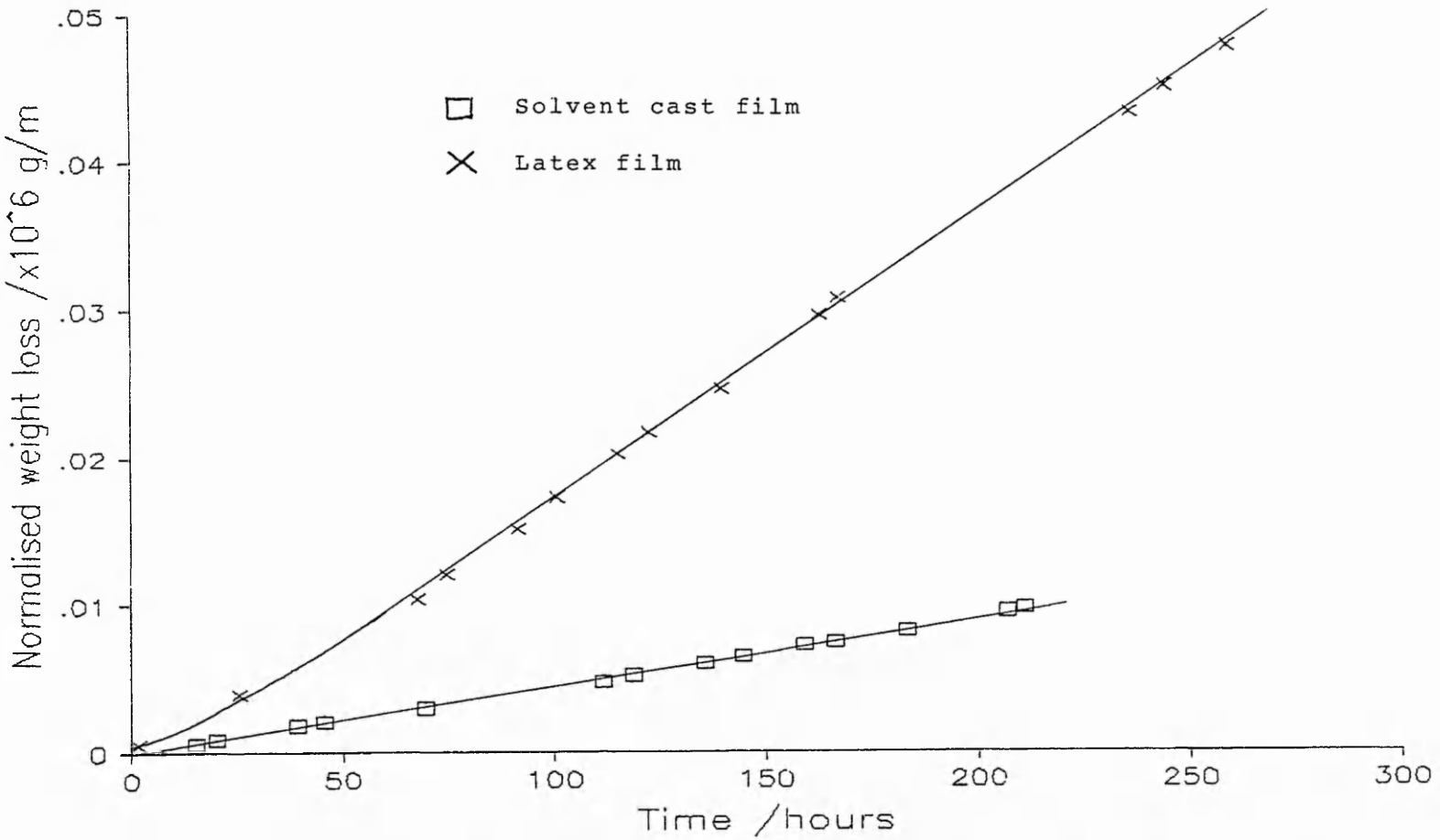

Figure VI:1 Weight loss vs time for latex and solvent cast films

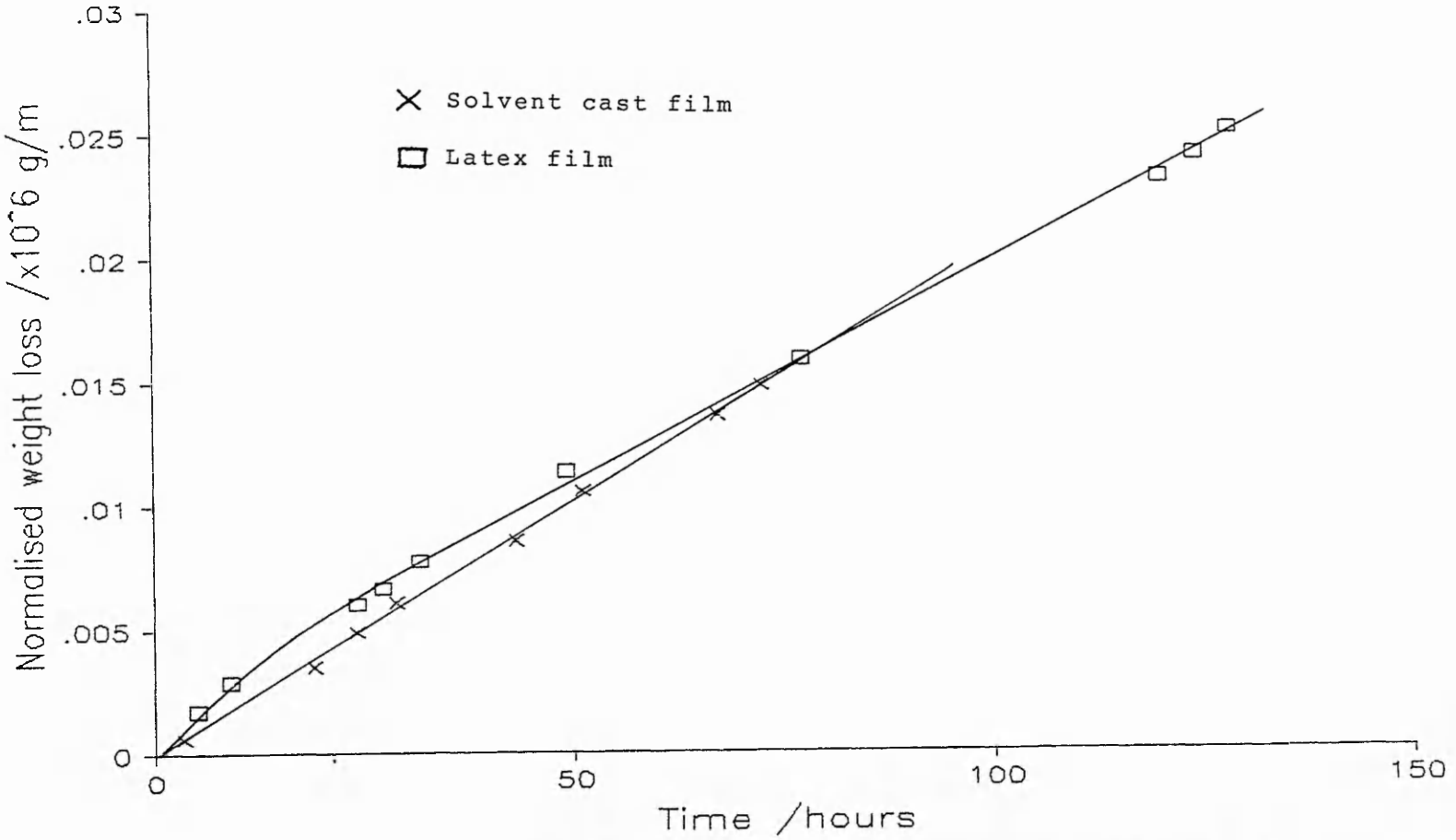

Figure VI:2 Weight loss vs time for films aged 1 month

lower than the equivalent film cast from an organic solution of the same polymer. List attributed this difference to the film morphology, which is reflected in the latex film having a greater density than the solvent cast film. The latex films used in this study were also found to have a higher density than solvent cast films of the same polymer. (see Section V.1.4 in Chapter V)

Banker et.al.[2] studied the water vapour permeability of solvent cast films of PBMA and some cellulose derivatives. They showed that the relatively hydrophobic poly(butyl methacrylate) showed a reasonably constant water vapour permeability coefficient with respect to film thickness. However, the relatively hydrophilic cellulose films had increasing permeability coefficients with increasing film thickness. For Fickian diffusion the permeability (flux) should be inversely proportional to the film thickness and this was also found to be the case for the permeabilities of PBMA solvent cast and latex films prepared in this work. A linear regression analysis showed that the plot had a positive intercept on the Y axis in agreement with Patel[1] and Banker et. al.[2]. The magnitude of the positive intercept was found to increase as the hydrophilic nature of the film increased[2] and was interpreted in terms of polymer-permeant interactions. In the present work, the theoretical prediction of the effect of film thickness on permeability shows reasonable agreement with the experimental values.

The water vapour permeability of solvent cast films showed little difference in permeability with respect to film orientation. The values were 1.73 ± 0.12 and

$1.76 \pm 0.11 \times 10^{-17}$ s $m^3 kg^{-1}$ for the lower and upper surface, respectively. The latex film gave a lower permeability when the lower surface was exposed to the water vapour. The values were 2.1 ± 0.45 and $3.1 \pm 0.56 \times 10^{-17}$ s $m^3 kg^{-1}$ for the lower and upper surface, respectively. This finding is contrary to that found for nitrophenol permeation through latex films, indicating that different interfacial processes control the permeability for aqueous solutes and water vapour.

Several instances of film asymmetry with respect to permeability have been reported in the literature. Abdel Aziz[5,9] reported that acrylic and methacrylic acid ester copolymer films cast from solution, showed an orientation effect for the permeation of aqueous solutes, with the lower surface having the higher permeability. This was attributed to gross differences in both the film surfaces and internal morphology. The upper surface had a more dense layer of polymer extending into the film interior, whilst the lower surface was a more open 'sponge' like structure similar to the bulk of the film interior. Chainey[3], showed an electron micrograph of a poly(butyl methacrylate) solvent cast film which exhibited some small pores in the upper surface and the presence of a dense layer, but the presence of any porosity in the interior of the film was not shown. The lack of any internal porosity in solvent cast films was shown earlier in this study.

Katz and Munk[10] showed that the polarity of the

substrate affects the water vapour permeability of the film. For polar polymers cast on polar substrates such as tin foil or glass the water vapour permeability was higher than when cast on nonpolar substrates, such as polyethylene. Also, the lower side of the film had the higher permeability. The orientation effect was attributed to the substrate attracting polar groups in the polymer, and thus concentrating these groups at the substrate surface. Yaseen[6] also demonstrated the increased water vapour permeability of film cast from polar substrates.

The evidence so far seems to suggest that, for solvent cast films, the lower surface should demonstrate the lower permeability, and none of the explanations can easily be attributed to latex films. In this study the solvent cast films were formed on a PTFE surface which is relatively nonpolar, and thus, the polarisation argument is not likely to apply. The appearance of the films may suggest a solution to this problem. In all cases, the lower substrate side of the film, was 'glossy'in appearance, in contrast to the more matt upper surface. This difference in the surface is likely to be due to surface roughness, which in turn would affect the area available for the absorption of water vapour. The small difference in the permeability of the solvent cast film with respect to orientation could be explained by an increased area available for absorption of only 1%. For latex films an increase in surface area of approximately 50% would be needed to account for the observed higher permeability of the upper surface. Electron micrographs shown in Chapter IV demonstrate the difference in appearance of the upper and lower surfaces of a latex film

(Plates IV:14 and IV:15). Clearly, the upper surface is more disrupted and has a higher surface area than the more planar lower surface. Using surface area differences to explain the orientation effect, absorption of water vapour into the film would be rate controlling. This is the opposite effect to that found for solute permeability, where desorption from the film was used to explain the orientation effect. Because PBMA is a relatively hydrophobic polymer[2], absorption of water vapour would be less favourable than desorption, and thus, the higher surface area available for water uptake would give the higher permeability, whereas the opposite was true for solute permeability because of the partition of the solute between the aqueous and the polymer phases.

VI.2. THE EFFECT OF ADDED SURFACTANT

Three different types of surfactants were used, a cationic, an anionic and a non ionic, all with the same hydrocarbon chain length. The anionic surfactant was sodium dodecyl sulphate (SDS), the cationic was dodecylethyldimethylammonium bromide (DEDAB), and the non-ionic was dodecyl tetraoxyethylene glycol monoether (C12E4). In order to establish a comparison between the three surfactants used the amount of surfactant added is reported in moles of surfactant per gram of polymer. Since they all contain the dodecyl hydrocarbon chain it is believed that differences only arise in the compatibility of the head group with the polymer, particularly during the latter stages of film formation.

VI.2.1 THE EFFECT OF ADDED SDS

The water vapour permeabilities of PBMA films with added SDS are shown in Table VI:1. As well as monitoring the effect of increasing surfactant concentration the effect on the permeability of film orientation and age was studied. The initial water vapour permeability for the surfactant free latex film was found to be 2.1 $x10^{-17}$ s $m^3 kg^{-1}$. This value was found to decrease as the concentration of added SDS increased, and a minimum permeability was found for a concentration of added surfactant of 150 $x10^{-6}$ moles SDS per gram of polymer. As the SDS concentration was increased above this value, the water vapour permeability increased again. Assuming that the area occupied by an SDS molecule was 0.5 nm^2[11], and the size of the latex particles was 400nm, the concentration required to just cover the latex particle surface would be 150 $x10^{-6}$ moles SDS per gram polymer. This value was in agreement for the SDS concentration required to give the film of the lowest permeability. The critical micelle concentration (CMC) of SDS in distilled water was determined by the conductometric method. The CMC was also determined in the presence of the latex, and the difference in the two values was attributed to the amount of surfactant adsorbed on the particle surface. The experimental value was 141 $x10^{-6}$ moles SDS per gram of polymer. This value is both in reasonable agreement with the predicted value, and the value required to give the lowest film permeability.

Conc SDS mole/gram polymer x10⁶	water vapour permeability coefficient x10¹⁷ s m³ kg⁻¹			
	Initial		After 1 month	
	film orientation to vapour		film orientation to vapour	
	lower	upper	lower	upper
0	2.1 ± 0.29	3.1 ± 0.56	1.4 ± 0.10	
78	1.8 ± 0.06	2.8 ± 0.33	1.2 ± 0.01	2.0 ± 0.1
150	1.0 ± 0.09	1.0 ± 0.08	0.9 ± 0.07	0.9 ± 0.07
178	1.8 ± 0.07	2.2 ± 0.22	2.2 ± 0.08	2.3 ± 0.04
258	2.5 ± 0.16	3.4 ± 1.85	3.5 ± 0.28	5.6 ± 0.78
350	2.7 ± 0.08	2.7 ± 0.26	2.8 ± 0.48	3.3 ± 0.40

Table VI:1 THE EFFECT OF ADDED SDS ON WATER VAPOUR PERMEABILITY

A sample of the film with the lowest permeability was analysed using the electron microscopic technique discussed in Chapter IV. Plate VI:1 shows a fracture cross section of the film, at the plate magnification a latex particle would have a diameter of 2 cm. Particle boundaries are not a prominent feature in this plate although there is some internal morphology. The micrograph shows no effects of the surfactant being exuded or forming a second phase, and thus, the fate of the surfactant during film formation remains uncertain. Plate VI:2 shows a similarly prepared sample of the film with the highest surfactant concentration employed in this study. A particle diameter would be 1.1 cm at the Plate

magnification. The appearance is similar to Plate VI:1, in that particle boundaries are hardly visible and again there seems to be no evidence of the surfactant, even though an amount well in excess of particle surface coverage was present in this sample. Plate VI:3 shows another fracture of the same sample as in Plate VI:2. In this case the fracture appears to have taken place through the interparticle regions, rather than through the particles. The effect of the excess surfactant is clear, since several patches of crystalline material(marked A) are visible. This same material is also present at the periphery and interstices of the particles (B). This suggests that the excess surfactant collects into small aggregates forming a defect in the film, and also in smaller aggregates in the interparticle interstices during the film formation process. The particles appear in a well ordered array as is clear from the plates described in Chapter IV, and there is some evidence that the particles are deformed. The top of the particles appear round rather than exhibiting the regular shape predicted earlier; this may be an artifact of the preparation. Even though the fracture took place at liquid nitrogen temperatures and the replica was made at the same temperature, the possibility of plastic deformation cannot be ruled out. During the actual fracture large amounts of energy are released, and this can be manifested as localised heating. Thus, the particle surface could have been warmed during the fracture and some of its features lost. This may then account for the rounded nature of the particles. The clear evidence of particle boundaries in Plate VI:3 indicates that the lack of particle boundaries in Plate VI:2 was

PLATE VI.1 TEM REPLICA OF FREEZE FRACTURE PBMA LATEX FILM WITH SURFACE COVERAGE OF SDS

SDS CONCENTRATION 150 X10^{-6} MOL/G

PLATE VI.2 TEM REPLICA OF FREEZE FRACTURE PBMA LATEX FILM WITH ADDED SDS

SDS CONCENTRATION 350 $\times 10^{-6}$ MOL/G

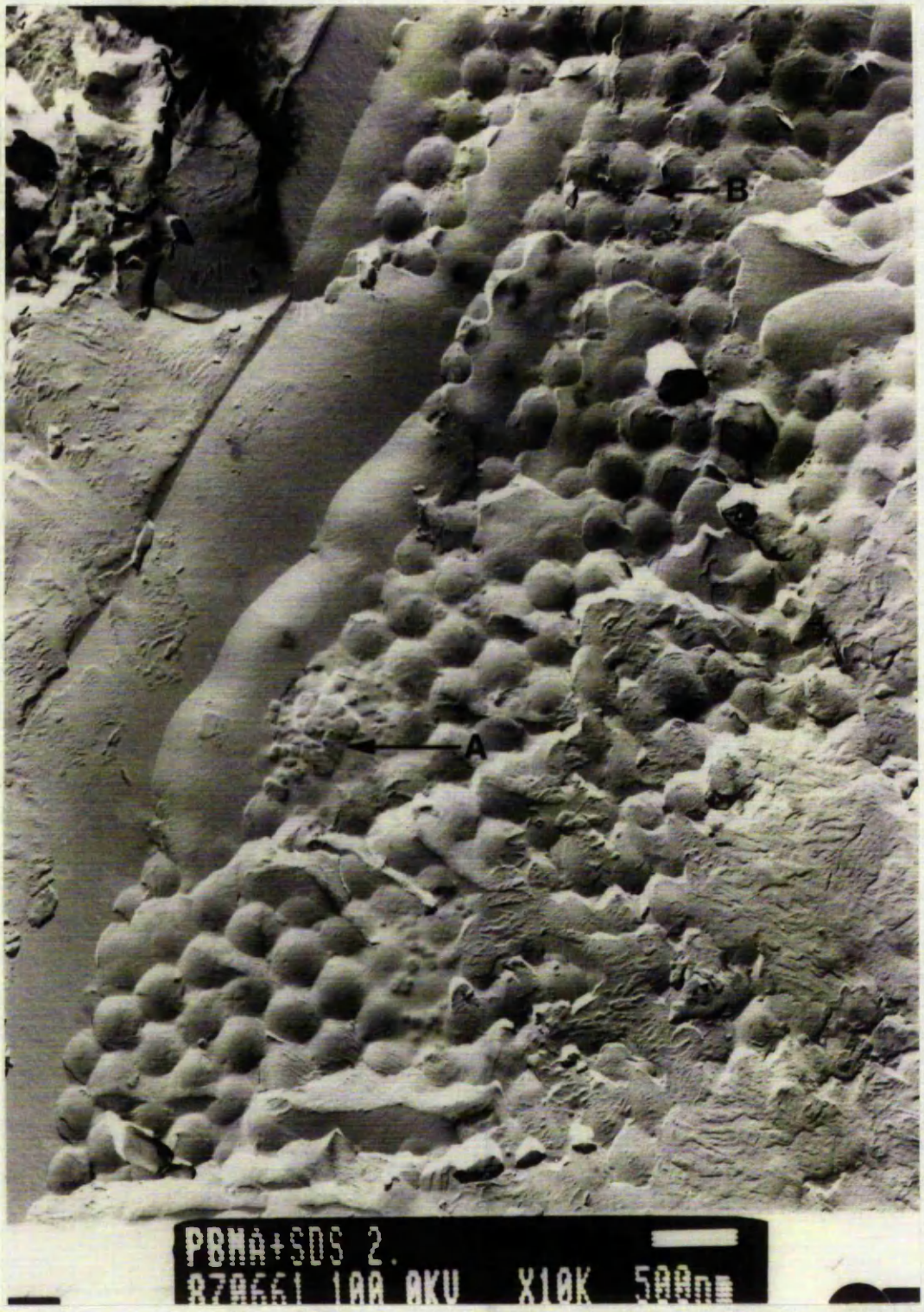

PLATE VI.3 TEM REPLICA OF FREEZE FRACTURE PBMA LATEX FILM WITH ADDED SDS

SDS CONCENTRATION 350 $\times 10^{-6}$ MOL/G

caused by the plane of fracture rather than totally coalesced particles.

The permeability coefficient was shown to decrease on aging for all the films containing less than 150 $x10^{-6}$ moles/gram polymer. Isaacs[12] showed that electrolyte permeability decreased on addition of surfactant to acrylic copolymer latex films, and that the permeability was reduced on aging. Bondy and Coleman[13] showed that the water vapour permeability decreased and the tensile strength increased with film age. The rate at which this occurred depended on film thickness. It was suggested[13] that the surfactant surrounding each particle must be displaced before the particles can fully coalesce, and that the displaced surfactant must migrate to the film surface, and thus in thicker films this process would take longer. The decrease in film permeability has been shown earlier in this study and elsewere[3] and was also interpreted in terms of the autohesion process increasing the interparticle coalescence. If the same arguement can be applied here, then small amounts of surfactant adsorbed on the particle surface seem not to impede this further gradual coalescence. In fact, the situation is improved, since the aged permeability coefficient decreases from the clean film value, to a minimum for the film having a monolayer coverage of surfactant.

At amounts of SDS above surface coverage the permeability coefficient was not reduced on aging, and in some instances increased. It appears that further gradual coalescence either is not occurring or other changes in the film morphology are having a greater effect on the film permeability. One of the possible fates of the

surfactant during film formation is to be absorbed by the polymer. At the point when the water is removed and the particles come into irreversible contact the hydrocarbon chain could collapse and subsequently be absorbed in the particle surface. For concentrations of surfactant below monolayer coverage this process could account for the lack of any exudations or a separate surfactant phase within the film. At greater concentrations, the excess surfactant could not be adsorbed onto the particles, which were already saturated with surfactant and thus must exude and form aggregates, as was shown in Plate VI:3

Considering the water vapour permeability in terms of the film structure in the presence of surfactant, the evidence in Plates VI:1 to VI:3 shows that the interparticle boundaries are present in films containing SDS. As was previously suggested, the presence of these regions, which are probably more hydrophilic than the bulk of the polymer, are responsible in part for the permeation through latex films, particularly so for water vapour. The lowest permeability resulted from a film with a surface coverage of SDS. Two possible explanations are proposed as follows.

A. The surfactant on the particle surface may aid the coalescence in the final stages of film formation, and thus, at concentrations lower than surface coverage, this effect would be diminished; this would account for the drop in permeability as the SDS concentration increases. At levels of addition greater than surface coverage the excess surfactant only serves to disrupt the film by forming small aggregates within the film, or residing in the interparticle interstices. This would account for the

increasing permeability when levels of addition above surface coverage are employed. The presence of hydrophilic groups on the surface causes the interparticle regions to remain after film formation is complete, due to the incompatibility of the hydrophilic entities with the hydrophobic interior of the latex particles.[14] However, it is possible that the dodecyl hydrocarbon chains plasticised the particle surface, thus making the autohesion process easier.

B. Durbin[15] described the film formation process in terms of the particle packing in the films. The order of particle packing in the film was determined by the latex particle stability. The more ordered particle packing resulted from the particles of the greatest stability. Durbin showed that polystyrene particles with a surface coverage of Aerosol MA displayed an ordered array at the air/latex interface, whilst the order was reduced at the latex/substate interface. This was attributed to the particles being initially stable during the early stages of film formation; then, as the water content was reduced the electric double layers on the particles were compressed by the increasing ionic strength of the dispersion medium. Thus, the particles became less stable and the packing order was lost. In the present study the permeability of the films decreased as the SDS concentration was increased up to surface coverage. As the amount of adsorbed surfactant increased the stability of the particles was increased accordingly. Thus, employing Durbins argument the particles would remain in stable suspension until a higher volume fraction of the polymer was achieved, and thus would pack in a more ordered

fashion. Once the concentration of SDS exceeded surface coverage the excess surfactant only serves to compress the electric double layer and bring about a loss of stability of the particles earlier during the film formation. However, Durbin gave evidence to show that small amounts of surfactant below a monolayer coverage seemed to destabilise the latex as the packing order was reduced in comparison with a surfactant free film, until surface coverage was reached. This was explained by the added surfactant contributing to the ionic strength of the water, and compressing the double layer on the particle to an extent that outweighed the added charge brought about by the adsorption of the surfactant. If Durbin's argument can be used to explain the observed permeability results two conclusions can be reached. Firstly, that the highly ordered array of particles results in a film with less defects and more polymer-polymer contacts. For a collection of particles which are not uniformly packed then the inclusion of voids within the film must result in the polymer particles having to distort to a greater degree to fill all the space. This may therefore lead to a less tortuous path through the film along the interparticle boundaries, and hence, the permeability is increased. Secondly, Durbin's observation that the lower surface was more ordered for surfactant concentrations at and above surface coverage of surfactant implies that the lower surface should have the lower permeability. This was not found for the films used in this work, and may be reconciled by the increased surface area of the upper surface suggested earlier, since the surfactant containing films showed the same glossy or matt appearance on the

relevant surfaces as was found for additive free films.

VI.2.2 THE EFFECT OF ADDED DEDAB

The effect of adding a cationic surfactant (DEDAB) was studied and the results are given in Table VI:2. Since the latex particles were stabilised by the sulphate groups on the surface arising from the initiator used in polymerisation, the particle surface was anionic in character. The surfactant used was of an opposite charge to the particle surface and thus the particle stability may have been affected at certain DEDAB concentrations. This was in fact observed; low levels of DEDAB addition (i.e., less than 100 $x10^{-6}$ moles/gram polymer) resulted in the latex coagulating immediately. This coagulation was assumed to be caused by the added surfactant neutralising the charge on the particles and thus colloidal stability was lost. At the concentrations employed in this study no coagulation was observed. This implies that the surfactant was rapidly adsorbed, and the charge on the particle was reversed. In the case of the cationic surfactant, the permeability coefficients are all higher than for films containing SDS at the corresponding concentrations. Since both of the surfactants used had the same hydrophobic tail, this difference could be attributed to the head group. The permeability was generally not a function of the DEDAB concentration. However, the permeability of the film at $164x10^{-6}$ moles per gram of polymer is lower than the others. This is slightly larger than the value for surface coverage obtained for SDS. Since the surfactant molecules are likely to adsorb on the particle surface by

Conc DEDAB mole/gram polymer x10⁶	water vapour permeability coefficient x10¹⁷ s m³ kg⁻¹			
	Initial		1 month	
	film orientation		film orientation	
	lower	upper	lower	upper
0	2.1±0.45	3.1±0.56	1.4 ± 0.10	
138	4.6±0.31	6.2±0.62	5.1 ± 0.29	6.0 ± 0.35
164	3.4±0.42	5.2±0.09	4.3 ± 0.11	5.7 ± 0.03
258	4.8±0.08	4.2±0.30	4.4 ± 0.36	4.5 ± 0.08
350	4.1±0.28	4.1±0.28	4.5 ± 0.14	5.3 ± 0.07

TABLE VI:2 THE EFFECT OF ADDED DEDAB ON WATER VAPOUR PERMEABILITY

the hydrophobic dodecyl chain (initially the DEDAB molecules will adsorb head first onto the negatively charged particle surface) the area occupied may be similar; only the relative size of the charged head groups would serve to increase the area occupied per chain.

Irrespective of film age and orientation, the permeability coefficient was higher than for the clean film, and there was no decrease in permeability on aging. These observations were contrary to those found for SDS in a similar range of concentrations and may be due to different film morphologies and the fate of the surfactant during film formation. A sample of the film containing the highest surfactant concentration was examined by the same electron microscope technique described earlier. Plate VI:4 shows a fracture cross section of the film; a particle diameter at the plate magnification would be 0.5

cm. As in the SDS containing film, none of the features found in the clean film are readily apparent. The particle boundaries are difficult to discern, and are either greatly reduced due to further gradual coalescence or masked by the excess surfactant present. Plate VI:5 shows the same sample at a higher magnification; here a particle diameter would be 1 cm. This micrograph shows both areas where the particles appear fractured and smoother areas which could be the particle surface. Although the fracture may not be over the particles as in Plate VI:3 of the SDS containing film, there seems little evidence of the type found earlier for the fate of the excess surfactant in the film. However, the overall texture of the fracture is different from the SDS film, and perhaps the rougher appearance is actually the surfactant spread over the fracture plane. If the surfactant formed layers or regions in between the particles then the fracture is likely to occur through these regions.

Since the permeability coefficients are increased by the addition of surfactant it would seem unlikely that increased coalescence of the particles is responsible for the lack of clear boundaries in the micrographs. It could, however, be argued that there was considerable particle coalescence and that the presence of a separate phase of surfactant within the film explained the increased film permeability by disruption the film morphology. The possibility of the surfactant being absorbed by the polymer, as postulated earlier for the anionic surfactant, should be considered as both the surfactants contain the same hydrocarbon chain. If this process did occur then the large size of the head group and the bromide counterion

PLATE VI.4 TEM REPLICA OF FREEZE FRACTURE PBMA LATEX FILM WITH ADDED DEDAB

DEDAB CONCENTRATION 350 x10^{-6} MOL/G

PLATE VI.5 TEM REPLICA OF FREEZE FRACTURE PBMA LATEX FILM WITH ADDED DEDAB

DEDAB CONCENTRATION 350×10^{-6} MOL/G

would serve to impede the autohesion process to a greater extent than for SDS. This possibility could account for the lack of a reduction in the film permeability with film age.

VI.2.3 THE EFFECT OF ADDED DODECYL TETRAOXYETHYLENE GLYCOL MONOETHER (C12E4)

The third surfactant studied was the non ionic C12E4. Since this surfactant had no charged head group it may be more compatible with the charged latex particle. Films prepared using this additive had a good transparent appearence, even at high levels of addition, which was not the case for the other surfactants studied. The films also seemed to be plasticised by the addition of the C12E4, giving very flexible but not tacky films. The resulting water vapour permeabilities are shown in Table VI:3

Conc C12E4 mole/gram polymer x10^6	water vapour permeability coefficient x10^{17} s $m^3 kg^{-1}$			
	Initial		1 month	
	film orientation		film orientation	
	lower	upper	lower	upper
0	2.1±0.45	3.1±0.56	1.4±0.10	
75	1.9±0.16	2.2±0.29	2.3±0.3	2.4±0.66
150	3.0±0.18	3.1±0.22	3.3±0.23	3.5±0.11
250	3.3±0.27	3.7±0.12	3.6±0.05	4.2±0.11
325	3.1±0.27	3.2±0.05	3.5±0.50	3.2±0.17

TABLE VI:3 THE EFFECT OF ADDED C12E4 ON WATER VAPOUR PERMEABILITY

The addition of the smallest amount of this surfactant appeared to slightly reduce the permeability coefficient initially, but, in general, the permeability coefficients were all similar. The permeability coefficients were not reduced on aging and in some cases a slight increase was found. These observations are similar to those found for the cationic surfactant. A fracture cross section of the film containing the highest concentration is shown in Plate VI:6; a particle diameter would be 1 cm at the plate magnification. The micrograph shows no evidence of the original latex particles, and this is consistent with the plasticised appearence of the film. If the surfactant did plasticise the film then the particles would have coalesced to a much greater extent, possibily causing them to lose their identity completely. Also, the plasticising effect would explain the increased permeability. The absence of any features in the fracture surface indicating particles could also be explained by the fracture plane being through a surfactant phase. However, the texture is similar to the fractured polymer shown for the clean films, and thus seems unlikely. The compatiblity of surfactant with the polymers in latex films has been demonstrated by Vanderhoff and his co-workers[16,17,18]. Surface exudations were found when the surfactant was incompatible with the polymer[17], although no exudations were found in other systems[18]. The possibility of some nonionic surfactants being soluble in, or compatible with, the polymer was also shown[16]. No exudations were found when a nonionic surfactant similar to the one used in this study was included in

PLATE VI.6 TEM REPLICA OF FREEZE FRACTURE PBMA LATEX FILM WITH ADDED C12E4

C12E4 CONCENTRATION 325 $x10^{-6}$ MOL/G

latex films of a styrene-butadiene copolymer[16]. However, when the number of moles of ethylene oxide in the surfactant was increased the surfactant became incompatible with the polymer, where it again was exuded to the surface. (This surfactant was subsequently readsorbed back into the film after oxidative chain scission of the polyethylene oxide chain).

In a recent study by Padget and Moreland[20] the addition of a nonionic surfactant was found to reduce the water permeability and increase the particle coalescence. This was only the case for surfactant additions up to surface coverage, and larger amounts of surfactant caused the water permeability to increase again. In the light of this experience the nonionic surfactant used in this study would probably be dissolved in the polymer, and this solubilisation would have both plasticised the particle surfaces and allowed complete coalescence of the latex particles. The postulate that the decrease in permeability was due to further gradual coalescence would be reinforced by the permeability of these films remaining unchanged with respect to film age, where particle boundaries had completely disappeared. The plasticising effect would also explain the increased permeability, as plasticisers are known to increase the water vapour permeability of both latex films[8] and solvent cast films.[19]

VI.3. THE EFFECT OF ADDED POTASSIUM CHLORIDE

To test the effect of residual inorganic material, on the water vapour permeability, potassium chloride was added to cleaned PBMA latex. All the films prepared were

opaque but never the less appeared to be continuous. The water vapour permeabilities are given in Table VI:4 The amount of added KCl was below the critical coagulation concentration for the latex, which was 0.763 mol/g polymer (0.0425 mol dm^{-3}). The results show that the permeability is greater for films containing KCl, but the magnitude is independent of both the amount of added KCl and the film orientation. The permeability was not reduced on aging, but showed an increase. During the aging period the films showed signs of the inorganic material being exuded. There was a white powder spread across the film surface together with large exudates of material. These were almost certainly KCl crystals being forced out of the polymer film.

Conc KCl mole/gram polymer x10^3	water vapour permeability coefficient x10^{17} s m^3 kg^{-1}			
	Initial		1 month	
	film orientation		film orientation	
	lower	upper	lower	upper
0	2.1±0.4	3.1±0.56	1.4±0.10	
0.89	4.8±0.3	4.3±0.25	6.5±0.54	8.5±0.49
1.79	6.3±0.4	4.3±0.5	6.2±0.27	5.8±0.07
5.38	4.8±0.2	4.3±0.4	5.5±0.22	5.9±0.14
7.18	4.6±0.8	7.4±0.15	4.9±0.87	7.4±2.0

TABLE VI:4 THE EFFECT OF ADDED KCL ON WATER VAPOUR PERMEABILITY

The amount of KCl added in terms of a percentage of the weight of polymer ranged from 6 to 54%, which, at the highest level represents a considerable proportion of the total film weight. A micrograph of the film containing this high percentage of KCl is shown in Plate VI:7; here a particle diameter would be 1 cm. The Plate shows no evidence of the 54% KCl present in this film. However, the partly coalesced particles are present, with the boundaries being discernible. The interparticle boundaries are, however not clear enough to show any ordering of the particles into packed arrays. With the large amount of KCl in this film the tendency for coagulation would increase as the film dried and the ionic strength of the remaining water increased. The coagulation would result in a less ordered film and may therefore lead to a greater permeability.

The fate of the inorganic material is not clear from the plate, but the appearence of the film, and the exudations, indicate that the KCl was concentrated at the film surface during film formation, and material trapped in the polymer near the surface was further forced to the surface during the aging process. This explanation is borne out by the permeability coefficients. If the inorganic material was homogeneously dispersed throughout the film then the film integrity, and hence its permeability, would change dramatically when the KCl went from occupying 6% to 54% of the total film. Since, to a first approximation, the permeability was unchanged then it is more probable that the inorganic material was not included in the film to any great extent, and only resided near the film surface.

PLATE VI.7 TEM REPLICA OF FREEZE FRACTURE PBMA LATEX FILM WITH ADDED KCl

KCl CONCENTRATION 7.18 $x10^{-3}$ MOL/G

VI.4. THE ADDITION OF POLYMERIC STABILISER

PBMA polymer latex films were prepared with the inclusion of two poly(vinylpyrrollidones) (PVP), of different molecular weights, 44,000 and 360,000. The concentration of each was such that a monolayer coverage of the particles would result[21]. The water vapour permeabilities were determined and are shown in Table VI:5 Electron micrographs of the aged samples were prepared in the usual manner and are shown in Plates VI:8 and VI:9. Plate VI:8 shows the sample containing the lower molecular weight PVP. The particle boundaries are clear and there is some evidence of the particles being deformed. Adhesion between the particles seems to be less than expected, since some of the particles clearly show their fractured interior and others show a smooth exterior. It is suggested that this feature is caused by the

PVP mol wt	Permeability coefficient s $m^3 kg^{-1}$ $x10^{17}$			
	Initial		1 month	
	film orientation		film orientation	
	lower	upper	lower	upper
44,000	4.1	6.6	2.8	4.2
360,000	17.0	22.2	15.5	19.2

TABLE VI:5 THE EFFECT OF PVP MOLECULAR WEIGHT ON WATER VAPOUR PERMEABILITY

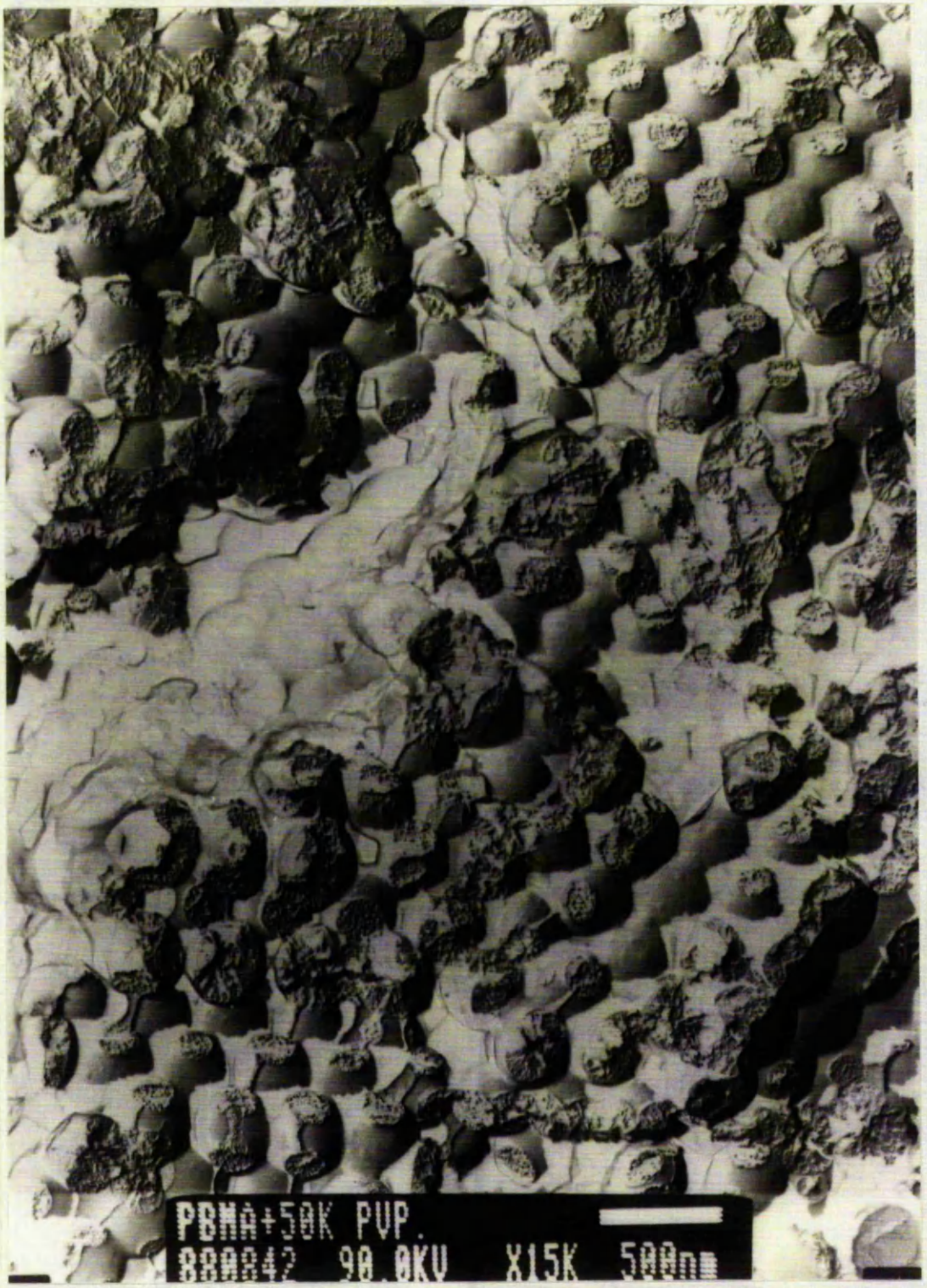

PLATE VI.8 TEM REPLICA OF FREEZE FRACTURE PBMA LATEX FILM WITH ADDED PVP MOL WT 44000

0.15g PVP ADDED TO 0.95g PBMA

PLATE VI.9 TEM REPLICA OF FREEZE FRACTURE PBMA LATEX FILM WITH ADDED PVP MOL WT 360000

0.15g PVP ADDED TO 0.95g PBMA

particles not being in intimate contact with all their near neighbours, and that the fractured surfaces result only from regions of good particle-particle coalescence. The order of the particle packing is good and would imply that the latex was stable during film formation and no coagulation occurred. The increased permeability for this sample in comparison with the clean film can therefore be explained by the lack of total coalescence throughout the sample, with the adsorbed polymer preventing coalescence to a limted degree. Plate VI:9 shows the fracture of the film containing the higher molecular weight PVP. Here, in contrast with the lower molecular weight sample no particle boundaries are easily identifiable. Although the particle-particle coalescence appears good, the permeability of this sample was much higher than the clean film, or the film containing the lower molecular weight PVP. Also obvious from the micrograph is the appearance of a second phase within the film. This material is likely to be the PVP, which may have been removed or desorbed from the particle surface during film formation, in order for a second phase to be produced. The increased permeability of this sample is likely to be a result of this second phase of PVP within the film.

VI.5. SUMMARY

The water vapour permeabilities of solvent cast PBMA films were found to be unaffected by film age. The upper surface had a slightly higher permeability, although the increase could be explained by a small increase in the surface area of the upper surface. The latex films, in

contrast, were found to have decreasing permeability with film age and the upper surface was more permeable. For latex films with no additives the reduction in film permeability is attributed to further gradual coalescence, which reduces permeability through the hydrophilic interparticle boundaries.

For films containing added surfactant, both the amount, and type of surfactant affected the film permeability. For small amounts of added anionic and nonionic surfactant the film permeability was reduced, although this was not found for the cationic surfactant. For the anionic surfactant the increased particle stability during film formation was described as the explanation for the reduction in film permeability. The fate of the surfactant up to surface coverage was not clear, but since the permeablity was reduced up to this point the surfactant could have been absorbed into the film with the charged groups remaining on the particle surface. The same explanation could have applied to the cationic surfactant, although the films did not show the same reduction in permeability on aging demonstrated with the anionic surfactant. Therefore, the increase in permeability due to the addition of cationic surfactant is probably a result of the incompatibility of the surfactant with the polymer, because of the large charged head group.

The nonionic surfactant, in all but the smallest concentration, gave a greater permeability than the clean film, and no aging was apparent. If the polymer was plasticised, and the particle boundaries had completely disappeared then it is not surprising that no reduction in

permeability was found, since this reduction was attributed earlier to further gradual coalescence. The generally higher permeability was also attributed to the plasticisation of the polymer.

The addition of the KCl, up to 50% by weight, did not affect the permeability to such a great extent as any of the surfactant additives. This was probably due to the KCl being forced to the film surface and the polymer film was only disrupted to a small extent.

The addition of PVP gave films of increased permeability, which was reduced on aging. The reduction in permeability indicates that an autohesion process was in operation, but the high final values, in comparison with the additive free film, suggest that particle coalescence was not as advanced, or there was a second phase of more permeable material within the film.

References

1. M.Patel, J.M.Patel, A.P.Lemberger;
J. Pharm. Sci., 53(3), 286 (1964).

2. G.S.Banker, A.Y.Gore, J.Swarbrick;
J. Pharm. Pharmac., 18, 457 (1966).

3. M.Chainey, M.C.Wilkinson, J.Hearn;
J.Polym. Sci., Polym. Chem. Ed., 23, 2947 (1985).

4. Idem., Makromol. Chem., Suppl. 10/11, 345 (1985).

5. S.A.M. Abdel-Aziz, P.A.M. Armstrong, W. Anderson;
J. Pharm. Pharmac., 25 (suppl 137) (1973).

6. M.Yaseen, K.V.S.N.Raju;
Prog. Org. Coat.,10, 125 (1982).

7. B.J.Hennessy, T.C.Stenning, J.A.Mead;
"The Permeability of Plastic Films.",
The Plastics Institute London (1966).

8. P.H.List, G.Kassis; Acta Pharmaceutica Technol.,
28, 1 (1982).

9. S.A.M. Abdel-Aziz; Ph.D Thesis, Strathclyde Univeristy 1976.

10. R.Katz, B.F.Munk; J.Oil Col. Chem. Assoc.,

52, 418, (1969).

11 N.Sutterlin in "Polymer Colloids II", R.M.Fitch (Ed.) Plenum Press, New York (1980).

12 F.K.Isaacs; J.Macromol Chem., 1(1), 163, (1966).

13 C.Bondy, M.M.Coleman; J. Oil Col. Chem. Assoc., 53, 555, (1970).

14 D.Distler, G.Kanig; Colloid Polym. Sci., 256, 1052, (1978).

15 D.P.Durbin; Ph.D Thesis, Lehigh University 1980.

16 J.W.Vanderhoff; Br. Polym. J., 2, 161, (1970).

17 E.B.Bradford, J.W.Vanderhoff; J.Macromol Chem., 1, 335, (1966).

18 Idem J.Macromol Sci. Phys, B6, 671, (1972).

19 S.Okor; Ph.D Thesis Strathclyde, University 1980.

20 J.C.Padget, P.J.Moreland; J.Coatings Technol., 55, 39, (1983).

21 I.W.Kellaway, N.M.Najib; Int. J. Pharmaceutics, 6, 285, (1980).

CHAPTER VII

CONTROLLED RELEASE DRUG COATINGS- A POSSIBLE APPLICATION FOR POLYMER LATICES

CHAPTER VII

CONTROLLED RELEASE DRUG COATINGS- A POSSIBLE APPLICATION FOR POLYMER LATICES

VII.1 INTRODUCTION.

The use of polymeric coatings for the control of drug release is of great interest to the pharmaceutical industry[1-7]. Several commercial products are available, although few are aqueous based. The use of aqueous based coatings removes any toxicological problems arising from residual solvents left in the coating and is therefore an important factor to consider; also the removal of solvents represents a considerable enviromental and fire risk.

For a drug coating to be of any real use the release profile of a specific drug through the coating must be known, and ideally this profile must be constant and linear, i.e., zero order. In reality, the release profiles are not linear as the drug bead or tablet is not a constant supply of the drug[7]. For release systems that rely on a concentration gradient to supply the driving force for release, the rate of release must decrease as the concentration of the drug in the tablet decreases. Initially, the change in concentration is small and the release rate could be reasonably linear, but as the amount of the drug released approaches higher amounts a reduction of release rate is inevitable, leading in some cases to first order type release profiles. Another important feature of any drug coating is the ability to control the

release through it, either by controlling the thickness, or the formulation of the coating[8,9]. The use of a latex coating would allow the release rate to be controlled via the degree of coalescence of the original latex particles. This would simply be a function of the coating and storage conditions for the surfactant-free latices used in this study, and not dependent on the common additives such as plasticisers and surfactants found in commercial supplies of aqueous based coating systems,e.g., Eudragit 30D.

VII.2 INITIAL WORK

In order to gain a brief insight into the possible performance of latex coatings for drug release uses, ascorbic acid beads where coated using the copper pan technique (see Chapter II). The latex was applied at two different temperatures, namely room temperature and approximately 45° C, where the temperatures were those of the tumbling mass of beads. Also, the effect of added surfactant was tested, since it was known that the commercially available latex coating system (Eudragit 30D) contained surfactant. Sodium dodecyl sulphate(SDS) was chosen, and was added at two different concentrations to the PBMA latex. The PHEMA latices were used as prepared.

Attempts were made to coat the beads using PHEMA latex, prepared surfactant-free and with 1.6 $x10^{-3}$ mol dm^{-3} SDS. In the former case the latex was approximately 2% W/W solids and in the latter, approximately 5%W/W. Samples of both of the PHEMA latices were used to coat beads at room temperature and at 45° C; in all cases the

release profile was the same as that of the uncoated beads. Therefore the coatings with PHEMA were unsuccessful as controlled release coatings when applied in this manner. The two possible reasons for this are; i) the latex was at low % solids and therefore relatively large amounts water were added along with the polymer and the coating thickness was very small, or ii) the hydrophilic PHEMA absorbed water rapidly and the coating ruptured allowing the release of the ascorbic acid unhindered.

The dissolution profiles for beads coated with PBMA by the pan technique were determined 24 hours after coating, and are shown in Figure VII:1. Clearly, the effect of increasing the coating temperature reduced the release rate, and this was consistent with the findings earlier in this study for solute permeation through free films. Here, the explanation is the same as given before, i.e., higher coating temperatures and longer drying times, increase the degree of particle-particle coalescence, and thus, the permeability of the interparticle regions decreases. The release rates for the films with added surfactant also show the expected results. The films were coated at room temperature and thus can be compared with the surfactant-free film coated at this temperature. Clearly, the release rate increased as the concentration of added surfactant increased. In view of these initial findings it seems clear that the temperature could be used to control the release rate through latex films.

As a comparison with the commercially available aqueous coating, Eudragit 30D, the nitrophenol permeability of Eudragit free films were determined in the same manner as PBMA free films in chapter V. The films

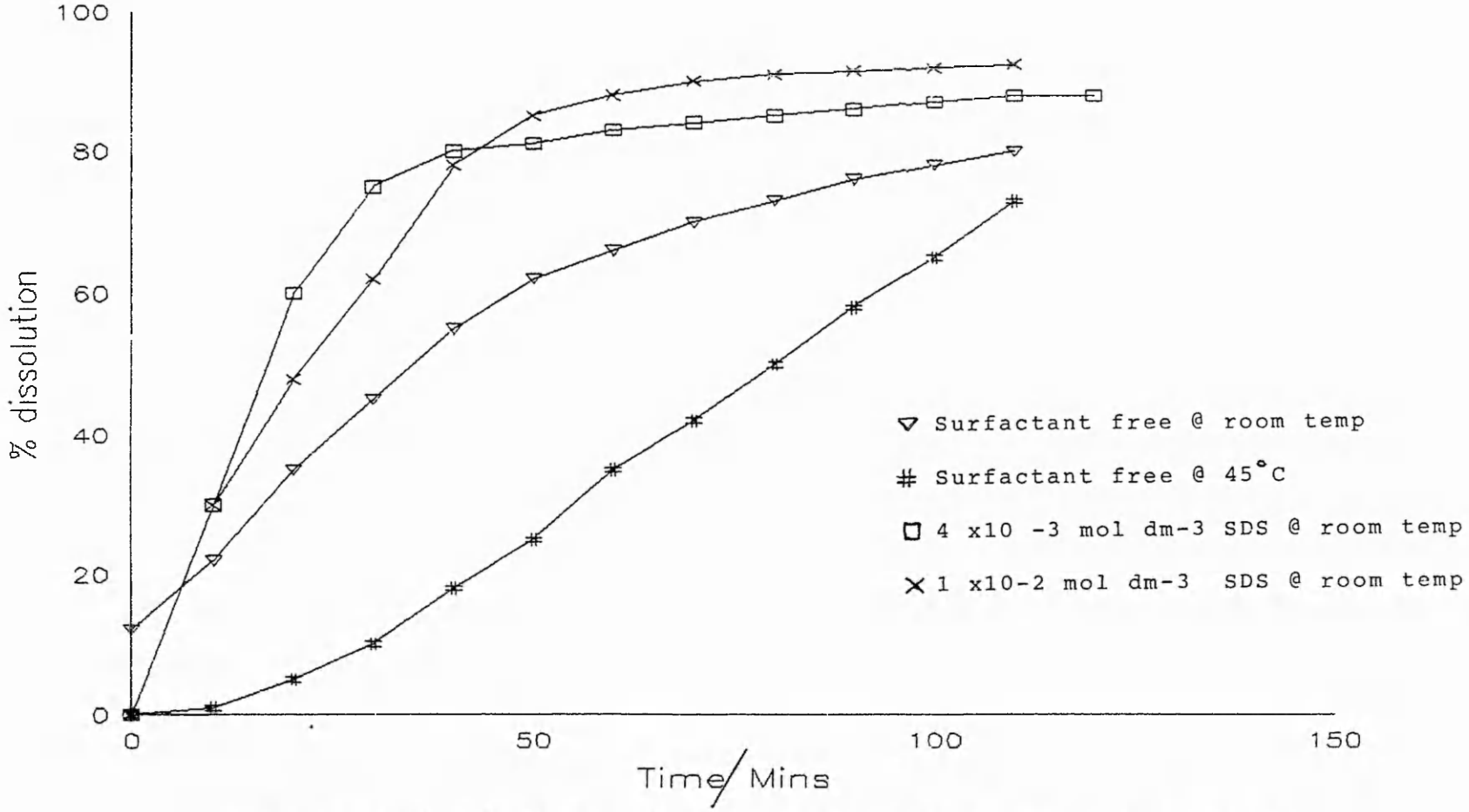

Figure VII:1 Dissolution profiles for PBMA coated ascorbic acid beads

were prepared at 80°C for three hours, and the permeabilities were determined 24 hours and one month after preparation. The initial permeability was 2×10^{-2} h^{-1} m^2 and the aged value was 5×10^{-2} h^{-1} m^2. These values were a factor of 100 greater than the values found for PBMA films prepared under the same conditions. The main reason for the large difference is likely to be the inclusion of lower alkyl acrylate and methacrylates polymers and surfactant, which were present in the Eudragit sample, and would give a film of increased permeability.

VII.3 THE EFFECT OF COATING TEMPERATURE

As ascorbic acid breaks down at temperatures above 40°C it could not sensibly be used in a study of the effect of coating temperature. Therefore, Ibuprofen beads were used, and were coated at 38,42,50 and 60 °C in the fluidised bed. The dissolution profiles were obtained 5 hours after coating by force drying the beads at 45°C. In addition to the effect of coating temperature the effect of aging at ambient temperature and at 60°C was also studied. Dissolution profiles were obtained for samples of the beads aged for 14 days at ambient temperature and for similar beads aged for a further two days at 60°C.

Coating temperature	Rate constant x 10^4 min^{-1}		
	5 Hours old.	Aged at room temp. 14 days	Further two days at 60°C
38	*	10.78	3.91
42	19.13	11.33	5.03
50	15.41	12.77	4.62
60	7.77	7.73	4.97

* this result was not available because of an instrument failure.

TABLE VII:7 THE EFFECT OF THE INITIAL COATING AND STORAGE TEMPERATURES ON THE RELEASE RATE

It is clear that aging the beads at 60°C for two days severely reduces the release rate. Figures VII:2, 3, 4 and 5, shows the reduction in release rate and the first order release profile of the beads aged at room temperature (ca. 25°C) and at 60°C. The shape of the profile for the beads aged at the higher temperature is still first order but the amount of curvature is much less, giving an almost linear release rate, and this is true regardless of the coating temperature. As the coating temperature increases the amount of coalsecence between the latex particles increases and this, as before, explains the reduction in the release rate. On storage at room temperature the coatings all show a reduction in release rate to roughly the same value, with the exception of the beads coated at 60°C. The effect of storing at the higher temperature is similar, in as much as the beads all age to the same value. This is in agreement with the

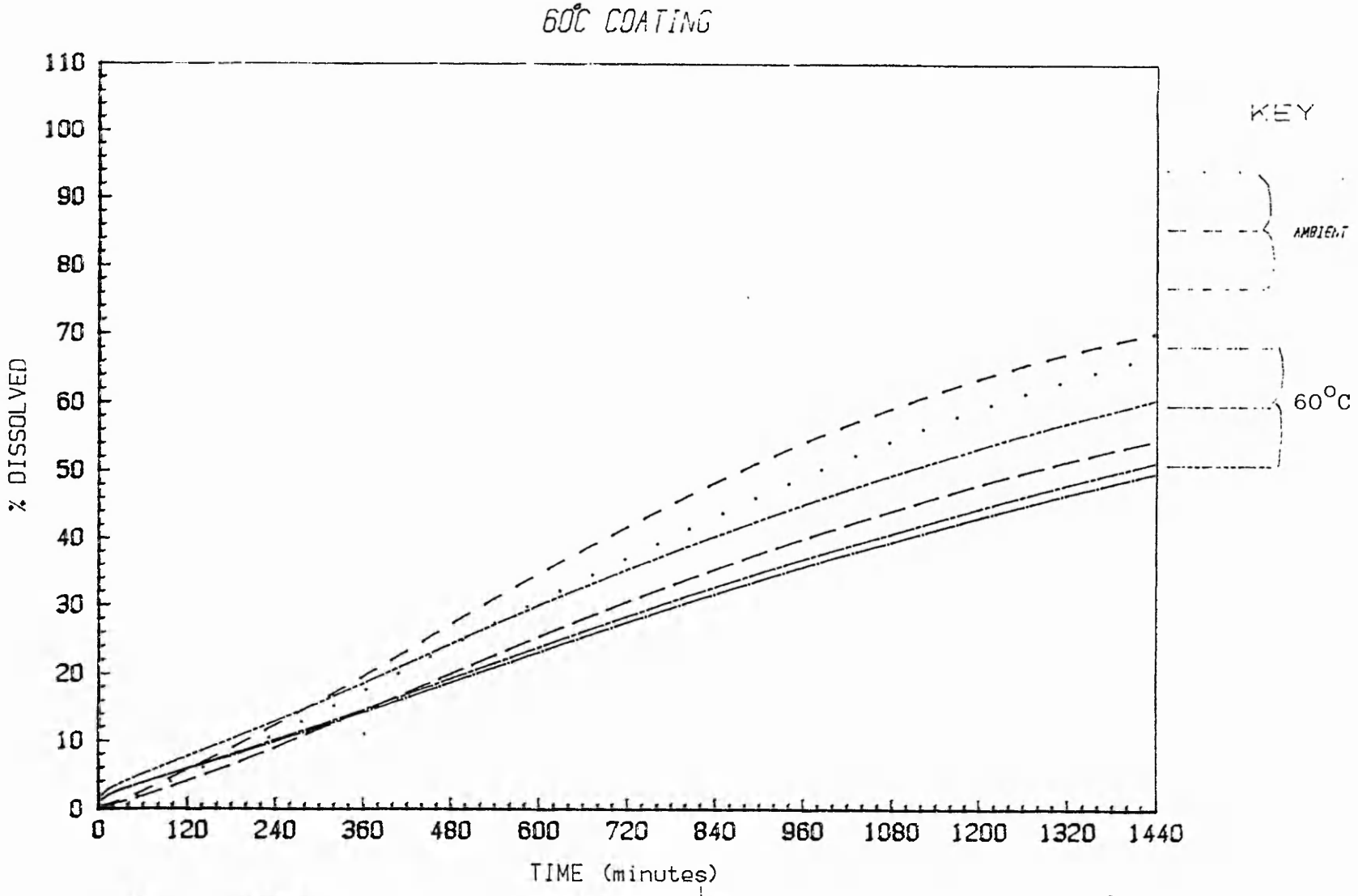

Figure VII:2 Dissolution profile for Ibuprofen beads coated at 60°C

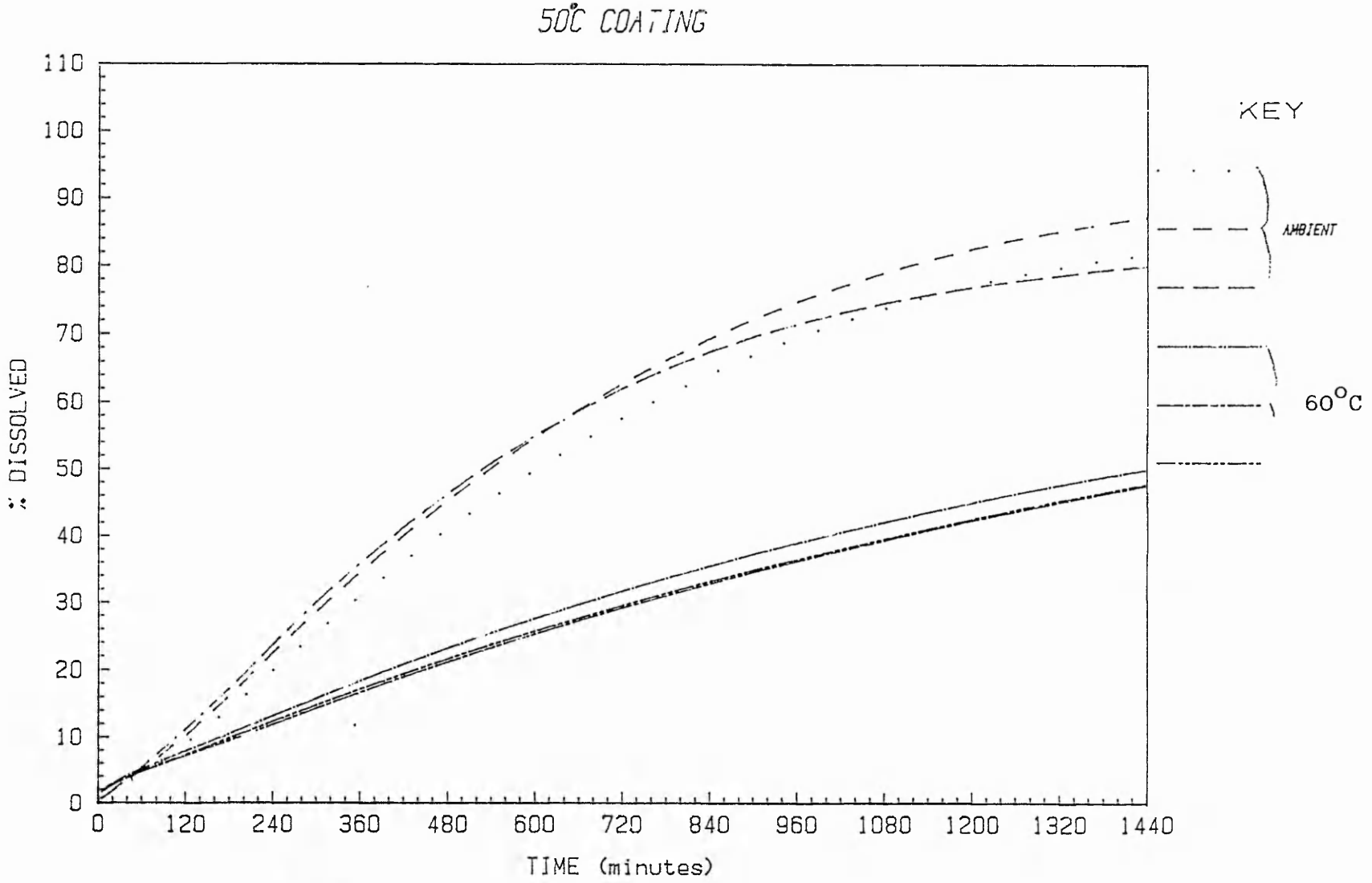

Figure VII:3 Dissolution profile for Ibuprofen beads coated at 50°C

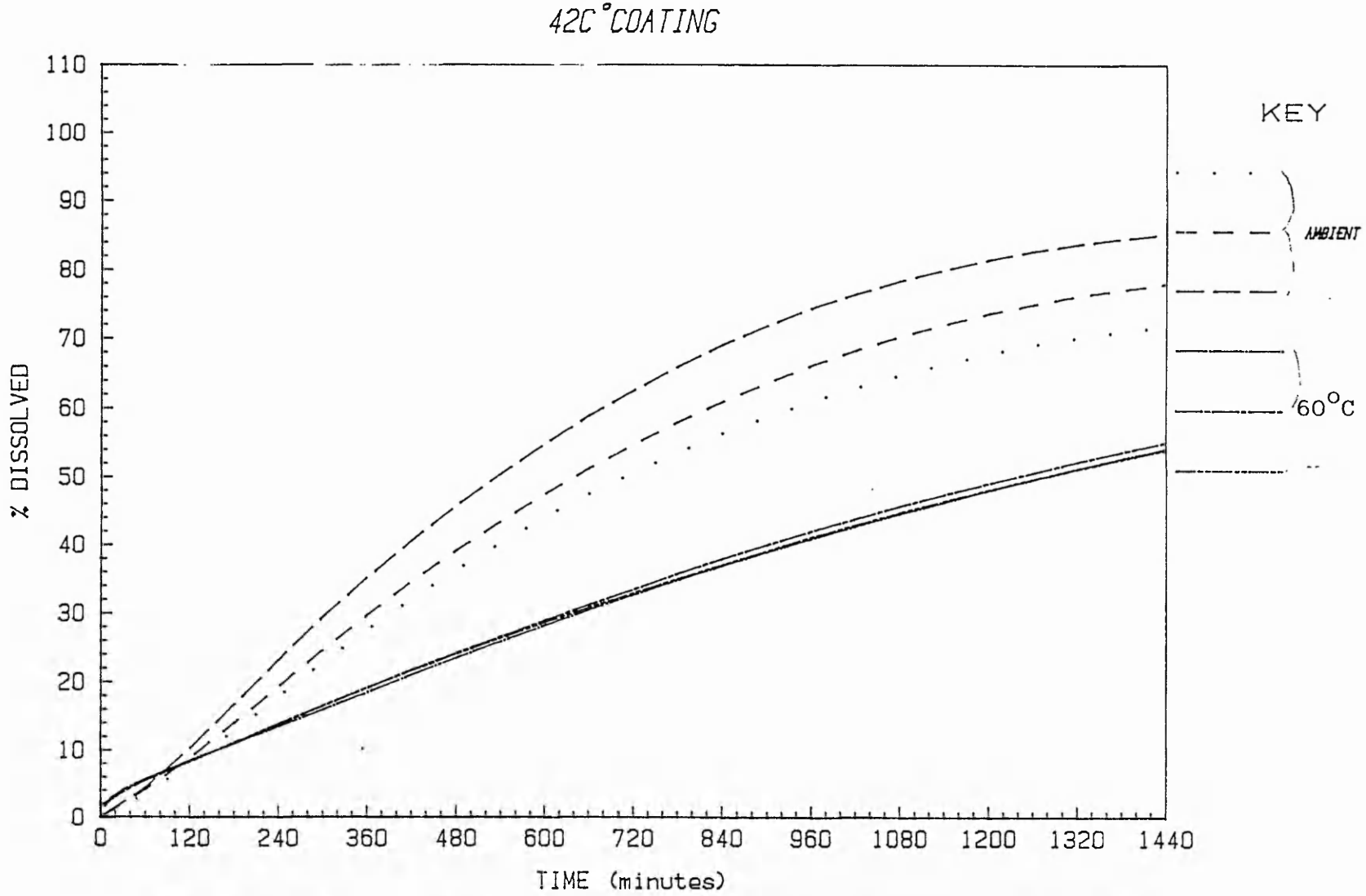

Figure VII:4 Dissolution profile for Ibuprofen beads coated at 42°C

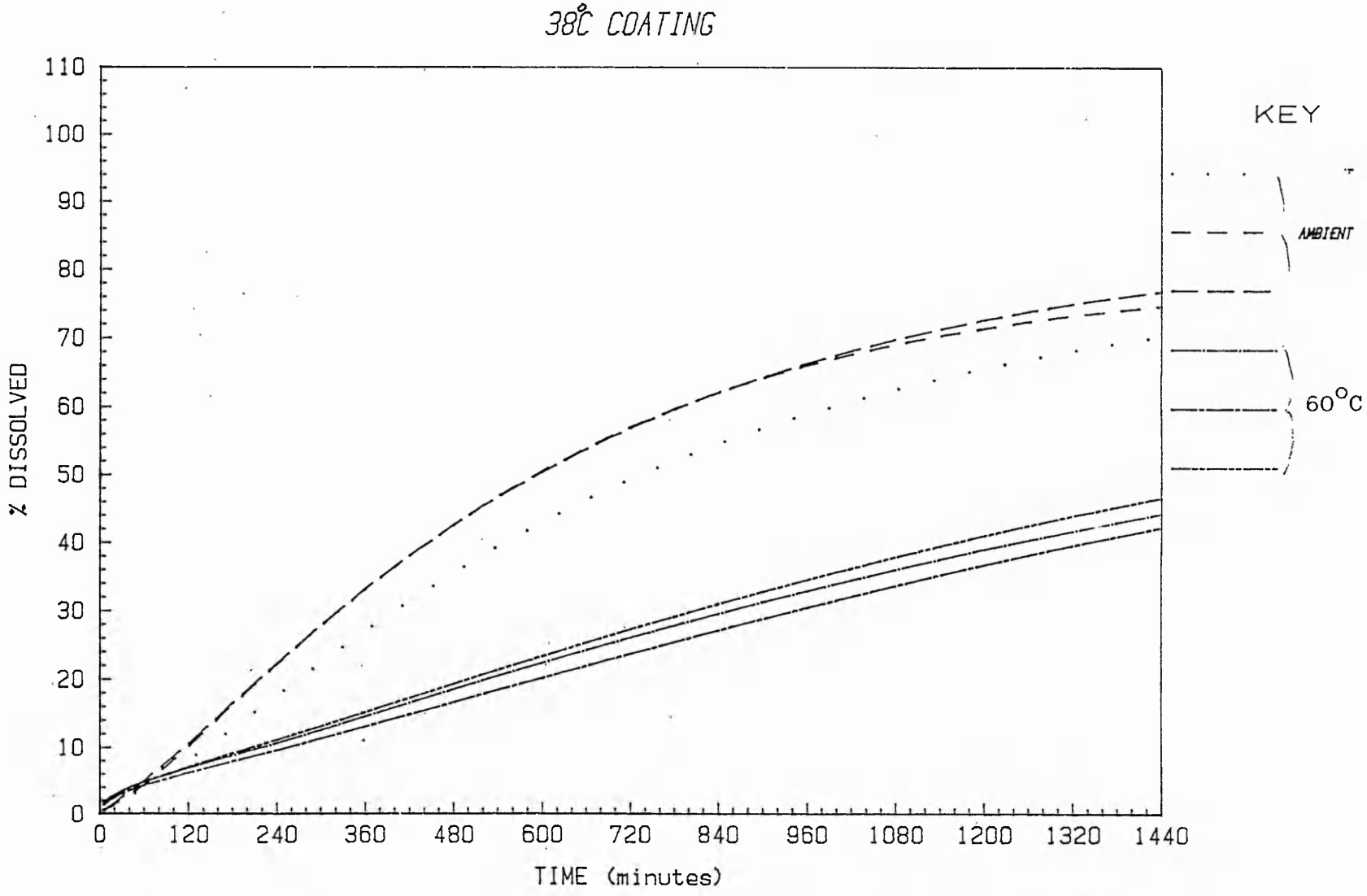

Figure VII:5 Dissolution profile for Ibuprofen beads coated at 38° C

findings for solute permeability through free films cast at various temperatures, i.e., the permeability was similar irrepective of casting temperature for films aged one month. It was also shown that the films aged to their final value in a much shorter time than the one month and 14 days would be in keeping with this observation (See section V.2.1.2). Similar findings were reported by Chainey[10] for the helium permeability of PBMA films cast at various temperatures. The permeability was found to reach a similar value within 14 days irrespective of casting temperature, with the films cast at the lowest temperatures aging at a faster rate. The exception to this pattern was the beads coated initially at 60°C, which appeared not to age, but had a release rate which was lower than the others. In this case, however, the release rate could be reduced further by heating at 60°C. This implies that the films had not reached their lowest release rate. To test this idea the beads were aged for a further two months and a portion was aged for two further days at 60°C. The release rates were determined for the aged beads and the beads heat treated again. The first order release rates are shown in Table VII:2.The results show that the two month old beads had not reached their ultimate release rate, since further heating at 60°C reduced the value for the release rate by a factor of three, indicating that further gradual coalescence could still be in operation.

First order rate constant of release $x10^4$ min^{-1}		
Coating temperature	Aged at room temp. 2 months	Plus extra 2 days at 60°C
38	6.46	2.18
42	6.98	2.5
50	6.7	1.24
60	3.91	1.05

TABLE VII:2 THE EFFECT OF STORAGE TIME AND TEMPERATURE ON THE RELEASE RATE FROM BEADS COATED AT VARIOUS TEMPERATURES

Scanning electron micrographs of the beads aged at room temperature and at 60°C were taken. The micrographs in Plates VII:1 to VII:9 show the beads two weeks after coating. Plates VII:1 to VII:3 show beads coated at 42, 50 and 60°C respectively. The surface of the beads appears to be crazed, and the amount of the crazing seems to be reduced as the coating temperature increases. The origin of these cracks probably derived from the stresses which develop during the film forming process. These stresses are affected by the rate of drying[11], the nature of the substrate[11] and the temperature (and hence the elasticity of the polymer). For a porous substrate the rate of water loss from the forming film is altered by absorption of the water by the substrate, and this, along with surface irregularities, can lead to crack formation[11]. Plates VII:4, 5 and 6 show the same beads at a higher magnification. A common feature of all the

sections was the dense compact layer with a rough surface, and some indication of porosity near the surface. A closer examination of the surface is shown in Plates VII:7 to 9. The open porous nature of the surface is particularly notable in the Plates VII:8 and 9 which correspond to the coatings at 50 and 60°C. Undoubtedly, both the fractured and porous nature of the surface was a great aid to drug release, although the coating generally seemed to be continuous over the surface of the bead.

The micrographs in Plates VII:10 to 13 show the 2 month aged beads after two days at 60°C. There are several features of interest here, firstly, the total absence of any crazing of the surface. The crazing appears to have healed when exposed to the higher temperature, with the obvious driving force for this being the polymer-air and polymer-polymer interfacial tensions. In Plate VII:11 the surface has an orange peel texture, which is probably due to the surface pores healing over. The second interesting feature in Plates VII:11, 12 and 13, is the sintering occurring between adjacent beads. In all three pictures the polymer has quite obviously flowed at the point of contact between two beads. This process is akin to the particle coalescence during film formation by latices and demonstrates the ease with which the polymer may flow at this temperature. The third quite striking feature is the appearance of crystalline material on the bead surface. Because of the large amount of this material being on the surface its origins cannot have been from the latex, but are more likely to be from the bead itself, and also this feature is most obvious for beads coated at the higher temperatures. A possible explanation for this is as

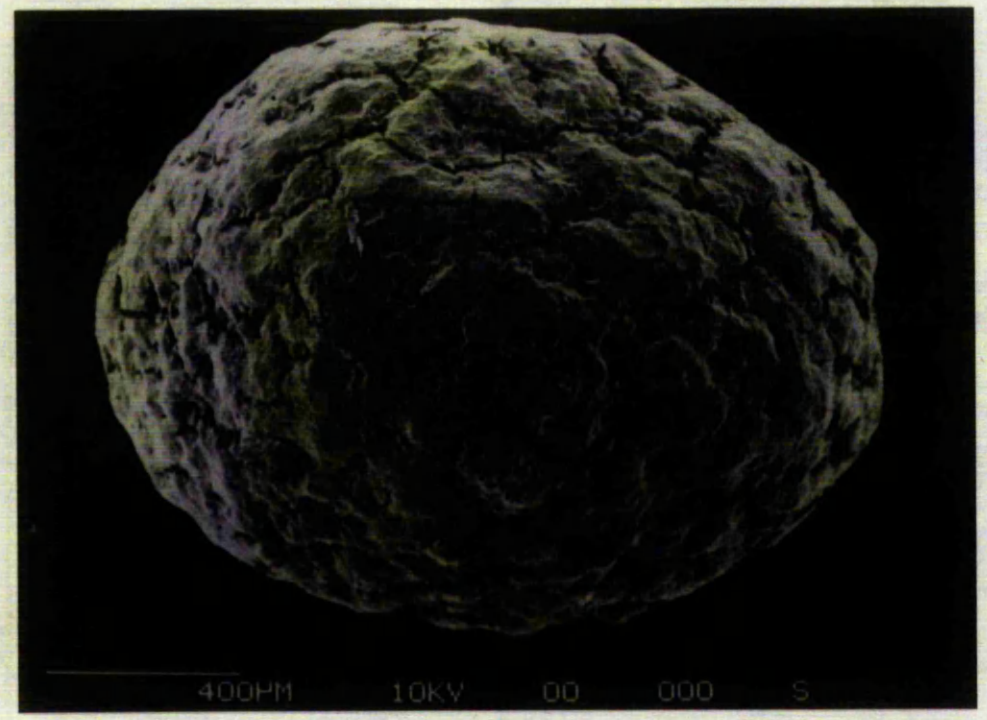

PLATE VII.1 BEAD COATED WITH PBMA AT 42°C.

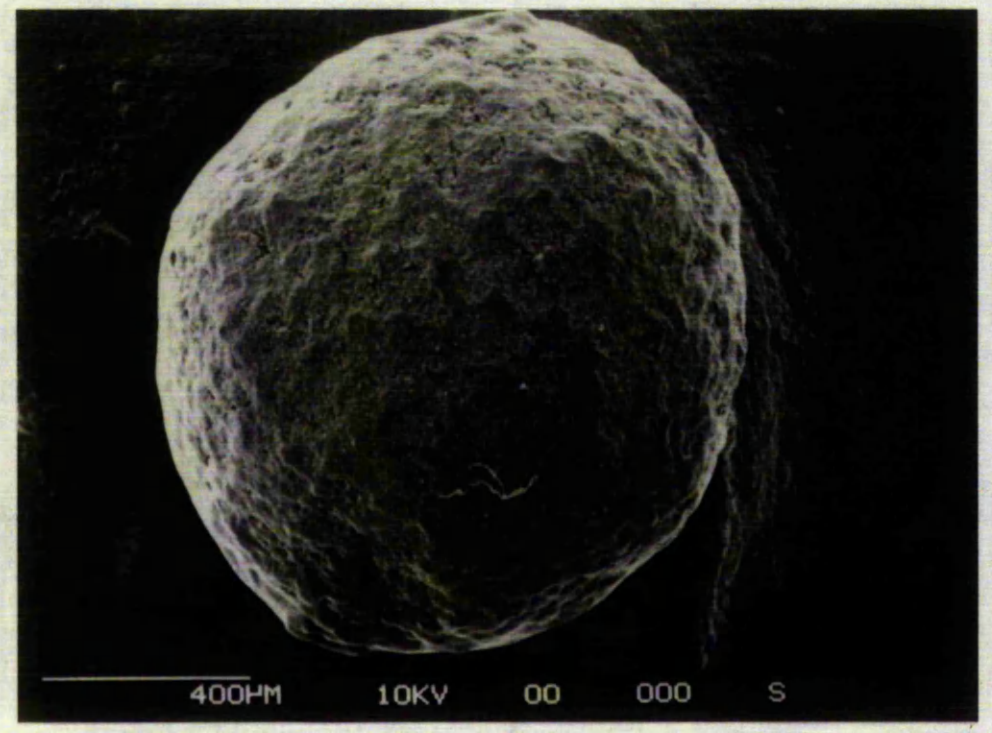

PLATE VII.2 BEAD COATED WITH PBMA AT 50°C.

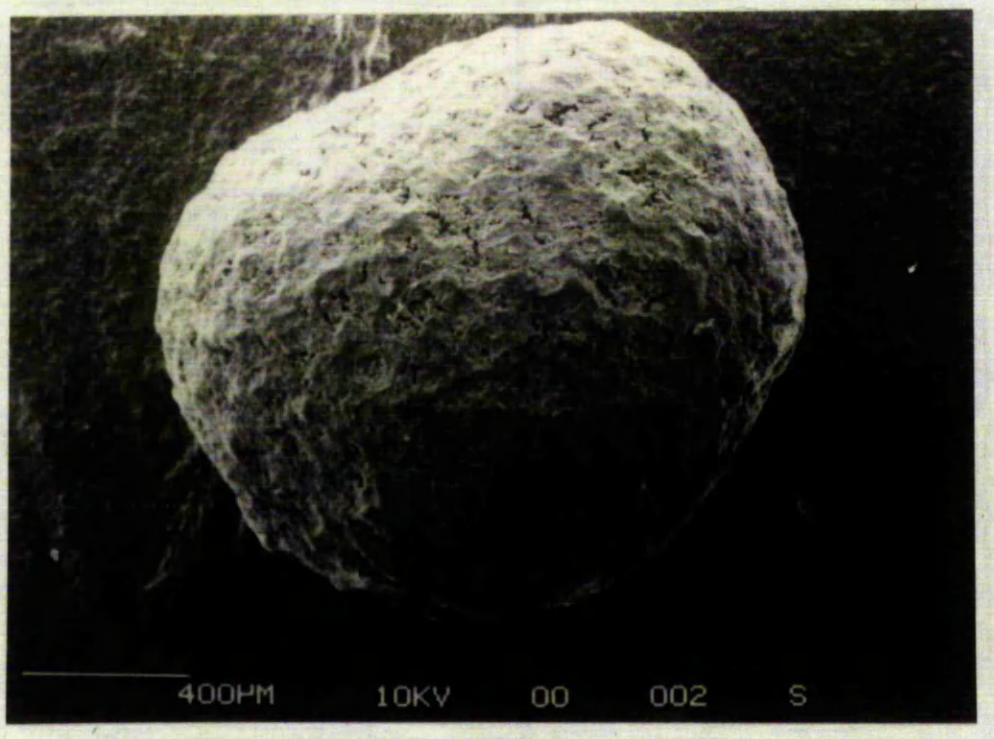

PLATE VII.3 BEAD COATED WITH PBMA AT 60°C.

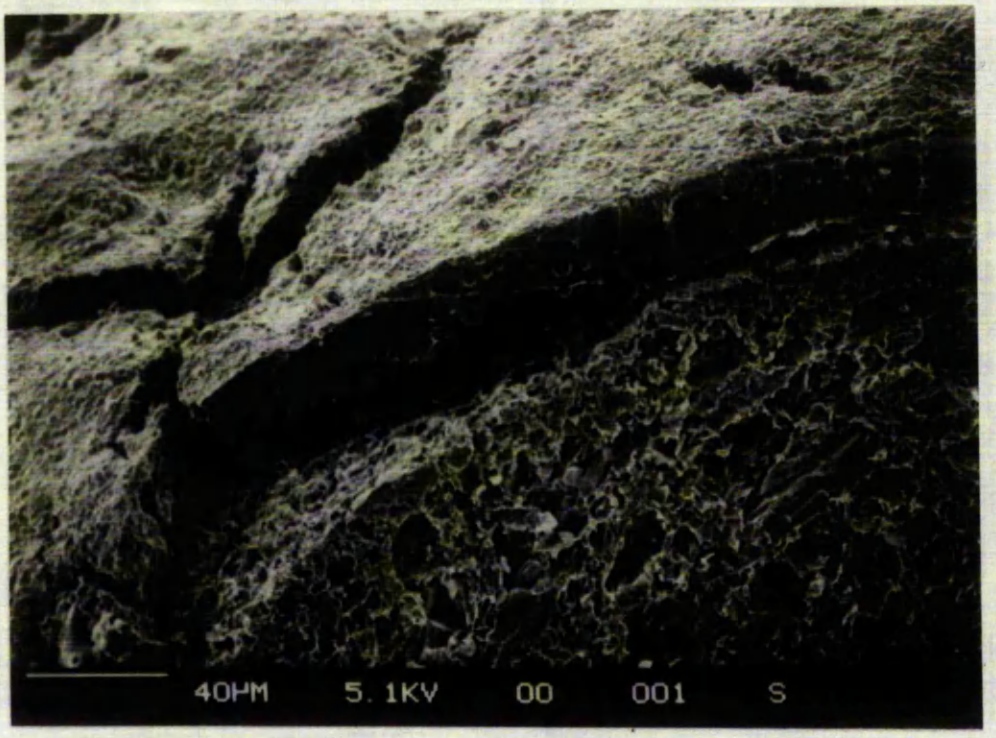

PLATE VII.4 BEAD COATED WITH PBMA AT 42°C.

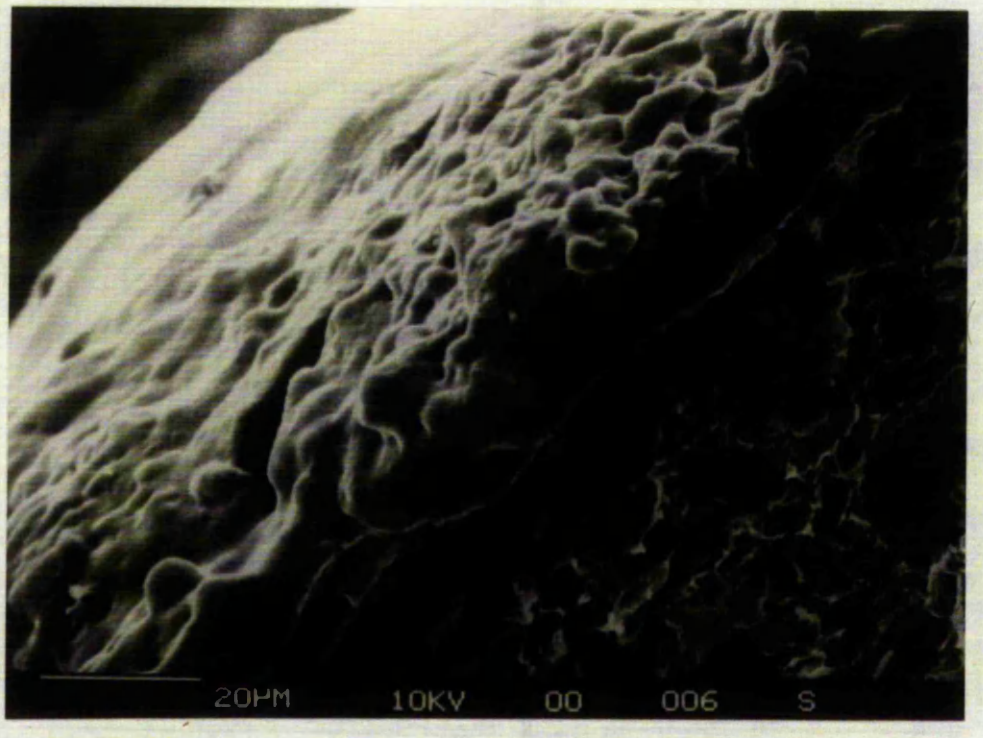

PLATE VII.5 BEAD COATED WITH PBMA AT 50°C.

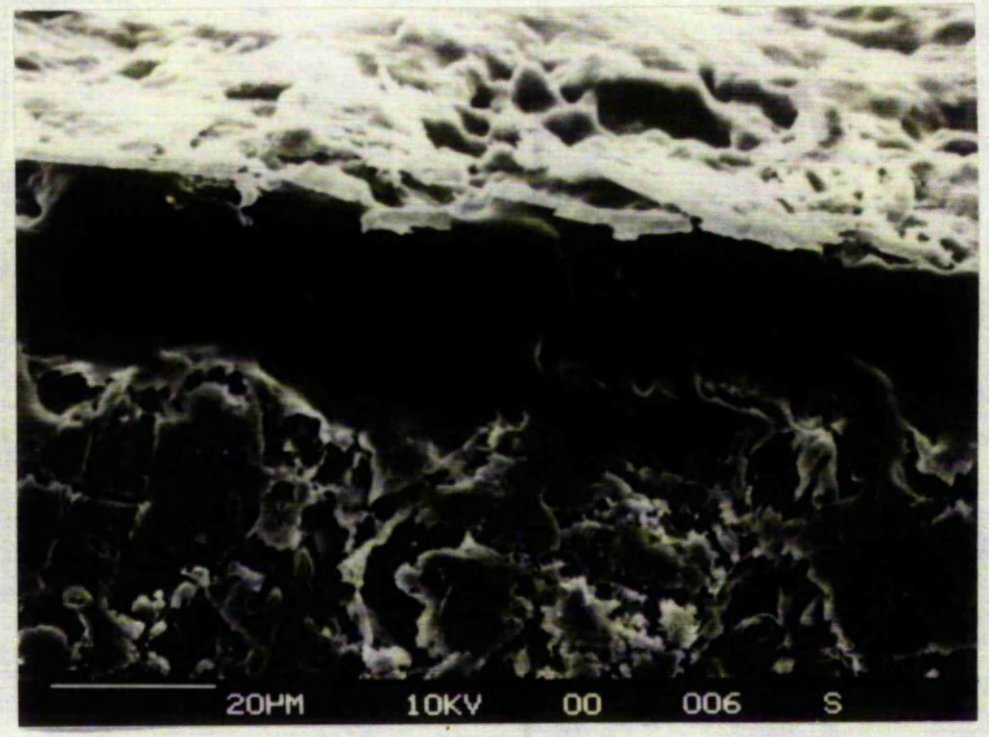

PLATE VII.6 BEAD COATED WITH PBMA AT 60°C.

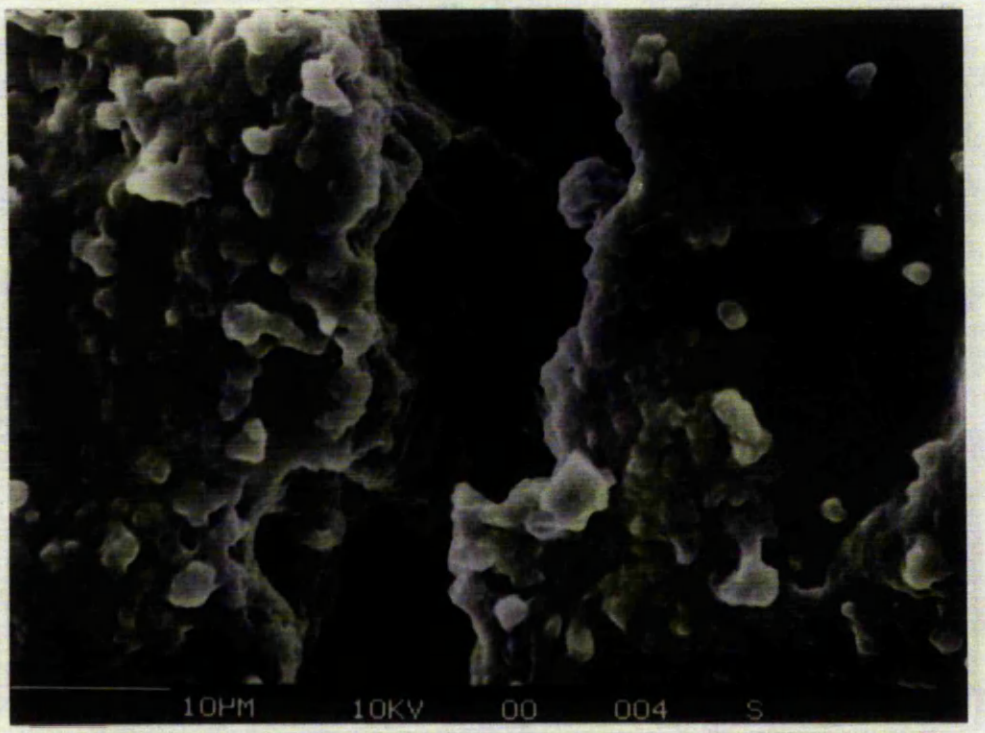

PLATE VII.7 BEAD COATED WITH PBMA AT 42°C.

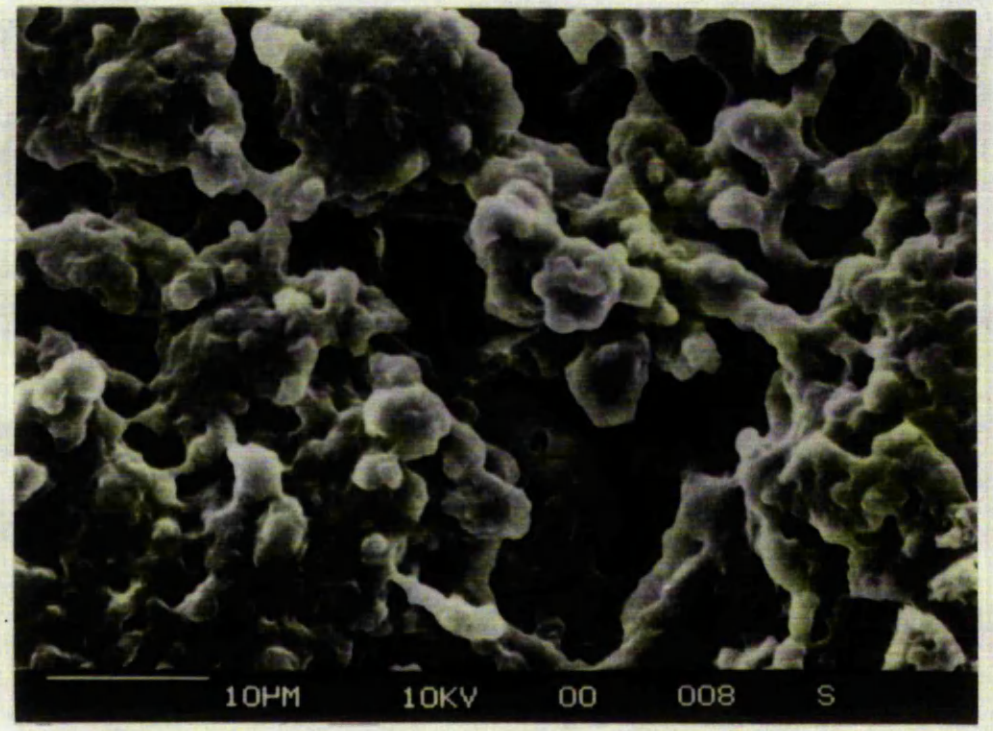

PLATE VII.8 BEAD COATED WITH PBMA AT 50°C.

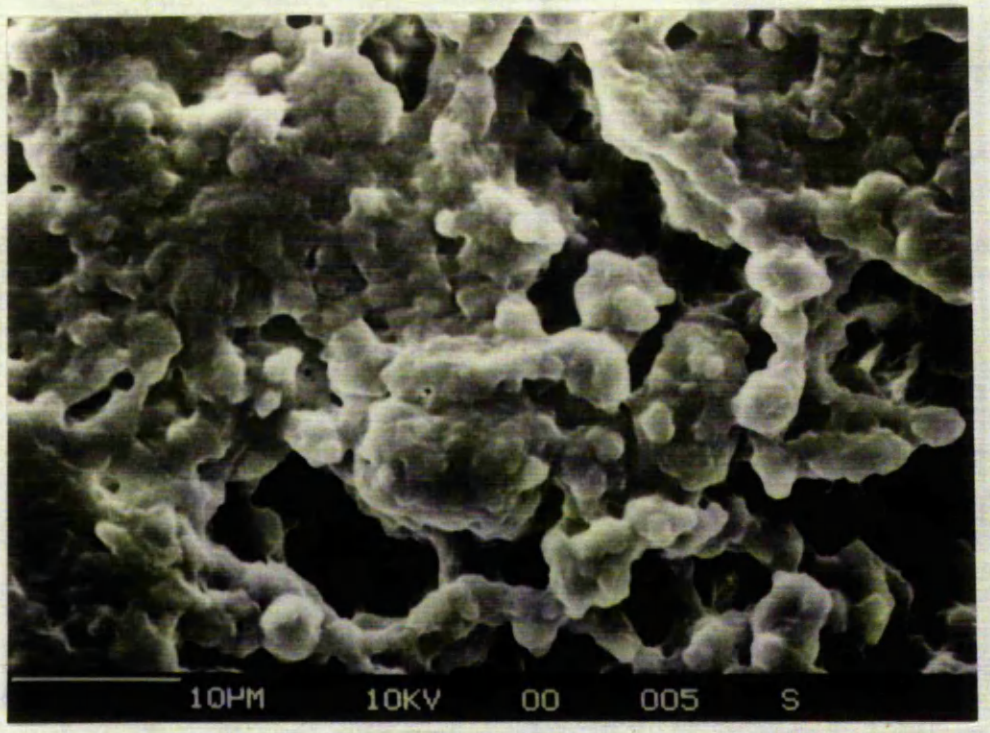

PLATE VII.9 BEAD COATED WITH PBMA AT 60°C.

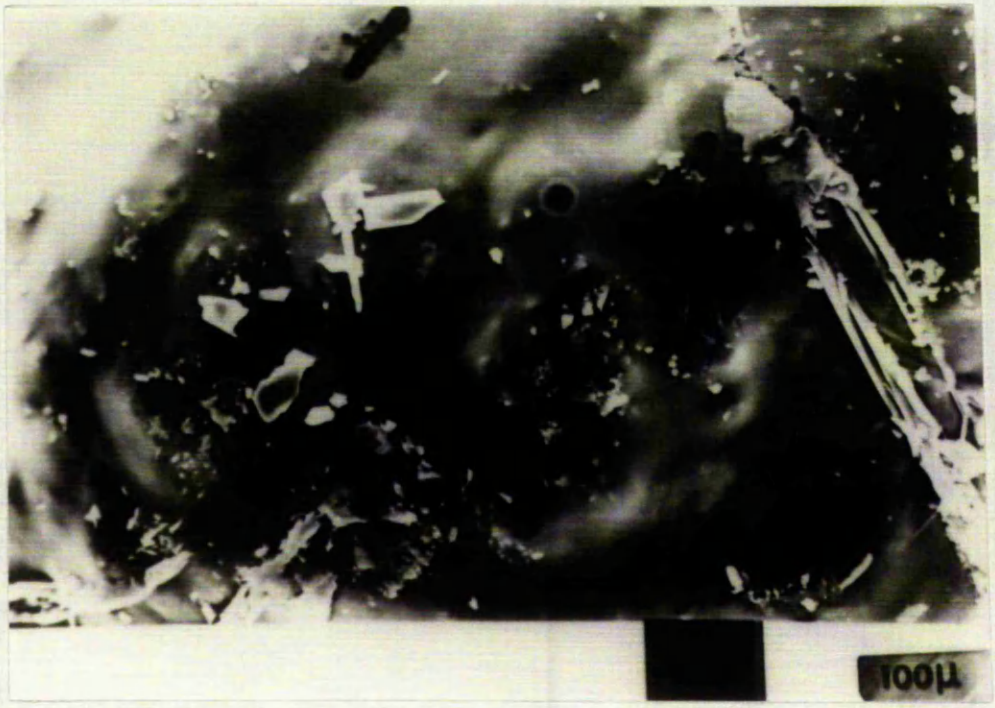

PLATE VII.10 BEAD COATED WITH PBMA AT 38°C. AGED TWO MONTHS PLUS TWO DAYS AT 60°C.

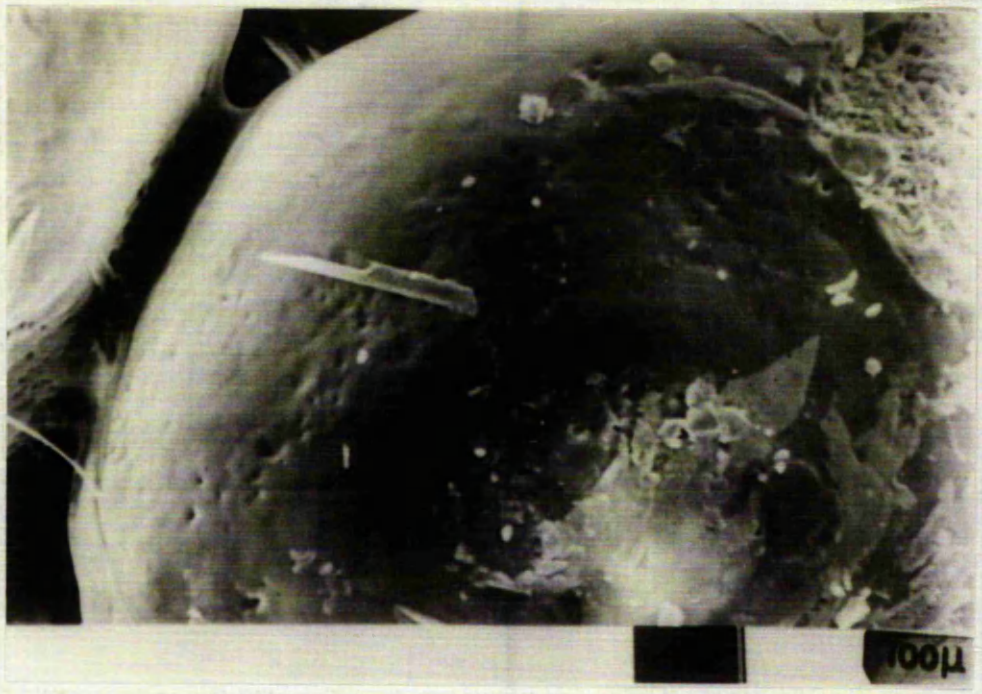

PLATE VII.11 BEAD COATED WITH PBMA AT 42°C. AGED TWO MONTHS PLUS TWO DAYS AT 60°C.

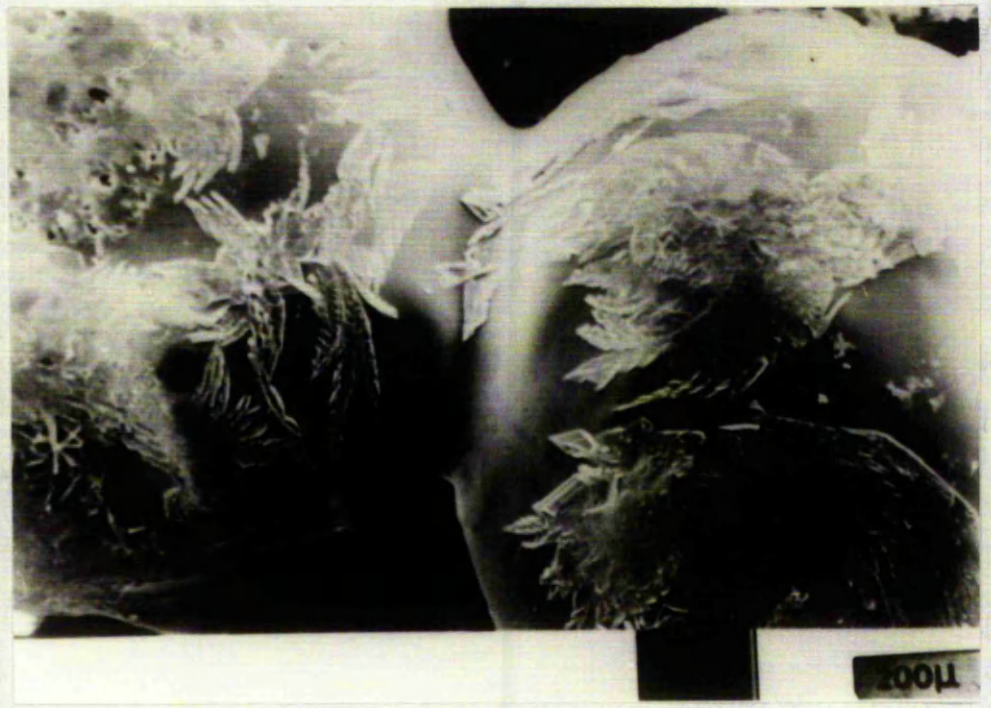

PLATE VII.12 BEAD COATED WITH PBMA AT 50°C. AGED TWO MONTHS PLUS TWO DAYS AT 60°C.

PLATE VII.13 BEAD COATED WITH PBMA AT 38°C. AGED TWO MONTHS PLUS TWO DAYS AT 60°C.

follows: When the wet latex was sprayed onto the beads some partial dissolution of the drug or the lactose took place, thus trapping some foriegn material in the drying latex film. The higher the coating temperature, the greater the amount of material that would be dissolved in the drying film. Thus, on aging and heat treating, this material was expelled from the film and appeared on the surface.

VII.4 CONCLUSIONS

The coating temperature affects the release rate of the drug through latex coated beads. In all cases the release profile changed on storage and the storage temperature affects the amount of aging. It was not clear from this preliminary work whether the beads had reached their lowest release rate after two months or whether they would all give the same release rate irrespective of coating temperature, given sufficient time. The crazed surface of the beads certainly played a dominant role in the release from the coated beads initially, but the heated beads still gave an appreciable release rate that presumably was through the polymer coating itself, since no crazing could be found in the micrographs of the heat treated beads. As to the role of the interparticle boundaries in the release process there is little evidence in this short study to support permeation through these regions, although for free films this seems to be a significant route for permeation. In conclusion, the rate of release was initially affected by the coating temperature, but a means of controlling this over any

significant period of time was not indicated, since the release rate decreased on storage. The occurrence of crazing in the surface served only to complicate the picture since it is not known whether the interparticle boundaries or the fractures in the film are responsible for the major transport process.

References

1. K.Lehmann, D.Dreher; Die Pharmazeutische Industrie, 34, 894 (1972).

2. D.Dreher; Pharma International, 1(2), 3 (1975).

3. K.Lehmann; APV Information service, 21(4), 255 (1975).

4. K.Lehmann, H.Bossler, D.Dreher; Pharmeutical Technol., 3(3), (1979).

5. K.Lehmann, D.Dreher; Technology & Product Manufacture, 2(4), 31 (1981).

6. S.C.Porter; Int.J.Pharm. Tech & Prod. Mfr., 3(1), 21 (1982).

7. K.Lehmann; Pharm Ind., 29, 396 (1967).

8. R.R.Crawford, O.K.Esmerian; J.Pharm Sci., 60, 312 (1971).

9. S.C.Porter; Pharm Technol., 4, 67 (1980).

10. M.Chainey, Ph.D Thesis, Trent Polytechnic, 1984.

11. G.P.Bierwagen; J.Coating Technol., 51(658), 117 (1979).

CHAPTER VIII

CONCLUSIONS

The work reported in this thesis concerns the permeability and morphology of model latex films derived from monodisperse, surfactant-free latices. This work was a continuation of a previous study in which gas permeability was used to study latex film morphology[1]. In this study the permeability of aqueous organic solutes, and water vapour were used. The morphology and permeability of PBMA latex films was studied along with films cast from core-shell and copolymers latices of PBMA with PMA. In addition to model surfactant-free films, water vapour permeability was used to study the effect on permeability of common additives found in most latex systems, such as surfactants. Along with the permeation studies, some work on the emulsion polymerisation of two different monomers was undertaken. The first was the relatively water insoluble BMA[2], and the second was highly water soluble HEMA, which is also a biomedically acceptable polymer[3].

The reaction kinetics of the emulsion polymerisation of BMA were found to agree with the Smith and Ewart Case III. For case III $n \gg 1$, which implies that the rate of radical termination and radical desorption are slow compared with the rate of radical entry into particles. The observations used to support this were, a) the large number of radicals per particle, and b) the dependence of the conversion rate on the total polymer volume, rather than the number of polymer particles. Also shown was the independence of the rate of

conversion with the initiator concentration. However, the particle size and number density changed considerably with variations in the initiator concentration, and it was found that the conversion rate per unit volume of polymer increased with increasing initiator concentration, again implying case III kinetics. The rate of conversion was found to be constant during most of the reaction, although the particle number density was decreasing during this period. To account for this it was postulated that the number of radicals per particle increased with increasing conversion. This was found to be the case when the expression given by Ugelstad[4] was used to calculate the average number of radicals per particle as a function of conversion.

Molecular weight studies showed evidence of low molecular weight material with a degree of polymerisation of approximately 10. It was suggested that this material was oligomeric species that had exceeded their water solubility. These oligomers were probably responsible for the nucleation of polymer particles. The presence of the oligomers throughout the reaction implied that these species were continually being formed, probably in the aqueous phase. The lack of new particle nucleation throughout the reaction could mean that the oligomers were terminated by heterocoagulation with larger polymer particles.

The surfactant-free emulsion polymerisation of HEMA was attempted and it was found that latices of relatively large particle size,i.e., 0.8-0.9 μm,were formed, irrespective of initiator concentration and ionic strength. Also, in the absence of surfactant, stable

latices could only be prepared up to a maximum solids concentration of 3%. In all surfactant-free latices prepared, the latex sedimented and coagulated irreversibly on storage. PHEMA latices prepared in the presence of SDS were found to give stable latices with solids concentrations up to 8%, and particle sizes in the range 60 to 700 nm. The surfactant containing latices were also stable on storage. It was suggested that the surfactant free PHEMA latices had low surface charge densities and were therefore relatively poorly stabilised. The production of a latex from a polymer that is accepted as being water soluble was probably the result of the high gel content found in these latices. It was postulated that this was a result of hydrogen abstraction of the monomer by the initiator which resulted in a highly branched or crosslinked polymer. It was also noted that the rate of polymerisation was dependent on the initiator concentration to the power 1.5. The same rate dependence was reported in the literature[5] for the decomposition of potassium persulphate in the presence of alcohols. It was concluded that polymerisation in the polymer particles was the more likely locus for polymerisation rather than the aqueous phase despite the high water solubility of the monomer.

Latex films prepared from surfactant-free PBMA were found to have little or no measurable porosity. Freeze fracture TEM replicates of the film interior showed highly ordered arrays of coalesced latex particles. Although the film was esssentially non porous, the latex particles had not totally coalesced, and the interparticle boundaries were clearly visible. It was suggested that the

particles were in close packed arrays and that a probable shape for the distorted latex particle was the rhombic dodecahedron.

The particle boundaries were still visible after one month indicating that the autohesion process[6] did not completely remove all of the original particle identity, which is consistant with the observations of Distler and Kanig[7]. The interparticle boundaries were completely removed only when the film was exposed to temperatures above the melting point of the polymer.

The permeabilities of PBMA films cast from solvent and prepared from surfactant-free latex were compared. It was found that the solvent cast film permeabilities could not be used to give a base line value for PBMA permeability, irrespective of any morphology resulting from film formation by the latex particles. Solvent cast films were found to have higher permeabilities, particularly to solutes, than latex films. It was reported that latex films had slightly higher densities than solvent cast films and this could account for the solvent cast films having higher permeabilities.

The permeability of surfactant-free latex films was found to obey Fick's laws with respect to film thickness and permeant concentration for aqueous solutions of nitrophenol. The permeability was shown to be dependent on the film orientation, with respect to the permeant and on the film preparation parameters. The effect of film orientation was described, with the film being least permeable when the upper surface of the film was in contact with the permeant. This was attributed to a combination of surface area effects, and the relative

solubilities of the solute in the polymer and water phases. The film permeability was shown to be dependent on the casting time and temperature. High casting temperatures and long the drying times produced films of low permeability. The reduction in permeability was attributed to greater coalescence of the latex particles when exposed to the higher temperature for longer times.

The latex film permeability was also found to be dependent on film age, with the permeability decreasing with time. This is in accordance with previous findings[2,8]. The decrease in film permeability was described in terms of the further gradual coalescence of the latex particles[9]; hence the permeability through the interparticle regions decreased. The permeability of several structurally related anilines indicated that the permeability through latex films was controlled by the partitioning of the solute between the film and water and not by molecular size (molecular weight). From the above evidence it was concluded that permeability through latex films is both through the bulk polymer itself, and also, through the interparticle regions. The interparticle regions would have a much higher free volume, and thus facilitate diffusion. However, the autohesion process would serve to decrease the free volume in these regions, and hence the overall film permeability would decrease.

The permeability of core-shell and copolymer films was studied. The core-shell polymers were prepared with a more hydrophilic PMA shell, and thus the hydrophilic nature of the interparticle regions would be increased. The permeability of both the core-shell and copolymer

films was found to decrease with time as was found previously[10]. The permeability of the aged films to nitrophenol solutions were reasonably similar in magnitude, and similar to that of the PMA homopolymer for volume fractions above 0.4 of the more permeable polymer(PMA). This was taken as suggesting that the permeability was through a PMA continuous phase within the film. A similar situation was found for water vapour permeability through the same films. The experimental permeabilities were compared with the values predicted by Higuchi[11] for permeability through heterogeneous films. The experimental results were greater than predicted, particularly at low volume fractions of the more permeable polymer. The probable reason for the lack of agreement between experimental and predicted permeabilities is permeability through the interparticle regions.

Water vapour permeability was used to study the effect of added surfactant and inorganic material on latex film permeability. The addition of small amounts of anionic surfactant, up to and including complete surface coverage resulted in a decrease in the film permeability. At concentrations above surface coverage the permeability increased again. This was attributed to greater particle stability during the film formation process, and hence a better packing order of the particles. At concentrations higher than surface coverage no extra stability could be achieved and the extra surfactant served to increase the ionic strength and hence decrease the particle stability. For cationic surfactants, no such minimum permeability was found and this was attributed to either a loss of particle stability on the addition of the surfactant, or, an

incompatibility of the surfactant's large head group with the polymer. For the non ionic surfactant again no minimum permeability was found, and the permeability increased on addition of the surfactant. In this case the plasticisation of the polymer by the surfactant could have caused the increased permeability. For all of the above surfactants the film permeability did not decrease on aging, as was recorded for the clean film, and also demonstated for gas permeability [1,8,10]. For the addition of polymeric stabilisers the permeability decreased on aging, but still showed larger permeabilities compared to the clean films. The permeability increased with the molecular weight of the stabiliser. The higher permeability was attributed to either a more permeable phase of stabiliser in the film or a decrease in the amount of particle coalescence. The addition of inorganic material to the film increased the permeability, but the increase was independent of the amount of material added. This was taken to suggest that the inorganic material was concentrated at the film surfaces, and an intact polymer film remained below the surface. This was further supported by the observation of white powder exudations on the film surface.

Chapter VII described the potential use of surfactant-free latices as controlled released drug coatings. Attempts were made to coat drug beads with both PBMA and PHEMA latex. Coatings of PHEMA proved to be ineffective as inhibitors for dissolution, either becasue of a low amount of polymer being present, or because of its hydrophilic character. Coatings of PBMA were much more effective at inhibiting dissolution.

It was found that the initial release rate of Ibuprofen from PBMA coated beads could be controlled by variations in the coating temperature. However, the release rate decreased on storage, and attained similar values for all but the highest coating temperatures. The release rate could be further decreased by storing the beads at elevated temperatures. This was either due to further gradual coalescence of the latex particles, or more probably a reduction in the amount of crazing in the coating surface. From the data presented it is concluded that these latices can find a potential application as coatings for drugs, and that the initial release rate can be controlled by the coating procedure. However, the aging of latex films serves to decrease the differences obtained initially. For use as genuine controlled release coatings, the aging process must be controlled, and perhaps varying amounts of crosslinking of the latex particles would serve to do this.

REFERENCES

1. M.Chainey; Ph.D Thesis, Trent Polytechnic, 1984.

2. N.Sutterlin in, "Polymer Colloids II", R.M.Fitch (Ed) Plenum publishers, New York (1980).

3. D.G.Pedly, P.J.Skelly, B.J.Tighe; Brit. Polym. J., 12, 99 (1980).

4. J.Ugelstad, P.C.Mork; Brit. Polym. J., 2, 31 (1970).

5. P.D.Barlett, J.D.Cotman; J.Am.Chem.Soc., 71, 1419 (1949).

6. S.S.Voyutskii; J,Polym.Sci., 32, 528 (1958).

7. D.Distler, G.Kanig; Colloid Polym. Sci., 256, 1052 (1978).

8. M.Chainey, M.C.Wilkinson, J.Hearn; J. Polym. Sci., Polym. Chem. Ed., 23, 2947 (1985).

9. J.W.Vanderhoff; Brit. Polym. J., 2, 161 (1970).

10. M.Chainey, M.C.Wilkinson, J.Hearn; Makromol Chem., Suppl. 10/11, 435 (1985).

11. W.I.Higuchi; J. Phys. Chem., 62, 649 (1958).

APPENDIX I

AN EXAMPLE OF GAS PERMEABILITY CALCULATIONS

$$\text{Flux} = \frac{V + 2ah}{H-h}\,\frac{dh}{dt}$$

V = volume of cavity = 2.085 cm^3

a = internal cross sectional area of capillary = 0.018 cm^2

h = height of mercury capillary at $t_{1/2}$

$\frac{dh}{dt}$ = rate of change of height in mercury capillary

Permeability coefficient: $P = \frac{\text{Flux} \times L \times 7.5 \times 10^{-8}}{A(H-h)}$

$P = sm^3\,kg^{-1}$

L film thickness, cm

A exposed area of film, cm^2

H atmospheric pressure, cmHg

Experimental values for a solvent cast PBMA film :

h = 1.3 cm dh/dt = 0.004697 cm sec^{-1}

A = 9.62 cm^2 H = 71.3 cmHg

L = 40×10^{-4} cm

Flux = 140.2×10^{6} $cm^3\,sec^{-1}$

Permeability coefficient = 6.25×10^{-17} $sm^3\,kg^{-1}$

APPENDIX II AN EXAMPLE OF SOLUTE PERMEABILITY CALCULATION

Permeability coefficient $P = \frac{dc}{dt} \frac{L}{A} \frac{V}{C_o}$

$\frac{dc}{dt}$ = rate of change in receiver solution g dm^{-3} s^{-1}

L = film thickness m

A = film area = 1.96 $x10^{-3}$ m^2

V = volume of receiver solution dm^3

C_o = initial donor concentration g dm^{-3}

Experimental values for a solvent cast PBMA film :

dc/dt = 5.37 $x10^{-5}$ g dm^{-3} h^{-1} V = 0.16 dm^3

C_o = 0.16 g dm^{-3} L = 23.06 $x10^{-6}$ m

Permeability coefficient = 6.3$x10^{-10}$ $h^{-1} m^2$

APPENDIX III AN EXAMPLE OF WATER VAPOUR PERMEABILITY CALCULATION

$P = \frac{dw/dt \; L \times 7.5x10^{-8}}{A \times 1.92}$

dw/dt = rate of weight loss g h^{-1}

L = thickness

A = area

1.92 = water vapour pressure at 81%RH 25° C (cmHg)

Experimental values for PBMA latex film:

A = 2.545 cm^2 dw/dt = 0.00256 g h^{-1} L = 10.26$x10^{-4}$ cm

Permeability coefficient = 1.12 $x10^{-17}$ s $m^3 kg^{-1}$

APPENDIX IV

EMULSION POLYMERISATION RECIPES FOR BUTYL METHACRYLATE

Monomer 50g, Double distilled water 450g

temperature 75°C, stirrer 250 rpm.

Code	KPS /g	NaCl /g	Code	KPS /g	NaCl /g	Code	KPS /g	NaCl /g
50	0.5	0.05	60	0.5	0.007	74	0.4	--
51	0.5	--	61	0.5	0.003	76	0.32	--
52	0.5	0.03	63	0.5	--	77	0.25	--
53	0.5	0.015	67	0.5	--	81	0.15	--
54	0.25	0.16	68	0.48	0.01	82	0.2	--
55	0.4	0.65	69	0.3	0.08	90	0.75	--
57	0.32	0.11	70	0.5	0.01	91	0.29	--
58	0.475	0.016	72	0.48	--	92	0.15	0.227
59	0.495	0.003	73	0.475	--			

APPENDIX V

EMULSION POLYMERISATION RECIPES FOR 2-HYDROXYETHYL METHACRYLATE

Monomer 12g, double distilled water 450g, stirrer 90 rpm

Code	KPS /g	NaCl /g	Temp °C	Code	KPS /g	SDS /g	Temp °C
32	0.1	--	75	34	0.1	0.52	60
44	0.1	--	60	35	0.1	0.05	60
45	0.05	0.32	75	36	0.1	0.20	60
46	0.08	0.13	75	38	0.1	0.31	60
48	0.08	0.22	75	47	0.08	--	75
49	0.1	--	90				

APPENDIX VI PBMA KINETIC DATA

Code 50			Code 51		
Time mins	Conversion %	Particle diameter/nm	Time mins	Conversion %	Particle diameter/nm
15	6.5	214	14	2.7	114
32	15.3	272	46	6.1	172
83	52.9	510	63	7.7	192
204	77.6	627	78	9.8	224
235	71.7	637	100	16.7	245
325	78.6	605	140	28.0	309
369	80.8	587	170	37.4	309
405	80.3	616	203	44.5	375
450	81.5	634	286	57.9	442
			409	82.6	576

Code 52			Code 53		
Time mins	Conversion %	Particle diameter/nm	Time mins	Conversion %	Particle diameter/nm
23	3.8	121	15	6.4	156
55	13.1	209	40	35.5	322
70	20.1	249	62	44.2	350
103	40.0	323	90	52.5	369
127	56.0	369	120	60.2	405
155	64.8	395	148	64.2	429
193	67.9	425	200	72.2	445
233	75.9	462	237	80.9	483
309	85.1	495	306	85.0	496
452	85.3	517			

Code 54			Code 55		
Time mins	Conversion %	Particle diameter/nm	Time mins	Conversion %	Particle diameter/nm
51	13.8	253	16	8.3	181
73	29.5	343	44	42.6	352
91	41.3	406	82	62.7	443
120	51.8	459	100	69.1	473
153	59.1	486	130	72.2	496
196	66.2	535	170	76.5	450
240	76.2	574	190	78.7	502
305	80.1	579	276	82.4	500
365	81.1	561	332	78.8	528
			428	79.0	584

Code 57			Code 58		
Time mins	Conversion %	Particle diameter/nm	Time mins	Conversion %	Particle diameter/nm
17	5.0	161	17	6.2	160
44	22.8	315	50	30.8	288
74	47.5	440	75	49.2	359
111	62.2	583	100	62.8	415
160	72.5	550	130	75.9	440
242	76.5	586	152	60.0	479
299	75.5	551	180	81.9	454
420	73.2	542	220	81.8	511
			308	78.5	459
			435	78.2	493

Code 59			Code 60		
Time mins	Conversion %	Particle diameter/nm	Time mins	Conversion %	Particle diameter/nm
20	5.8	146	20	7.3	190
58	29.3	279	46	32.2	319
95	49.7	330	71	59.9	390
123	57.0	351	96	77.1	460
166	64.5	394	123	83.8	490
195	68.3	398	153	85.1	464
237	79.0	415	238	86.5	469
327	81.9	417	280	85.2	475
405	83.2	433	314	86.9	483

Code 61			Code 63		
Time mins	Conversion %	Particle diameter/nm	Time mins	Conversion %	Particle diameter/nm
18	5.7	173	33	14.7	226
50	27.0	303	70	38.9	312
97	59.6	392	101	53.8	362
114	66.3	406	123	61.1	373
168	75.7	411	148	67.8	406
231	77.7	429	192	74.3	403
300	79.5	435	248	75.8	395
			375	76.2	410

Code 67			Code 68		
Time mins	Conversion %	Particle diameter/nm	Time mins	Conversion %	Particle diameter/nm
33	12.2	212	31	13.1	197
60	30.6	306	51	24.9	252
86	42.6	329	80	42.1	309
110	52.7	350	110	58.2	349
140	60.9	361	142	73.5	371
190	72.8	377	190	84.7	385
273	73.1	394	250	86.9	392
373	86.9	408	347	87.3	389
435	89.6	397	465	89.6	397

Code 69			Code 70		
Time mins	Conversion %	Particle diameter/nm	Time mins	Conversion %	Particle diameter/nm
32	9.9	195	26	8.2	170
63	30.8	316	60	29.7	259
89	45.5	324	83	44.0	298
140	59.9	380	111	60.2	334
199	69.8	401	143	72.3	353
268	76.8	442	186	82.2	379
391	77.2	420	226	85.9	381
491	77.7	421	275	85.2	393
			425	86.5	392

Code 72			Code 73		
Time mins	Conversion %	Particle diameter/nm	Time mins	Conversion %	Particle diameter/nm
24	26.5	159	20	5.9	140
41	35.9	262	40	15.1	209
60	58.9	312	60	26.9	254
80	67.5	334	80	40.4	293
120	74.3	336	110	55.8	361
178	85.4	356	144	64.5	390
265	86.4	364	204	79.2	401
360	86.9	345	271	86.0	418
			400	87.5	421

Code 74			Code 76		
Time mins	Conversion %	Particle diameter/nm	Time mins	Conversion %	Particle diameter/nm
21	3.8	141	30	14.8	206
51	12.9	225	50	55.3	274
70	18.5	225	70	50.1	316
90	22.5	253	92	70.5	370
111	26.3	257	112	80.1	397
145	46.0	317	155	93.3	416
190	69.4	374	212	94.1	426
250	84.4	391	348	92.4	410

Code 77			Code 81		
Time mins	Conversion %	Particle diameter/nm	Time mins	Conversion %	Particle diameter/nm
27	10.3	171	15	20.7	239
55	29.0	273	37	32.2	429
75	44.7	326	63	60.2	556
96	62.6	365	111	83.7	650
131	84.9	404	150	84.4	640
174	87.4	406	178	90.4	629
247	86.7	406	247	90.0	653
420	84.1	426	390	91.1	635

Code 82			Code 90		
Time mins	Conversion %	Particle diameter/nm	Time mins	Conversion %	Particle diameter/nm
20	5.7	257	22	36.6	372
38	14.5	339	44	65.8	526
60	30.8	455	76	77.8	580
80	44.1	473	111	86.0	662
123	72.7	588	153	88.8	596
178	90.2	589	200	89.3	605
240	91.9	656	335	90.0	613
370	92.3	618			

Code 91			Code 92		
Time mins	Conversion %	Particle diameter/nm	Time mins	Conversion %	Particle diameter/nm
23	17.7	408	16	7.3	274
40	43.9	615	40	29.0	444
65	61.3	718	60	46.6	579
92	70.8	722	86	67.6	586
123	86.6	771	118	79.9	644
154	92.6	794	178	89.5	726
258	94.7	765	264	88.3	708
452	95.0	720	454	87.3	608

APPENDIX VII HEMA KINETIC DATA

Code 32			Code 34		
Time mins	Conversion %	Particle diameter/nm	Time mins	Conversion %	Particle diameter/nm
5	11.4	304	52	92.0	37.2
15	41.1	554	72	100	41.5
30	72.8	657	107	100	43.0
45	83.4	769	200	100	48.1
65	90.4	776	245	100	50.0
90	91.5	784	600	100	59.2
123	100	796			
150	100	845			

Code 35			Code 36		
Time mins	Conversion %	Particle diameter/nm	Time mins	Conversion %	Particle diameter/nm
5	11.2	152	5	24.4	58.9
10	8.6	201	15	23.5	82.0
15	7.1	242	25	28.6	96.5
25	26.9	301	35	34.7	110
35	21.6	368	45	44.6	129
45	27.3	417	63	70.6	145
60	35.6	502	107	77.6	168
90	57.2	627	150	89.1	169
120	64.8	684	235	91.9	170
300	85.0	701			

Code 38			Code 44		
Time mins	Conversion %	Particle diameter/nm	Time mins	Conversion %	Particle diameter/nm
15	19.9	71.7	1	69.2	225
22	21.0	73.1	4	84.1	417
30	28.9	78.5	8	88.0	576
37	46.0	86.6	13	95.6	632
55	51.7	104	20	96.0	703
75	85.4	120	30	97.6	776
100	88.6	123	45	96.0	725
150	91.1	126	75	95.0	716
204	89.9	126			

Code 44		
Time mins	Conversion %	Particle diameter/nm
7	15.0	227
12	28.4	298
20	29.7	436
30	34.7	539
51	34.5	638
300	88.0	1004

Code 45		
Time mins	Conversion %	Particle diameter/nm
5	9.0	248
10	23.9	361
15	23.6	498
22	31.5	550
32	30.6	663
45	50.6	760
60	64.3	956
133	73.7	983
240	76.0	920

Code 46		
Time mins	Conversion %	Particle diameter/nm
5	21.0	312
10	23.0	523
15	40.0	640
24	61.2	653
32	67.5	724
48	85.0	960
60	83.5	936
108	84.3	941
360	88.6	890

Code 47		
Time mins	Conversion %	Particle diameter/nm
6	15.0	282
11	33.5	408
17	60.4	549
25	65.5	596
37	73.3	657
55	82.5	733
85	84.3	759
145	79.8	732
210	87.2	750

Code 48		
Time mins	Conversion %	Particle diameter/nm
5	24.5	295
10	44.1	431
15	65.2	609
25	64.2	645
35	67.7	796
46	74.1	878
60	82.3	920
102	84.7	983
138	81.7	1004
300	84.3	963